GEOTECHNICAL DATA REPORT
SPECIAL BLOCK TEST
CHEMISTRY AND METALLURGY RESEARCH FACILITY REPLACEMENT (CMRR) PROJECT
LOS ALAMOS NATIONAL LABORATORY
LOS ALAMOS, NEW MEXICO
KLEINFELDER PROJECT NO. 19435
REV. 0

Kleinfelder DCN: 19435.SBT.7-ALB05RP001

Prepared for:
Los Alamos National Laboratory
Los Alamos, New Mexico

Submitted to:
Tom Andrews, Project Manager
DMJM H+N
201 3rd St. NW, Suite 600
Albuquerque, New Mexico 87112

Prepared by:
Kleinfelder, Inc.
8300 Jefferson NE, Suite B
Albuquerque, New Mexico 87113

Joseph P. Laird, P.E.
Lead Project Engineer

Alan Kuhn, Ph.D., P.E., R.P.G.
Senior Geotechnical Engineer

John North, P.E.
Kleinfelder Project Manager

JOSEPH P. LAIRD NEW MEXICO 15873 5/31/07 LICENSED PROFESSIONAL ENGINEER

ALAN K. KUHN NEW MEXICO 6798 5/31/07 REGISTERED PROFESSIONAL ENGINEER

JOHN S. NORTH NEW MEXICO 13211 5/31/07 REGISTERED PROFESSIONAL ENGINEER

KLEINFELDER

May 31, 2007

Copyright 2007, Kleinfelder
All Rights Reserved

THIS DOCUMENT WAS PREPARED FOR USE ONLY BY THE CLIENT, ONLY FOR THE PURPOSES STATED, AND WITHIN A REASONABLE TIME FROM ITS ISSUANCE. PLEASE READ THE "LIMITATIONS" SECTION OF THIS REPORT.

TABLE OF CONTENTS

SECTION **PAGE**

LIST OF ACRONYMS AND ABBREVIATIONS 4
1 INTRODUCTION 5
1.1 PURPOSE 5
1.2 SCOPE AND CONTENT OF REPORT 7
1.3 TOPOGRAPHIC BASELINE 7
2 FIELD INVESTIGATION 7
2.1 AREA OF INVESTIGATION 7
2.2 SITE LOCATIONS AND DESCRIPTIONS 8
2.2.1 TA-61 Borrow Pit (Source A) 8
2.2.2 Mortandad Canyon (Source B) 8
2.2.3 CMRR Site Location and Description (Source C) 9
2.2.4 Two-Mile Canyon (Source D) 9
2.3 GEOLOGIC SETTING 9
2.4 BLOCK EXTRACTION 10
2.5 SAND-CONE DENSITY TESTS 14
2.6 IN PLACE DENSITY BY DRIVE CYLINDER METHOD 14
2.7 SPECTRAL ANALYSIS OF SURFACE WAVE TESTING 17
3 LABORATORY TESTING 23
3.1 KLEINFELDER, INC., LABORATORY 24
3.1.1 Unconfined Compression Tests 25
3.1.2 Specific-Gravity Tests 27
3.1.3 Particle-Size Analyses 28
3.2 ADVANCED TERRA TESTING 28
3.3 UNIVERSITY OF TEXAS AT AUSTIN 30
3.4 UNIVERSITY OF CALIFORNIA, BERKELEY 33
3.4.1 Cyclic Stress Ratio and Test Condition 34
3.4.2 Initial CSS Test Phase 35
3.4.3 Expanded CSS Test Phase 37
4 DISCUSSION OF RESULTS AND CONCLUSIONS 38
4.1 SAMPLE PREPARATION 38
4.2 VOLUME AND DENSITY CHARACTERISTICS 38
4.3 GRADATION 40
4.4 COMPRESSIVE STRENGTH 40
4.5 DYNAMIC PROPERTIES 40
4.6 SEISMICALLY INDUCED COMPACTION 41
4.7 CONCLUSIONS 41
5 LIMITATIONS 42
6 REFERENCES 43

Copyright 2007, Kleinfelder

TABLE OF CONTENTS (Continued)

SECTION **PAGE**

Appendix A – Area of Investigation ……A-1 – A-18

Figure A.1 – Facility Map Showing Investigation Areas
Figure A.2 – Bandelier Tuff Nomenclature
Plate A.3 – Geologic and Geomechanical Glossary of Terms
Figures A.4 through A.13 - Special Block Test Photographs
Table A.1 – Summary of Sample Locations

Appendix B – Summary of Kleinfelder Field and Laboratory Test Results……B-1 – B-13

Figure B.1– Density and Unit Weight of Soil In Place by Sand-Cone Method
Figures B.2 through B.4 – Density of Soil In Place by the Drive Cylinder Method
Figures B.5 through B.8 – Unconfined Compression Test Results with Stress-Strain Plots
Figure B.9 – Unconfined Compression Test Results without Stress-Strain Plots
Figure B.10 – Grain Size Distribution
Table B.1 – Summary of Specific Gravity Tests and Particle Size Analyses

Appendix C – Report of Field and Laboratory Testing Performed by the University of Texas at Austin……C-1 – C-109

Appendix D – Results of Laboratory Testing Performed by Advanced Terra Testing……...D-1 – D-16

Appendix E – Report of Cyclic Simple Shear Testing Performed by the University of California, Berkeley……...……..E-1 – E-62

Appendix F – Calculation – Estimate of Cyclic Stress Ratio for CMRR……..F-1 – F-10

Appendix G – Summary Description of Quality Control Plan …….....G-1 – G-2

Copyright 2007, Kleinfelder

LIST OF ACRONYMS AND ABBREVIATIONS

amsl	above mean sea level
ASTM	American Society for Testing and Materials
ATT	Advanced Terra Testing
bgs	below ground surface (at time of measurement)
CMRR	Chemistry and Metallurgy Research Facility Replacement
CSR	cyclic stress ratio
CSS	cyclic simple shear
DCN	document control number
DMJMH+N	Daniel Mann Johnson Mendenhall and Holmes and Narver
DOE	Department of Energy
ft	feet
G/SIR	Geotechnical/Seismic Investigation Report
KA	Kleinfelder, Inc.
KSL	Kellogg, Brown & Root, Inc.; Shaw Environmental and Infrastructure, Inc.; and Los Alamos Technical Associates, Inc.
LANL	Los Alamos National Laboratory
NQA-1	Nuclear Quality Assurance Level-1 Standard
pcf	pounds per cubic foot
PIDAS	Personnel Intrusion Detection Awareness System
psf	pounds per square foot
QA	quality assurance
Qbt2	Unit 2 of the Tshirege Member
Qbt3	Unit 3 of the Tshirege Member
$Qbt3_L$	Lower Unit 3 of the Tshirege Member
$Qbt3_U$	Upper Unit 3 of the Tshirege Member
Qbt4	Unit 4 of the Tshirege Member
RC/TS	resonant column and torsional shear
SASW	spectral analysis of surface waves
SBT	special block test
SIC	seismically induced compaction
SOP	standard operating procedure
SQAP	Subcontractor Quality Assurance Plan
UCB	University of California, Berkeley
UC	unconfined compressive
UT	University of Texas at Austin
V_s	shear-wave velocity
V_p	compression-wave velocity

Copyright 2007, Kleinfelder

1 INTRODUCTION

Kleinfelder, Inc. (KA) has prepared this report of the Special Block Test (SBT), which is a companion effort associated with the geotechnical/seismic investigation report (G/SIR) of the Chemistry and Metallurgy Research Facility Replacement (CMRR) project. This report is part of the overall deliverable-product requirements for Task 109 of the Daniel Mann Johnson Mendenhall and Holmes and Narver (DMJMH+N) contract with Los Alamos National Laboratory (LANL). This investigation was completed in accordance with the following documents:

- Kleinfelder, Inc., Block Sampling Test Plan, document control number (DCN) 19435.SBT.16-ALB04WP001 Rev. 1, March 18, 2005 (Kleinfelder, 2005)
- Kleinfelder, Inc., "Spectral Analysis of Surface Waves (SASW) Plan," DCN 19435.SBT.17-ALB04WP001 Rev. 0, December 3, 2004 (Kleinfelder, 2004d)
- Los Alamos National Laboratory, CMR Replacement Project, "Block Sampling Plan," CMRR-PLAN-013, Revision 0, June 10, 2004 (LANL, 2004a)
- Los Alamos National Laboratory, CMR Replacement Project, Block Sampling Quality Procedure, CMRR-QA-010, Revision 1, June 17, 2004 (LANL, 2004b)

1.1 Purpose

The purpose of the SBT investigation was to characterize near surface, readily accessible geologic formation materials from sites near to CMRR for use in the geotechnical characterization and recommendations for CMRR. Testable samples of the subject geologic materials at CMRR were difficult to collect because of their depth below the ground surface and their relative fragility.

Block samples (BS) of tuff were extracted by LANL from a nearby borrow pit that contains exposures of the lower nonwelded to poorly welded portion of Unit 3 of the Tshirege member of Bandelier tuff ($Qbt3_L$). This stratum was generally encountered at a depth of about 75 and 125 feet (ft) below ground surface (bgs) within the footprint of the CMRR site. Preliminary analyses

Copyright 2007, Kleinfelder

by Houston and Costantino (2003) have confirmed Kleinfelder's opinion that the behavior of this stratum is critical to the results of ground motion analyses for the CMRR site.

Before the current phase of field work at CMRR, there were significant challenges associated with obtaining quality, undisturbed samples of $Qbt3_L$ stratum using the drilling techniques employed. Due to its poorly welded, fragile, low-density structure, it was extremely difficult to obtain undisturbed, testable samples of the $Qbt3_L$. Sampling with continuous-tube and air-rotary advanced Geo-Barrel samplers produced variable but often poor recovery and, with a few exceptions, yielded samples usually too weak or disturbed for testing of intact properties. Additionally, the borehole walls in $Qbt3_L$ were prone to raveling and collapse. Consequently, the SBT program was developed and employed as a parallel investigation tract to the main CMRR G/SIR with the following objectives:

- Obtain undisturbed block samples for primary laboratory testing in the event that specialized undisturbed borehole sampling of the subsequent G/SIR was unsuccessful,
- Evaluate the spatial variability of the $Qbt3_L$ layer at different areas of LANL by a variety of independent investigative methods including spectral analysis of surface wave (SASW) testing, *in-situ* density testing, index testing, and petrographic analyses,
- Obtain preliminary results of dynamic properties by performing laboratory resonant column/torsional shear (RC/TS) tests and compare these results to field SASW test results, as well as assist in the development of RC/TS testing protocol for subsequent G/SIR testing, and
- Evaluate the potential of the $Qbt3_L$ stratum to undergo significant vertical strains under earthquake loading (i.e., seismically induced compaction [SIC]) by performing cyclic simple shear (CSS) tests, obtain preliminary results of dynamic properties at high shearing strain, and assist in developing CSS testing protocol for subsequent G/SIR testing.

Subsequent to the initiation of the SBT program, KA has been successful in obtaining high quality Pitcher tube samples of $Qbt3_L$ as part of the G/SIR at CMRR. Because this study was

Copyright 2007, Kleinfelder

completed at the same Nuclear Quality Assurance Level -1 Standard (NQA-1) as CMRR, the results of the SBT program will be used to supplement the results of the G/SIR where applicable.

1.2 Scope and Content of Report

Section 2 describes the field investigation, including a discussion of the project sites and the block extraction process, and the results of *in-situ* density and geophysical testing. Section 3 summarizes the results of laboratory testing. Section 4 presents a summary discussion of completed field and laboratory results as well as a recommended testing protocol to be incorporated into the CMRR Cyclic Simple Shear (CSS) laboratory test plan.

1.3 Topographic Baseline

All elevations and plan coordinates utilized in this report were provided by LANL and are based on either LANL GPS measurements or survey data. Elevations are measured above mean sea level (amsl) based on National Geodetic Vertical Datum (NGVD). Plan coordinates are based on the New Mexico State Plane Coordinate System. Kleinfelder did not perform any independent survey of locations presented in this report.

2 FIELD INVESTIGATION

2.1 Area of Investigation

A site plan showing the sampling areas of this study is presented as Figure A.1 of Appendix A. This site plan includes the location of samples taken for petrographic analyses (Lewis et al., 2005) and geologic contacts, as mapped by Gardner et al. (1999). The four areas of investigation for this study, referred to hereafter as Source A through D, are defined below:

Source A: TA-61, E. Jemez Road Borrow Pit (approximately one mile northeast of Site C)

Source B: Mortandad Canyon, adjacent canyon north of the CMRR site (approximately 1000 ft northeast of Site C

Source C: CMRR site

Source D: Two-Mile Canyon, adjacent canyon south of the CMRR site (approximately 500 to 750 feet south to southwest of Site C

Copyright 2007, Kleinfelder

2.2 Site Locations and Descriptions

The CMRR site (Source C), is where $Qbt3_L$ is located below the present ground surface. Its stratigraphic depth is expected to be within the zone influenced by the proposed below-grade foundation for CMRR. Sources A, B, and D are nearby areas where $Qbt3_L$ outcrops; these sites were used to obtain near-surface tuff samples and to perform *in-situ* geophysical measurements for comparison with the $Qbt3_L$ tuff between the different areas. The following subsections describe the four areas of investigation for the SBT project.

2.2.1 TA-61 Borrow Pit (Source A)

The TA-61 borrow pit is located south of Jemez Road, (known locally as the truck route), about one mile northeast of the CMRR site. Source A was the most accessible site of this study to obtain undisturbed samples of $Qbt3_L$. All block samples utilized for this study were extracted from the TA-61 borrow pit, while other techniques described in this report were used to evaluate the spatial variability of $Qbt3_L$ at other locations. The top elevations of the block samples ranged from about 7125.0 to 7127.5 ft above mean sea level (amsl). In addition to collecting samples for petrographic analyses, LANL Earth and Environmental, Environmental Geology and Spatial Analysis Sciences Department (EES-9) geologists also staked the Qbt3/Qbt2 contact in Sandia Canyon, just south of the borrow pit. This contact was surveyed at 7104.5 ft amsl; thus, the block samples were extracted about 20 ft above the contact. Based on our visual observation and inspection of the site photographs, it appears that as much as 40 to 50 ft of overburden, including $Qbt3_U$ and $Qbt3_L$, had been removed from the north face of the borrow pit at the block sample location before our investigation.

2.2.2 Mortandad Canyon (Source B)

The Mortandad Canyon site is located along an unpaved road, north of Pecos Drive, that leads to the base of the canyon. The $Qbt3_L$ outcrop is on a north-facing road cut, with a maximum height of about 12 to 14 ft and is located about 1,000 feet from the CMRR site. Due to the large amount of excavation that would be required to safely extract block samples, only SASW testing, petrographic samples (by LANL EES-9), and drive cylinder sampling were completed at Source

Copyright 2007, Kleinfelder

B. As indicated on Figure A.1, the Qbt3/Qbt2 contact is at about 7140 ft amsl near the sampled locations. The sample locations appear to be about 27 ft above the $Qbt3_L$/Qbt2 contact assuming an average sample elevation of 7167 ft amsl, based on LANL's GPS measurements.

2.2.3 CMRR Site Location and Description (Source C)

The proposed CMRR site is located on the Pajarito Mesa, adjacent to and south of the TA-55 Personal Intrusion Detection Alarm System (PIDAS). The CMRR site is bounded by Pajarito Road to the south, Pecos Drive to the east, and PIDAS fencing for the Plutonium Facility #4 to the north and west. The project area lies along the top of a mesa, with existing surface elevations varying from about 7260 to 7310 ft amsl. The project area is currently used as a parking lot, part of which is paved. The western portion of the site has been graded to create a relatively level parking area and is currently unpaved.

The focus layer of this investigation, $Qbt3_L$, is generally about 50 to 55 ft thick, based on the completed borings. This layer has a top elevation ranging from about 7210 to 7226 ft amsl within the CMRR footprint.

2.2.4 Two-Mile Canyon (Source D)

As shown on Figure A.1, the Qbt3/Qbt2 contact also outcrops in portions of Two-Mile Canyon, located south of Pajarito Road and the CMRR site; however a continuous outcrop of $Qbt3_L$ in this portion of Two-Mile Canyon was not observed due to the colluvial soil cover. For this reason, block sampling and SASW testing was not feasible at Source C. LANL EES-9 geologists collected several samples just downslope of a boulder-strewn area, about 500 to 750 ft from the CMRR site. Samples for in-place density testing were also collected by drive cylinder method near the EES-9 sampling location.

2.3 Geologic Setting

The general geologic setting of the entire LANL Complex was established by previous studies specifically contained or cited in the references, most notably Broxton and Reneau (1995), as illustrated in Figure A.2 of Appendix A. The mesa and surrounding terrain are composed of

Copyright 2007, Kleinfelder

volcanic ashflow and ashfall tuffs of the Bandelier Tuff. Unit 4 and Unit 3 of the upper Tshirege Member of the Bandelier Tuff underlie the ground surface of the Pajarito Mesa. The remainder of this section discusses the geologic and geomechanical properties of these layers. A glossary of applicable terms is presented as Plate A.3 of Appendix A.

Unit 4, denoted as Qbt4, is a poorly to moderately welded, soft to moderately hard, pumice-poor ash-flow tuff with a thin (<1.0 foot) crystal-rich pyroclastic surge deposit at its base. Unit 4 has been partially eroded over about half of the CMRR site and has been completely eroded along the southwest edge of the site; however, thicknesses of 15 to 20 ft remain in some places over the CMRR site.

Unit 3 of the Tshirege Member of the Bandelier Tuff has two portions: an upper reddish-gray, moderately welded, moderately hard tuff with 10 to 30 percent pumice fragments and abundant phenocrysts (macroscopic mineral crystals) denoted as $Qbt3_U$, and a lower portion that is poorly welded, soft, light-gray ash with shards and pumice fragments denoted as $Qbt3_L$. $Qbt3_L$, the focus stratum of the SBT investigation, is believed to be continuous across the entire mesa on which TA-55 is located.

The more welded portions of both Qbt4 and $Qbt3_U$ contain numerous natural fractures within the overall rock mass. $Qbt3_L$ has a more soil-like matrix which generally does not support fractures.

2.4 Block Extraction

The block samples were extracted from Source A in general accordance with LANL's Block Sampling Quality Procedure CMRR-QA-010 Revision 1 (2004b). One or both of Ms. Catherine Goetz, geologist, and Mr. Joe Laird, P.E., of KA were present during the collection of block samples by LANL to observe the extraction process and to assume custody of the samples. The blocks were extracted and packaged under the direction of Mr. Nathan Yost, P.E., of LANL by by laborers and carpenters employed by the maintenance and operations contractor to LANL, Kellogg, Brown & Root, Inc. (KSL); Shaw Environmental and Infrastructure, Inc.; and Los Alamos Technical Associates, Inc. Photographs of the block extraction process were taken by KA personnel and are presented as Figure A.4 through A.13 of Appendix A.

Copyright 2007, Kleinfelder

LANL EES-9 Geologists determined the general excavation area for the block extraction. The surface area intended for block sampling was stripped of disturbed material with the bucket of a backhoe. A trenching machine was used to carve out trenches within the block sample area. Wood planks were used to reduce the contact pressure the trenching machine tracks exerted to the ground surface. The trenches were excavated to a depth of about two feet. Once the trenches were excavated, KSL laborers used hand saws and battery-powered drills to carve pedestals of the tuff.

Exposed pedestals of tuff were wrapped in plastic. An oversized wooden box (4 of 6 sides) was then placed over the pedestal. Sheetrock joint compound was poured into the gaps between the box and the pedestal and allowed to set for about 30 minutes. The top of the box was placed over the exposed, freshly set joint compound and was screwed into the sides of the box. Non-resettable 5 g and 10 g Drop-N-Tell shock indicators were placed on the sides of the box in three orthogonal directions before the base of the pedestal was sawed off. The entire base of the pedestal was cut using hand saws. Four laborers, one at each side handle, lifted the block sample out of the ground, inverted it, and placed the top side of the box on the ground. After a spacer was affixed to the bottom side of the sample, plastic wrap was placed on the bottom and additional joint compound was placed. Following a 30-minute period, the bottom piece of the box was screwed in to the sides of the box. Four laborers returned the box to its upright position before placing it in the transport vehicle. The block samples were encased in bubble-wrap and wrapped in the 2-inch-thick sheet of foam.

Dr. Gardner and Dr. Lavine of LANL EES-9 visited the site during block excavation and confirmed that the excavated material consisted of $Qbt3_L$. Except where noted in Table 2.1, intact tuff cubes of approximately 10 to 14 inches per side were successfully sampled. The top few inches of the tuff typically became dry and/or disaggregated before encasement due to environmental conditions, including solar and wind exposure.

LANL relinquished the critical-care samples to Kleinfelder who transported them to the KA - Albuquerque laboratory for storage and then subsequent testing and/or distribution to other testing laboratories. The samples were handled and transported according to the KA Standard

Copyright 2007, Kleinfelder

Operating Procedure (SOP) KA5901-08, "Sampling Labeling, Handling, and Transport" (Kleinfelder, 2004c). Sampling and transport notes of the 14 block samples, documented by KA, are presented in Table 2.1. A summary of all of the sampling locations is presented as Table A.1 in Appendix A.

Copyright 2007, Kleinfelder

Table 2.1 – Summary of Notes Made During Sampling and Transport

Block Sample Designation	Top Elevation, ft	Sampling Notes, Shock Indicator History	Destination Laboratory
Test Block	7125.0 *	Vertical 5-g shock indicator tripped during transport to KA.	KA
BS-1	7125.4	5-g vertical shock indicator tripped at KA Lab, date of tripping unknown. All others untripped.	ATT
BS-2	7125.3	One vertical and one horizontal 5-g shock indicators tripped at site.	KA
BS-3	7125.2	No tripped shock indicators.	UCB
BS-4	7125.4	Vertical 5-g shock indicator tripped during vehicle transport to KA.	ATT
BS-5	7125.4	No tripped shock indicators.	UT
BS-6	7125.6	Vertical 5-g shock indicator tripped at site.	KA, reserve
BS-7	7125.7	Thin in-filled crack observed at base, SW to NE. No tripped shock indicators.	KA, reserve
BS-8	7125.6	No tripped shock indicators.	KA, reserve
BS-9	7125.9	No tripped shock indicators.	UT
BS-12	7127.3	Top SW corner of block sloughed off during site carving, tapers to full block at bottom. Filled-in with additional joint compound. Vertical 5-g shock indicator tripped during vehicle transport to KA.	KA
BS-13	7127.5	Vertical 5-g shock indicator tripped at site.	UCB
BS-14	7127.4	NE corner to north-central portion of block sloughed off during site carving. Filled-in with additional joint compound. No tripped shock indicators.	ATT
BS-15	7126.7	NW corner of block sloughed off during site carving. Filled-in with additional joint compound. 5-g vertical shock indicator tripped during unloading at University of Texas at Austin.	UT
BS-16	7126.7	No tripped shock indicators.	UCB

* Estimated, based on a bottom elevation of 7123.6 ft amsl

ATT – Advanced Terra Testing

UCB – University of California, Berkeley

UT – University of Texas at Austin

Copyright 2007, Kleinfelder

2.5 Sand-Cone Density Tests

KA performed four sand-cone density tests at the block extraction area of Source A on April 5, 2004, to obtain *in-situ* density values at the block sample test area. The tests were performed below the base of the removed block pedestals according to ASTM D 1556-00, "Standard Test Method for Density and Unit Weight of Soil In-Place by the Sand-Cone." The results of these tests were used for comparison of *in-situ* density of the $Qbt3_L$ layer at Source A to the density of the limited access sites (Source B and D) and the CMRR site (Source C). The results of the in-place density testing are presented on Figure B.1 of Appendix B and are summarized in Table 2.2. The corresponding sample void ratio and porosity values are also presented, based on an average tested specific gravity of 2.56 of all Source A samples.

Table 2.2 – Summary of Sand Cone Density Test Results at Source A

Test Location	Elevation (ft amsl)[1]	Moisture Content (%)	Wet Density (pcf)	Dry Density (pcf)	Specific Gravity (dim)[2]	Void Ratio, *e* (dim)	Porosity, *n* (dim)
BS-5	7123.9	6.1	86.8	81.8	2.56	0.95	0.49
BS-9	7124.4	4.5	86.7	83.0	2.56	0.92	0.48
BS-16	7125.2	4.6	86.6	82.8	2.56	0.93	0.48
BS-12	7125.8	4.8	93.2	88.9	2.56	0.80	0.44
	Average	**5.0**	**88.3**	**84.1**	**2.56**	**0.90**	**0.47**

[1]Estimated, assuming 1.5 ft below top of block survey elevation
[2]Assumed, based on average of all specific gravity test results from Source A (Table 3.3)

2.6 In Place Density By Drive Cylinder Method

KA utilized the drive-cylinder method at Sources A, B, and D to obtain tube samples for subsequent density testing and index property laboratory testing. The inclusion of the drive cylinder testing allowed comparison of the $Qbt3_L$ layer index properties of the limited access

Copyright 2007, Kleinfelder

sites (Sources B and D) to those of Sources A and C. The drive cylinder samples were tested for unit weight in accordance with SOP KA5901-14 (Kleinfelder, 2004a), and ASTM D 2937, "Density of Soil In-Place by the Drive Cylinder Method".

Four drive cylinder samples of $Qbt3_L$ were obtained at Source A on December 9 through 10, 2004. The Source A samples were obtained just below the existing ground surface, approximately 10 ft west and 10 ft east of the center of the first SASW array. The Source B and D samples were obtained on December 16, 2004, and December 10, 2004, respectively. These samples were within 1 to 2 ft of the referenced petrographic sample taken previously by EES-9. An EES-9 geologist surveyed these locations.

The sampling records of the drive samples, as well as the results of the subsequent laboratory measurements, are presented on Figures B.2 through B.4 of Appendix B. Care was taken to begin sampling below the exposed partially frozen ground surface. The samples at Sources A and D were driven vertically into the exposed subgrade. The samples taken at Source B were driven at angles ranging from about 10 to 45 degrees from vertical since the exposed surface was an inclined road-cut wall. Photograph 12 illustrates the sliding drop hammer driving an inclined sample tube into the road cut wall. A close-up picture of the 4-inch-diameter, 5-inch-high sample tube is presented on Photograph No. 13.

The samples were handled and transported according to KA SOP 5901-08. The samples were measured at the KA laboratory in Albuquerque, NM. Where the extracted tuff sample was not flush with the sampler, the sampler was reamed to an even length during the laboratory trimming phase. The corrected cylinder volume was used for subsequent calculations. Summaries of the density test results are presented as Tables 2.3 through 2.5. Additional laboratory testing, including particle-size analyses and specific-gravity tests, were performed on some of the drive samples, as discussed in Section 3.1.

Copyright 2007, Kleinfelder

Table 2.3 – Summary of In Place Density Test Results at Source A by Drive Cylinder Method

Test Location	Elevation (ft amsl)	Moisture Content (%)	Wet Density (pcf)	Dry Density (pcf)	Specific Gravity (dim)	Void Ratio, *e* (dim)	Porosity, *n* (dim)
TA-61-1A	7124.7	6.9	82.8	77.5	2.58	1.08	0.52
TA-61-1B	7130.0	7.9	84.6	78.5	2.57	1.04	0.51
	Average	**7.4**	**83.7**	**78.0**	**2.57**	**1.06**	**0.51**

Table 2.4 – Summary of In-Place Density Test Results at Source B by Drive Cylinder Method

Test Location*	Elevation (ft amsl)*	Moisture Content, (%)	Wet Density (pcf)	Dry Density (pcf)	Specific Gravity (dim)	Void Ratio, *e* (dim)	Porosity, *n* (dim)
MC-1	7164	8.0	92.6	85.7	2.54	0.85	0.46
MC-2	7165	7.1	91.4	85.4	2.56	0.87	0.47
MC-3	7166.7	4.7	90.4	86.3	2.56	0.85	0.46
MC-4	7168.1	10.1	95.3	86.6	2.55	0.84	0.46
	Average	**7.5**	**92.4**	**86.0**	**2.55**	**0.85**	**0.46**

*Test locations and elevations as presented by Lewis, et al. (2005). See Table A.1 for corresponding EES-9 sample number.

Copyright 2007, Kleinfelder

Table 2.5 – Summary of In-Place Density Test Results at Source D by Drive Cylinder Method

Test Location*	Elevation (ft amsl)	Moisture Content (%)	Wet Density (pcf)	Dry Density (pcf)	Specific Gravity (dim)	Void Ratio, *e* (dim)	Porosity, *n* (dim)
TMC-1	7183.9	9.5	91.5	83.6	2.56	0.91	0.48
TMC-2	7177.7	9.5	96.1	87.7	2.58	0.84	0.46
TMC-3	7176.5	9.9	98.1	89.3	2.55	0.78	0.44
TMC-4	7183.9	13.3	101.7	89.8	2.57	0.79	0.44
	Average	**10.6**	**96.9**	**87.6**	**2.57**	**0.83**	**0.45**

*Test locations and elevations as presented by Lewis, et al. (2005). See Table A.1 for corresponding EES-9 sample number.

2.7 Spectral Analysis of Surface Wave Testing

SASW testing was performed by Prof. Kenneth Stokoe, P.E., and Mr. Brady Cox of the University of Texas at Austin (UT) during the period from December 9, 2004 to December 10, 2004. Mr. Joe Laird, P.E., of KA and Mr. Nathan Yost, P.E., of LANL were present for project oversight during the SASW field work. The *in-situ* testing was performed according to "Seismic Testing by the Spectral-Analysis-of-Surface-Waves (SASW) Method at Los Alamos National Laboratory," prepared by UT, 2004. A stand-alone report prepared by UT, "Special Block Tests of Bandelier Tuff: Field Seismic and Dynamic Laboratory Tests, Los Alamos National Laboratory," dated November 7, 2005, is presented as Appendix C.

SASW testing was employed as a means to compare the *in-situ* dynamic properties of the $Qbt3_L$, principally shear wave velocity, V_S, between the various sites of this study. SASW was also used for comparison to the laboratory, V_S values obtained by RC/TS testing of the block samples.

The SASW survey coordinates are presented on Table A.1 of Appendix A. SASW surveys at Source A were offset about 100 to 200 ft east of the former test block sampling area and performed over sloping ground. The offset was necessitated by the partial excavation of the test

Copyright 2007, Kleinfelder

block area by the borrow pit operators. As shown on the Table A.1, the center elevation of the TA-61-1 and TA-61-2 surveys, performed parallel to each other, are about 0 to 2 ft higher and 3 to 5 ft higher, respectively, than the surface of the block samples locations. The TA-61-3 survey was off set about 200 ft east of and at a surface elevation about 19 to 21 ft higher than the block area. Photograph 14 was taken during this survey, facing to the west. The former test block area is located at the base of the ramp to the bottom of the borrow pit.

The waveform data analyses for the completed SASW surveys were performed at UT. The iterative-forward modeling process was performed using the computer program WinSASW, Version 1.2.3, which matches the theoretical surface wave dispersion curve with an average experimental dispersion curve for evaluation of the *in-situ* velocity profile.

The three Source A SASW surveys were used to develop interpreted V_S and compression wave velocity (V_P) profiles. Based on the geologic contact information provided by LANL EES-9, all three of the generated profiles were measured within $Qbt3_L$ to a depth of at least 20 feet. Summaries of the interpreted velocity measurements are presented in Tables 2.6 through 2.8. All depths and elevations are presented from the center point of the test array. An assumed mass density of 85 pounds per cubic feet (pcf) and an assumed Poisson's Ratio of 0.33 (based on Merrick and Associates, 1995) were used for the data reduction. While the actual measured *in-situ* density of this unit varies only slightly, this is of secondary importance in the overall forward modeling process, which primarily considers the variation of shear wave velocity. The shear wave velocity changes (increases) rapidly with corresponding increases in effective confining pressure at these shallow test depths.

SASW testing was also completed along the road cut at Source B, as shown in Photograph 15. The survey was completed between petrographic sample locations CMRR-10 and CMRR-13 at about 7165 ft amsl. The spacing of the impact source and geophones was varied to generate an effective horizontal sampling depth (into the road cut) of about 15 ft. The overburden above the SASW array was about 8 to 10 ft at the road cut face and continued to slope upward. As such, the effective pressure of the tested tuff likely increases with deeper penetration into the hillside. The corresponding increase of velocity with deeper penetration into the hillside is presented in

Copyright 2007, Kleinfelder

Table 2.9. An assumed mass density of 85 pcf and Poisson's Ratio of 0.33 were used for the data reduction.

Table 2.6 – Summary of Velocity Measurements, SASW Testing at TA-61-1

Below Ground Surface to Top Depth of Layer (ft bgs)	Below Ground Surface to Bottom Depth of Layer (ft bgs)	Elevation at Top of Layer (ft bgs)	Elevation at Bottom of Layer (ft bgs)	Shear Wave Velocity, V_s (ft/sec)	Compression Wave Velocity, V_P (ft/sec) [1]
Profile 1					
0	0.5	7127.5	7127.0	600[2]	1191[2]
0.5	1.1	7127.0	7126.4	200	397
1.2	3.4	7126.4	7124.2	430	854
3.4	15.4	7124.2	7112.2	530	1052
15.4	21.7	7112.2	7105.8	710	1410
Profile 2					
0	0.5	7127.5	7127.0	600[2]	1191[2]
0.5	1.0	7127.0	7126.5	170	338
1.0	3.5	7126.5	7124.0	370	735
3.5	14.5	7124.0	7113.0	490	973
14.5	21.7	7113.0	7105.8	710	1410

ft bgs = feet below ground surface

ft/sec = feet per second

[1] Compression wave velocity was not measured, but estimated based on an assumed Poisson's Ratio, measured shear wave velocity, and the relationship between these two based on wave propagation theory.
[2] These relatively high velocities are likely influenced by previous vehicular traffic over the ground or frozen ground conditions.

Copyright 2007, Kleinfelder

Table 2.7 – Summary of Velocity Measurements, SASW Testing at TA-61-2

Below Ground Surface to Top Depth of Layer (ft bgs)	Below Ground Surface to Bottom Depth of Layer (ft bgs)	Elevation at Top of Layer (ft bgs)	Elevation at Bottom of Layer (ft bgs)	Shear Wave Velocity, V_s (ft/sec)	Compression Wave Velocity, V_P (ft/sec) [1]
Profile 1					
0	0.4	7130.7	7130.3	420[2]	834[2]
0.4	0.7	7130.3	7130.0	300	596
0.7	1.5	7130.0	7129.2	350	695
1.5	4.5	7129.2	7126.2	430	854
4.5	14.5	7126.2	7116.2	530	1052
14.5	22.2	7116.2	7108.5	720	1429
Profile 2					
0	0.3	7130.7	7130.4	390[2]	774[2]
0.3	0.6	7130.4	7130.1	200	397
0.6	1.4	7130.1	7129.3	330	655
1.4	4.4	7129.3	7126.3	370	735
4.4	13.4	7126.3	7117.3	500	993
13.4	22.2	7117.3	7108.5	710	1410

ft bgs = feet below ground surface

ft/sec = feet per second

[1] Compression wave velocity was not measured, but estimated based on an assumed Poisson's Ratio, measured shear wave velocity, and the relationship between these two based on wave propagation theory.
[2] These relatively high velocities are likely influenced by previous vehicular traffic over the ground or frozen ground conditions.

Copyright 2007, Kleinfelder

Table 2.8 – Summary of Velocity Measurements, SASW Testing at TA-61-3

Below Ground Surface to Top Depth of Layer (ft bgs)	Below Ground Surface to Bottom Depth of Layer (ft bgs)	Elevation at Top of Layer (ft bgs)	Elevation at Bottom of Layer (ft bgs)	Shear Wave Velocity, V_s (ft/sec)	Compression Wave Velocity, V_P (ft/sec) [1]
Profile 1					
0	0.2	7146.5	7146.5	275	546
0.2	1.7	7146.3	7144.8	350	695
1.7	5.2	7144.8	7141.3	420	834
5.2	8.2	7141.3	7138.3	580	1151
8.2	13.2	7138.3	7133.3	650	1290
13.2	26.4	7133.3	7120.1	750	1489
26.4	28.2	7120.1	7118.3	750	1489
Profile 2					
0	0.2	7146.5	7146.5	280	556
0.2	1.7	7146.3	7144.8	410	814
1.7	5.2	7144.8	7141.3	450	893
5.2	8.2	7141.3	7138.3	580	1151
8.2	13.2	7138.3	7133.3	650	1290
13.2	26.4	7133.3	7120.1	750	1489
26.4	28.2	7120.1	7118.3	750	1489

ft bgs = feet below ground surface

ft/sec = feet per second

[1] Compression wave velocity was not measured, but estimated based on an assumed Poisson's Ratio, measured shear wave velocity, and their relation based on wave propagation theory.

Copyright 2007, Kleinfelder

SASW testing was also planned for Source D. However, due to the persistent colluvial soil layer along Two-mile Canyon, a continuous layer of exposed $Qbt3_L$ could not be identified by LANL EES-9. As such, it was determined in the field by UT, KA, and LANL that there was not an adequate location for a linear array of SASW testing to be performed. Thus, due to a potential for misleading waveforms to be generated, the SASW survey was not performed at Source D.

Table 2.9 – Summary of Velocity Measurements, SASW Testing at Source B

Road Cut Wall to Lateral Distance of Layer (ft bgs)	Road Cut Wall to Lateral Distance of Layer (ft bgs)	Test Elevation at Road Cut Wall (ft bgs)	Shear Wave Velocity, V_s (ft/sec)	Compression Wave Velocity, V_P (ft/sec) [1]
0	1.0	7165	1820[2]	3613[2]
1.0	4.0	7165	420	834
4.0	9.0	7165	730	1449
9.0	15.2	7165	950	1886

ft bgs = feet below ground surface

ft/sec = feet per second

[1] Compression wave velocity was not measured, but estimated based on an assumed Poisson's Ratio, measured shear wave velocity, and the relationship between these two based on wave propagation theory.
[2] These relatively high velocities are likely influenced by previous vehicular traffic over the ground or frozen ground conditions.

The $Qbt3_L$ velocity profiles of the completed SASW arrays at Source A and B are plotted on Figure 3 of Appendix C. Based on the tabulated data and this illustration, it is apparent that there is a significant increase in the $Qbt3_L$ shear wave velocity with an increase in depth and corresponding rise in effective stress. This is indicative of more soil-like material, as opposed to a more indurated rock unit that exhibits more uniform dynamic properties relative to changes in effective stress. The three TA-61 profiles exhibit a similar stair-stepped pattern, where *Vs* increases with depth. Although profile TA-61-3 indicates a slightly steeper increase in shear wave velocity than the two profiles completed at lower elevations, the predominate factor

Copyright 2007, Kleinfelder

affecting *Vs* appears to be effective stress, rather than any elevation-related material property change within $Qbt3_L$. While it is difficult to directly compare the two SASW sites because the Source B testing was performed in a horizontal plane, both arrays appear to have velocity properties in the same order of magnitude for shallow depths. We note that Tables 2.6, 2.7 and 2.9 indicate an anomalous, high velocity surface layer of less than one-foot thick. It is our opinion that this is due to overconsolidated surface crust, densificiation caused by surface traffic, frozen ground, or a combination thereof.

As illustrated on Figure 4 of the main report in Appendix C, the shear velocity versus depth profile obtained from SASW testing of $Qbt3_L$ lies within the range of value predicted for a dry sand, based on previous studies at UT (Menq, 2003). As shown in the addendum to the main report, the SASW data was also compared to the Menq relationship using the index properties of the $Qbt3_L$ material. The comparative plots illustrate the effect of mean effective confining pressure (represented as an equivalent depth) from the ground surface to a depth of 22 feet. Due to the uncertainty of the actual *in-situ* state of stress, K_o values of 0.5 and 1.0 were both used in the stress-to-depth conversion to show how this parameter affects the correlation. It is important to note that $Qbt3_L$ was encountered at a drilled depth of about 75 ft below the existing ground surface at the CMRR site and is subject to a considerably higher effective stress. It is anticipated that the trend of increasing shear velocity with depth can be extrapolated to higher effective pressures. The G/SIR production RC/TS tests for $Qbt3_L$, as well as other *in-situ* tests such as seismic downhole testing, will further define the dynamic soil property profiles of this layer at the CMRR site.

3 LABORATORY TESTING

Samples from the various sources were delivered to the KA Albuquerque geotechnical testing laboratory for storage, cataloging, distribution to specialty geotechnical laboratories, and conventional geotechnical testing. The purpose of the laboratory testing program was to:

- Perform a limited number of geomechanical tests on the block samples (Source A) such that a set of preliminary geotechnical properties could be developed that could

Copyright 2007, Kleinfelder

be used to estimate the approximate range of performance of the $Qbt3_L$ under static and dynamic loading conditions,

- Perform a series of index tests on samples of the $Qbt3_L$ from all four sources to compare basic properties between the four source sites, and

- Using the index laboratory tests, evaluate and determine if the results are similar and if it is justifiable to use the preliminary geotechnical properties from Source A at the CMRR site (Source C).

The laboratory testing program was completed using four separate laboratories. Conventional geomechanical and index testing was performed at Kleinfelder's geotechnical laboratory in Albuquerque, New Mexico. Advanced Terra Testing (ATT) in Lakewood, Colorado completed more sophisticated static geotechnical testing. Dynamic laboratory testing was completed at the University of Texas, Austin (UT) and at the University of California, Berkeley (UCB). Specifically, UT performed Resonant Column and Torsional Shear (RC/TS) testing of samples milled from the block samples. Cyclic Simple Shear (CSS) tests were performed at UCB on samples milled from the block samples. Details of the specific laboratory tests performed and summaries of the results are presented in the following sections of the report.

3.1 Kleinfelder, Inc., Laboratory

Conventional strength and index property tests were performed at the Kleinfelder laboratory in Albuquerque, New Mexico. Unconfined compression tests, as well as unit weight and moisture content tests, were performed on two separate block samples of $Qbt3_L$ that were extracted from the TA-61 borrow pit. Laboratory sieve analyses and specific gravity tests were also performed on these samples. Tests were performed on samples retrieved from each of the two correlation sources (B and D). These tests were performed according to the specifications of the CMRR Special Block Test, Block Sample Test Plan (Kleinfelder, 2005). As part of the CMRR G/SIR, the same series of tests was performed on a 6-inch-diameter Pitcher Tube sample from boring DSC-1 for comparison purposes. Photographs of selected laboratory operations are referenced in

Copyright 2007, Kleinfelder

the following sections. The photographs are identified by photo number and are contained in Appendix A.

3.1.1 Unconfined Compression Tests

The unconfined compression test samples were extracted from the test blocks using hand saws, (see Photograph 16) to reduce the sample disturbance to the structural fabric of the tuff. Once a rough-hewn sample was extracted from the block, the sample was placed in a soil lathe and manually trimmed while turning to form a cylindrical specimen, as shown in Photograph 17. Due to the persistent presence of lithics, pumice, and other inclusions within the tuff matrix, as well as the fragile nature of this poorly welded material, it was difficult to carve a testable cylindrical specimen, and many of the samples developed mechanical fractures during trimming and had to be discarded. Fortunately, the overall size of the block samples was large enough for multiple opportunities to trim acceptable samples.

Kleinfelder performed these tests in general accordance with ASTM D 2938, "Unconfined Compressive Strength of Rock Core Specimens". Moisture content and unit weight tests were performed as a part of this test. One unconfined compression test was completed for BS-12, while two tests were completed for BS-2. Additionally, a compression test was completed on a sample from the Test Block, before the SBT test plan approval. While a portion of this block likely included colluvial soil, the tested sample appeared to consist of intact $Qbt3_L$ material and the results are therefore included for comparison. Typical photographs at the start of loading the test block sample and after failure are presented as Photographs 18 and 19, respectively. The test results, including the stress-versus-strain plots, are presented on Figures B.6 through B.9 of Appendix B and summarized on Table 3.1.

Copyright 2007, Kleinfelder

Table 3.1 – Summary of Unconfined Compression Tests on Carved Block Samples

Test Location	Elevation (ft amsl)	Unconfined Compressive Strength, (psf)	Axial Strain at Failure, (%)	Moisture Content (%)	Dry Density (pcf)	Void Ratio, *e** (dim)	Porosity, *n** (dim)
BS-12	7127.3	562	0.9	6.1	78.1	1.04	0.51
BS-2, NW	7125.3	1377	1.4	4.7	87.7	0.81	0.45
BS-2, NE	7125.3	1402	1.2	4.3	81.2	0.95	0.49
Test Block	7123.6	2108	3.4	6.6	77.6	1.06	0.51
	Average	**1362**	**1.7**				

*For BS-2 and BS-12, calculated void ratio and porosity values are based on measured specific gravity of 2.54 and 2.55, respectively. For test block sample, the Source A average specific gravity value of 2.56 was used.

Based on unconfined compressive strength (UC) values, which vary from 562 to 2108 pounds per square foot (psf), the $Qbt3_L$ samples have unconfined strengths below the lower limit of an extremely weak rock (Hoek, 2000). These low UC values are typical of this poorly welded tuff, with only minimal apparent cohesion. The stress-versus-strain curves presented on Figures B.5 through B.8 and the low axial strains at failure, which ranged from 0.9 to 3.4 percent, illustrate the brittle failure mechanism as the weak edge-to-edge particle bonds are broken. It is important to note that this material exhibits significantly higher shear-strength properties under confined conditions, as indicated by the triaxial compression tests results discussed in Section 3.2.

In addition to the block samples, a Pitcher tube sample from CMRR (DSC-1, 91.0 to 92.0 ft) was extracted by first cutting the tube in half, then making two longitudinal cuts with a Dremel cutting tool. There was a thin sheen of drilling mud present on the outside of the sample, but otherwise the sample appeared to be undisturbed. The nominally 6-inch-diameter sample was trimmed at both edges. For comparative purposes, this large-diameter sample was tested in unconfined compression. Due to its large size, it necessitated testing of the sample in a concrete compression loading frame. Although the length-to-diameter (L:D) ratio was only 1.54 (ASTM

Copyright 2007, Kleinfelder

standards are L:D 2.0 to 2.5), the shortened height did not appear to inhibit failure planes during compressional loading. The results of this test are presented on Figure B.9 of Appendix B and summarized in Table 3.2. The results of this large diameter test are within the range of recorded UC values from the previously presented results.

Table 3.2 – Summary of Unconfined Compression Test on CMRR Sample

Test Location	Elevation (ft amsl)	Unconfined Compressive Strength (psf)	Axial Strain at Failure (%)	Moisture Content (%)	Dry Density (pcf)	Void Ratio, *e** (dim)	Porosity, *n** (dim)
DSC-1	7203.6	1074	0.8	6.9	86.3	0.85	0.46

*The calculated void ratio and porosity values are based on measured specific gravity of 2.56

3.1.2 Specific-Gravity Tests

Kleinfelder performed fifteen specific-gravity tests as part of the SBT program in general accordance with ASTM D854-02, "Standard Test Methods for Specific Gravity of Soil Solids Using Soil Pycnometer". Where these tests coincided with a density test, they are presented on Tables 2.3, 2.4, 2.5, and 3.1. A partial summary of specific-gravity values from the different sources is presented below in Table. 3.3. A full summary of results is presented on Table B.1 of Appendix B. Two additional tests, performed by ATT, are included in the summary for Source A presented in Table 3.3. The specific gravity of the $Qbt3_L$ samples across the four source sites is relatively consistent, varying from 2.54 and 2.58 and averaging 2.56.

Table 3.3 – Summary of Specific Gravity Tests at Different Sources

Test Location	Number of Tests	Low Value	High Value	Average Value
Source A	8	2.54	2.58	2.56
Source B	4	2.54	2.56	2.55
Source C	1	2.56	2.56	2.56
Source D	4	2.55	2.58	2.57
			Overall Average	**2.56**

Copyright 2007, Kleinfelder

3.1.3 Particle-Size Analyses

Particle-size analyses were performed on ten samples from Sources A, C, and D, including several of the block samples and drive samples. The tabular and graphical results of percent finer by weight are summarized on Table B.1 and Figure B.10, respectively. After the initial dry weighing of the samples, the samples were soaked in a pan for a minimum of 12 hours. The poorly welded samples, which were predominately disaggregated after the soaking phase, were then wet-sieved through a No. 200 sieve in accordance with ASTM D 1140-00, "Standard Test Methods for Amount of Material in Soils Finer Than the No. 200 Sieve, Method A". The retained material was dried and later tested through the coarse sieves according to ASTM C 136-01, "Standard Test Method for Sieve Analysis of Coarse and Fine Aggregates".

As indicated on Figure B.10, the grain-size distribution is similar for all ten samples. The $Qbt3_L$ tuff is predominantly sand-sized, as indicated by 80 to 86 percent of all particles falling within the range of coarse to fine sand. A total of 12 to 16 percent of the tuff passes through the No. 200 sieve, indicating some silt-sized or finer material. One to 5 percent of material was gravel-sized or higher, and likely includes pumice or lithics. Based on this particle size distribution, this stratum would be classified as a silty sand (SM), according to the Unified Soil Classification System.

3.2 Advanced Terra Testing

Triaxial compression (TRX) tests were performed on a sample from block BS-4 and a sample from block BS-14 at the ATT laboratory in Lakewood, Colorado. These tests were performed to evaluate the shear strength and stiffness properties of $Qbt3_L$ under static loading. Additional laboratory tests, including unit weight, bulk density, and specific-gravity tests as applicable, were also performed on these samples. The laboratory test report prepared by ATT is presented as Appendix D.

As detailed in the SBT laboratory test plan, the test confining pressure was chosen to be the estimated mean effective stress at the existing mid-point of the $Qbt3_L$ layer at CMRR (102.5 ft). Because the at-rest earth coefficient, K_o, was not accurately known, two tests were performed to

Copyright 2007, Kleinfelder

bound this estimated pressure between a range of reasonable values. Assuming a K_o of 1.0 and 0.5, mean effective pressures of 9,600 psf and 6,300 psf, respectively, were estimated and subsequently used for test confining pressure.

Following the removal of the block sample cover and top layer of joint compound, ATT was able to obtain test samples by hydraulically pushing test-sized, sharpened-cutting-edge, thin-walled tubes into the encased tuff and extruding the sample from the tube. Photographs of samples before and after testing are provided as part of the ATT laboratory testing results presented in Appendix D. The tests were performed by ATT in accordance with ASTM D 2664-95A, "Standard Test Method for Triaxial Compressive Strength of Undrained Rock Core Specimens without Pore Pressure Measurements".

The samples were also fitted with dial gauges to measure axial strain and to develop elastic moduli in accordance with ASTM D5407, "Standard Method for Elastic Moduli of Undrained Intact Rock Core Specimens in Triaxial Compression without Pore Pressure Measurements." However, the samples were too weak (poorly welded) and sensitive to be tested in the rock-compression device. As such, radial-strain gauges could not be used and Poisson's ratio could not be obtained for the samples. Therefore, a modified version of ASTM 5407 was employed for this testing. A summary of the ATT tests results are presented in Table 3.4.

Table 3.4 – Summary of Triaxial Compression Tests on Block Samples

Test Location (1)	Elev. (ft amsl)	Confining Pressure (psf)	Deviator Stress at Failure (psf)	Young's Modulus (ksf)	Axial Strain at Failure (%)	Mc (%)	Dry Density (pcf)	Void Ratio, *e** (dim)	Porosity *n** (dim)
BS-4	7125.4	6,300	19,002	850	7.6	2.5	80.0	1.01	0.50
BS-14	7127.4	9,400	26,293	1138	10.5	4.2	83.6	0.90	0.47

*The calculated void ratio and porosity values are based on measured specific gravity of 2.58 for BS-4 and a specific gravity of 2.55 for BS-14
ksf – kips per square foot

By comparing the UC values presented in Tables 3.1 and 3.2, the confined samples exhibit notably higher strength values under lateral confinement, as well as higher axial strains at failure.

Copyright 2007, Kleinfelder

Following the completion of additional conventional triaxial compression and triaxial stress path tests in the G/SIR, Kleinfelder will further evaluate the shear strength and static deformation relationship of this material at simulated *in-situ* conditions .

3.3 University of Texas at Austin

RC/TS testing was performed at the UT Soil Dynamics Laboratory in Austin, Texas, to characterize the dynamic properties, shear modulus (G), and damping ratio (D) of $Qbt3_L$ at low to high shear strains. The shear modulus and damping ratio degradation curves are required for subsequent ground response and soil-structure interaction analyses.

Two RC/TS test series were performed on block sample BS-15 of $Qbt3_L$ that was extracted from the TA-61 borrow pit. Two block samples are being held in reserve at UT. The tests were performed under the direction of Prof. Kenneth Stokoe, P.E. of UT according to the procedures in UT's Technical Procedures for Resonant Column and Torsional Shear Testing of Soil and Rock Samples (UT, 2000). This test procedure has been quality-assurance-approved at similar Department of Energy sites and will be provided with the final test results. A stand-alone UT report presenting a discussion of sample preparation and testing, laboratory RC/TS, as well as a discussion of data trends and comparison to published relationships, is presented in Appendix C.

Resonant column tests were performed at isotropic confining pressures ranging from 216 psf to 13,824 psf. Due to excessive tilting of Specimen No. 1, however, this test series was performed to a confining pressure of only 3,456 psf. The results of both tests were similar and indicated that dynamic properties of the $Qbt3_L$ samples are highly dependent on effective confining pressure, as shown on Figure 5 and Figure 6 of Appendix C. In effect, this material behaves similar to a sand when compared to typical published relationships of log-shear velocity and log-shear modulus versus log-confining pressure. As the isotropic confining pressure of Specimen No. 2 increased from 216 psf to 13,824 psf, there was a corresponding increase in shear velocity and shear modulus from 388 to 1,098 ft/sec and 390 to 3,172 ksf, respectively. For the same increase of confining pressure, material damping ratios decreased from about 1.87 to 0.51 percent. A summary of low-amplitude dynamic properties is presented is Table. 3.5. For comparative

Copyright 2007, Kleinfelder

purposes, the closest test point to the estimated mean effective pressure at the mid-layer depth of $Qbt3_L$ at the CMRR site is 6,920 psf.

RC/TS tests were also performed in the non-linear range for both specimens at confining pressures of 864 and 3,456 psf. As the test shearing strain exceeds about 0.001%, the dynamic properties begin their non-linear behavior as G decreases and D increases, with corresponding high-amplitude shearing strain increases. The normalized shear modulus (G/G_{max}) and D degradation plots with respect to increasing shearing strain are presented on Figure 8 and Figure 9 of Appendix C. Summaries of the G/G_{max} and D with respect to peak shearing strain are presented in Tables D.3 through D.10 of Appendix C. The shapes of these degradation curves are also consistent with published relationships for sandy soils.

Copyright 2007, Kleinfelder

Table 3.5 – Summary of Low-Amplitude Resonant Column Test Results

Test Location	Isotropic Confining Pressure, psf	Low-Amplitude Shear Wave Velocity, V_s (ft/sec)	Low-Amplitude Shear Modulus, G_{max} (ksf)	Low-Amplitude Material Damping Ratio, D_{min} (%)	Mc (%)	Initial Dry Density (pcf)	Initial Void Ratio, *e** (dim)	Initial Porosity, *n** (dim)
BS-15, Specimen 1	216	335	311	1.76	6.0	83.8	0.91	0.48
	432	402	445	1.42				
	864	471	614	1.22				
	1728	572	907	0.93				
	3456	683	1299	0.68				
BS-15, Specimen 2	216	388	390	1.87	5.3	79.1	1.02	0.50
	432	451	527	1.63				
	864	531	730	1.24				
	1728	598	929	1.03				
	3456	729	1385	0.85				
	6912	900	2139	0.65				
	13,824	1098	3172	0.51				

*The calculated void ratio and porosity values are based on measured specific gravity of 2.56. The elevation of BS-15 is 7126.7 ft amsl.

Copyright 2007, Kleinfelder

3.4 University of California, Berkeley

CSS testing was performed at the University of California, Berkeley (UCB) geotechnical laboratory. The CSS tests were performed to evaluate the potential for vertical strains of $Qbt3_L$ due to seismically induced shear stresses (i.e., seismically induced compaction [SIC]). SIC may occur as a result of a breakdown of the structural fabric of the $Qbt3_L$ layer during cyclic loading, leading to densification and possible settlement of the ground above.

A conventional CSS test is generally performed on sand by remolding test material within a wire-wrapped membrane. The wire-wrapped membrane maintains a K_o condition (no radial strain) during cyclic shearing of the sample. In this manner the apparatus allows only vertical stains to occur which provides data on one-dimensional vertical strain and thus provides a measure of potential for SIC.

The $Qbt3_L$ has a relatively high porosity and void ratio and relatively low unit weight. The concern is that this material could densify if the very weak bonds (welding) between adjacent particles are damaged during seismic shaking. Because of this very fragile, intact nature it is not likely that any meaningful results will be collected by performing CSS test in a conventional manner using remolded material. What was determined is that carefully milled (shaped) samples of intact $Qbt3_L$ were necessary and that a cell confining stress must be maintained in an attempt to simulate K_o conditions during testing. Therefore, tests on the block samples were performed utilizing only cell confining pressures to mimic *in-situ* confining stresses and to attempt to limit to zero any radial strain and thus mimic K_o conditions. During tests on block samples only vertical strain was measured.

After the block samples were tested, the testing program was expanded to attempt to resolve issues associated with state of stress and measurement of radial strain. The expanded program included experimentation to measure radial strain on the outside of a latex membrane using elastomeric gauges (EG) as well as a test using the wire-wrapped membrane with a slightly undersized milled sample in which Ottawa sand was placed in the annular space.

Copyright 2007, Kleinfelder

The samples were prepared and tested by Dr. Michael Riemer of UCB and tested according to UCB Procedure 018420-PROC-04, Rev. 1 (UCB, 2004). The report prepared by Dr. Riemer, "Feasibility Study of Cyclic Simple Shear Testing of Volcanic Tuff at UC Berkeley," dated April 30, 2007, is presented as Appendix E. The report combines the results from the initial testing of block samples, as well as secondary phase of experimental testing of CMRR Pitcher tube samples conducted to resolve concerns of sample stress ratio encountered during testing and to further develop the most appropriate test protocol for subsequent CSS tests of CMRR samples.

3.4.1 Cyclic Stress Ratio and Test Condition

A preliminary baseline estimate of cyclic stress ratio (CSR) equal to 0.155 was developed for the site using the average value of simplified procedures developed by Seed and Idriss (1982) and Seed et al. (2003). The estimated CSR was used in lieu of a site-specific value that may be later obtained from a detailed ground response analysis. In both simplified approaches, the CSR is based on a probabilistic seismic hazard assessment dominant earthquake magnitude of 6.0 with a peak horizontal ground surface acceleration of 0.33g. A calculation brief, which summarizes the results of both methods, is presented in Appendix F.

To capture expected uncertainty of the CSR value, we bracketed the tests by performing them at the following stress levels relative to the preliminary baseline estimate value:

- 5 cycles at 0.5 CSR
- 10 cycles at 1.0 CSR (Preliminary Baseline)
- 10 cycles at 2.0 CSR

Each sample was tested at these three cyclic stress levels to evaluate the variation in cyclic response and corresponding strain levels of interest.

The number of cycles for each of these three CSR values was based on an approximation of the average number of significant stress cycles that would be expected with the earthquake magnitude identified. A frequency of 0.25 hertz was used for all testing.

Copyright 2007, Kleinfelder

3.4.2 Initial CSS Test Phase

The initial test plan included four CSS tests to be performed on block samples of $Qbt3_L$ that were extracted from the TA-61 borrow pit. Isotropic and anisotropic tests series were performed on samples from blocks BS-13 and BS-16. Details of block sample trimming and preparation procedures are presented in Section 4.0 of the Appendix E report.

The estimated mean effective stress at the existing mid-point of the $Qbt3_L$ layer at CMRR was used as the basis for the test confining pressure. The samples were tested based on a depth of 102.5 feet below ground surface. The K_o values were initially selected to represent the range of possible lateral effective stress conditions at the site. For the isotropic tests (K_o = 1.0), the mean effective stress as this depth is approximately 9,400 psf. However, the confining pressure used was limited by the capacity of the testing apparatus to about 7,000 psf. The anisotropic companion tests were performed at a confining pressure of about 4,700 psf with a vertical deviatoric stress of about 4,700 psf, thus simulating a K_o = 0.5 condition. The results of these tests correspond to specimens LANL-2 through LANL-5, as summarized on Table 3.6.

The results of the tests indicated that anisotropically consolidated specimens developed considerably higher vertical strain (0.23 to 0.38 percent at 1.0 CSR) during cyclic loading than isotropically consolidated specimens (0.08 to 0.11 percent at 1.0 CSR). Both consolidation loading conditions resulted in considerable vertical strains prior to actual cyclic testing.

Copyright 2007, Kleinfelder

Table 3.6 - Summary of Cyclic Simple Shear Test Results

		Preparation Conditions				Test Conditions			Cyclic Test Results		
Specimen	Sample	Vert. stress psf	Lateral stress psf	Vert. strain (%)*	Dry density pcf**	Test	CSR	# cycles	Shear strain (%)	Approx. G (ksf)	Vert. Strain (%)
LANL-2	BS-13	9545	4657	2.15	86.2	Cyc 1	0.08	5	0.104	702	0.08
						Cyc 2	0.16	10	0.255	581	0.38
						Cyc 3	0.32	10	0.880	345	1.10
LANL-3	BS-13	7101	6892	1.05	83.7	Cyc 1	0.07	5	0.070	716	0.03
						Cyc 2	0.14	10	0.170	608	0.11
						Cyc 3	0.29	10	0.470	449	0.21
LANL-4	BS-16	7352	7018	0.8	82.4	Cyc 1	0.08	5	0.062	804	0.02
						Cyc 2	0.16	10	0.190	585	0.08
						Cyc 3	0.31	10	0.850	261	0.22
LANL-5	BS-16	9502	4657	1.33	86.2	Cyc 1	0.08	5	0.085	909	0.08
						Cyc 2	0.15	10	0.250	585	0.23
						Cyc 3	0.31	10	0.825	355	0.43
LANL-6	DSC-1, R-27	7122	6976	0.79	92.4	Cyc 1	0.08	5	0.137	432	0.04
						Cyc 2	0.17	10	0.460	265	0.09
						Cyc 3	0.35	10	1.210	201	0.23
LANL-7	DSC-1, R-27	9398	4699	1.43	83.7	Cyc 1	0.08	5	0.126	547	0.10
						Cyc 2	0.15	10	0.317	448	0.30
						Cyc 3	0.30	10	1.100	259	0.73
LANL-8	DSC-1, R-28	9712	4386	0.93	78.7	Cyc 1	0.07	5	0.107	652	0.07
						Cyc 2	0.15	10	0.260	545	0.26
						Cyc 3	0.29	10	0.750	374	0.67
LANL-9	DSC-1, R-28	8396	$k^*(\sigma_v)$	1.54	89.9	Cyc 1	0.08	5	0.119	547	0.09
						Cyc 2	0.15	10	0.300	426	0.23
						Cyc 3	0.30	10	0.860	297	0.80
EG-1	Ottawa Sand	5764	5514	0.21	103.6	Cyc 1	0.11	5	0.137	441	0.11
						Cyc 2	0.22	10	0.458	266	0.15
						Cyc 3	0.41	10	1.370	163	0.45
EG-2	Ottawa Sand	7310	3655	0.96	103.0	Cyc 1	0.11	5	0.080	927	0.23
						Cyc 2	0.21	10	0.230	627	0.64
						Cyc 3	0.37	10	0.658	407	1.21

* The net vertical strain calculated from the observed vertical deformation during static stress application, less the rebound during unloading

** Estimated values based on displaced volumes after testing, and including mass of expoxy, and Ottawa sand for LANL-9

Copyright 2007, Kleinfelder

3.4.3 Expanded CSS Test Phase

As introduced earlier, the initial testing utilized an alternative method to permit testing of the undisturbed samples. Cell confining pressure was used rather than a wire-wrapped membrane to attempt to simulate a K_o (zero lateral strain) condition. The outcome of this initial method was the realization that the lateral (radial) strain could not be measured and thus we could not resolve the components of vertical strain versus volumetric strain. We also could not evaluate which state of stress was applicable (isotropic or something less than isotropic).

To resolve these issues we performed an expanded CSS test program. The main focus of the expanded program was to utilize elastomeric gauges (EG) to monitor radial strain such that this component of the overall volumetric strain could be mathematically eliminated to provide a better measure of the one-dimensional vertical strain. The tests utilizing EGs would still be performed utilizing cell confining pressure to contain the sample and simulate the mean effective stress. Another type of test was also employed to attempt to return to the more standard method of CSS testing using a wire-wrapped membrane and thus attempt to produce a true K_o condition (zero lateral strain). This test still involved an intact sample of the $Qbt3_L$; however, the sample was milled to a slightly smaller diameter than the membrane to allow the membrane to be placed over the sample. Once this was accomplished, the annular space between the membrane and the sample was backfilled with Ottawa sand to establish positive contact between the sample and the inside wall of the membrane

Tests EG-1 and EG-2 were performed on Ottawa sand samples for calibration of the EGs, prior to testing with intact $Qbt3_L$ samples. The remaining four CSS tests were completed using samples from Pitcher tubes R-27 and R-28 from CMRR boring DSC-1. Details of the Pitcher tube sample trimming and preparation, as well as the application of EGs, are presented in Section 4.0 of the Appendix E report. The results of these tests are also summarized on Table 3.6.

Specimens LANL-6 and LANL-7, which were fitted with EGs, were tested at similar loading conditions as the block samples and exhibited vertical strains of 0.09 percent and 0.30 percent for isotropic and anisotropic loading conditions, respectively for the preliminary baseline CSR value (1.0 x CSR). The EG measurements during static loading indicated that the anisotropic

Copyright 2007, Kleinfelder

stress conditions resulted in a slightly dilative (radial bulging) behavior, while isotropic loading resulted in a slightly contractive behavior. LANL-8, also fitted with EGs, was performed by varying the lateral stress conditions during static loading to evaluate the ratio at which zero lateral strain occurs and thus develop an approximate measure of K_o. For this sample (Pitcher tube R28 of boring DSC-1), a stress ratio of about 0.45 was estimated for static conditions. A CSS test was performed at this stress ratio, resulting in 0.26 percent vertical strain at 1.0 CSR. The sample exhibited slight, but increasingly higher dilative behavior as the cyclic stress was increased.

The final test (LANL-9) was performed on the undersized sample placed inside the wire-wrapped membrane and backfilled with Ottawa sand. The results of this test are generally similar to those of the anisotropically consolidated tests, with a vertical strain of 0.23 percent at 1.0 CSR.

4 DISCUSSION OF RESULTS AND CONCLUSIONS

4.1 Sample Preparation

The special block test program was successful in retaining representative samples of $Qbt3_L$ in the TA-61 borrow pit. Although each of the testing laboratories reported challenges during the sample preparation phase of testing, all laboratories were ultimately able to satisfactorily prepare the samples. Successful methods of trimming included the use of hand saws and a soil lathe, as well as hydraulically pushing a test-size thin walled tube into the block specimen.

Kleinfelder was ultimately able to obtain undisturbed samples of $Qbt3_L$ at CMRR using large diameter Pitcher tubes. Similar techniques developed during the SBT program will be implemented during the production phase testing of the CMRR G/SIR.

4.2 Volume and Density Characteristics

Field and laboratory geotechnical tests were performed at all four source locations and resulted in similar test results. Average dry density values of the four sources ranged from 82.3 to 87.6 pcf. A summary of all sample dry density test results with respect to elevation for the four

Copyright 2007, Kleinfelder

sources is presented as Figure 4.1. Dry density values of samples extracted at depth from the CMRR site are within the range of values measured from near-surface samples of the canyon sites. As summarized in Table 3.3, the average specific gravity varied from 2.55 to 2.57 for all sources used. Based on measurements of density and specific gravity, sample void ratio and porosity were calculated and also exhibit good comparison between the four sources.

Figure 4.1 - Comparison of Dry Density at Sources A through D

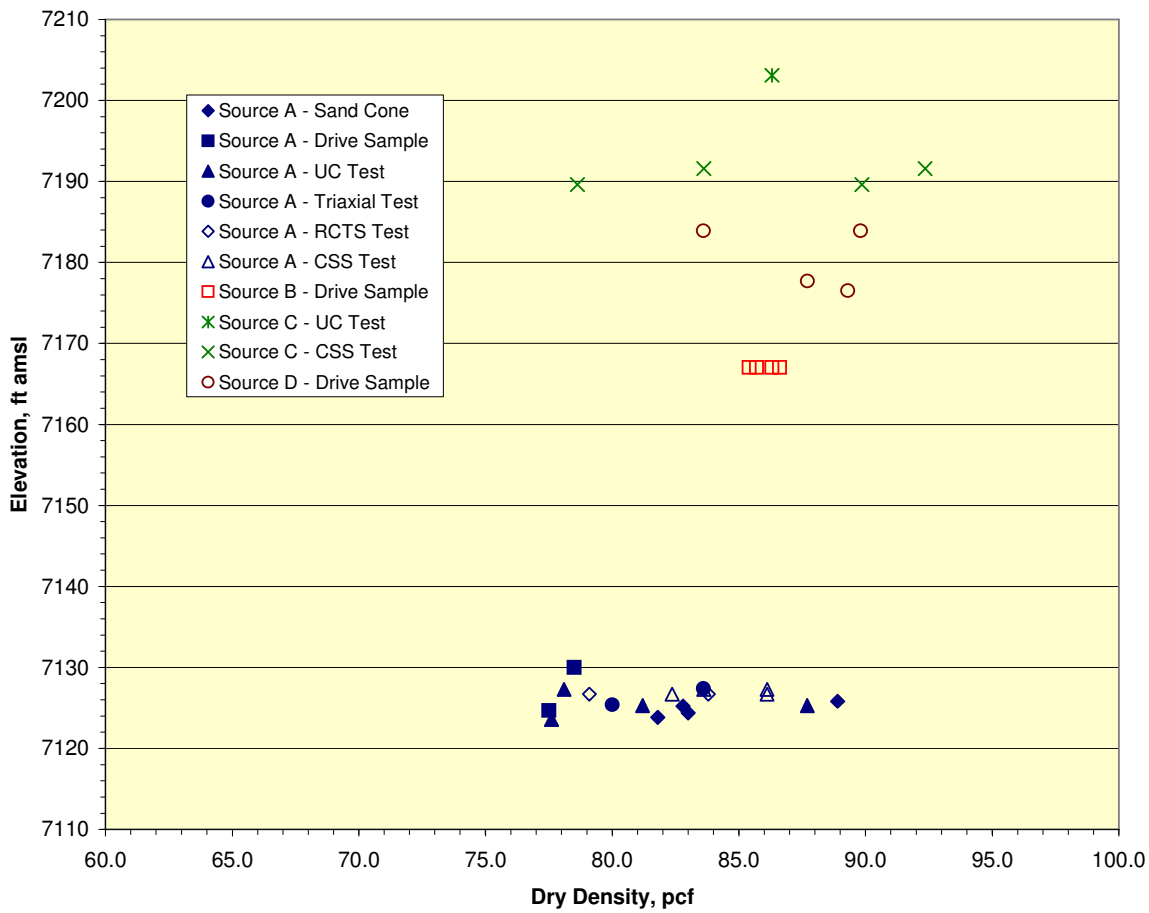

4.3 Gradation

Based on the completed particle size analyses at three of the four sources, the material consistently classified as a silty sand (SM). As indicated on Figure B.10, the gradational changes with respect to sieve size are also strikingly consistent across the sampling source locations.

4.4 Compressive Strength

$Qbt3_L$ exhibits extremely low rock strength values under unconfined conditions based on the limited quantity of $Qbt3_L$ strength data. The very weak particle bonding was broken at very low strains, about 1 to 3 percent, and resulted in UC values ranging from 562 to 2,108 psf. Consistent with the behavior of granular soils, the samples exhibited a significant increase in shear strength under lateral confinement. Triaxial compression tests performed at confining pressures of 6,300 and 9,400 psf, resulted in compressive strengths of 19,002 and 26,293 psf, respectively. Following the completion of additional compression tests in the G/SIR, Kleinfelder will further evaluate this relationship, including developing a modified Mohr-Coulomb failure envelope.

4.5 Dynamic Properties

Field and laboratory dynamic testing indicates that $Qbt3_L$ exhibits a relatively low shear velocity and corresponding shear modulus, both of which are affected by their state of stress (i.e., depth below ground surface). SASW testing at Source A resulted in shear velocity measurements that varied from about 300 ft/sec near the surface to about 750 ft/sec at a depth of 25 feet. As shown in Figure 18 and Figure 19 of Appendix C, which compare the SASW data to RC/TS data converted to an equivalent depth, the increase in shear velocity was also observed in the laboratory tests and matched reasonably well with the field data. The results of RC/TS tests in both the linear and non-linear stress ranges indicate that the dynamic properties of $Qbt3_L$ are comparable to published relationships of dry sand.

If the RC/TS data of the SBT study are extrapolated to the estimated depth and corresponding *in-situ* effective pressure at the CMRR site, V_s is in the range of the 900 to 1,050 ft/sec, which is

Copyright 2007, Kleinfelder

comparable to values measured in downhole geophysical surveys performed at the CMRR site. The RC/TS testing of the G/SIR will later be used for more detailed comparison.

4.6 Seismically Induced Compaction

CSS testing was performed to evaluate the potential for SIC of $Qbt3_L$ during and after seismic shaking. The evaluation of settlement due to static building loads and backfill will be performed by separate numerical modeling. The tests were completed on both block samples from Source A and Pitcher samples from the CMRR site. CSS tests of anisotropically loaded samples as well as a sample laterally confined by a wire-reinforced membrane resulted in a vertical strain of 0.23 to 0.38 percent at the estimated CSR of 0.155. Dr. Riemer reported these strains to be less than those measured by comparative tests of dense sands and compacted fills. Applying these vertical strains over the entire 50-foot-thick $Qbt3_L$ layer, we estimate that a range of about 1 to 2 inches of SIC is possible for 1.0 CSR. Higher strains and thus greater SIC are possible with higher levels of CSR. However, it is likely that some substantial portion of the strain observed is due to sample disturbance.

Based on the available test results, and considering the relatively small total strains measured, it is our opinion that the potential for collapse of the $Qbt3_L$ is highly unlikely during the maximum credible earthquake. This is based on limited data and evolving methodologies and procedures. To better evaluate SIC we recommend that production CSS tests be performed as planned. We also recommend that production testing be performed using the combination of under-reamed and backfilled samples in conjunction with the wire-wrapped membrane.

4.7 Conclusions

The basic field and laboratory testing data (Bulk Density, In-Place Density by Sand Cone and Drive Cylinder Method, Particle Size Analysis, Moisture Content, Specific Gravity, Void Ratio, Porosity) collected from the four separate sources generally compares well, showing relatively low spatial variability within $Qbt3_L$. We recommend that results of this study be used to supplement the database of the ongoing CMRR G/SIR.

Copyright 2007, Kleinfelder

The measured shear velocity profiles of *in-situ* seismic SASW testing, as well as laboratory RC/TS test results converted to a shear velocity-depth profile, compared similarly for the range of pressures tested. The measured linear and non-linear dynamic properties of $Qbt3_L$ also compared well to published relationships of dry sand. This relationship will be further developed by the results of the production RC/TS tests.

The results of CSS tests indicate that despite the low-density structure of $Qbt3_L$, relatively low vertical strains were recorded using the preliminary baseline CSR. We recommend that additional testing be performed throughout the $Qbt3_L$ vertical profile of the CMRR sample to further refine these initial results. We recommend that these tests be performed using the under-reamed sample/wire-reinforced membrane method to more easily achieve the zero lateral strain condition anticipated for *in-situ* earthquake conditions. Although comparable results were also obtained with samples prepared in an unreinforced membrane under anisotropic loading conditions, the uncertainty of maintaining the zero lateral strain condition can be eliminated with the wire-reinforced membrane.

5 LIMITATIONS

The recommendations contained in this report are based upon the field exploration, laboratory tests, and Kleinfelder's understanding of the proposed facility, its design, and construction. Subsurface data used in the preparation of this report were obtained from sampled material, as well as *in-situ* testing methods. It is anticipated that variations in the subsurface soil and tuff conditions may exist. The nature and extent of variations may not be evident until construction occurs.

This report was prepared in accordance with generally accepted standards of practice at the time the report was written. No warranty, expressed or implied, is made. It is the client's responsibility to see that all parties to the project, including the designer, contractor, subcontractors, etc., are made aware of this report in its entirety. The use of information contained in this report for design and construction bidding purposes should be done at the user's option and risk.

Copyright 2007, Kleinfelder

Other standards or documents referenced in any given standard cited in this report, or otherwise relied upon by the authors of this report, are only mentioned in the given standard; they are not incorporated into it or "included by reference" as that latter term is used relative to contracts or other matters of law.

This report may be used only by the client and only for the purposes stated, within reasonable time from the issuance. Land or facility use, site conditions (both on- and off-site), regulations, or other factors may change over time, and additional work may be required with the passage of time.

6 REFERENCES

American Society of Testing and Materials (ASTM), 2002, Standard test methods for specific gravity of soil solids using soil pycnometer, ASTM D 854-02.

American Society of Testing and Materials (ASTM), 2001, Standard test method for sieve analysis of coarse and fine aggregates, ASTM C 136-01.

American Society of Testing and Materials (ASTM), 2000, Standard test methods for amount of material in soils finer than the no. 200 sieve, method A," ASTM D 1140-00.

American Society of Testing and Materials (ASTM), 2000, Standard test method for density and unit weight of soil in place by the sand cone, ASTM D 1556-00.

American Society of Testing and Materials (ASTM), 2000, Density of soil in-place by the drive cylinder method, ASTM D 2937-00.

American Society of Testing and Materials (ASTM), 1995, Standard test method for triaxial compressive strength of undrained rock core specimens without pore pressure measurements, ASTM D 2664-95A.

American Society of Testing and Materials (ASTM), 1995, Unconfined compressive strength testing of intact rock core specimens, ASTM D 2938-95.

Bieniawski, Z.T., 1989, Engineering Rock Mass Calculations, Wiley, New York.

Broxton, D.E. and S.L. Reneau, 1995, Statigraphic nomenclature of the Bandelier tuff for the Environmental Restoration Project at Los Alamos National Laboratory, Los Alamos National Laboratory report LA-13010-MS, 21 pp.

Copyright 2007, Kleinfelder

Gardner, J.N., et al., 1999, Structural geology of the northwestern portion of Los Alamos National Laboratory, Rio Grande rift, New Mexico: Implications for seismic surface rupture potential from TA-3 to TA-55: Los Alamos National Laboratory report LA-13589-MS, 112 pp.

Hoek, E., 2000, Practical rock engineering course notes, http://www.rocscience.com/hoek/ PracticalRockEngineering.asp.

Houston, T.E., and C.J. Costantino, 2003, Site response sensitivity study for the CMRR facility.

Kleinfelder, Inc., 2005, Block sampling test plan, DCN 19435.SBT.16-ALB04WP001 Rev. 1, March 18, 2005.

Kleinfelder, Inc., 2004a, Density of soil in-place by the drive cylinder method, SOP 5901-14, Rev. 1.

Kleinfelder, Inc., 2004b, Estimation of cyclic shear ratio for CMRR calculation, Calculation No. 19435.SBT.16ALB04CA001, Rev. 0.

Kleinfelder, Inc., 2004c, Sampling labeling, handling and transport, SOP-5901-8, Rev. 4.

Kleinfelder, Inc., 2004d, Spectral analysis of surface waves (SASW) plan, DCN 19435.SBT.17-ALB04WP001 Rev. 0.

Lewis, C.J., R.G. Warren, J.N. Gardner, S.Chipera, and A.Lavine, 2005, Petrographic and geochemical analyses of Bandelier tuff unit Qbt3 from boreholes at the Chemistry and Materials Research Replacement Site and nearby outcrops, Los Alamos National Laboratory, New Mexico: Los Alamos National Laboratory report LA-UR-05-3841, 64 pp.

Los Alamos National Laboratory, 2004a, Block Sampling Plan, CMR Replacement Project: Los Alamos National Laboratory plan CMRR-PLAN-013, Revision 0.

Los Alamos National Laboratory, 2004b, Block Sampling Quality Procedure, CMR Replacement Project: Los Alamos National Laboratory report CMRR-QA-010, Revision 1.

Merrick & Company, 1995, Engineering report on the properties and characteristics of volcanic tuff at the Los Alamos National Laboratory.

Seed, H.B. and I.M. Idriss, 1982, Ground motions and soil liquefaction during earthquakes, Earthquake Engineering Research Institute.

Seed, R.B., et al., 2003, Recent advances in soil liquefaction engineering – a unified and consistent framework, 26th Annual ASCE Geotechnical Spring Seminar.

University of California, Berkeley (UCB), 2004, Cyclic simple shear testing to evaluate likely seismic response of volcanic tuff, Procedure 018420-PROC-04, Rev. 1.

University of Texas at Austin (UT), 2004, Spectral-analysis-of-surface-waves (SASW) method at Los Alamos National Laboratory."

Copyright 2007, Kleinfelder

University of Texas at Austin (UT), 2000, Technical procedures for resonant column and torsional shear testing of soil and rock samples, Procedure PBRCTS-1 Rev. 4.

Woodward Clyde Federal Services (WCFS), 1995, Seismic hazards evaluation of the Los Alamos National Laboratory.

Copyright 2007, Kleinfelder

Appendix A

Area of Investigation

Figure A.1 – Facility Map Showing Investigation Areas
Figure A.2 – Bandelier Tuff Nomenclature
Plate A.3 – Geologic and Geomechanical Glossary of Terms
Figures A.4 through A.13 – Special Block Test Photographs
Table A.1 – Summary of Sample Locations

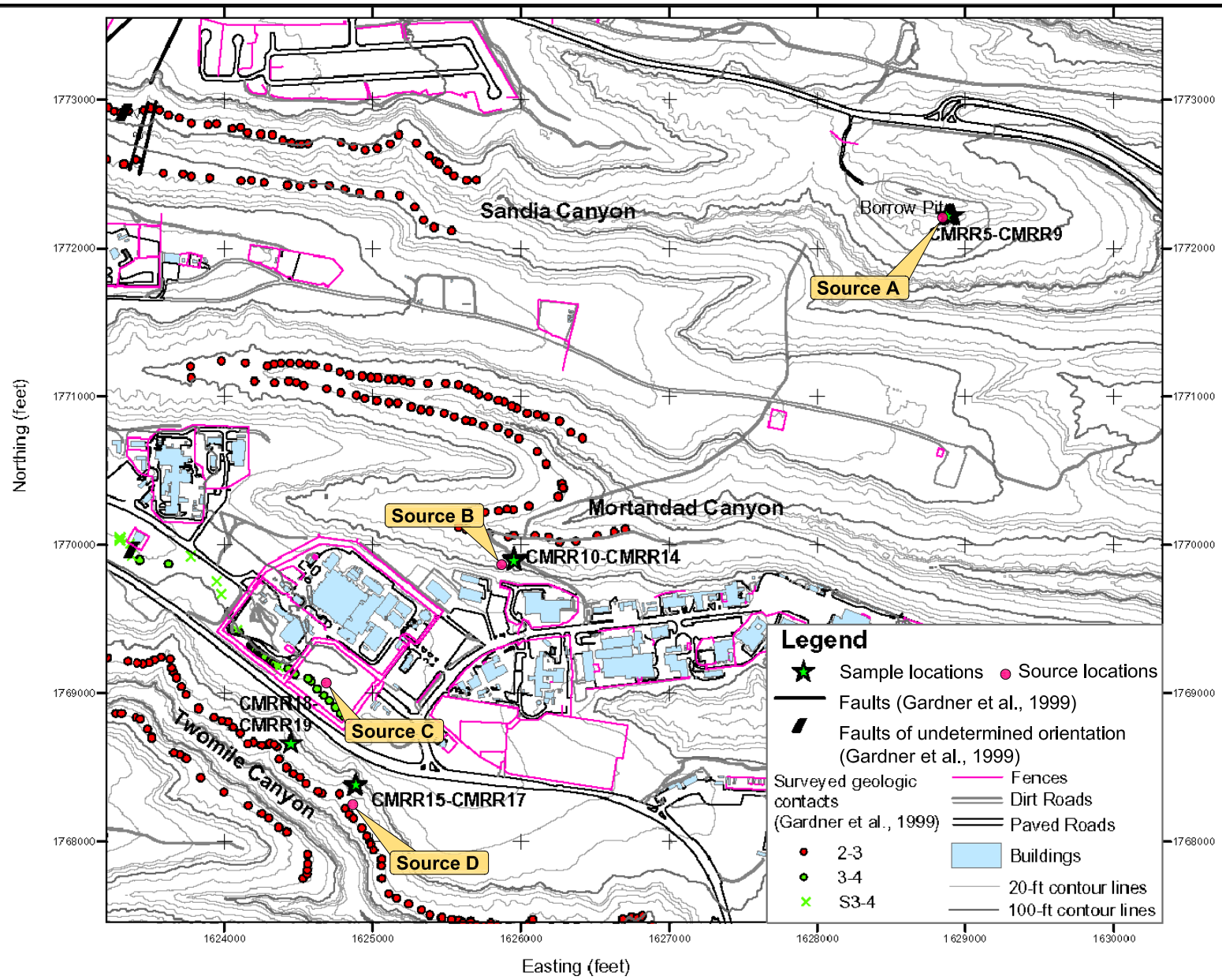

Notes:
1. Map showing the area of investigation for the special block tests, CMRR project. Surveyed geologic contacts and faults are from Gardner et al. (1999). Contour interval=20 ft. Grid is in the State Plane Coordination System (feet), New Mexico Central Zone, NAD83.
2. Source: Lewis, C.J., R.G. Warren, J.N. Gardner, S.Chipera, and A.Lavine, 2005, Petrographic and geochemical analyses of Bandelier tuff unit Qbt3 from boreholes at the Chemistry and Materials Research Replacement Site and nearby outcrops, Los Alamos National Laboratory, New Mexico: Los Alamos National Laboratory report LA–UR–05–3841, 64 pp.

KLEINFELDER

Drawn By: C. Landon	Date: May 2007
Project No.: 19435	Drawing No.:19435_204_0.dwg
Scale: None	Drawing Category: A

FACILITY MAP SHOWING INVESTIGATION AREAS
Chemistry & Metallurgical Research Replacement Project
Los Alamos National Laboratory
Los Alamos, New Mexico

FIGURE
A.1

G:\Geotech\Projects\19435 CMRR\4.0\Special Block Test\Figures\Rev 0\19435_204_0.dwg

Copyright 2007, Kleinfelder

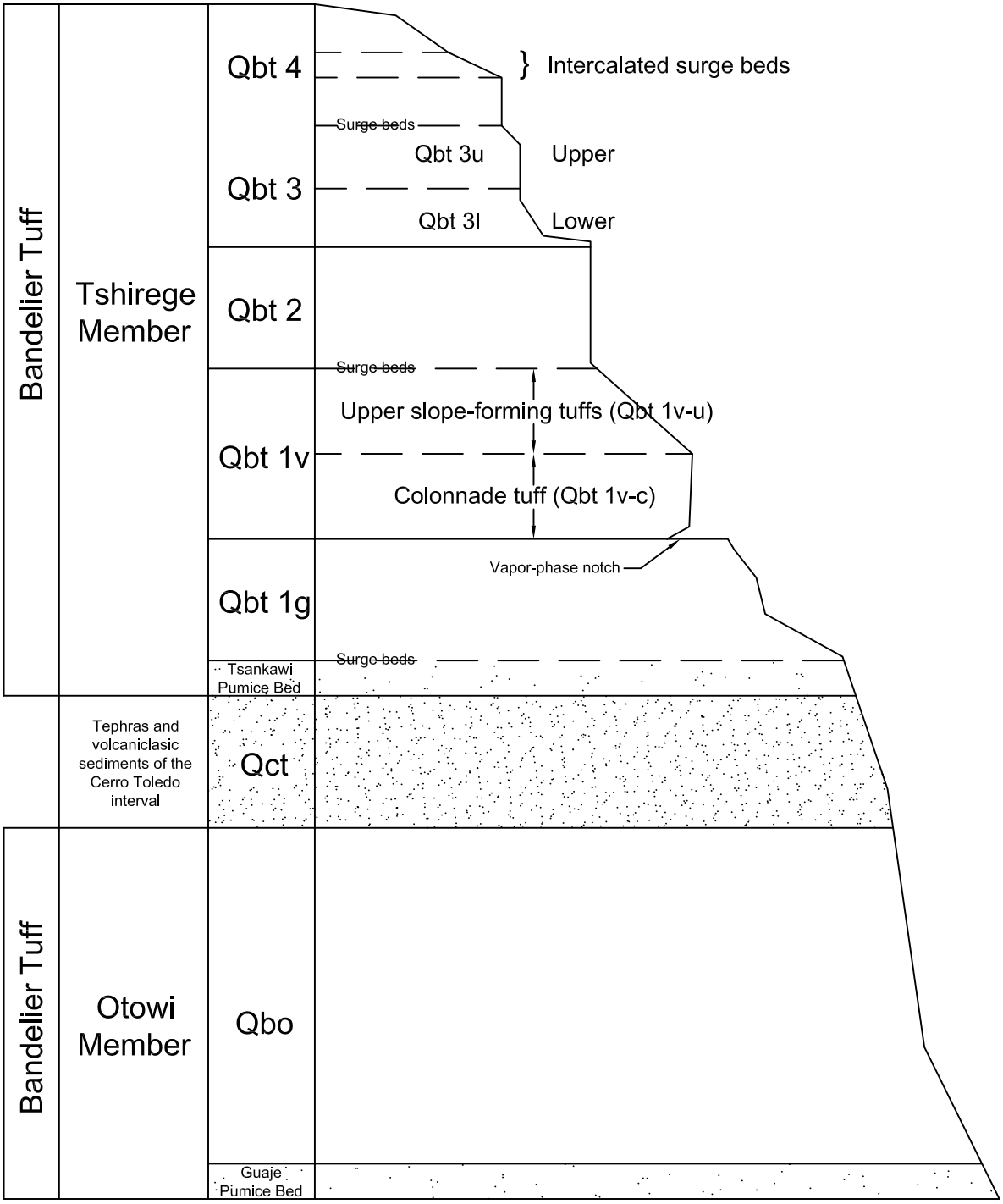

KLEINFELDER		BANDELIER TUFF NOMENCLATURE Chemistry & Metallurgical Research Replacement Project Los Alamos National Laboratory Los Alamos, New Mexico	FIGURE A.2
Drawn By: C. Landon	Date: May 2007		
Project No.: 19435	Drawing No.:19435_205_0.dwg		
Scale: None	Drawing Category: A		

G:\Geotech\Projects\19435 CMRR\v4.0\Special Block Test\Figures\Rev 0\19435_205_0.dwg

PLATE A.3 – GEOLOGIC AND GEOMECHANICAL GLOSSARY OF TERMS

Ash – pyroclastic material generally under 4 mm in size

Fill – soil or broken tuff material used to raise or restore ground surface

Lithic – rock fragment included in the tuff derived from an earlier geologic process

Mafics – iron/magnesium-rich minerals such as pyroxene

Mechanical fractures – fractures or breaks in the tuff due to the mechanical process of collecting the samples; i.e., not naturally occurring fractures

N/R – no recovery

Organics – vegetable matter, including roots

Phenocrysts – larger individual mineral crystals in a finer-grained matrix

Pumice – highly vesicular volcanic glass

Pyroclastic – Mineral fragments ejected into the air from volcanic eruptions and deposited as ashfalls or ashflows

Pyroxene – mafic silicate mineral

Qbt3 – Unit 3 of the Tshirege Member of the Bandelier Tuff of Quaternary age

Qbt4 – Unit 4 of the Tshirege Member of the Bandelier Tuff of Quaternary age

Quartz – naturally occurring crystalline form of silica

RMR – Rock Mass Rating (Bieniawski, 1989). A system that rates a rock mass using strength, RQD, joint (fracture) spacing, joint condition, and groundwater conditions. Total RMR rating can range from a low of 8 to the highest (best) rating of 100. Orientation of joints can also be considered, as appropriate.

RQD – Rock Quality Designation. A means of characterizing rock mass quality of tuff core, expressed as the ratio (percentage) of the sum of the lengths of all pieces of sound rock core greater than 4 inches divided by the total length of the run. In calculating the sum of pieces to be counted, only natural geologic fractures are considered; mechanical breaks caused by drilling or handling are disregarded. For the purposes of the CMRR project, rock is sound if it withstands squeezing by hand. This standard is substantially lower than that usually applied to evaluating rock soundness in RQD evaluations.

Copyright 2007, Kleinfelder

PLATE A.3 – GEOLOGIC AND GEOMECHANICAL GLOSSARY OF TERMS (CONT.)

Sanidine – feldspathic silicate mineral with a characteristic bluish play of colors.

Strength – Ability of material to withstand stress with rupture.

Tuff – indurated pyroclastic ash consisting of grains generally finer than 4 mm. In this study, the term tuff is used to include the ashy matrix, as well as the pumice, lithic fragments, and phenocrysts.

Weathering – chemical or mechanical degradation of tuff and constituent minerals over time. Descriptive terms are fresh (FR), slightly (SL), moderately (MOD), and very highly (H) weathered.

Welding – process that promotes the union or cohesion of glassy fragments by thermal fusion and/or vapor-phase mineralization after deposition and subsequent cooling of tuff.

Terminology for *In-situ* Tuff

General Property	Descriptive Term	Visual or Physical Properties
Weathering	Very Weathered	Abundant fractures coated with oxides, carbonates, sulfates, mud, etc., thorough discoloration, rock disintegration, mineral decomposition.
	Moderately Weathered	Some fracture coating, moderate or localized discoloration, little to no effect on cementation, slight mineral decomposition.
	Slightly Weathered	A few stained fractures, slight discoloration, little to no effect on cementation, no mineral decomposition.
	Fresh	Unaffected by weathering agents, no appreciable change with depth.
Fracturing	Intensely Fractured	Less than 1" spacing
	Very Fractured	1" to 6" spacing
	Moderately Fractured	6" to 12" spacing
	Slightly Fractured	12" to 36" spacing
	Solid	36" spacing or greater
Stratification	Thinly Laminated	Less than 1/10"
	Laminated	1/10" to 1/2"
	Very Thinly Bedded	1/2" to 2"
	Thinly Bedded	2" to 2 feet
	Thickly Bedded	more than 2 feet

Copyright 2007, Kleinfelder

PLATE A.3 – GEOLOGIC AND GEOMECHANICAL GLOSSARY OF TERMS (CONT.)

Terminology for *In-situ* Tuff (Cont.)

Hardness	Soft	Can be dug by hand and crushed by fingers.
	Moderately Hard	Friable, can be gouged deeply with knife and will crumble readily under light hammer blows.
	Hard	Knife scratch leaves dust trace, will withstand a few hammer blows before breaking.
	Very Hard	Scratched with knife with difficulty, difficult to break with hammer blows.
Welding	Poorly Welded Tuffs (non-welded to partially welded tuffs in some literature)	Poorly to non-indurated and easily crumbled into flour-like. Some zones display some strength and may produce intact core with short lengths. Some core produces thin wafers that are friable and easily broken by hand. The core is lightweight and very low density. The pumices have significant void space within the pumice structures. Pumices that survive the drilling are open, not elongated. Pumice aspect ratios are roughly equant to 2:1.
	Moderately Welded Tuffs	Appear to be moderately indurated and break readily with light hammer blows. Pumices are elongated with some appearance of structure. Approximate pumice aspect ratios are 2:1 to 6:1. Generally, the core remains intact for lengths of several inches to feet.
	Strongly Welded Tuffs	Strongly indurated and have pumice aspect ratios of roughly >6:1. Generally, the core remains intact, solid, and dense with flattening of pumices such that little evidence of the pumices may remain. Strongly welded tuffs are not often encountered. They require hammers to break apart core, and also require air rotary drilling to obtain sample.

Copyright 2007, Kleinfelder

Photo No. 1 - Block extraction site, near south cut slope of TA-61 Borrow Pit

Photo No. 2 - Preparation of block extraction area with backhoe bucket

KLEINFELDER		SPECIAL BLOCK TEST PHOTOGRAPHS Chemistry & Metallurgical Research Replacement Project Los Alamos National Laboratory Los Alamos, New Mexico	FIGURE **A.4**
Drawn By: C. Landon	Date: May 2007		
Project No.: 19435	Drawing No.:19435_206_0.dwg		
Scale: None	Drawing Category: A		

G:\Geotech\Projects\19435 CMRR\4.0\Special Block Test\Figures\19435_206_0.dwg

Photo No. 3 - Lateral cuts excavated by trenching machine, positioned on wooden planks

Photo No. 4 - Laborer trimming block pedestal with hand saw

KLEINFELDER		SPECIAL BLOCK TEST PHOTOGRAPHS Chemistry & Metallurgical Research Replacement Project Los Alamos National Laboratory Los Alamos, New Mexico	FIGURE **A.5**
Drawn By: C. Landon	Date: May 2007		
Project No.: 19435	Drawing No.:19435_207_0.dwg		
Scale: None	Drawing Category: A		

G:\Geotech\Projects\19435 CMRR\4.0\Special Block Test\Figures\Rev 0\19435_207_0.dwg

Photo No. 5 - Excavated pedestal of Qbt3L tuff

Photo No. 6 - Excavated pedestal of Qbt3L tuff
(Notice the crack and sloughing of front right corner)

KLEINFELDER		**SPECIAL BLOCK TEST PHOTOGRAPHS** Chemistry & Metallurgical Research Replacement Project Los Alamos National Laboratory Los Alamos, New Mexico	FIGURE **A.6**
Drawn By: C. Landon	Date: May 2007		
Project No.: 19435	Drawing No.:19435_208_0.dwg		
Scale: None	Drawing Category: A		

G:\Geotech\Projects\19435 CMRR\4.0\Special Block Test\Figures\Rev 0\19435_208_0.dwg

Photo No. 7 - Tuff pedestal being wrapped with clear plastic, prior to placement of box around pedestal

Photo No. 8 - Placement of joint compound in annulus between tuff pedestal and box

KLEINFELDER		SPECIAL BLOCK TEST PHOTOGRAPHS Chemistry & Metallurgical Research Replacement Project Los Alamos National Laboratory Los Alamos, New Mexico	FIGURE **A.7**
Drawn By: C. Landon	Date: May 2007		
Project No.: 19435	Drawing No.:19435_209_0.dwg		
Scale: None	Drawing Category: A		

G:\Geotech\Projects\19435 CMRR\4.0\Special Block Test\Figures\Rev 0\19435_209_0.dwg

Photo No. 9 - 5g and 10g shock indicators placed on sample box after lid screwed into top of box

Photo No. 10 - Bottom of block sample after It Is detached from pedestal by hand saw

KLEINFELDER		SPECIAL BLOCK TEST PHOTOGRAPHS Chemistry & Metallurgical Research Replacement Project Los Alamos National Laboratory Los Alamos, New Mexico	FIGURE **A.8**
Drawn By: C. Landon	Date: May 2007		
Project No.: 19435	Drawing No.:19435_210_0.dwg		
Scale: None	Drawing Category: A		

G:\Geotech\Projects\19435 CMRR\4.0\Special Block Test\Figures\Rev 0\19435_210_0.dwg

Photo No. 11 - Block sample encased in bubble wrap and placed on foam sheet for transport

Photo No. 12 - Drive cylinder sampling at Source B (Mortandad Canyon)

KLEINFELDER		SPECIAL BLOCK TEST PHOTOGRAPHS Chemistry & Metallurgical Research Replacement Project Los Alamos National Laboratory Los Alamos, New Mexico	FIGURE **A.9**
Drawn By: C. Landon	Date: May 2007		
Project No.: 19435	Drawing No.:19435_211_0.dwg		
Scale: None	Drawing Category: A		

G:\Geotech\Projects\19435 CMRR\4.0\Special Block Test\Figures\Rev 0\19435_211_0.dwg

Photo No. 13 - Close-up of drive cylinder sample prior to extraction from Source B road cut wall

Photo No. 14 - SASW survey TA-61-3 at Source A

KLEINFELDER		**SPECIAL BLOCK TEST PHOTOGRAPHS** Chemistry & Metallurgical Research Replacement Project Los Alamos National Laboratory Los Alamos, New Mexico	FIGURE **A.10**
Drawn By: C. Landon	Date: May 2007		
Project No.: 19435	Drawing No.:19435_212_0.dwg		
Scale: None	Drawing Category: A		

G:\Geotech\Projects\19435 CMRR\4.0\Special Block Test\Figures\Rev 0\19435_212_0.dwg

Photo No. 15 - SASW testing into road cut wall in Mortandad Canyon (Source B)

Photo No. 16 - Trimming of unconfined compression sample using hand saws

KLEINFELDER		SPECIAL BLOCK TEST PHOTOGRAPHS Chemistry & Metallurgical Research Replacement Project Los Alamos National Laboratory Los Alamos, New Mexico	FIGURE **A.11**
Drawn By: C. Landon	Date: May 2007		
Project No.: 19435	Drawing No.:19435_213_0.dwg		
Scale: None	Drawing Category: A		

G:\Geotech\Projects\19435 CMRR\4.0\Special Block Test\Figures\Rev 0\19435_213_0.dwg

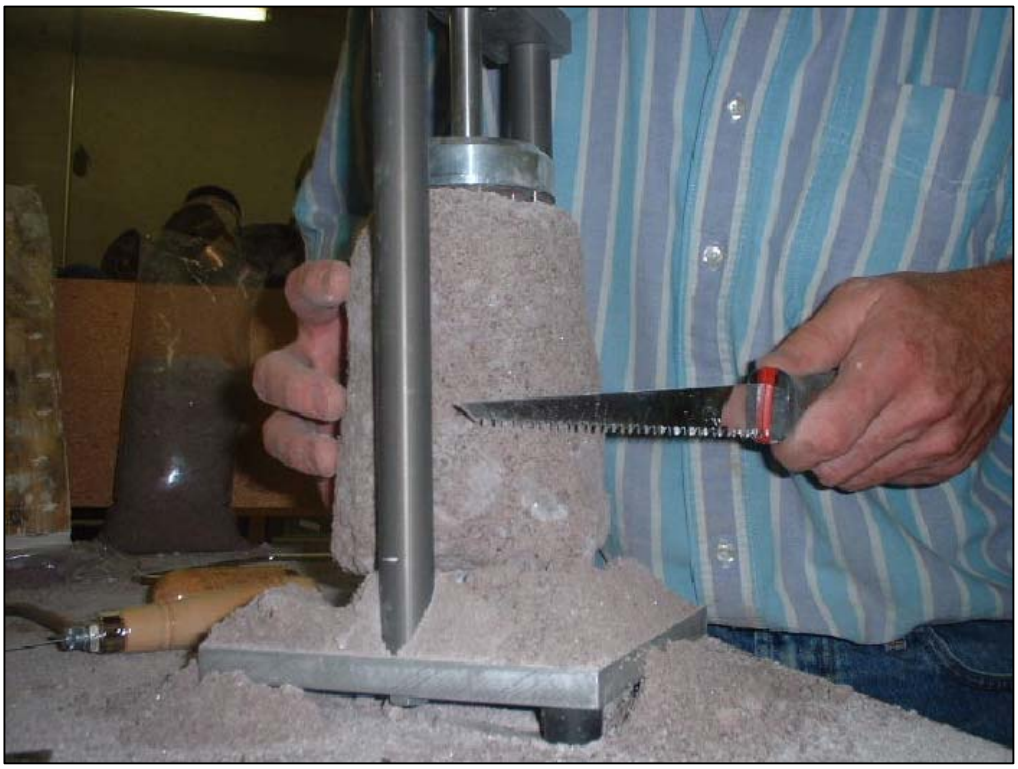

Photo No. 17 - Using hand saw and soil lathe to trim unconfined compression sample into cylindrical shape

Photo No. 18 - Unconfined compression test of tuff near start of loading

KLEINFELDER		SPECIAL BLOCK TEST PHOTOGRAPHS Chemistry & Metallurgical Research Replacement Project Los Alamos National Laboratory Los Alamos, New Mexico	FIGURE **A.12**
Drawn By: C. Landon	Date: May 2007		
Project No.: 19435	Drawing No.:19435_214_0.dwg		
Scale: None	Drawing Category: A		

G:\Geotech\Projects\19435 CMRR\4.0\Special Block Test\Figures\Rev 0\19435_214_0.dwg

Photo No. 19 - Unconfined compression test of tuff after failure

KLEINFELDER		SPECIAL BLOCK TEST PHOTOGRAPHS Chemistry & Metallurgical Research Replacement Project Los Alamos National Laboratory Los Alamos, New Mexico	FIGURE **A.13**
Drawn By: C. Landon	Date: May 2007		
Project No.: 19435	Drawing No.:19435_215_0.dwg		
Scale: None	Drawing Category: A		

G:\Geotech\Projects\19435 CMRR\4.0\Special Block Test\Figures\Rev 0\19435_215_0.dwg

TABLE A.1
SUMMARY OF SAMPLE LOCATIONS

Sample Number	Sample Survey Location Coordinates and Elevations			Remarks
	Northing (ft)	Easting (ft)	Elevation (amsl ft)	
Block Samples (Source A)[1]				
Test Block	1772226	1628870	7123.6	Elevation taken at base of sample
BS-1	1772227	1628884	7125.4	Elevation taken at top of sample
BS-2	1772225	1628884	7125.3	Elevation taken at top of sample
BS-3	1772224	1628884	7125.2	Elevation taken at top of sample
BS-4	1772225	1628885	7125.4	Elevation taken at top of sample
BS-5	1772224	1628885	7125.4	Elevation taken at top of sample
BS-6	1772228	1628887	7125.6	Elevation taken at top of sample
BS-7	1772226	1628887	7125.7	Elevation taken at top of sample
BS-8	1772225	1628888	7125.6	Elevation taken at top of sample
BS-9	1772228	1628890	7125.9	Elevation taken at top of sample
BS-12	1772229	1628908	7127.3	Elevation taken at top of sample
BS-13	1772228	1628909	7127.5	Elevation taken at top of sample
BS-14	1772226	1628909	7127.4	Elevation taken at top of sample
BS-15	1772228	1628904	7126.7	Elevation taken at top of sample
BS-16	1772226	1628905	7126.7	Elevation taken at top of sample
SASW, Center Point of Test Array (Source A)[1]				
TA-61-1	1772222	1629014	7127.5	Elevation taken at surface
TA-61-2	1772226	1629025	7130.7	Elevation taken at surface
TA-61-3	1772233	1629098	7146.5	Elevation taken at surface
SASW, Center Point of Test Array (Source B)[2]				
Mortandad Canyon	1769912	1625959	7165	Near CMRR-10 sample
Sand Cone Density Tests (Source A)[1]				
BS-5	1772224	1628887	7123.9	Elevation estimated, assuming 1.5 ft below top of block survey elevation
BS-9	1772229	1628908	7124.4	Elevation estimated, assuming 1.5 ft below top of block survey elevation
BS-16	1772226	1628905	7125.2	Elevation estimated, assuming 1.5 ft below top of block survey elevation
BS-12	1772229	1628908	7125.8	Elevation estimated, assuming 1.5 ft below top of block survey elevation
Drive Cylinder Samples (Source A)[1]				
TA-61-1A	1772220	1629005	7124.7	10 ft west of TA-61-1 SASW center
TA-61-1B	1772225	1629023	7130.0	10 ft east of TA-61-1 SASW center

TABLE A.1 (CONT.)
SUMMARY OF SAMPLE LOCATIONS

Sample Number	Sample Survey Location Coordinates and Elevations			Remarks
	Northing (ft)	Easting (ft)	Elevation (amsl ft)	
Drive Cylinder Samples (Source B)[2]				
MC-1	1769916	1625956	7164	Near CMRR-11 sample
MC-2	1769910	1625956	7165	Near CMRR-10 sample
MC-3	1769912	1625959	7166.7	Near CMRR-12 sample
MC-4	1769906	1625955	7168.1	Near CMRR-14 sample
Drive Cylinder Samples (Source D)[2]				
TMC-1	1768396	1624890	7183.9	1 ft south of CMRR-17 sample
TMC-2	1768384	1624885	7177.7	1 ft southwest of CMRR-16 sample
TMC-3	1768385	1624881	7176.5	1 ft south of CMRR-15 sample
TMC-4	1768396	1624890	7183.9	2 ft north of CMRR-17 sample
Large Diameter Pitcher Sample[1]				
DSC-1	1769120	1624740	7203.6	91.0 ft to top of sample
Mapped Contact (Source A)[1]				
Qbt2/Qbt 3 Contact	1771907	1628702	7104.5	Sandia Canyon contact, near TA-61 borrow pit, staked by LANL EES-9
Deep Seismic Borings (Source C)[1]				
DSC-1A	1769131	1624750	7161.4	Estimated Qbt2/ Qbt3 contact
DSC-1B	1769117	1624755	7161.8	Estimated Qbt2/ Qbt3 contact
DSC-2	1769148	1625263	7154.9	Estimated Qbt2/ Qbt3 contact
DSC-2A	1769121	1625220	7155.1	Estimated Qbt2/ Qbt3 contact

[1] Survey information performed by KSL and provided by LANL
[2] Survey information, as presented by Lewis et al. (2005)

Appendix B

Summary of Kleinfelder Field and Laboratory Test Results

Figure B.1 – Density and Unit Weight of Soil In Place by Sand Cone Method

Figures B.2 through B.4 – Density of Soil In Place by Drive Cylinder Method

Figures B.5 through B.8 – Unconfined Compression Test Results (With Stress-Strain Plots)

Figure B.9 – Unconfined Compression Test Results (Without Stress-Strain Plot)

Figure B.10 – Grain Size Distribution

Table B.1 – Summary of Specific Gravity Tests and Particle Size Analyses

FIGURE B.1 - DENSITY AND UNIT WEIGHT OF SOIL IN PLACE BY SAND-CONE METHOD (ASTM D1556)

Project Name:	CMRR - Special Block Test	Project Number:	19435
Project Manager:	John North	Project Task Number:	SBT.15
Cone Number:	95	Plate Number: A1	Date Test Performed: 5/6/2004

		Test 1	Test 2	Test 3	Test 4
Test Number:		Test 1	Test 2	Test 3	Test 4
Site Plan Reference:		TA-61	TA-61	TA-61	TA-61
Test Location:		Borrow Pit Area Test Location 5	Borrow Pit Area Test Location 9	Borrow Pit Area Test Location 16	Borrow Pit Area Test Location 12
Test Elevation:		7123.9	7124.4	7125.2	7125.8
Jar Identification:		A	2	C	D
	Embedded Calculation				
REFERENCE SAND: (1) Initial Weight Reference Sand & Tare (Grams)	Enter value	5463.4	5694.5	5581.1	5785.3
(2) Final Weight Reference Sand & Tare (Grams)	Enter value	2568.4	2892.0	2582.5	2947.2
(3) Gross Weight Reference Sand Used (Grams)	(1) - (2)	2895.0	2802.5	2998.6	2838.1
(4) Correction for Cone (Grams)	Enter value	1633.0	1633.0	1633.0	1633.0
(5) Net Weight Reference Sand Used (Grams)	(3) - (4)	1262.0	1169.5	1365.6	1205.1
(6) Density Reference Sand (Pounds/Cu-Ft)*	Enter value	87.07	87.07	87.07	87.07
TESTED SOIL: (7) Wet Weight Tested Soil and Tare (Grams)	Enter value	1481.8	1387.3	1535.4	1501.6
(8) Weight Tare (Grams)	Enter value	223.7	221.6	176.9	212.7
(9) Wet Weight Tested Soil (Grams)	(7) - (8)	1258.1	1165.7	1358.5	1288.9
(10) Wet Density Tested Soil (P.C.F.)	[(6)*(9)]/(5)	86.80	86.79	86.62	93.12
(11) Dry Weight Tested Soil and Tare (Grams)	Enter value	1409.2	1337.5	1475.2	1442.0
(12) Dry Weight Tested Soil (Grams)	(11) - (8)	1185.5	1115.9	1298.3	1229.3
(13) Water Weight (Grams)	(9) - (12)	72.6	49.8	60.2	59.6
(14) In-Place Moisture Content	(13) / (12)	0.061	0.045	0.046	0.048
(15) In-Place Moisture Content (Percent)	(14)*100	6.1%	4.5%	4.6%	4.8%
(16) Dry Density Tested Soil (P.C.F.)	(10) / [1+ (14)]	81.8	83.0	82.8	88.9
(17) Laboratory Maximum Dry Density (P.C.F.)	Enter value	N/A	N/A	N/A	N/A
(18) Maximum Dry Density (Percent)	[(16) / (17)]*100	N/A	N/A	N/A	N/A

* See test records for Reference Sand, Laboratory Number 04-113

Acceptance Criteria: Maximum Dry Density in Percent (18) shall be equal to or greater than: NA % and In-place Moisture Content in Percent (15) shall be equal to NA +/- NA %

Comments: None

Lab Technician: Jesse Carlin / JDL FOR JC / 5/6/04
Print Name / Signature / Date

Checked By: Joe Laird / / 6/14/04
Print Name / Signature / Date

Kleinfelder Inc., 8300 Jefferson NE Suite B, Albuquerque, NM 87113 KA Form ASTM D1556, Rev 0

Copyright 2007, Kleinfelder

FIGURE B.2 - SOURCE A DENSITY OF SOIL IN PLACE BY THE DRIVE-CYLINDER METHOD (ASTM D2937-00)

Project Name	CMRR - SBT	Project Number	19435
Project Location	TA-61, E. JEMEZ ROAD BORROW PIT	Project Task Number	SBT.14
Project Manager	J. NORTH	Field Sampling Date	12/9/2004

Sample Number			TA-61-1	TA-61-2		
Test Location			TA-61-1 SASW, 10' WEST OF CENTER	TA-61-1 SASW, 10' EAST OF CENTER		
Test Elevation			7224.7	7130.0		
		Embedded Calculation				
DRIVE CYLINDER DATA	(1) Drive Cylinder Identification Number	Enter value	C-1	C-7		
	(2) Cylinder Tare Weight + Pan (grams)	Enter value	775.0	777.0		
	(3) Cylinder Diameter, Avg of 4 meas. (in.)	Enter value	3.82	3.83		
	(4) Cylinder Height (in.)	Enter value	4.71	4.28		
	(5) Cylinder Volume (in.^{3})	$\pi * [(3)^2/4] * (4)$	53.93	49.28		
SAMPLING NOTES	(6) No. of Blows to Drive 1/2" Below Surface	Enter value	52	32		
	(7) Sample Conditions (Disturbed?, Flush?)	Enter Description	0.146" at top and 0.148" at bottom reamed to even depth	Flush at top of material fell out of bottom, reamed to 0.713"		
	(8) Sample Description	Enter Description	Light gray tuff, very hard at base	Light gray tuff, some to trace pumice		
TESTED SOIL	(9) Wet Weight Tested Soil and Tare (Grams)	Enter value	1947.2	1871.5		
	(10) Wet Weight Tested Soil (Grams)	(9) - (2)	1172.3	1094.5		
	(11) Wet Density Tested Soil (lb/ft^3)	[(10)/(5)]*3.81	82.8	84.6		
	(12) Dry Weight Tested Soil and Tare (Grams)	Enter value	1871.7	1791.6		
	(13) Dry Weight Tested Soil (Grams)	(12) - (2)	1096.8	1014.6		
	(14) Water Weight (Grams)	(10) - (13)	75.5	79.9		
	(15) In-Place Moisture Content	(14) / (13)	0.069	0.079		
	(16) In-Place Moisture Content (Percent)	(15)*100	6.9%	7.9%		
	(17) Dry Density Tested Soil (lb/ft^3)	(11) / [1+ (15)]	77.5	78.5		
	(18) Laboratory Maximum Dry Density (lb/ft^3)	Enter value	N/A	N/A		
	(19) Maximum Dry Density (Percent)	[(17) / (18)]*100	N/A	N/A		

Acceptance Criteria: Maximum Dry Density in Percent (19) shall be equal to or greater than: N/A % and In-place Moisture Content in Percent (16) shall be equal to N/A +/- N/A %

Comments: Cylinder height and weight adjusted for volume calculation where retained sample not flush

Lab Testing Technician: Jesse Carlin / JC for JC / 12/14/04
Print Name / Signature / Date

Checked By: Joe Laird / [signature] / 12/22/04
Print Name / Signature / Date

Kleinfelder Inc., 8300 Jefferson NE Suite B, Albuquerque, NM 87113

KA Form ATSM D2937, Rev 0

FIGURE B.3 - SOURCE B DENSITY OF SOIL IN PLACE BY THE DRIVE-CYLINDER METHOD (ASTM D2937-00)

Project Name	CMRR - SBT	Project Number	19435
Project Location	Mortandad Canyon, LA	Project Task Number	SBT.14
Project Manager	J. NORTH	Field Sampling Date	12/15/2004

			MC-1	MC-2	MC-3	MC-4
Sample Number			MC-1	MC-2	MC-3	MC-4
Test Location			Near CMRR-11 sample	Near CMRR-10 sample	Near CMRR-12 sample	Near CMRR-14 sample
Test Elevation			7164	7165	7166.7	7168.1
		Embedded Calculation				
DRIVE CYLINDER DATA	(1) Drive Cylinder Identification Number	Enter value	C-9	C-11	C-10	C-16
	(2) Cylinder Tare Weight + Pan (grams)	Enter value	921.3	919.1	914.6	1143.8
	(3) Cylinder Diameter, Avg of 4 meas. (in.)	Enter value	3.83	3.84	3.84	3.83
	(4) Cylinder Height (in.)	Enter value	4.61	4.51	3.62	4.44
	(5) Cylinder Volume (in.^{3})	$\pi * [(3)^2/4] * (4)$	53.10	52.20	41.97	51.15
SAMPLING NOTES	(6) No. of Blows to Drive 1/2" Below Surface	Enter value	225, 30 deg-vert.	162, 10 deg-vert.	225, 45 deg-vert.	425, 30 deg-vert.
	(7) Sample Conditions (Disturbed?, Flush?)	Enter Description	Near flush bottom, 0.381" reamed to even depth on top.	Near flush bottom, 0.483" reamed to even depth on top.	Near flush bottom, 1.376" reamed to even depth on top.	Near flush bottom, 0-1/2" divot @ top replaced with cuttings.
	(8) Sample Description	Enter Description	Gray tuff	Gray tuff, some pumice	Gray tuff, harder at base	Gray tuff, harder, crystalline at base
TESTED SOIL	(9) Wet Weight Tested Soil and Tare (Grams)	Enter value	2211.2	2171.7	1910.0	2423.5
	(10) Wet Weight Tested Soil (Grams)	(9) - (2)	1289.9	1252.6	995.4	1279.7
	(11) Wet Density Tested Soil (lb/ft^3)	[(10)/(5)]*3.81	92.6	91.4	90.4	95.3
	(12) Dry Weight Tested Soil and Tare (Grams)	Enter value	2115.5	2088.4	1865.4	2306.2
	(13) Dry Weight Tested Soil (Grams)	(12) - (2)	1194.2	1169.3	950.8	1162.4
	(14) Water Weight (Grams)	(10) - (13)	95.7	83.3	44.6	117.3
	(15) In-Place Moisture Content	(14) / (13)	0.080	0.071	0.047	0.101
	(16) In-Place Moisture Content (Percent)	(15)*100	8.0%	7.1%	4.7%	10.1%
	(17) Dry Density Tested Soil (lb/ft^3)	(11) / [1+ (15)]	85.7	85.4	86.3	86.6
	(18) Laboratory Maximum Dry Density (lb/ft^3)	Enter value	N/A	N/A	N/A	N/A
	(19) Maximum Dry Density (Percent)	[(17) / (18)]*100	N/A	N/A	N/A	N/A

Acceptance Criteria: Maximum Dry Density in Percent (19) shall be equal to or greater than: N/A % and In-place Moisture Content in Percent (16) shall be equal to N/A +/- N/A %

Comments: Cylinder height and weight adjusted for volume calculation where retained sample not flush

Lab Testing Technician: Jesse Carlin / [signature] / 12/17/04
Print Name / Signature / Date

Checked By: Joe Laird / [signature] / 12/22/04
Print Name / Signature / Date

Kleinfelder Inc., 8300 Jefferson NE Suite B, Albuquerque, NM 87113

KA Form ATSM D2937, Rev 0

FIGURE B.4 - SOURCE D DENSITY OF SOIL IN PLACE BY THE DRIVE-CYLINDER METHOD (ASTM D2937-00)

Project Name	CMRR - SBT	Project Number	19435
Project Location	TA-61, E. JEMEZ ROAD BORROW PIT	Project Task Number	SBT.14
Project Manager	J. NORTH	Field Sampling Date	12/10/2004

	Sample Number		TMC-1	TMC-2	TMC-3	TMC-4
	Test Location		Near CMRR-17 sample 1' south	Near CMRR-16 sample, 1'SW	Near CMRR-15 sample 1'S	Near CMRR-17 2'N
	Test Elevation		7183.9	7177.7	7176.5	7183.9
		Embedded Calculation				
DRIVE CYLINDER DATA	(1) Drive Cylinder Identification Number	Enter value	C-15	C-12	C-2	C-14
	(2) Cylinder Tare Weight + Pan (grams)	Enter value	781.0	766.9	772.3	779.5
	(3) Cylinder Diameter, Avg of 4 meas. (in.)	Enter value	3.84	3.84	3.82	3.83
	(4) Cylinder Height (in.)	Enter value	4.98	4.99	4.99	4.99
	(5) Cylinder Volume (in.^{3})	$\pi * [(3)^2/4] * (4)$	57.67	57.79	57.19	57.49
SAMPLING NOTES	(6) No. of Blows to Drive 1/2" Below Surface	Enter value	28	20	44	36
	(7) Sample Conditions (Disturbed?, Flush?)	Enter Description	Near flush at top and bottom	Near flush, top and bottom	1/4" Divot over 1/2 of base, near flush at top	Flush at bottom, near flush on top
	(8) Sample Description	Enter Description	Gray and orange-brown tuff	gray tuff with some pumice	Gray tuff	Gray orange-brown tuff, hard crystal-rich
TESTED SOIL	(9) Wet Weight Tested Soil and Tare (Grams)	Enter value	2166.6	2223.7	2245.2	2313.6
	(10) Wet Weight Tested Soil (Grams)	(9) - (2)	1385.6	1456.8	1472.9	1534.2
	(11) Wet Density Tested Soil (lb/ft^3)	[(10)/(5)]*3.81	91.5	96.1	98.1	101.7
	(12) Dry Weight Tested Soil and Tare (Grams)	Enter value	2046.9	2097.7	2112.5	2133.8
	(13) Dry Weight Tested Soil (Grams)	(12) - (2)	1265.9	1330.8	1340.2	1354.4
	(14) Water Weight (Grams)	(10) - (13)	119.7	126.0	132.7	179.8
	(15) In-Place Moisture Content	(14) / (13)	0.095	0.095	0.099	0.133
	(16) In-Place Moisture Content (Percent)	(15)*100	9.5%	9.5%	9.9%	13.3%
	(17) Dry Density Tested Soil (lb/ft^3)	(11) / [1+ (15)]	83.6	87.7	89.3	89.8
	(18) Laboratory Maximum Dry Density (lb/ft^3)	Enter value	N/A	N/A	N/A	N/A
	(19) Maximum Dry Density (Percent)	[(17) / (18)]*100	N/A	N/A	N/A	N/A

Acceptance Criteria: Maximum Dry Density in Percent (19) shall be equal to or greater than: N/A % and In-place Moisture Content in Percent (16) shall be equal to N/A +/- N/A %

Comments: Cylinder height and weight adjusted for volume calculation where retained sample not flush

Lab Testing Technician: Jesse Carlin / [signature] / 12/14/04
Print Name / Signature / Date

Checked By: Joe Laird / [signature] / 12/22/04
Print Name / Signature / Date

Kleinfelder Inc., 8300 Jefferson NE Suite B, Albuquerque, NM 87113

KA Form ATSM D2937, Rev 0

FIGURE B.5 - BS-12, UNCONFINED COMPRESSION TEST (ASTM D 2938)

Project Name	CMRR	Sample No.:	05-006-1	Job #	19345 SBT.3A
Location	LANL, TA-61			Date Tested	14-Jan-05
Sample Location	BS-12	Elevation, ft	7127.3	Tested by	Jesse Carlin
Description of Sample	Light gray, poorly-welded tuff (Qbt3L)			Checked by	Joe Laird
Proving Ring #	Humboldt 393	Apparatus #	115-2-203	Average Load Factor	9.14 (lbs/div)

Physical Dimensions	
Intial Diameter	2.992 in.
Initial Height	6.268 in.
Initial Area	0.0488 sq. ft.

Physical Properties	
Bulk Unit Weight (Moist)	82.8 pcf
Bulk Unit Weight (Dry)	78.1 pcf
Moisture Content	6.1 %

UNCONFINED COMPRESSIVE STRENGTH	562 psf
UNIT STRAIN at failure	0.9%
STRAIN RATE	1.22 %/min

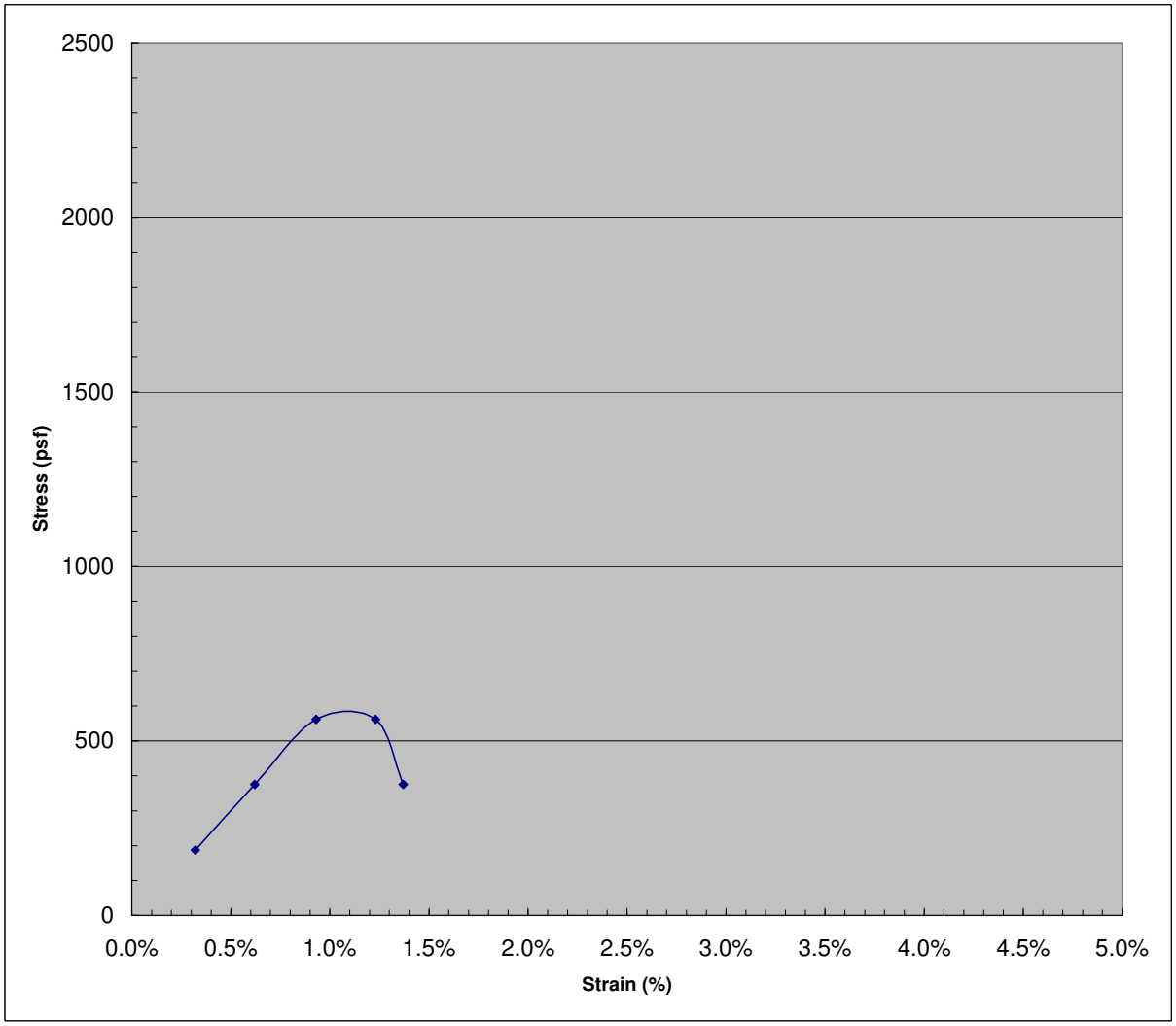

FIGURE B.6 - BS-2, NW, UNCONFINED COMPRESSION TEST (ASTM D 2938)

Project Name	CMRR-SBT	Sample No.:	05-045	Job #	19345 SBT.3A
Location	LANL, TA-61			Date Tested	15-Mar-05
Sample Location	BS-2, NW	Elevation, ft	7125.3	Tested by	Jesse Carlin
Description of Sample	Light gray, poorly welded tuff (Qbt3L)			Checked by	Joe Laird

Proving Ring #	Humboldt 393	Apparatus #	115-2-203	Average Load Factor	9.14 (lbs/div)

Physical Dimensions	
Intial Diameter	3.658 in.
Initial Height	7.316 in.
Initial Area	0.0730 sq. ft.

Physical Properties	
Bulk Unit Weight (Moist)	91.8 pcf
Bulk Unit Weight (Dry)	87.7 pcf
Moisture Content	4.7 %

Note: Unit weight values obtained from average of two tests using ASTM D 4531, Method B.

UNCONFINED COMPRESSIVE STRENGTH	1377 psf
UNIT STRAIN at failure	1.4%
STRAIN RATE	0.79 %/min

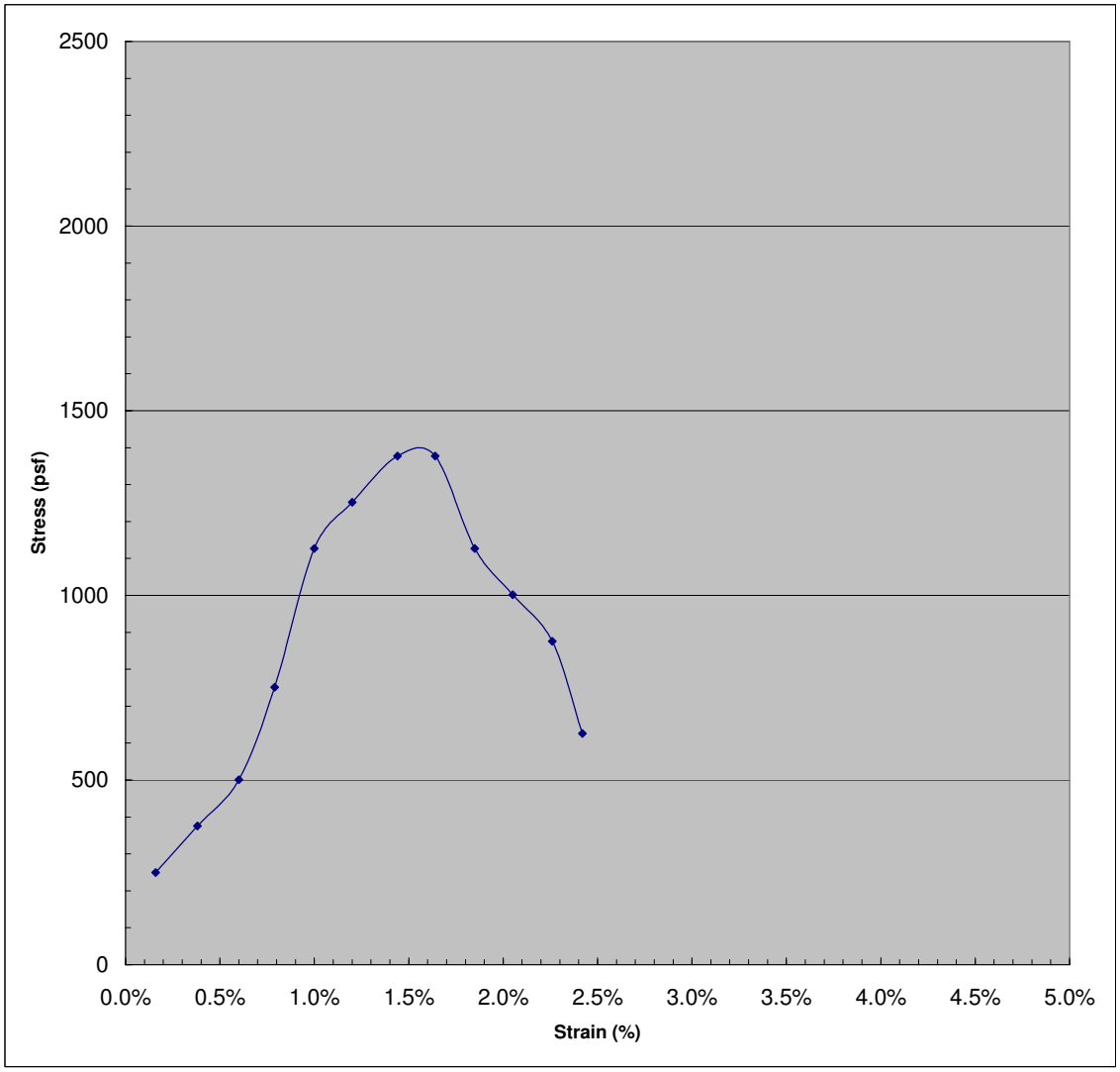

FIGURE B.7 - BS-2, NE, UNCONFINED COMPRESSION TEST (ASTM D 2938)

Project Name	CMRR-SBT	Sample No.:	05-045-2	Job #	19345 SBT.3A
Location	LANL, TA-61			Date Tested	15-Mar-05
Sample Location	BS-2, NE	Elevation, ft	7125.3	Tested by	Jesse Carlin
Description of Sample	Light gray, poorly-welded tuff (Qbt3L)			Checked by	Joe Laird

Proving Ring #	Humboldt 393	Apparatus #	115-2-203	Average Load Factor	9.14 (lbs/div)

Physical Dimensions	
Intial Diameter	3.625 in.
Initial Height	7.069 in.
Initial Area	0.0717 sq. ft.

Physical Properties	
Bulk Unit Weight (Moist)	84.9 pcf
Bulk Unit Weight (Dry)	81.2 pcf
Moisture Content	4.3 %

UNCONFINED COMPRESSIVE STRENGTH	1402 psf
UNIT STRAIN at failure	1.2%
STRAIN RATE	0.8 %/min

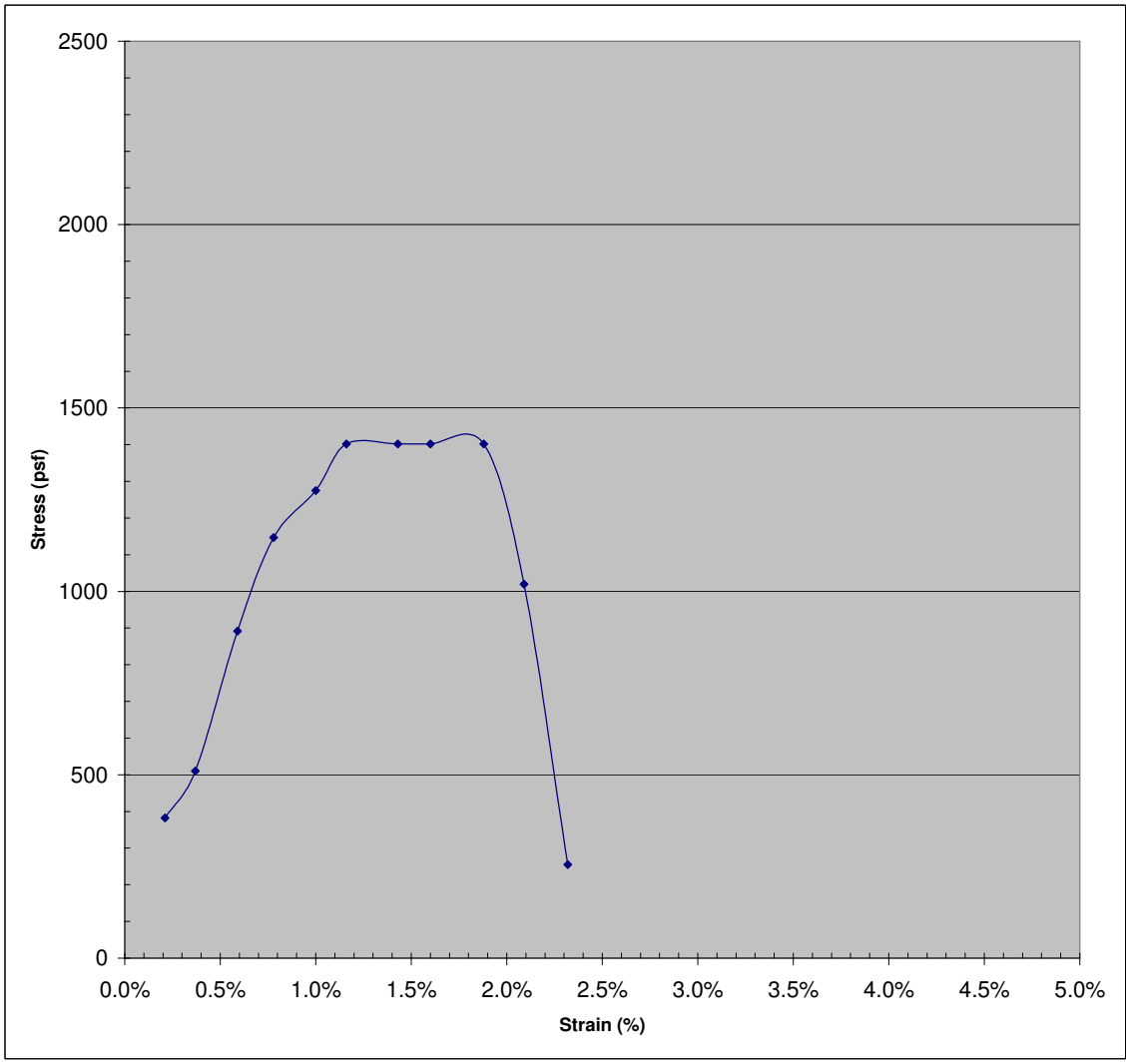

FIGURE B.8 - TEST BLOCK, UNCONFINED COMPRESSION TEST (ASTM D 2938)

Project Name	CMRR	Sample No.:	Test-1	Job #	19345 SBT.3A
Location	TA-61			Date Tested	7-Jul-04
Sample Location	Test Block	Elevation, ft	7123.6	Tested by	Stephen Woodall
Description of Sample	Bandaler Unit3			Checked by	Joe Laird

Proving Ring #	Humboldt 393	Apparatus #	115-2-203	Average Load Factor	9.14 (lbs/div)

Physical Dimensions	
Intial Diameter	2.957 in.
Initial Height	5.655 in.
Initial Area	0.0477 sq. ft.

Physical Properties	
Bulk Unit Weight (Moist)	82.7 pcf
Bulk Unit Weight (Dry)	77.6 pcf
Moisture Content	6.6 %

UNCONFINED COMPRESSION at failure	2108 psf
UNIT STRAIN at failure	3.4%
STRAIN RATE	2.29 %/min

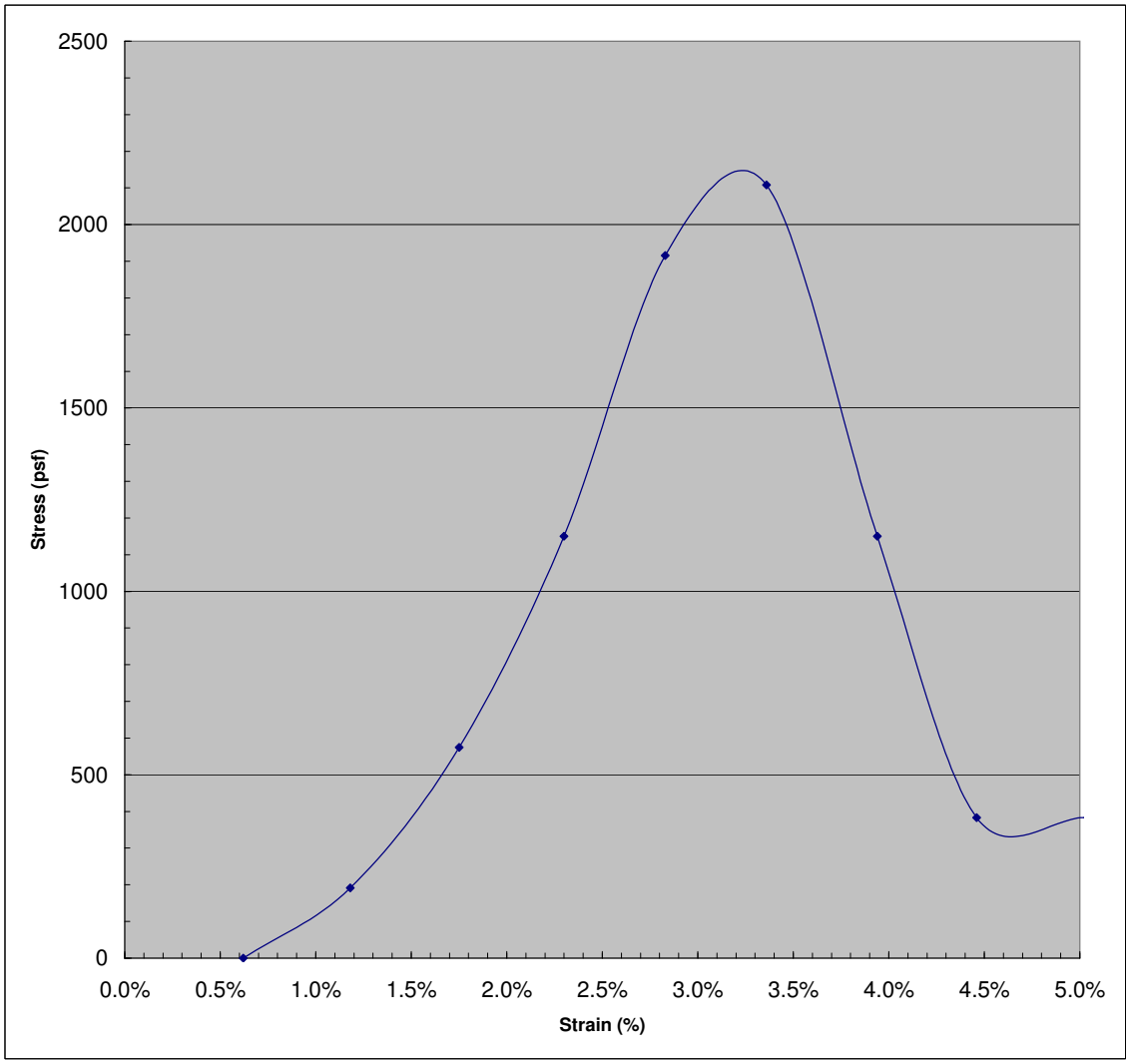

FIGURE B.9 - UNCONFINED COMPRESSION TEST (ASTM D2936)

DSC-1 Run 24 @ 91.0'-92.0'				Weight of Wet Specimen (g)			5666.80
(N) 1769120, (E) 1624740, Elevation 7203.6 ft amsl (Top of Sample)							
Wet Specimen Weight (g)	6111.70	Water Content (%)		6.9		Diameter (in)	5.79
Dry Specimen Weight (g)	5745.60	Sample Type		6" Tube		Area (in^2)	26.32
Weight of Water (g)	366.10	Unit Weight Wet (pcf)		92.3		Height (in)	8.89
Tare Weight (g)	444.90	Unit Weight Dry (pcf)		86.3		Volume (in^3)	233.95
Weight of Dry Specimen (g)	5300.70						

Load Dial	Axial Load (lbs)	Total Strain (in)	Unit Strain (%)	Corrected Area (in^2)	Unconfined Compressive Strength, psi	Unconfined Compressive Strength, psf
	197.95	0.070	0.8%	26.53	7.5	1074

Dial Indicator # 002573668
Calipers # 001100216

Tested By	Jesse Carlin
Date Tested	12/15/2004
Reviewed By	Joe Laird
Date Reviewed	12/20/2004

04-253-1 Unconfined Compression

Copyright 2007, Kleinfelder

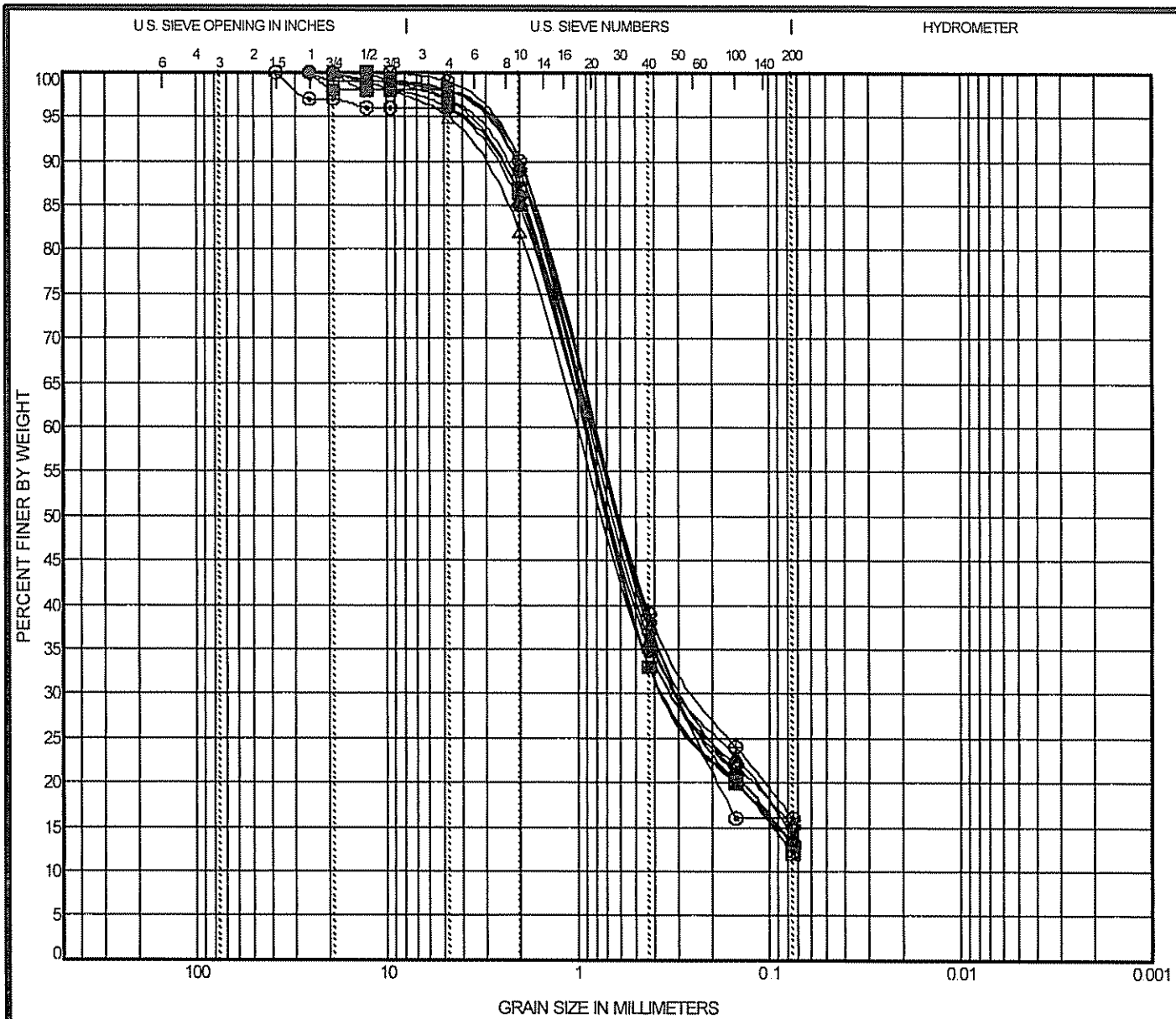

COBBLES	GRAVEL		SAND			SILT OR CLAY
	coarse	fine	coarse	medium	fine	

	Specimen Identification		D100	D60	D30	D10	%Gravel	%Sand	%Silt	%Clay
●	SBT_BS-02_NE	7125.3	25.4	0.922	0.293		4.0	83.0	13.0	
⊠	SBT_BS-02_NW	7125.3	12.7	0.922	0.334		3.0	85.0	12.0	
▲	SBT_BS-12_1A	7125.8	19.05	0.857	0.263		2.0	84.0	14.0	
★	SBT_BS-12_1B	7125.8	12.7	0.897	0.334		2.0	85.0	13.0	
⊙	SBT_DSC-1	7203.6	38.1	0.864	0.291		4.0	80.0	16.0	
✿	SBT_TA-61-1	7124.7	19.05	0.908	0.285		3.0	82.0	15.0	
○	SBT_TA-61-2	7130.0	25.4	0.818	0.26		2.0	85.0	13.0	
△	SBT_TMC-1	7183.9	19.05	0.998	0.334		5.0	82.0	13.0	
⊗	SBT_TMC-2	7177.7	9.525	0.832	0.277		1.0	86.0	13.0	
⊕	SBT_TMC-3	7176.5	19.05	0.815	0.228		2.0	82.0	16.0	

KLEINFELDER

FIGURE B.10 - GRAIN SIZE DISTRIBUTION

Project: CMRR - Special Block Tests

Location: LANL, TA-55

Project Number: 19435

US GRAIN SIZE KA 19435 7 22 05.GPJ TRINITY.GDT 10/24/05

Copyright 2007, Kleinfelder

TABLE B.1 – SUMMARY OF SPECIFIC GRAVITY TESTS AND PARTICLE SIZE ANALYSES

Location, Sample No.	Elevation (ft amsl)	Grain Size Distribution (Percent Passing)							Moisture Content (%)	Specific Gravity (dim)
		#200	#100	#40	#10	#4	3/8"	3/4"		
Source A Samples										
BS-2, NE	7125.3	13	21	35	85	96	98	98	4.3	2.54
BS-2, NW	7125.3	12	20	33	87	97	99	100	5.2	2.54
BS-12, 1A	7125.8	14	23	36	89	98	98	100	6.1	2.55
BS-12, 1B	7125.8	13	20	33	89	98	99	100	N/A	N/A
TA-61-1	7124.7	15	22	35	86	97	99	99	6.1	2.58
TA-61-2	7130.0	13	21	38	90	98	99	99	4.5	2.58
Source B Samples										
MC-1	7164*	No test performed							8.0	2.54
MC-2	7165*	No test performed							7.1	2.56
MC-3	7166.7	No test performed							4.7	2.56
MC-4	7168.1	No test performed							10.1	2.55

Copyright 2007, Kleinfelder

TABLE B.1. SUMMARY OF SPECIFIC GRAVITY TESTS AND PARTICLE SIZE ANALYSES (CONT.)

Location, Sample No.	Elevation (ft amsl)	Grain Size Distribution (Percent Passing)							Moisture Content (%)	Specific Gravity (dim)
		#200	#100	#40	#10	#4	3/8"	3/4"		
Source C Samples										
DSC-1	7203.6	16	16	38	86	96	96	97	6.9	2.56
Source D Samples										
TMC-1	7183.9	13	20	33	82	95	98	100	9.5	2.56
TMC-2	7177.7	13	20	37	90	99	100	100	9.5	2.58
TMC-3	7176.5	16	24	39	89	98	99	100	9.9	2.55
TMC-4	7183.9	No test performed							13.3	2.57

*Elevation to nearest foot provided by LANL EES-9 personnel, Lewis et al (2005)

Appendix C

Addendum to UT Report

Report of Field and Laboratory Testing Performed by the University of Texas at Austin

Placeholder for Addendum

Placeholder for Addendum

Placeholder for Addendum

Placeholder for Addendum

Placeholder for Addendum

Placeholder for Addendum

Placeholder for Addendum

Placeholder for Addendum

SPECIAL BLOCK TESTS (SBT) OF BANDELIER TUFF (Qbt3L): FIELD SEISMIC AND DYNAMIC LABORATORY TESTS, LOS ALAMOS NATIONAL LABORATORY

for

Kleinfelder, Inc.
Albuquerque, New Mexico

by

Dr. Kenneth H. Stokoe, II
Brady Cox
Yin-Cheng Lin
Won Kyoung Choi
Seong Yeol Jeon
Jung Jae Lee

November 7, 2005

K. H. Stokoe II
7 Nov. 05

Geotechnical Engineering Report GR05-4
Geotechnical Engineering Center
Civil, Architectural, and Environmental Engineering Department
The University of Texas at Austin

TABLE OF CONTENTS

TABLE OF CONTENTS 2

LIST OF FIGURES 3

LIST OF TABLES 10

1. INTRODUCTION 12

2. FIELD SEISMIC TESTS 12

2.1. Field Shear Wave Velocity Profiles 13

2.2. Comparison of Field V_s Profiles of Intact Qbt3L and Predicted V_s Profiles for Loose Sand 16

3. DYNAMIC LABORATORY TESTS 19

3.1 Dynamic Properties at Small Strains 19

3.2 Dynamic Properties in the Nonlinear Range 23

4. COMPARISON OF LABORATORY AND EMPIRICAL RESULTS 23

5. COMPARISON OF V_S VALUES OF THE QBT3L MEASURED IN THE FIELD AND LABORATORY 36

6. REFERENCES 36

APPENDIX A: SEISMIC TESTING BY THE SPECTRAL-ANALYSIS-OF-SURFACE-WAVES (SASW) METHOD 38

APPENDIX B: FIELD RESULTS AND SHEAR WAVE VELOCITY PROFILES FROM FOUR SASW TEST SITES 48

APPENDIX C: BACKGROUND ON THE COMBINED RESONANT COLUMN AND TORSIONAL SHEAR (RCTS) EQUIPMENT 62

APPENDIX D: LABORATORY RESULTS OF COMBINED RESONANTCOLUMN AND TORSIONAL SHEAR (RCTS) TESTS OFTWO SPECIMENS FROM BLOCK SAMPLE #15, TA 61 70

LIST OF FIGURES

Figure 1 Comparison of the V_s Profiles at Sites TA-61-1, TA-61-2 and TA-61-3 at Los Alamos National Laboratory 14

Figure 2 Comparison of the V_s Profiles at Sites TA-61-1, TA-61-2, TA-61-3 and Mortandad Canyon at Los Alamos National Laboratory 15

Figure 3 Comparison of the V_s Profiles in the Intact Lower Unit 3, Bandelier Tuff at Sites TA-61-1, TA-61-2, TA-61-3 and Mortandad Canyon at Los Alamos National Laboratory 17

Figure 4 Comparison of V_s Profiles Determined for the Intact Qb3L with V_s Profiles Predicted for Loose Dry Sand 18

Figure 5 Variation in Low-Amplitude Shear Wave Velocity with Isotropic Confining Pressure of the Two Intact Specimens from Block Sample #15 (Lower Unit 3, Bandelier Tuff (Qbt3L)) as Determined from Resonant Column (RC) Tests 20

Figure 6 Variation in Low-Amplitude Shear Modulus with Isotropic Confining Pressure of the Two Intact Specimens from Block Sample #15 (Lower Unit 3, Bandelier Tuff (Qbt3L)) as Determined from Resonant Column (RC) Tests 21

Figure 7 Variation in Low-Amplitude Material Damping Ratio with Isotropic Confining Pressure of the Two Intact Specimens from Block Sample #15 (Lower Unit 3, Bandelier Tuff (Qbt3L)) as Determined from Resonant Column (RC) Tests 22

Figure 8 Variation in Shear Modulus with Shearing Strain of the Two Intact Specimens from Block Sample #15 (Lower Unit 3, Bandelier Tuff (Qbt3L)) at an Isotropic Confining Pressure of 0.86 ksf (41 kPa) from Resonant Column (RC) and Torsional Shear (TS) Tests 24

Figure 9 Variation in Material Damping Ratio with Shearing Strain of the Two Intact Specimens from Block Sample #15 (Lower Unit 3, Bandelier Tuff (Qbt3L)) at an Isotropic Confining Pressure of 0.86 ksf (41 kPa) from Resonant Column (RC) and Torsional Shear (TS) Tests 25

Figure 10 Variation in Normalized Shear Modulus with Shearing Strain of the Two Intact Specimens from Block Sample #15 (Lower Unit 3, Bandelier Tuff (Qbt3L)) at an Isotropic Confining Pressure of 0.86 ksf (41 kPa) from Resonant Column (RC) and Torsional Shear (TS) Tests 26

Copyright 2007, Kleinfelder

Figure 11 Comparison between the Trend Line for a Dry Loose Sand Predicted by Menq (2003) and the Variation in Low-Amplitude Shear Wave Velocity with Isotropic Confining Pressure of the Two Intact Specimens from Block Sample #15 (Lower Unit 3, Bandelier Tuff (Qbt3L)) as Determined from Resonant Column (RC) Tests 27

Figure 12 Comparison between the Trend Line for a Dry Loose Sand Predicted by Menq (2003) and the Variation in Low-Amplitude Shear Modulus with Isotropic Confining Pressure of the Two Intact Specimens from Block Sample #15 (Lower Unit 3, Bandelier Tuff (Qbt3L)) as Determined from Resonant Column (RC) Tests 28

Figure 13 Comparison between the Trend Line for a Dry Loose Sand Predicted by Menq (2003) and the Variation in Low-Amplitude Material Damping Ratio with Isotropic Confining Pressure of the Two Intact Specimens from Block Sample #15 (Lower Unit 3, Bandelier Tuff (Qbt3L)) as Determined from Resonant Column (RC) Tests 29

Figure 14 Comparison between the Trend Line for a Dry Loose Sand Predicted by Seed et al. (1986) and the Variation in Shear Modulus with Shearing Strain of the Two Intact Specimens from Block Sample #15 (Lower Unit 3, Bandelier Tuff (Qbt3L)) as Determined from Resonant Column (RC) Tests 30

Figure 15 Comparison between the Trend Line for a Dry Loose Sand Predicted by Seed et al. (1986) and the Variation in Material Damping Ratio with Shearing Strain of the Two Intact Specimens from Block Sample #15 (Lower Unit 3, Bandelier Tuff (Qbt3L)) as Determined from Resonant Column (RC) Tests 31

Figure 16 Comparison between the Trend Line for a Dry Loose Sand Predicted by Menq (2003) and Darendeli (2001) and the Variation in Normalized Shear Modulus with Shearing Strain of the Two Intact Specimens from Block Sample #15 (Lower Unit 3, Bandelier Tuff (Qbt3L)) as Determined from Resonant Column (RC) Tests 32

Figure 17 Comparison between the Trend Line for a Dry Loose Sand Predicted by Menq. (2003) and Darendeli (2001) and the Variation in Material Damping Ratio with Shearing Strain of the Two Intact Specimens from Block Sample #15 (Lower Unit 3, Bandelier Tuff (Qbt3L)) as Determined from Resonant Column (RC) Tests 33

Figure 18 Comparison of Field-Measured V_s Profiles at the TA-61 Borrow Pit and Laboratory-Predicted V_s Profiles (K_o = 0.5, γ_t = 85 pcf) of the Qbt3L 34

Copyright 2007, Kleinfelder

Figure 19 Comparison of Field-Measured V_s Profiles at the TA-61 Borrow Pit and Laboratory-Predicted V_s Profiles (K_o = 1.0, γ_t = 85 pcf) of the Qbt3L 35

Figure A.1 Approximate Distribution of Vertical Particle Motion with Depth for Two Surface Waves with Different Wavelengths 40

Figure A.2 Typical SASW Field Arrangement and Associated Phase Spectrum Measurement from One Source-Receivers Set-Up 41

Figure A.3 Unwrapped Phase Spectrum and Associated Dispersion Curve from Testing at One Receiver Spacing as Shown in Figure A.2a 42

Figure A.4 Typical Receiver Arrangements and Associated Dispersion Curves 43

Figure A.5 Developing the Field Dispersion Curve and Matching a Theoretical Curve to It 45

Figure A.6 Shear Wave Velocity Profile Determined from the Forward-Modeling Process Shown in Figure A.5c 46

Figure B.1 Experimental and Theoretical Dispersion Curves for Site TA-61-1 at Los Alamos National Laboratory 49

Figure B.2 Shear Wave Velocity Profiles of Site TA-61-1 from Fitting the Experimental Dispersion Curve 50

Figure B.3 Experimental and Theoretical Dispersion Curves for Site TA-61-2 at Los Alamos National Laboratory 52

Figure B.4 Shear Wave Velocity Profiles of Site TA-61-2 from Fitting the Experimental Dispersion Curve 53

Figure B.5 Experimental and Theoretical Dispersion Curves for Site TA-61-3 at Los Alamos National Laboratory 55

Figure B.6 Shear Wave Velocity Profiles of Site TA-61-3 from Fitting the Experimental Dispersion Curve 56

Figure B.7 Experimental and Theoretical Dispersion Curves for the Mortandad Canyon Site at Los Alamos National Laboratory 58

Figure B.8 Shear Wave Velocity Profile at the Mortandad Canyon Site from Fitting the Experimental Dispersion Curve 59

Copyright 2007, Kleinfelder

Figure B.9 Comparison of V_s Profiles of Sites TA-61-1, TA-61-2, TA-61-3 and Mortandad Canyon at Los Alamos National Laboratory 61

Figure C.1 Simplified Diagram of a Combined Resonant Column (RC) and Torsional Shear (TS) Device (Confining Chamber not Shown) 64

Figure C.2 An Example of the Dynamic Response Curve Measured in the RC Test 64

Figure C.3 Material Damping Measurement in the RC Test Using the Free-Vibration Decay Curve 66

Figure C.4 Material Damping Measurement in the RC Test Using the Half-Power Bandwidth (Same Specimen as Shown in Figure C.3) 66

Figure C.5 An Example of a Hysteresis Loop Measured in the TS Test 68

Figure C.6 Examples of Equipment-Generated Damping Measured in the Resonant Column Device Using Metal Specimens (from Hwang, 1997) 68

Figure D.1 Variation in Low-Amplitude Shear Wave Velocity with Isotropic Confining Pressure of the Two Intact Specimens from Block Sample #15 (Lower Unit 3, Bandelier Tuff (Qbt3L)) as Determined from Resonant Column (RC) Tests 71

Figure D.2 Variation in Low-Amplitude Shear Modulus with Isotropic Confining Pressure of the Two Intact Specimens from Block Sample #15 (Lower Unit 3, Bandelier Tuff (Qbt3L)) as Determined from Resonant Column (RC) Tests 72

Figure D.3 Variation in Low-Amplitude Material Damping Ratio with Isotropic Confining Pressure of the Two Intact Specimens from Block Sample #15 (Lower Unit 3, Bandelier Tuff (Qbt3L)) as Determined from Resonant Column (RC) Tests 73

Figure D.4 Variation in Estimated Total Unit Weight with Isotropic Confining Pressure of the Two Intact Specimens from Block Sample #15 (Lower Unit 3, Bandelier Tuff (Qbt3L)) as Determined from Resonant Column (RC) Tests 74

Figure D.5 Variation in Shear Modulus with Shearing Strain of the Two Intact Specimens from Block Sample #15 (Lower Unit 3, Bandelier Tuff (Qbt3L)) at an Isotropic Confining Pressure of 0.86 ksf (41 kPa) from Resonant Column (RC) and Torsional Shear (TS) Tests 75

Copyright 2007, Kleinfelder

Figure D.6 Variation in Shear Modulus with Shearing Strain of the Two Intact Specimens from Block Sample #15 (Lower Unit 3, Bandelier Tuff (Qbt3L)) at an Isotropic Confining Pressure of 3.46 ksf (166 kPa) from Resonant Column (RC) and Torsional Shear (TS) Tests 76

Figure D.7 Variation in Normalized Shear Modulus with Shearing Strain of the Two Intact Specimens from Block Sample #15 (Lower Unit 3, Bandelier Tuff (Qbt3L)) at an Isotropic Confining Pressure of 0.86 ksf (41 kPa) from Resonant Column (RC) and Torsional Shear (TS) Tests 77

Figure D.8 Variation in Normalized Shear Modulus with Shearing Strain of the Two Intact Specimens from Block Sample #15 (Lower Unit 3, Bandelier Tuff (Qbt3L)) at an Isotropic Confining Pressure of 3.46 ksf (166 kPa) from Resonant Column (RC) and Torsional Shear (TS) Tests 78

Figure D.9 Variation in Material Damping Ratio with Shearing Strain of the Two Intact Specimens from Block Sample #15 (Lower Unit 3, Bandelier Tuff (Qbt3L)) at an Isotropic Confining Pressure of 0.86 ksf (41 kPa) from Resonant Column (RC) and Torsional Shear (TS) Tests 79

Figure D.10 Variation in Material Damping Ratio with Shearing Strain of the Two Intact Specimens from Block Sample #15 (Lower Unit 3, Bandelier Tuff (Qbt3L)) at an Isotropic Confining Pressure of 3.46 ksf (166 kPa) from Resonant Column (RC) and Torsional Shear (TS) Tests 80

Figure D.11 Variation of (a) Shear Modulus and (b) Material Damping Ratio with Number of Cycles for Spec. No. 1 from Block Sample #15 (Lower Unit 3, Bandelier Tuff (Qbt3L)) at an Isotropic Confining Pressure of 0.86 ksf (41 kPa) from Torsional Shear (TS) Tests 81

Figure D.12 Variation of (a) Shear Modulus and (b) Material Damping Ratio with Number of Cycles for Spec. No. 1 from Block Sample #15 (Lower Unit 3, Bandelier Tuff (Qbt3L)) at an Isotropic Confining Pressure of 3.46 ksf (166 kPa) from Torsional Shear (TS) Tests 82

Figure D.13 Variation in Shear Modulus and Specimen Height with Shearing Strain of Spec. No. 1 from Block Sample #15 (Lower Unit 3, Bandelier Tuff (Qbt3L)) as Determined from Resonant Column (RC) Tests at Two Different Isotropic Confining Pressures: (a) 0.86 ksf (41 kPa) and (b) 3.46 ksf (166 kPa) 83

Copyright 2007, Kleinfelder

Figure D.14 Variation of (a) Shear Modulus and (b) Material Damping Ratio with Number of Cycles for Spec. No. 2 from Block Sample #15 (Lower Unit 3, Bandelier Tuff (Qbt3L)) at an Isotropic Confining Pressure of 0.86 ksf (41 kPa) from Torsional Shear (TS) Tests 84

Figure D.15 Variation of (a) Shear Modulus and (b) Material Damping Ratio with Number of Cycles for Spec. No. 2 from Block Sample #15 (Lower Unit 3, Bandelier Tuff (Qbt3L)) at an Isotropic Confining Pressure of 3.46 ksf (166 kPa) from Torsional Shear (TS) Tests 85

Figure D.16 Variation in Shear Modulus and Specimen Height with Shearing Strain of Spec. No. 2 from Block Sample #15 (Lower Unit 3, Bandelier Tuff (Qbt3L)) as Determined from Resonant Column (RC) Tests at Two Different Isotropic Confining Pressures: (a) 0.86 ksf (41 kPa) and (b) 3.46 ksf (166 kPa) 86

Figure D.17 Comparison between the Trend Line for a Dry Loose Sand Predicted by Menq (2003) and the Variation in Low-Amplitude Shear Wave Velocity with Isotropic Confining Pressure of the Two Intact Specimens from Block Sample #15 (Lower Unit 3, Bandelier Tuff (Qbt3L)) as Determined from Resonant Column (RC) Tests 87

Figure D.18 Comparison between the Trend Line for a Dry Loose Sand Predicted by Menq (2003) and the Variation in Low-Amplitude Shear Modulus with Isotropic Confining Pressure of the Two Intact Specimens from Block Sample #15 (Lower Unit 3, Bandelier Tuff (Qbt3L)) as Determined from Resonant Column (RC) Tests 88

Figure D.19 Comparison between the Trend Line for a Dry Loose Sand Predicted by Menq (2003) and the Variation in Low-Amplitude Material Damping Ratio with Isotropic Confining Pressure of the Two Intact Specimens from Block Sample #15 (Lower Unit 3, Bandelier Tuff (Qbt3L)) as Determined from Resonant Column (RC) Tests 89

Figure D.20 Comparison between the Trend Line for a Dry Loose Sand Predicted by Menq (2003) and Darendeli (2001) and the Variation in Shear Modulus with Shearing Strain of the Two Intact Specimens from Block Sample #15 (Lower Unit 3, Bandelier Tuff (Qbt3L)) as Determined from Resonant Column (RC) Tests 90

Figure D.21 Comparison between the Trend Line for a Dry Loose Sand Predicted by Menq (2003) and Darendeli (2001) and the Variation in Normalized Shear Modulus with Shearing Strain of the Two Intact Specimens from Block Sample #15 (Lower Unit 3, Bandelier Tuff (Qbt3L)) as Determined from Resonant Column (RC) Tests 91

Copyright 2007, Kleinfelder

Figure D.22 Comparison between the Trend Line for a Dry Loose Sand Predicted by Menq. (2003) and Darendeli (2001) and the Variation in Material Damping Ratio with Shearing Strain of the Two Intact Specimens from Block Sample #15 (Lower Unit 3, Bandelier Tuff (Qbt3L)) as Determined from Resonant Column (RC) Tests 92

Figure D.23 Comparison between the Trend Line for a Dry Loose Sand Predicted by Seed et al. (1986) and the Variation in Shear Modulus with Shearing Strain of the Two Intact Specimens from Block Sample #15 (Lower Unit 3, Bandelier Tuff (Qbt3L)) as Determined from Resonant Column (RC) Tests 93

Figure D.24 Comparison between the Trend Line for a Dry Loose Sand Predicted by Seed et al. (1986) and the Variation in Material Damping Ratio with Shearing Strain of the Two Intact Specimens from Block Sample #15 (Lower Unit 3, Bandelier Tuff (Qbt3L)) as Determined from Resonant Column (RC) Tests 94

Copyright 2007, Kleinfelder

LIST OF TABLES

Table B.1 Parameters Used to Develop the Theoretical Dispersion Curve at Site TA-61-1, Profile 1 51

Table B.2 Parameters Used to Develop the Theoretical Dispersion Curve at Site TA-61-1, Profile 2 51

Table B.3 Parameters Used to Develop the Theoretical Dispersion Curve at Site TA-61-2 , Profile 1 54

Table B.4 Parameters Used to Develop the Theoretical Dispersion Curve at Site TA-61-2 , Profile 2 54

Table B.5 Parameters Used to Develop the Theoretical Dispersion Curve at Site TA-61-3, Profile 1 57

Table B.6 Parameters Used to Develop the Theoretical Dispersion Curve at Site TA-61-3, Profile 2 57

Table B.7 Parameters Used to Develop the Theoretical Dispersion Curve at the Mortandad Canyon Site 60

Table D.1 Variation in Low-Amplitude Shear Wave Velocity, Low-Amplitude Shear Modulus, Low-Amplitude Material Damping Ratio and Estimated Total Unit Weight with Isotropic Confining Pressure of Spec. No. 1 from Block Sample #15 (Lower Unit 3, Bandelier Tuff (Qbt3L)) as Determined from Resonant Column (RC) Tests..... 95

Table D.2 Variation in Low-Amplitude Shear Wave Velocity, Low-Amplitude Shear Modulus, Low-Amplitude Material Damping Ratio and Estimated Total Unit Weight with Isotropic Confining Pressure of Spec. No. 2 from Block Sample #15 (Lower Unit 3, Bandelier Tuff (Qbt3L)) as Determined from Resonant Column (RC) Tests..... 95

Table D.3 Variation in Shear Modulus, Normalized Shear Modulus, Material Damping Ratio and Specimen Height with Shearing Strain from RC Tests of Spec. No. 1 from Block Sample #15 (Lower Unit 3, Bandelier Tuff (Qbt3L)); Isotropic Confining Pressure , σ_o' = 0.86 ksf (41 kPa)..... 96

Table D.4 Variation in Shear Modulus, Normalized Shear Modulus and Material Damping Ratio with Shearing Strain from TS Tests of Spec. No. 1 from Block Sample #15 (Lower Unit 3, Bandelier Tuff (Qbt3L)); Isotropic Confining Pressure , σ_o' = 0.86 ksf (41 kPa)..... 96

Copyright 2007, Kleinfelder

Table D.5 Variation in Shear Modulus, Normalized Shear Modulus, Material Damping Ratio and Specimen Height with Shearing Strain from RC Tests of Spec. No. 1 from Block Sample #15 (Lower Unit 3, Bandelier Tuff (Qbt3L)); Isotropic Confining Pressure , σ_o' = 3.46 ksf (166 kPa) 97

Table D.6 Variation in Shear Modulus, Normalized Shear Modulus and Material Damping Ratio with Shearing Strain from TS Tests of Spec. No. 1 from Block Sample #15 (Lower Unit 3, Bandelier Tuff (Qbt3L)); Isotropic Confining Pressure , σ_o' = 3.46 ksf (166 kPa) 97

Table D.7 Variation in Shear Modulus, Normalized Shear Modulus, Material Damping Ratio and Specimen Height with Shearing Strain from RC Tests of Spec. No. 2 from Block Sample #15 (Lower Unit 3, Bandelier Tuff (Qbt3L)); Isotropic Confining Pressure , σ_o' = 0.86 ksf (41 kPa) 98

Table D.8 Variation in Shear Modulus, Normalized Shear Modulus and Material Damping Ratio with Shearing Strain from TS Tests of Spec. No. 2 from Block Sample #15 (Lower Unit 3, Bandelier Tuff (Qbt3L)); Isotropic Confining Pressure , σ_o' = 0.86 ksf (41 kPa) 98

Table D.9 Variation in Shear Modulus, Normalized Shear Modulus, Material Damping Ratio and Specimen Height with Shearing Strain from RC Tests of Spec. No. 2 from Block Sample #15 (Lower Unit 3, Bandelier Tuff (Qbt3L)); Isotropic Confining Pressure , σ_o' = 3.46 ksf (166 kPa) 99

Table D.10 Variation in Shear Modulus, Normalized Shear Modulus and Material Damping Ratio with Shearing Strain from TS Tests of Spec. No. 2 from Block Sample #15 (Lower Unit 3, Bandelier Tuff (Qbt3L)); Isotropic Confining Pressure , σ_o' = 3.46 ksf (166 kPa) 99

Table D.11 Variation of Shear Modulus and Material Damping Ratio with Number of Cycles for Spec. No. 1 from Block Sample #15 (Lower Unit 3, Bandelier Tuff (Qbt3L)) at Isotropic Confining Pressures of 0.86 ksf (41 kPa) and 3.46 ksf (166 kPa) from Torsional Shear (TS) Tests 100

Table D.12 Variation of Shear Modulus and Material Damping Ratio with Number of Cycles for Spec. No. 2 from Block Sample #15 (Lower Unit 3, Bandelier Tuff (Qbt3L)) at Isotropic Confining Pressures of 0.86 ksf (41 kPa) and 3.46 ksf (166 kPa) from Torsional Shear (TS) Tests 100

Copyright 2007, Kleinfelder

1. INTRODUCTION

This report summarized the findings from a study that was performed by the University of Texas at Austin (UT) for the Chemistry and Metallurgical Research Replacement (CMRR) project at Los Alamos National Laboratory (LANL). The objectives of the study were to: (1) characterize in the field the small-strain shear wave velocity, V_s, of the Lower Unit 3, Bandelier Tuff (Qbt3L), and (2) characterize the dynamic properties of intact Qbt3L specimens over a range in confining pressures and shearing strains in the laboratory. The first objective was accomplished with field seismic tests using surface waves at four sites at LANL. The second objective was accomplished using two intact specimens that were hand carved from a large block sample of Qbt3L material and tested in the Soil Dynamics Laboratory at UT. Combined resonant column and torsional shear (RCTS) equipment was used in the laboratory to evaluate the dynamic material properties.

The UT study is part of a larger study that was performed by Kleinfelder, Inc. (KA), Albuquerque, New Mexico. The KA study is called the special block tests (SBT). All field and laboratory work that was performed by UT personnel was conducted under NQA-1 standards with equipment that was within the one-year calibration period. All documentation of equipment calibration is contained in Volume 3 of Geotechnical Engineering Report GR05-5 from UT to Kleinfelder, Inc.

2. FIELD SEISMIC TESTS

Field seismic tests were performed at LANL during December 8 through 10, 2004. The spectral-analysis-of-surface-waves (SASW) method was employed. The SASW method is a non-invasive and non-destructive seismic method that involves generation and measurement of Rayleigh-type surface waves. Appendix A contains a discussion of the SASW test procedures used to collect the field data and the analysis used in the laboratory to determine the V_s profiles.

SASW tests were performed at four sites. At each site, the Qbt3L material was exposed at the ground surface. Three sites were located in the TA-61 Borrow Pit. The borrow pit is also the area where the Qbt3L SBT samples were recovered. The three SASW test sites were located in the vicinity of the SBT sampling area. The fourth SASW site was in Mortandad Canyon. A fifth site in Two-Mile Canyon was also investigated during field testing, but the Qbt3L outcrop and surrounding area were found to be insufficient in lateral dimensions for testing.

Copyright 2007, Kleinfelder

The purpose of the SASW tests was to determine V_s profiles to a maximum depth of about 15 ft. Therefore, receivers spacings (in Figure A.2) ranging from 1 to 24 ft were used. The seismic source was hand-held hammers, and the receivers were 4.5-Hz geophones. This equipment is the same equipment that has been used in SASW testing at the Yucca Mountain site for the U.S. Department of Energy (DOE). The recording equipment was a 4-channel Agilent waveform recorder (Model 35670A). The 4-channel waveform recorder was field calibrated for timing and phase using a calibrated waveform generator. The geophones, analyzer and waveform generator were all calibrated to an NQA-1 level prior to field testing.

The forward modeling process that was used to determine the V_s profile from the field-measured dispersion curve was performed in the laboratory at UT (see discussion in Appendix A). The forward modeling process was done with computer program WinSASW, version 1.23. This exact program, computer platforms and personnel are the ones presently qualified and working on the Yucca Mountain project for DOE.

2.1 Field Shear Wave Velocity Profiles

The three V_s profiles determined at the TA-61 Borrow Pit are shown in Figure 1. The field dispersion curves, theoretical dispersion curves used to fit the field data and the tabulated V_s profiles are given in Appendix B. The field dispersion curve at each site has been fit with two theoretical dispersion curves; hence, with two V_s profiles. Each of the two profiles varies only slightly from the other. The variability present in each field dispersion curve lead to the decision to use two V_s profiles to fit the measured field data.

As seen in Figure 1, the V_s profiles at the three sites in the TA-61 Borrow Pit are very similar. Within one foot of the ground surface, a thin stiffer zone was measured. This stiffer zone is assumed to result from compaction of the Qbt3L material due to machinery traffic at the borrow pit. Also, below a depth of 20 ft, Mr. Joe Laird of KA indicated that the material type may change. Therefore, the V_s profiles between 1 and 20 ft are assumed to represent the undisturbed (intact) Qbt3L. These V_s profiles show a gradually increasing shear wave velocity, from an average V_s of about 375 fps at 2 ft to about 725 fps at 20 ft.

The Vs profile evaluated at the Mortandad Canyon site is presented with the three TA-61 profiles in Figure 2. The canyon site differs from the borrow pit sites in the following three aspects: (1) SASW testing was performed on an exposed vertical cut along a gravel road in

Copyright 2007, Kleinfelder

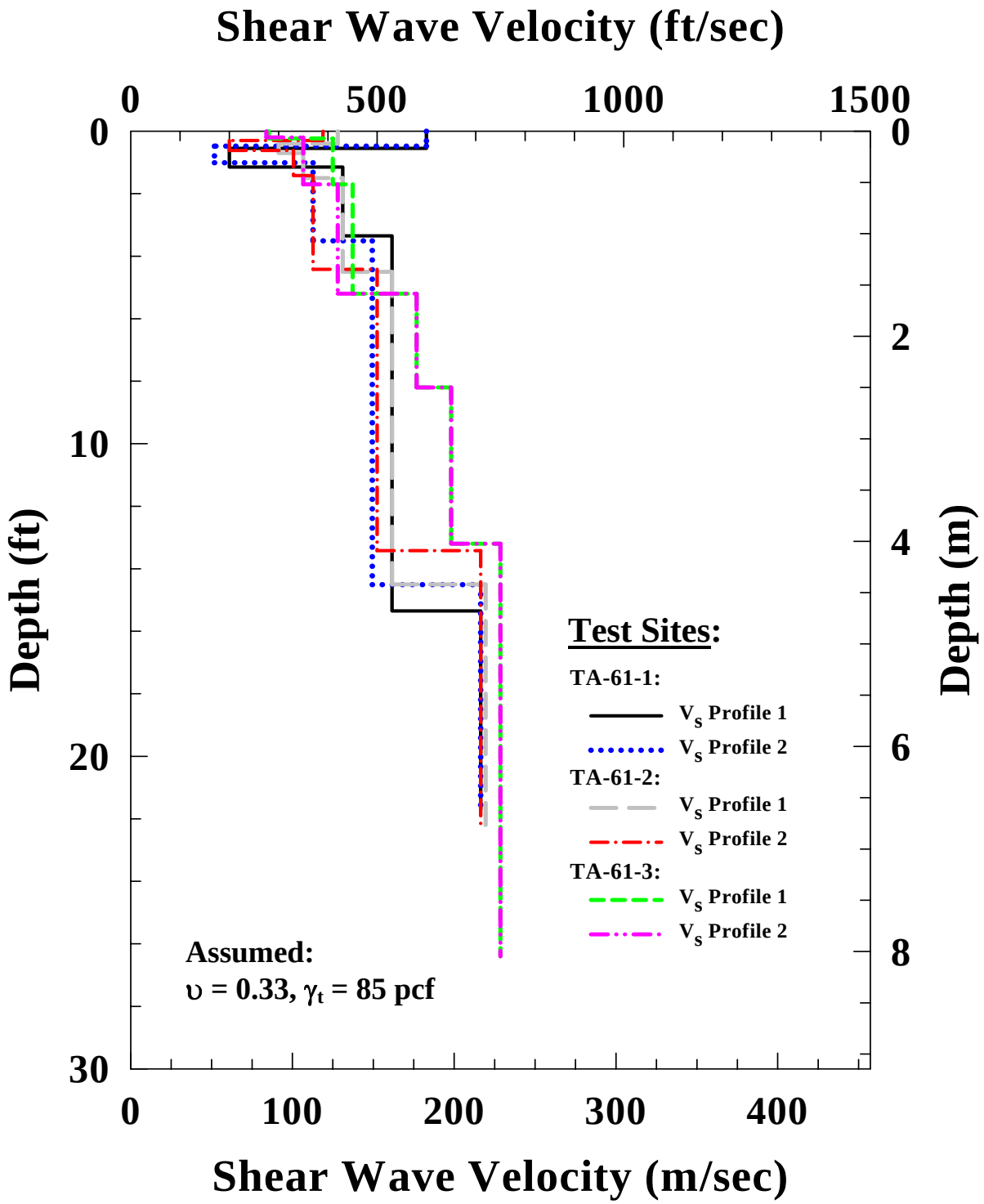

Figure 1 Comparison of the V_s Profiles at Sites TA-61-1, TA-61-2 and TA-61-3 at Los Alamos National Laboratory

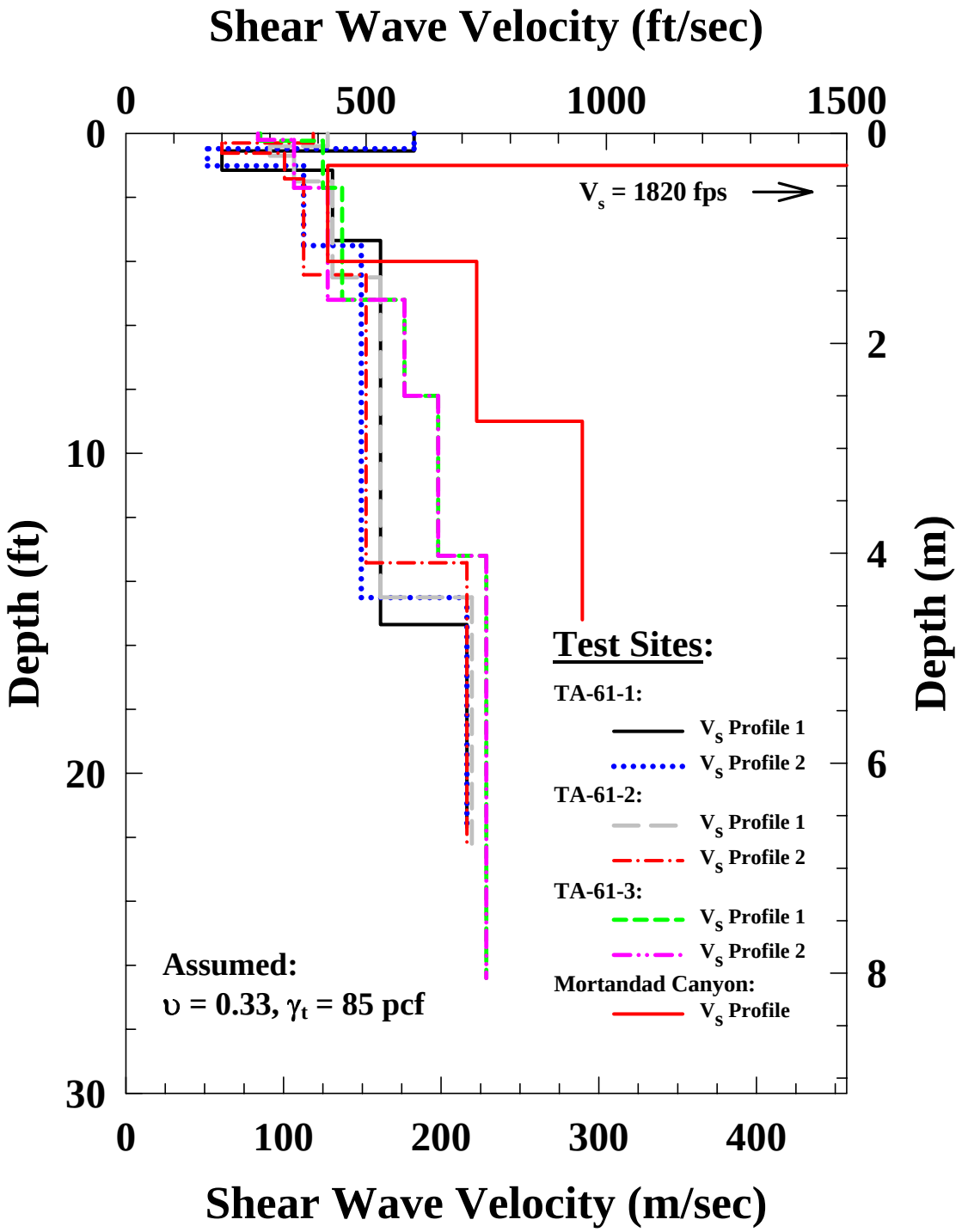

Figure 2 Comparison of the V_s Profiles at Sites TA-61-1, TA-61-2, TA-61-3 and Mortandad Canyon at Los Alamos National Laboratory

Mortandad Canyon, (2) the exposed material was covered with snow, and (3) the Qbt3L material behind the vertical cut has an upward sloping surface. The V_s profile at the canyon site shows two special features: (1) a very stiff surface layer about one-foot thick, and (2) a somewhat stiffer layer at a depth greater than 9 ft. The first feature is attributed to partially frozen shallow material which was determined visually and by shoveling. The second feature, a stiffer layer at a depth greater than about 9 ft (hence, a distance behind the vertical cut of about 9 ft) is attributed by Mr. Joe Laird to a possible material change. The remainder of the V_s profile is assumed to represent undisturbed Qbt3L.

The V_s profiles from the four sites that represent only the intact Qbt3L are presented in Figure 3.

2.2. Comparison of Field V_s Profiles of Intact Qbt3L and Predicted V_s Profiles for Loose Sand

It is interesting to compare the V_s profiles measured in the intact Qbt3L with V_s profiles predicted for a loose, dry sand. The sand is represented by a material with the following properties:

void ratio, e = 0.75,
mean grain size, D_{50} = 0.4 mm,
uniformity coefficient, C_u = 2.0,
specific gravity, G_s = 2.65, and
dry unit weight = 94.5 pcf.

The study by Menq (2003) was used to predict V_s of the dry sand. The coefficient of earth pressure at rest, K_0, was assumed to vary from a normally consolidated soil, K_0 = 0.5, to a moderately overconsolidated soil with K_0 = 1.0. The V_s profiles of the sand and Qbt3L are compared in Figure 4. As seen in the figure, the Qbt3L exhibits V_s values in the top 20 ft that are generally in the range of the values predicted for a normally consolidated to moderately overconsolidated loose sand. In this case, the loose sand has a relative density in the range of 30 to 50 percent.

Copyright 2007, Kleinfelder

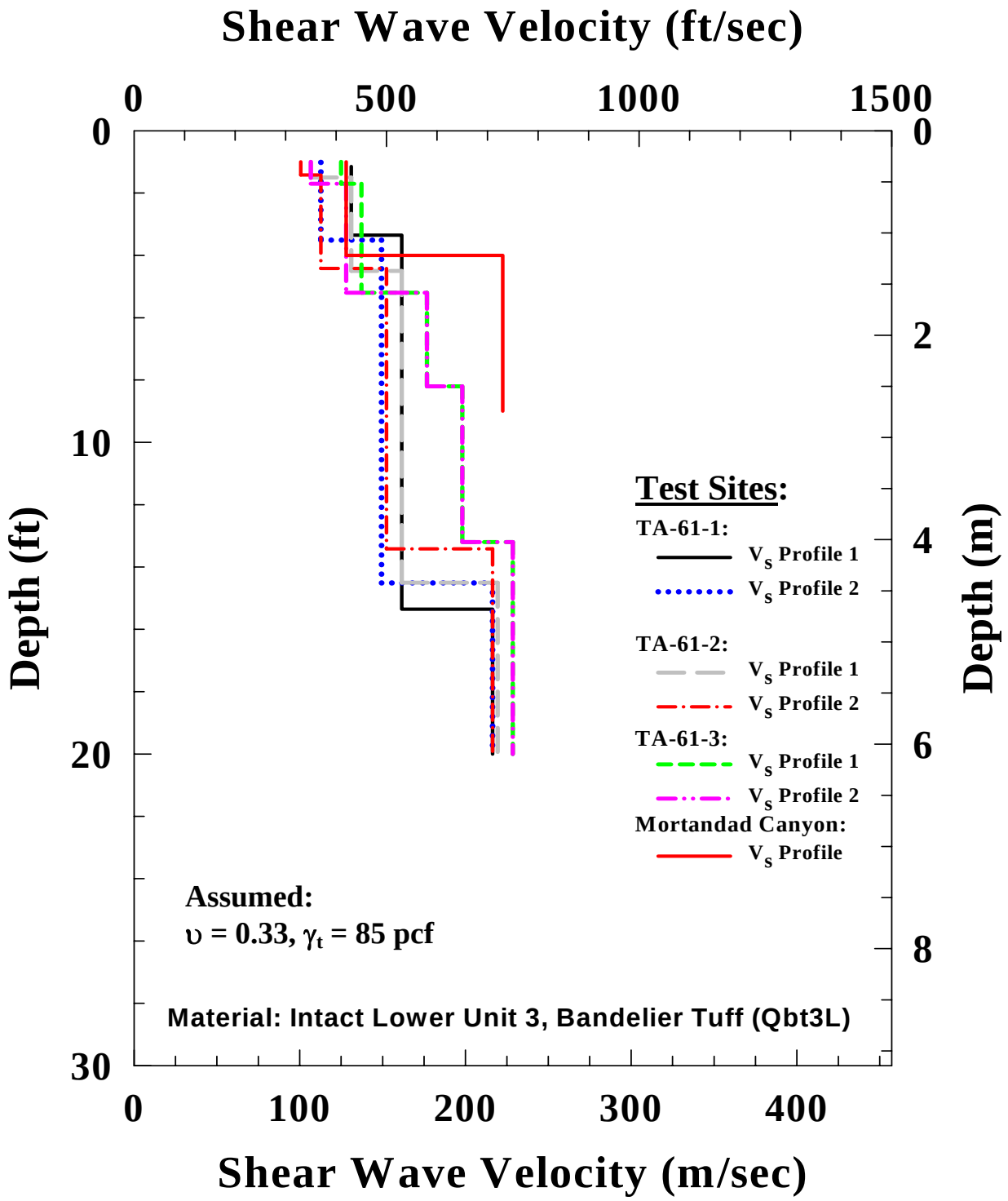

Figure 3 Comparison of the V_s Profiles in the Intact Lower Unit 3, Bandelier Tuff at Sites TA-61-1, TA-61-2, TA-61-3 and Mortandad Canyon at Los Alamos National Laboratory

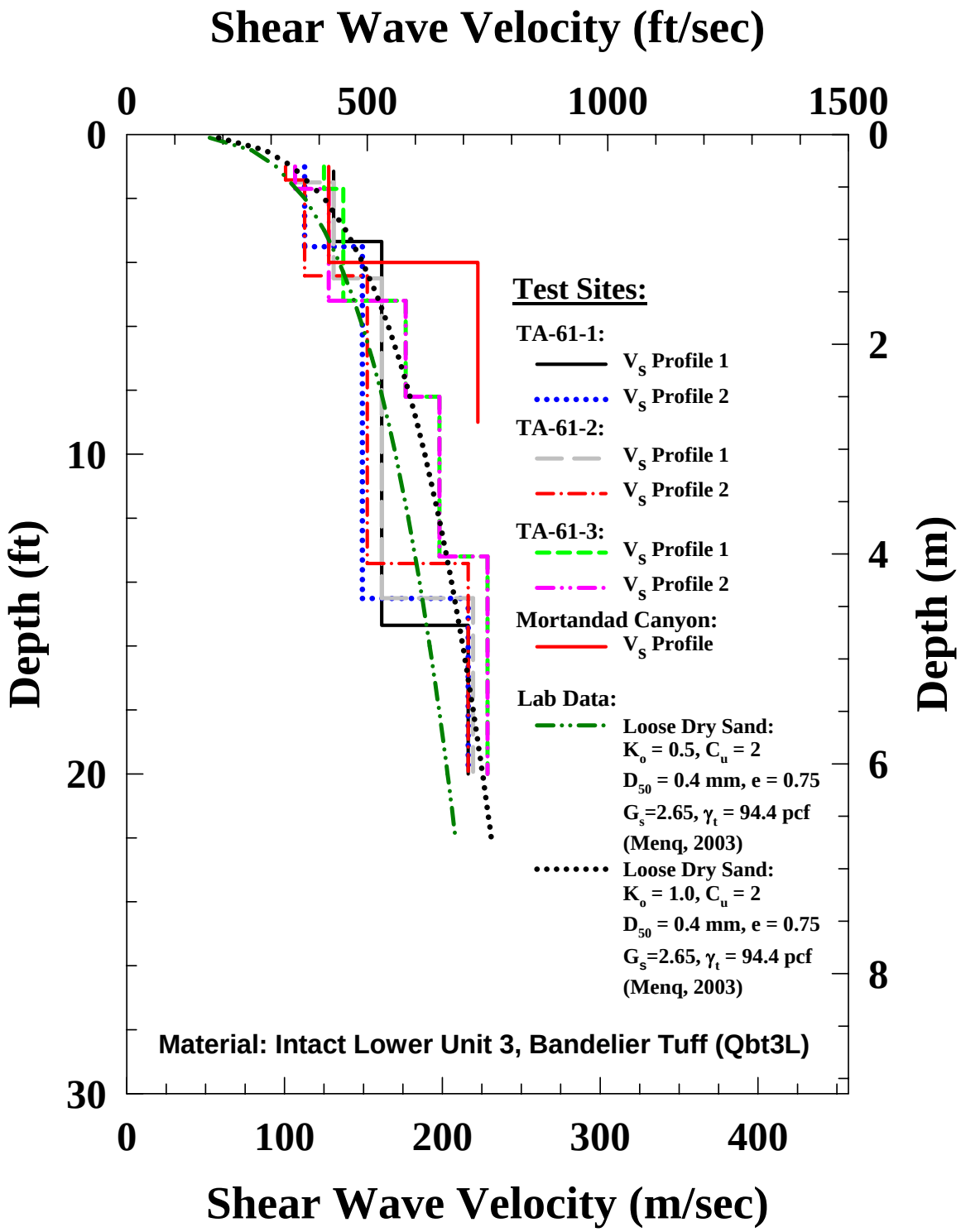

Figure 4 Comparison of V_s Profiles Determined for the Intact Qb3L with V_s Profiles Predicted for Loose Dry Sand

3. DYNAMIC LABORATORY TESTS

Dynamic laboratory tests were performed on two intact specimens of Qbt3L material in January and February, 2005. Combined resonant column and torsional shear (RCTS) equipment was used to evaluate the effects of various parameters on V_s, shear modulus, G, and material damping in shear, D. The RCTS equipment has a fixed-free configuration, with the bottom of the specimen fixed and torsional excitation applied at the top. Appendix C contains a discussion of the RCTS equipment, test procedures and data analysis.

The effects of the following parameters on the dynamic properties of the Qbt3L material were studied:

isotropic confining pressure, σ_0,

shearing strain amplitude, γ,

loading frequency, f, and

number of loading cycles, N.

The results of the laboratory study are presented in graphical and tabular forms in Appendix D. The key results are discussed below.

3.1 Dynamic Properties at Small Strains

Dynamic soil and rock properties are often determined in the laboratory in the strain range where the properties are independent of shearing strain amplitude, γ. These measurements are often called "small-strain" or "low-amplitude" measurements, and the resulting shear wave velocity, shear modulus and material damping terms are denoted as V_s, G_{max} and D_{min}, respectively. One test method that works well in this strain range is the resonant column (RC) method. Testing generally involves performing measurements at shearing strains less than 0.001%.

The variations of V_s, G_{max} and D_{min} with isotropic confining pressure, σ_0, as determined from RC tests are shown in Figures 5, 6 and 7, respectively. The results from both intact Qbt3L specimens are shown in each figure. As seen in the figures, the log V_s - log σ_0, log G_{max} - log σ_0 and log D_{min} - log σ_0 relationships determined with the two specimens are very similar. The log V_s - log σ_0 and log G_{max} - log σ_0 relationships also show a trend with confining pressure similar to that expected for sands (Hardin, 1978) as shown by the measured relationships closely paralleling the dashed trend lines in Figures 5 and 6, respectively.

Copyright 2007, Kleinfelder

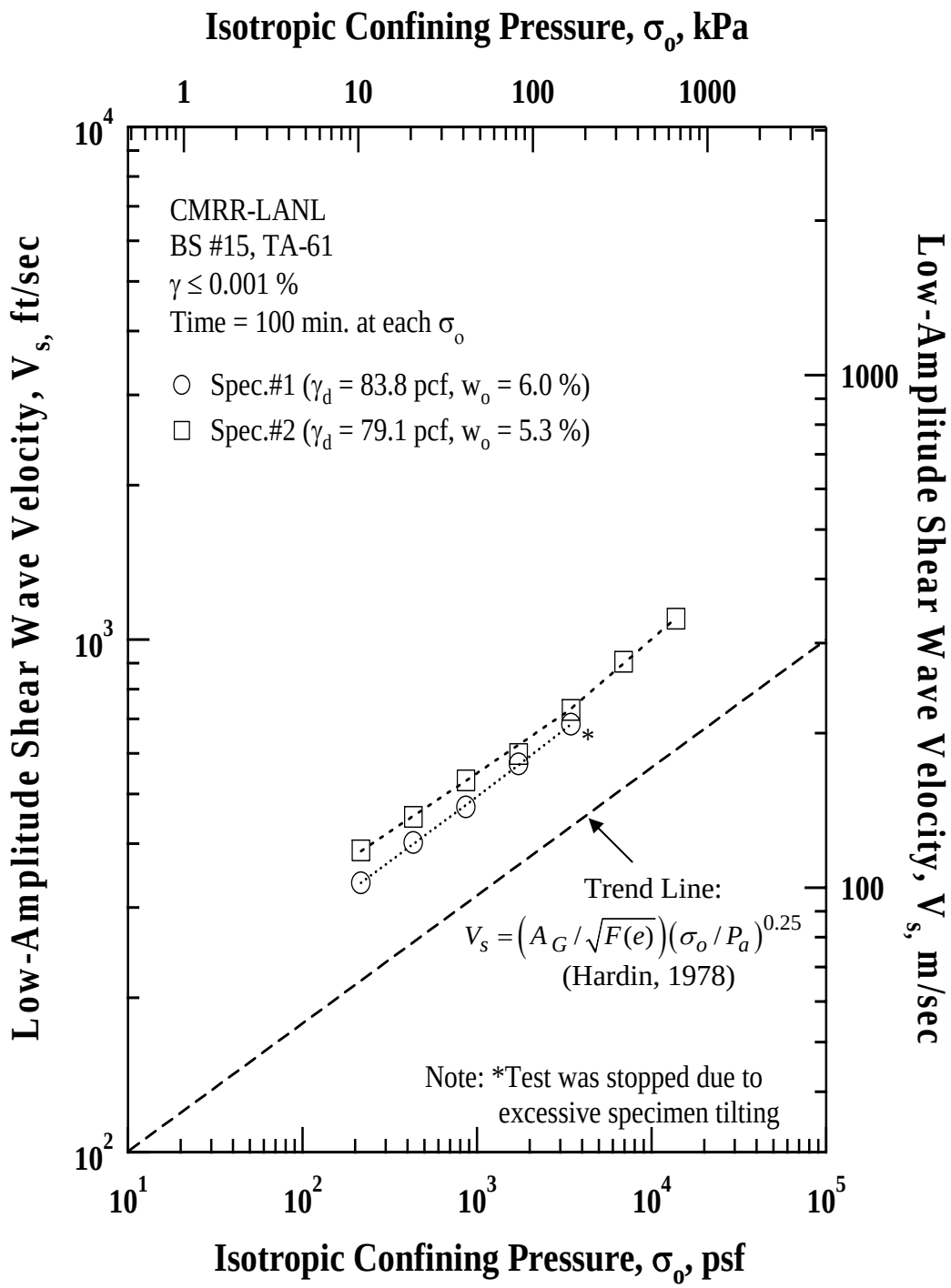

Figure 5 Variation in Low-Amplitude Shear Wave Velocity with Isotropic Confining Pressure of the Two Intact Specimens from Block Sample #15 (Lower Unit 3, Bandelier Tuff (Qbt3L)) as Determined from Resonant Column (RC) Tests

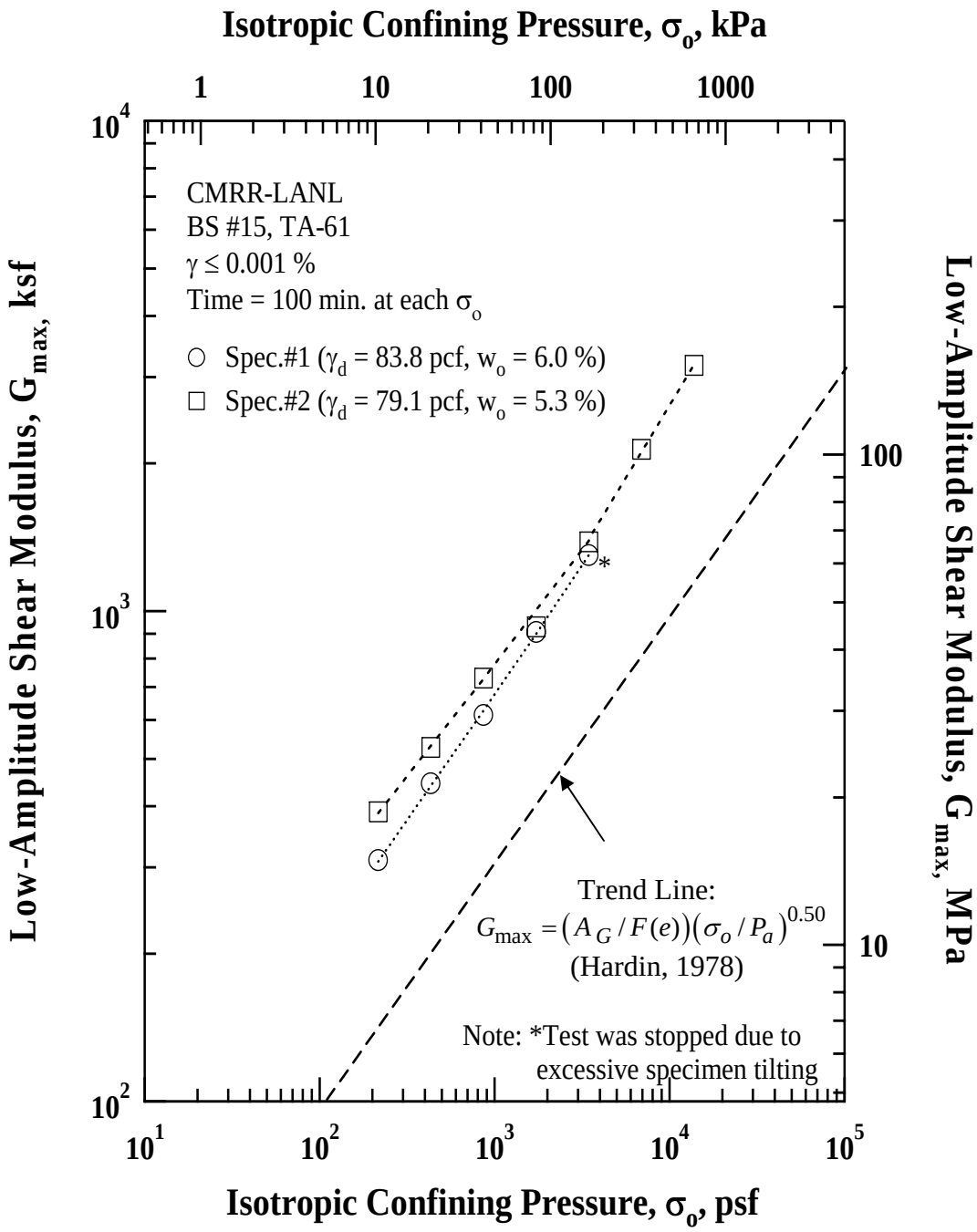

Figure 6 Variation in Low-Amplitude Shear Modulus with Isotropic Confining Pressure of the Two Intact Specimens from Block Sample #15 (Lower Unit 3, Bandelier Tuff (Qbt3L)) as Determined from Resonant Column (RC) Tests

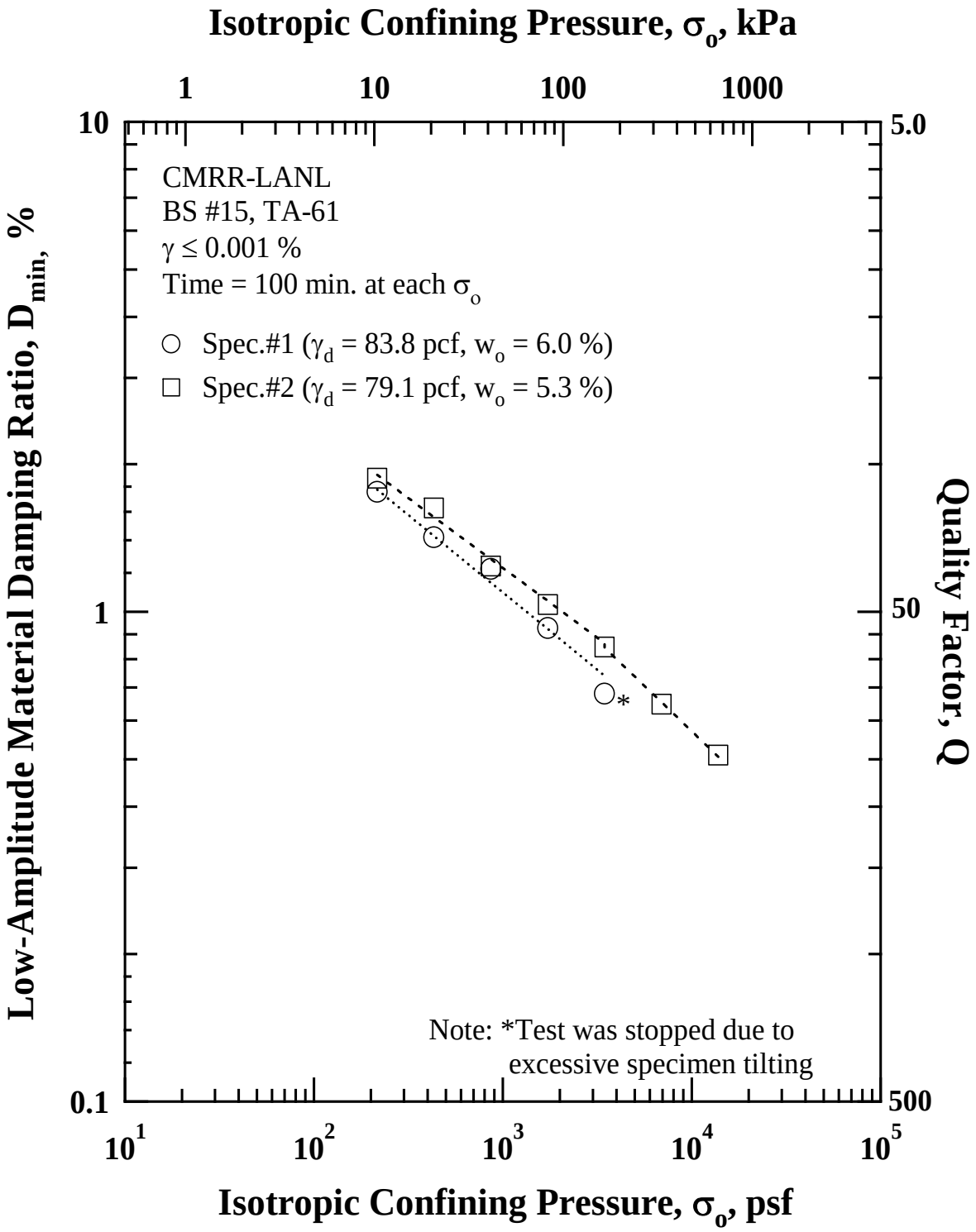

Figure 7 Variation in Low-Amplitude Material Damping Ratio with Isotropic Confining Pressure of the Two Intact Specimens from Block Sample #15 (Lower Unit 3, Bandelier Tuff (Qbt3L)) as Determined from Resonant Column (RC) Tests

3.2 Dynamic Properties in the Nonlinear Range

As shearing strains exceed 0.001%, shear modulus, G, and material damping in shear, D, of soils become nonlinear. In the nonlinear range, G decreases and D increases as γ increases. This behavior is clearly demonstrated by the Qbt3L specimens in both the RC and TS tests. The G-log γ relationships of the two specimens at an isotropic confining pressure of 6 psi (41 kPa) are shown in Figure 8. The nonlinear D-log γ relationships at the same confining pressure are shown in Figure 9. The results in these two figures also show that the effects of excitation frequency, f, and number of loading cycles, N, are not very important because the TS measurements (f = 0.5 Hz and N = 10 cycles) and the RC measurements (f > 20 Hz and N ~ 1000 cycles) are very similar.

The variation in the normalized shear modulus, G/G_{max}, with γ at σ_0 = 6 psi (41 kPa) is shown in Figure 10. In this figure, both the RC and TS measurements from both intact samples are shown. The agreement from all measurements is excellent.

4. COMPARISON OF LABORATORY AND EMPIRICAL RESULTS

The linear measurements performed on the Qbt3L specimens in the laboratory can be compared with empirical results determined from earlier laboratory studies. Such a comparison is shown in Figures 11, 12, and 13 for the log V_s - log σ_0, log G_{max} - log σ_0 and log D_{min} - log σ_0 relationships, respectively. The relationships for the loose, dry sand described in Section 2.2 are compared with the RC measurements in these figures. As seen in Figures 11 and 12, the trends in V_s and G_{max} are well predicted, with the laboratory values slightly overestimated by the empirical relationships (Menq, 2003). The log D_{min} - log σ_0 relationship is, however, not predicted as well as seen in Figure 13.

The nonlinear measurements performed on the Qbt3L specimens are compared with the well known empirical relationships proposed by Seed et al. (1986) for sands. Comparison of the G/G_{max} - log γ relationships is shown in Figure 14. Comparison of the D-log γ relationships is shown in Figure 15. The G/G_{max} - log γ relationship of the intact Qbt3L specimens is slightly underpredicted and the D-log γ relationship is slightly overpredicted. On the other hand, the prediction of the measured nonlinear behavior is somewhat improved when Menq's (2003) empirical results are used as seen in Figures 16 and 17.

Copyright 2007, Kleinfelder

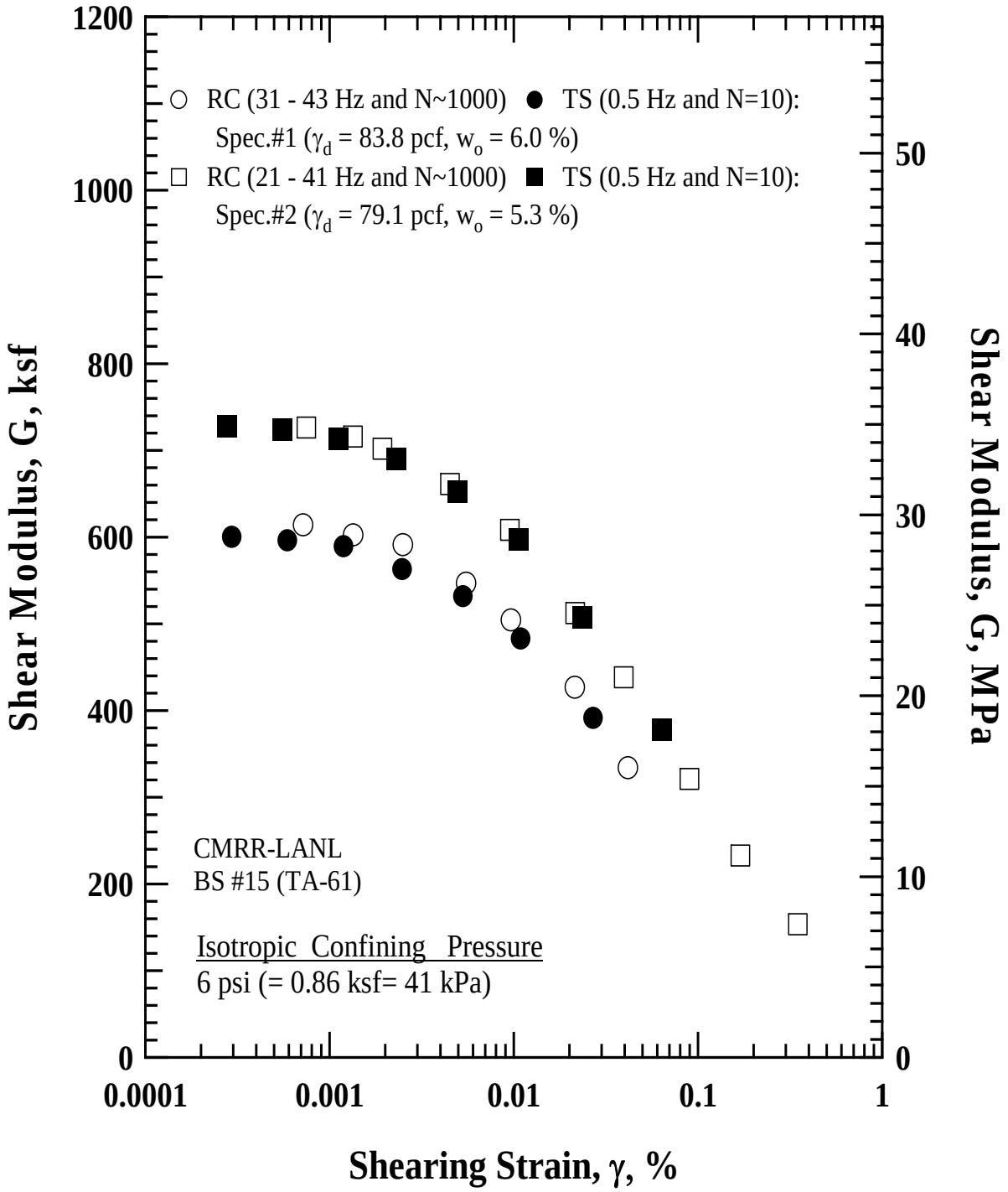

Figure 8 Variation in Shear Modulus with Shearing Strain of the Two Intact Specimens from Block Sample #15 (Lower Unit 3, Bandelier Tuff (Qbt3L)) at an Isotropic Confining Pressure of 0.86 ksf (41 kPa) from Resonant Column (RC) and Torsional Shear (TS) Tests

Copyright 2007, Kleinfelder

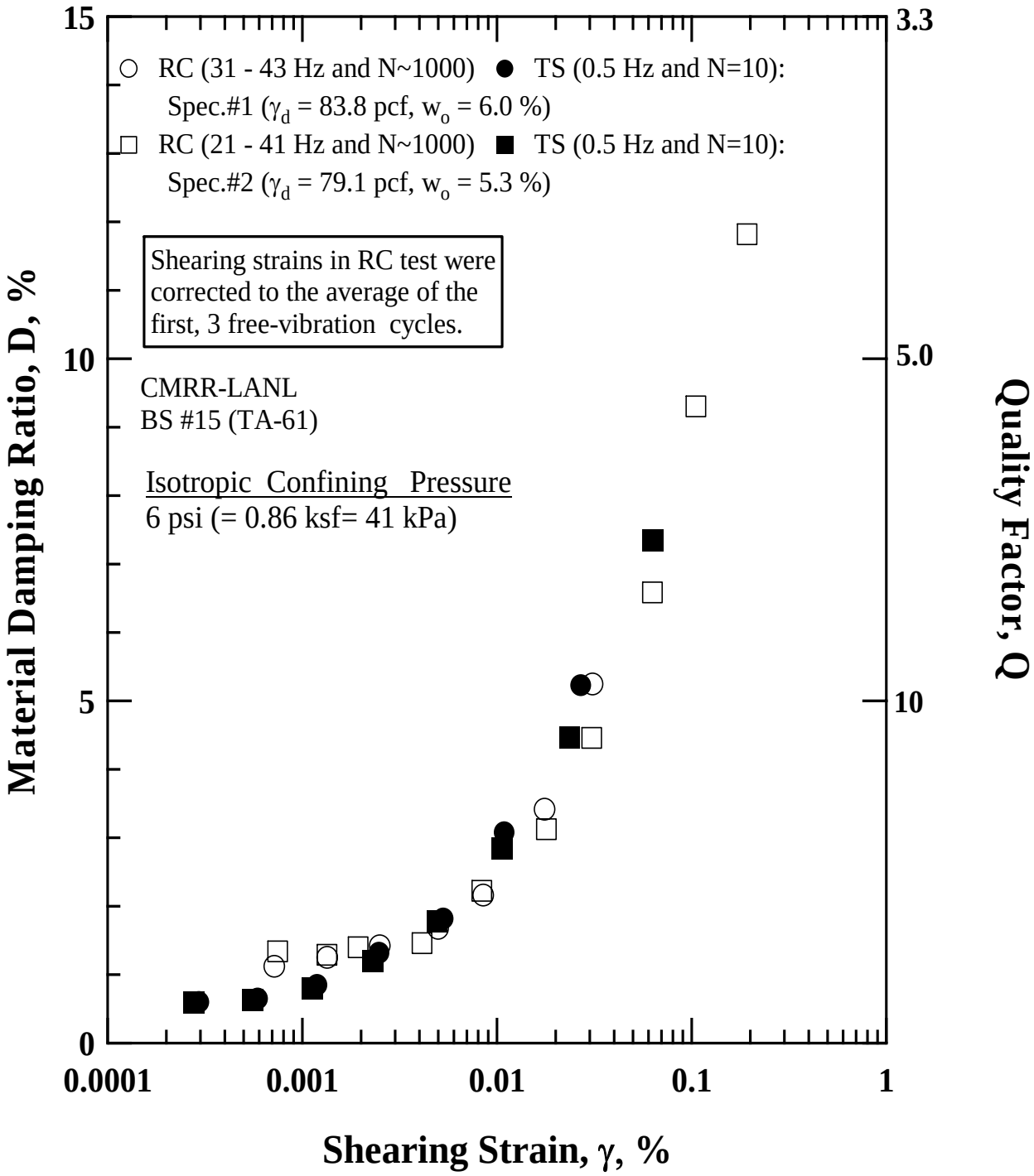

Figure 9 Variation in Material Damping Ratio with Shearing Strain of the Two Intact Specimens from Block Sample #15 (Lower Unit 3, Bandelier Tuff (Qbt3L)) at an Isotropic Confining Pressure of 0.86 ksf (41 kPa) from Resonant Column (RC) and Torsional Shear (TS) Tests

Copyright 2007, Kleinfelder

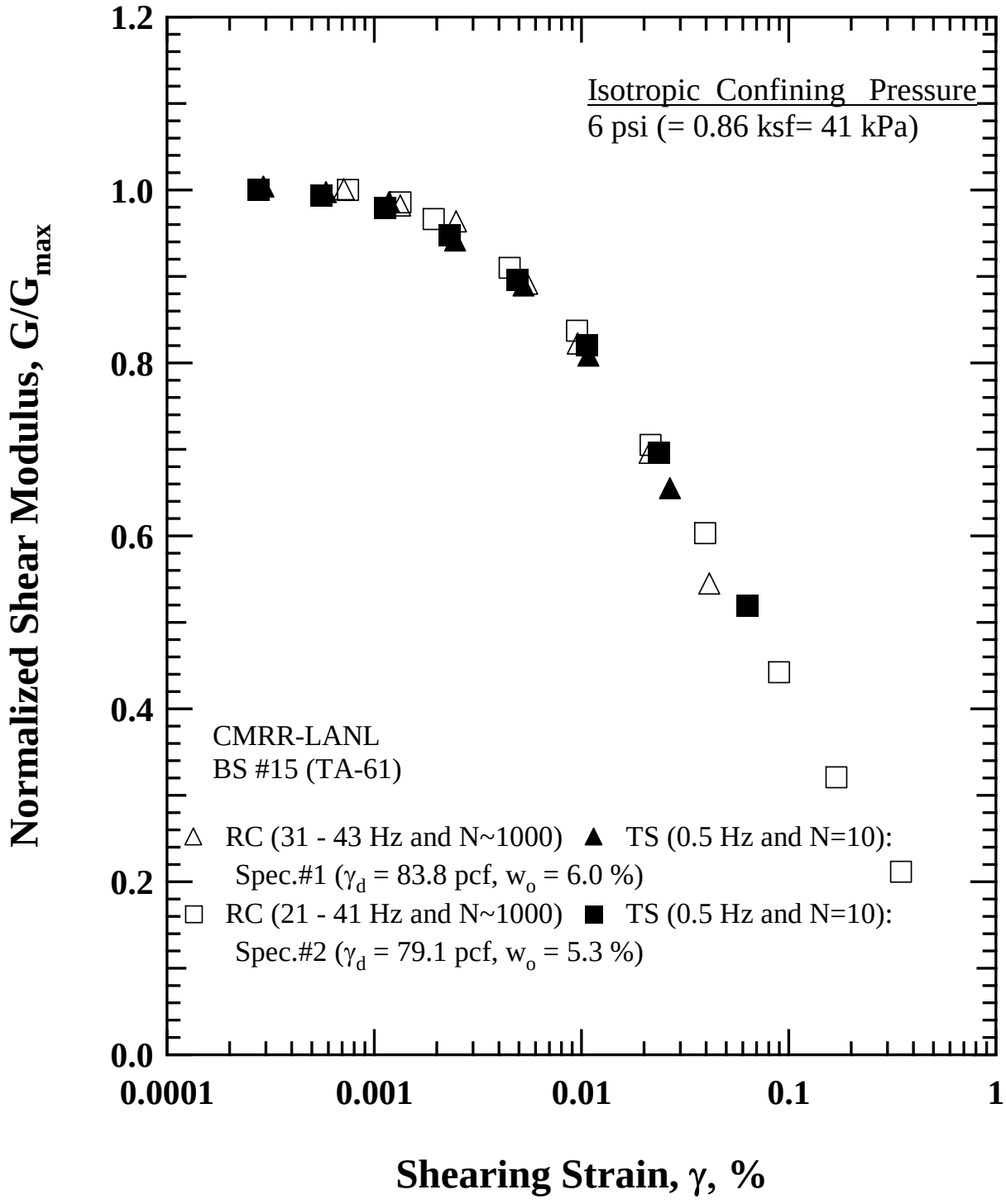

Figure 10 Variation in Normalized Shear Modulus with Shearing Strain of the Two Intact Specimens from Block Sample #15 (Lower Unit 3, Bandelier Tuff (Qbt3L)) at an Isotropic Confining Pressure of 0.86 ksf (41 kPa) from Resonant Column (RC) and Torsional Shear (TS) Tests

Copyright 2007, Kleinfelder

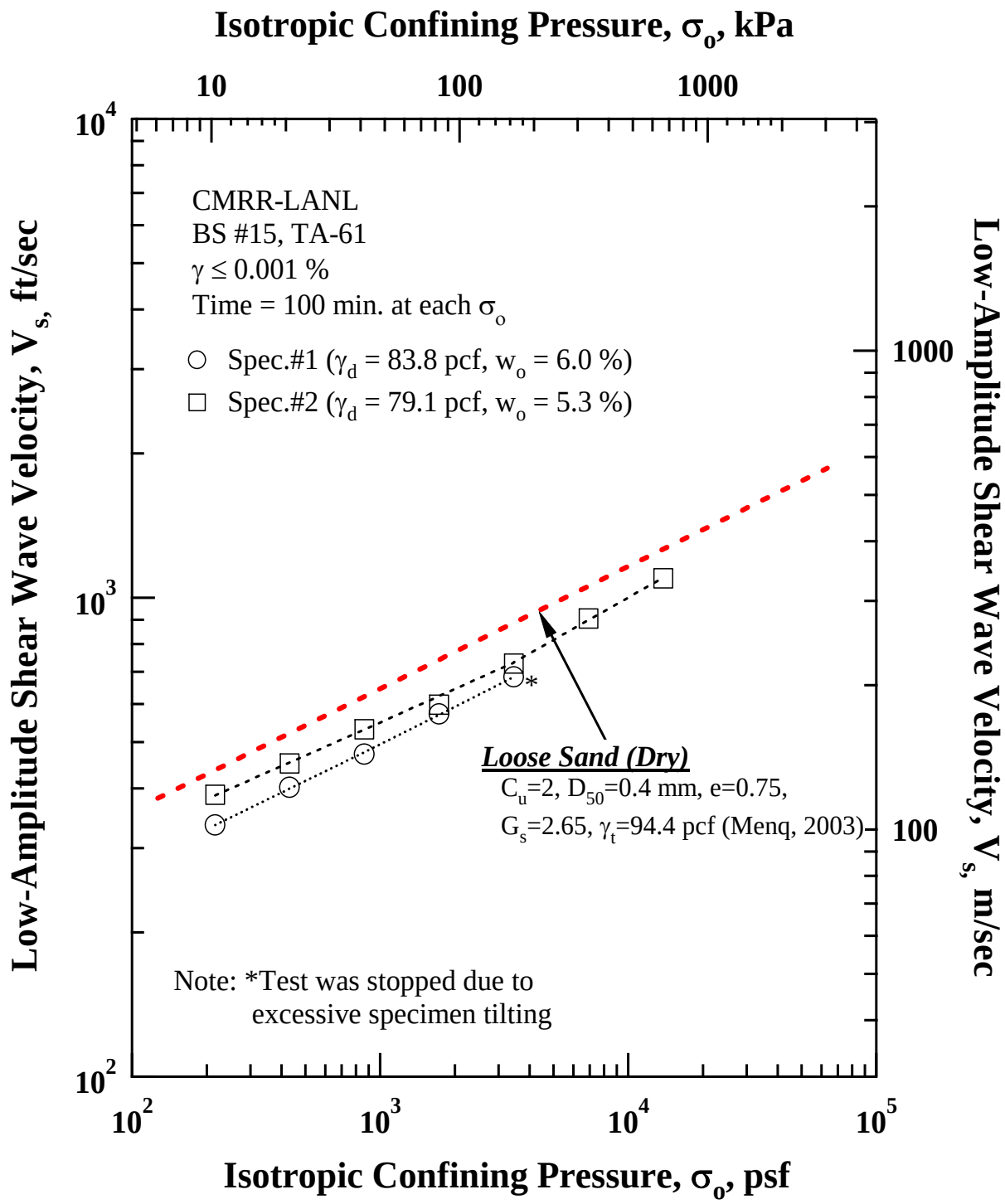

Figure 11 Comparison between the Trend Line for a Dry Loose Sand Predicted by Menq (2003) and the Variation in Low-Amplitude Shear Wave Velocity with Isotropic Confining Pressure of the Two Intact Specimens from Block Sample #15 (Lower Unit 3, Bandelier Tuff (Qbt3L)) as Determined from Resonant Column (RC) Tests

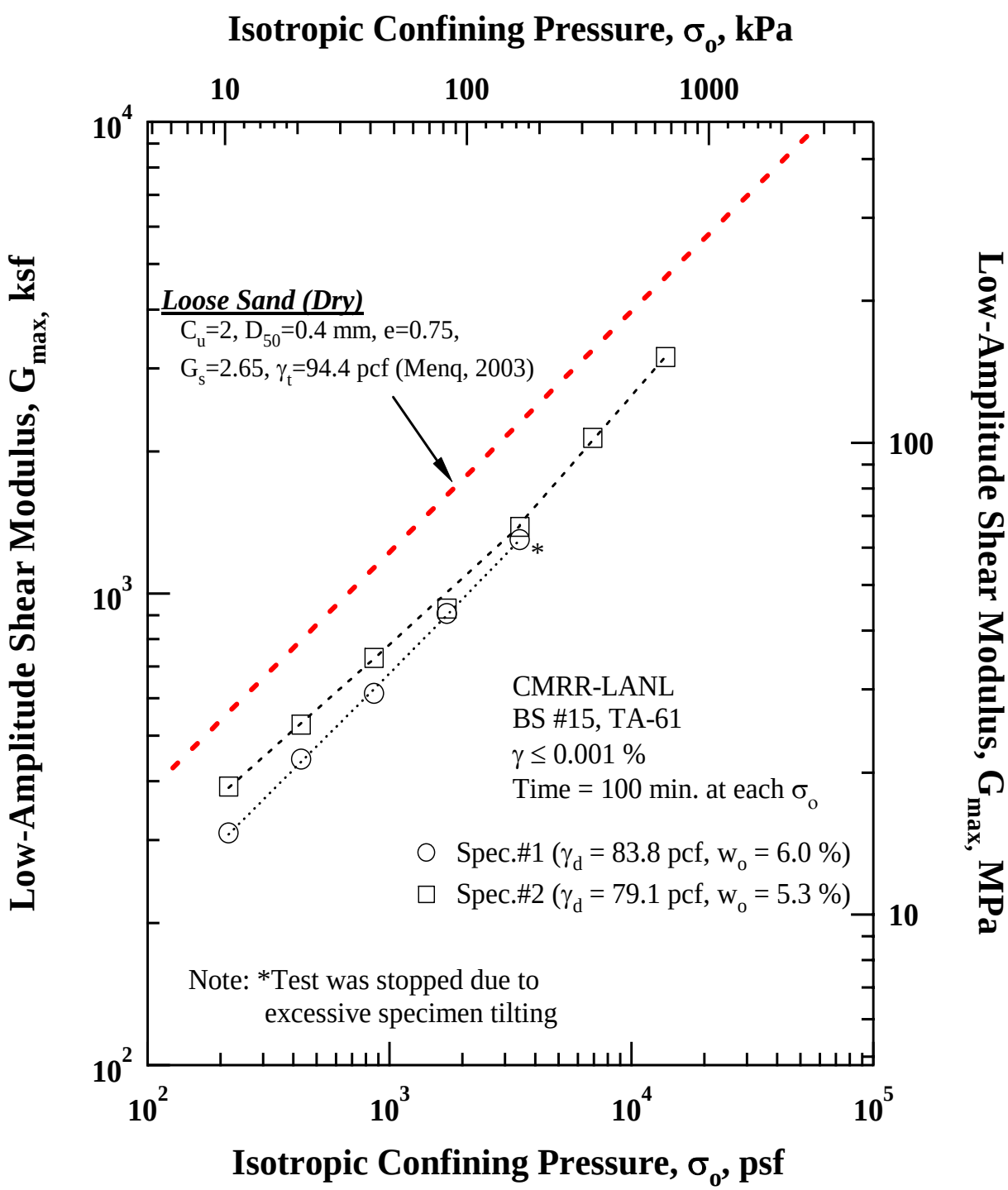

Figure 12 Comparison between the Trend Line for a Dry Loose Sand Predicted by Menq (2003) and the Variation in Low-Amplitude Shear Modulus with Isotropic Confining Pressure of the Two Intact Specimens from Block Sample #15 (Lower Unit 3, Bandelier Tuff (Qbt3L)) as Determined from Resonant Column (RC) Tests

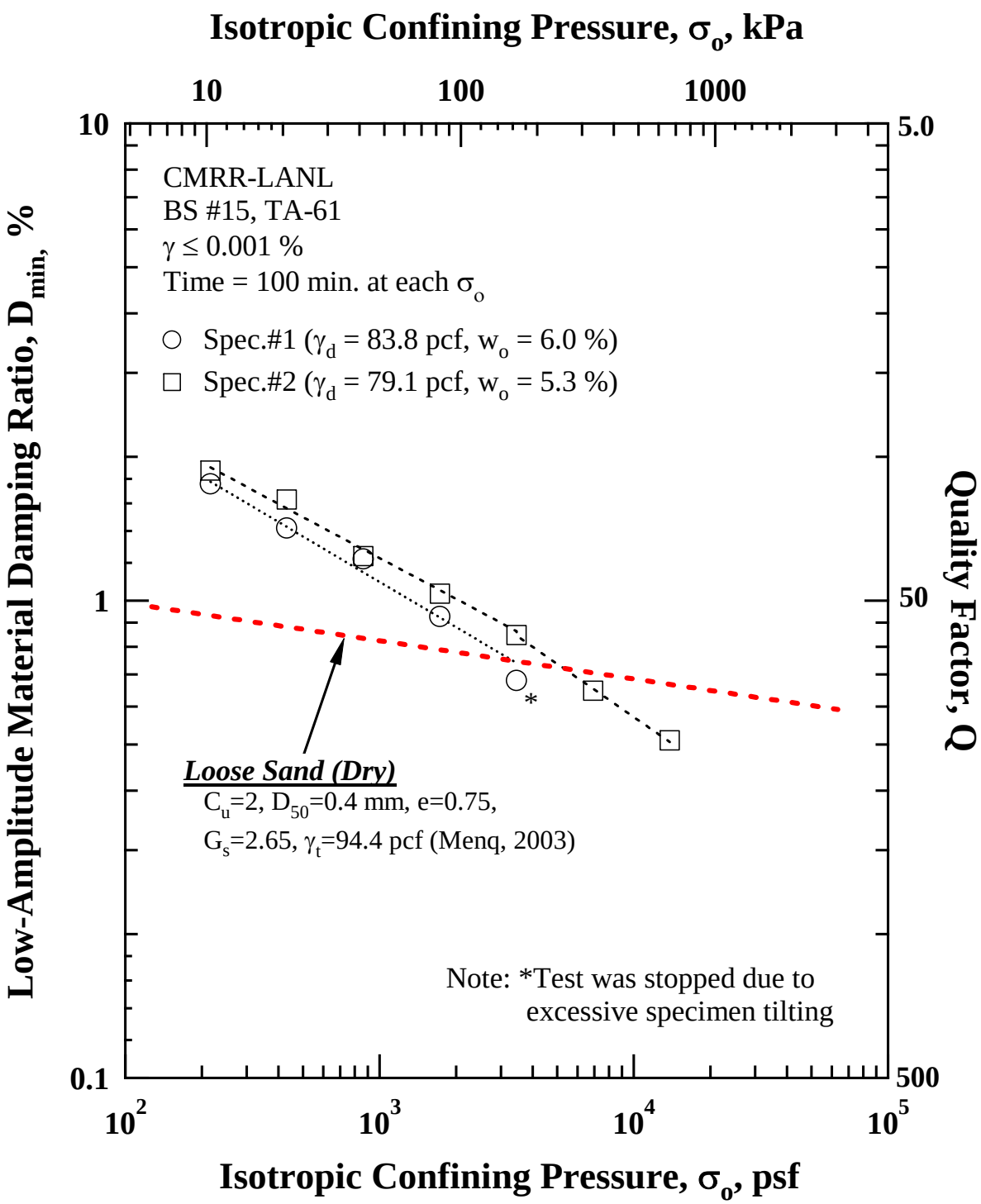

Figure 13 Comparison between the Trend Line for a Dry Loose Sand Predicted by Menq (2003) and the Variation in Low-Amplitude Material Damping Ratio with Isotropic Confining Pressure of the Two Intact Specimens from Block Sample #15 (Lower Unit 3, Bandelier Tuff (Qbt3L)) as Determined from Resonant Column (RC) Tests

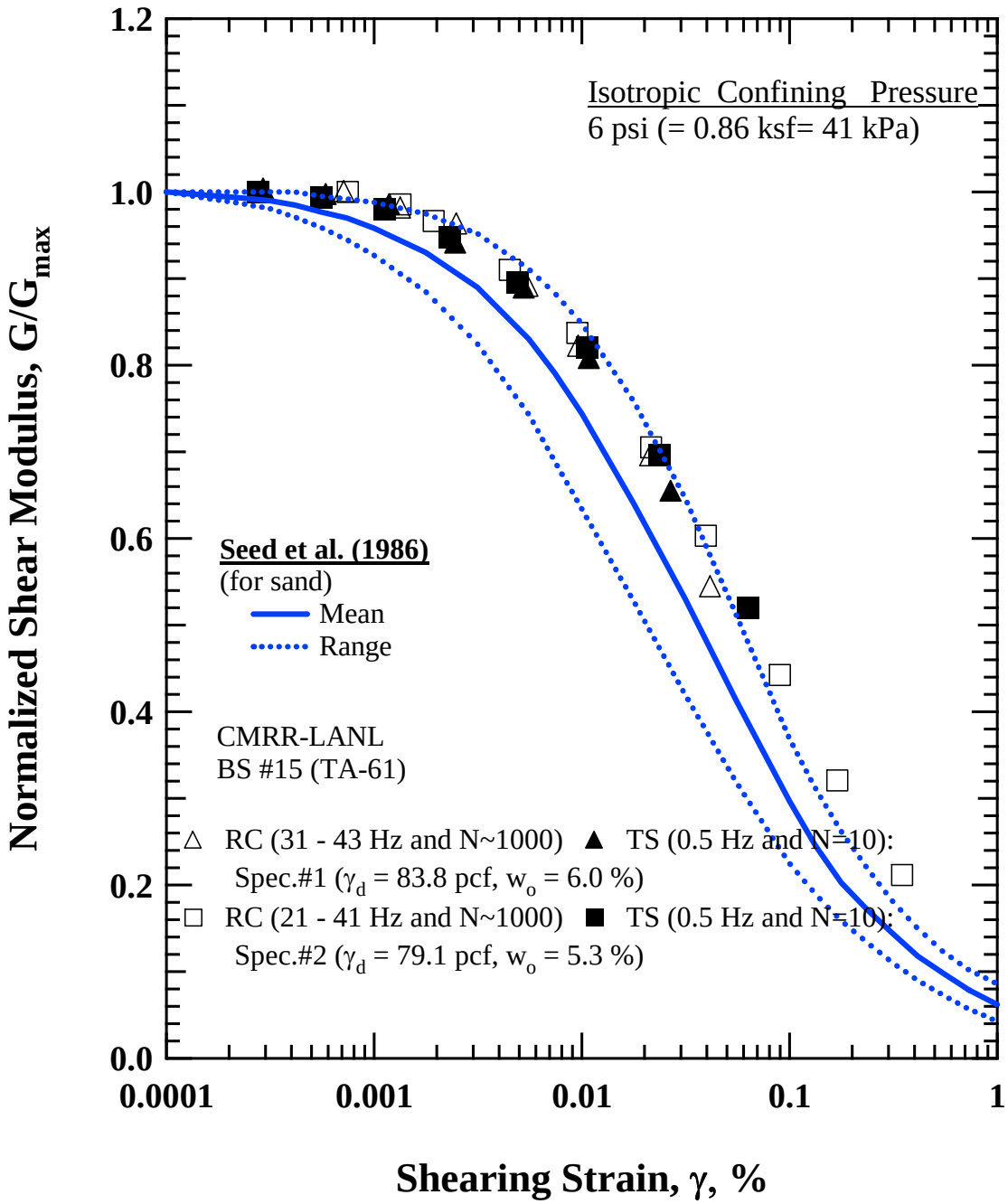

Figure 14 Comparison between the Trend Line for a Dry Loose Sand Predicted by Seed et al. (1986) and the Variation in Shear Modulus with Shearing Strain of the Two Intact Specimens from Block Sample #15 (Lower Unit 3, Bandelier Tuff (Qbt3L)) as Determined from Resonant Column (RC) Tests

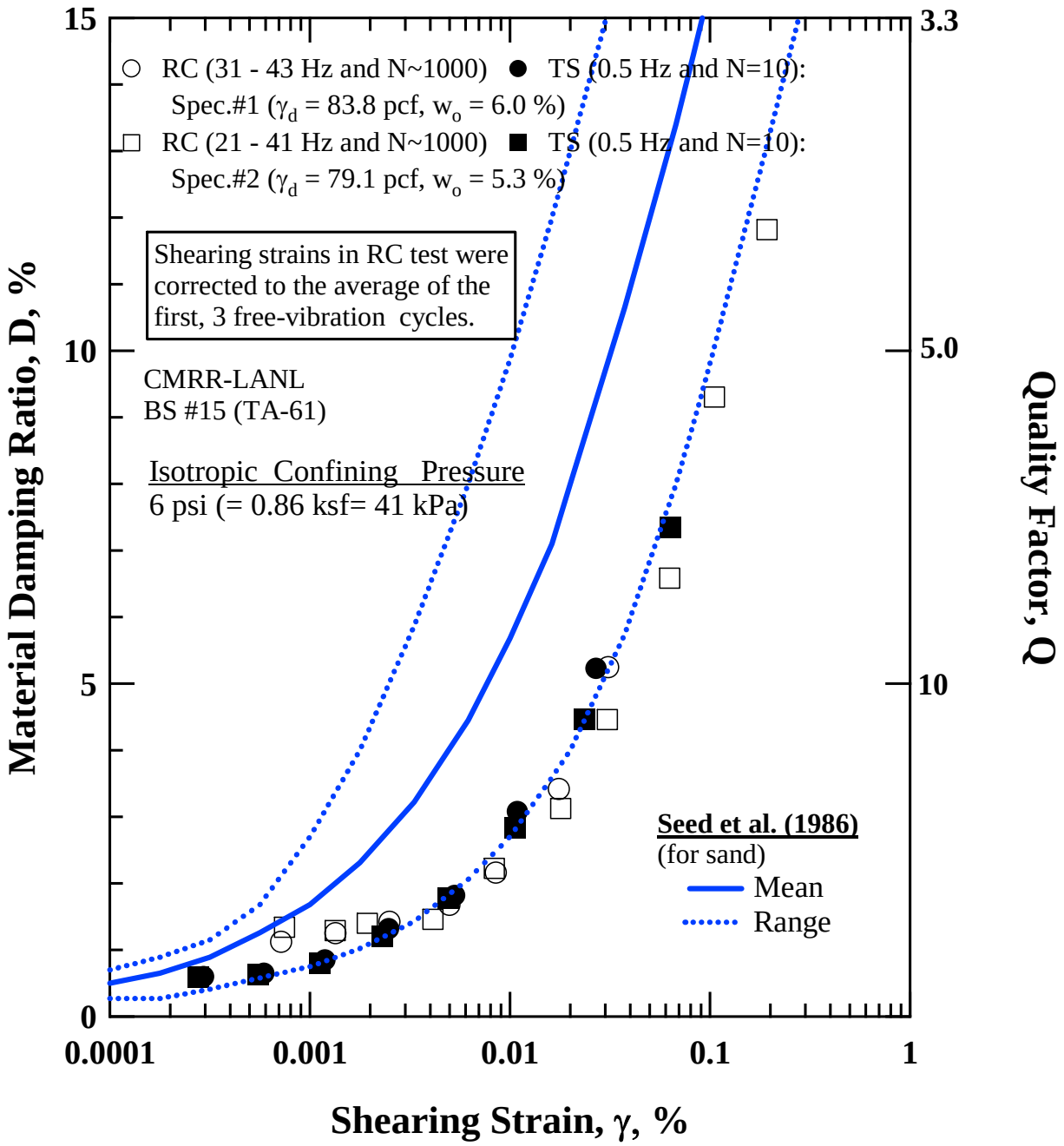

Figure 15 Comparison between the Trend Line for a Dry Loose Sand Predicted by Seed et al. (1986) and the Variation in Material Damping Ratio with Shearing Strain of the Two Intact Specimens from Block Sample #15 (Lower Unit 3, Bandelier Tuff (Qbt3L)) as Determined from Resonant Column (RC) Tests

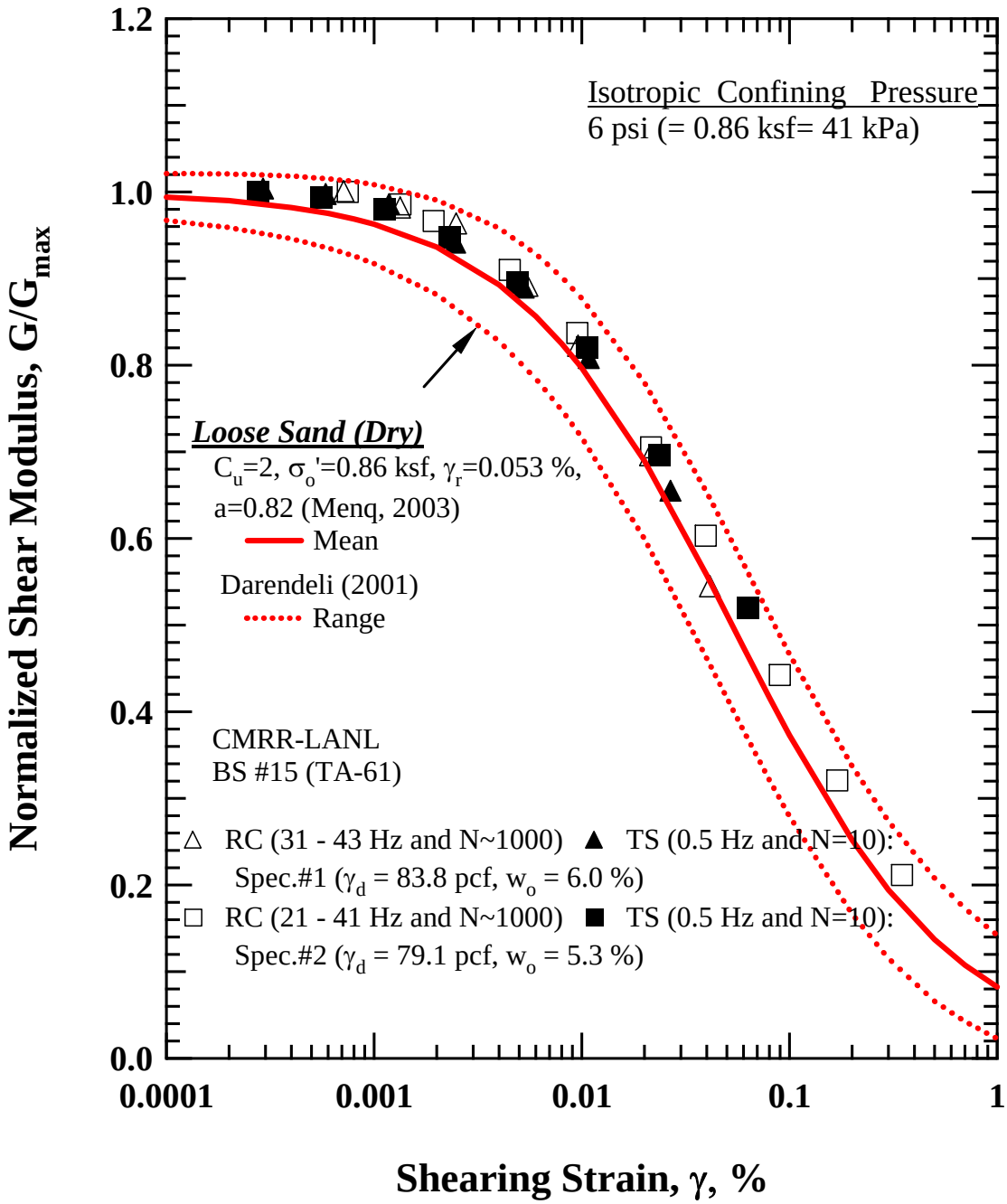

Figure 16 Comparison between the Trend Line for a Dry Loose Sand Predicted by Menq (2003) and Darendeli (2001) and the Variation in Normalized Shear Modulus with Shearing Strain of the Two Intact Specimens from Block Sample #15 (Lower Unit 3, Bandelier Tuff (Qbt3L)) as Determined from Resonant Column (RC) Tests

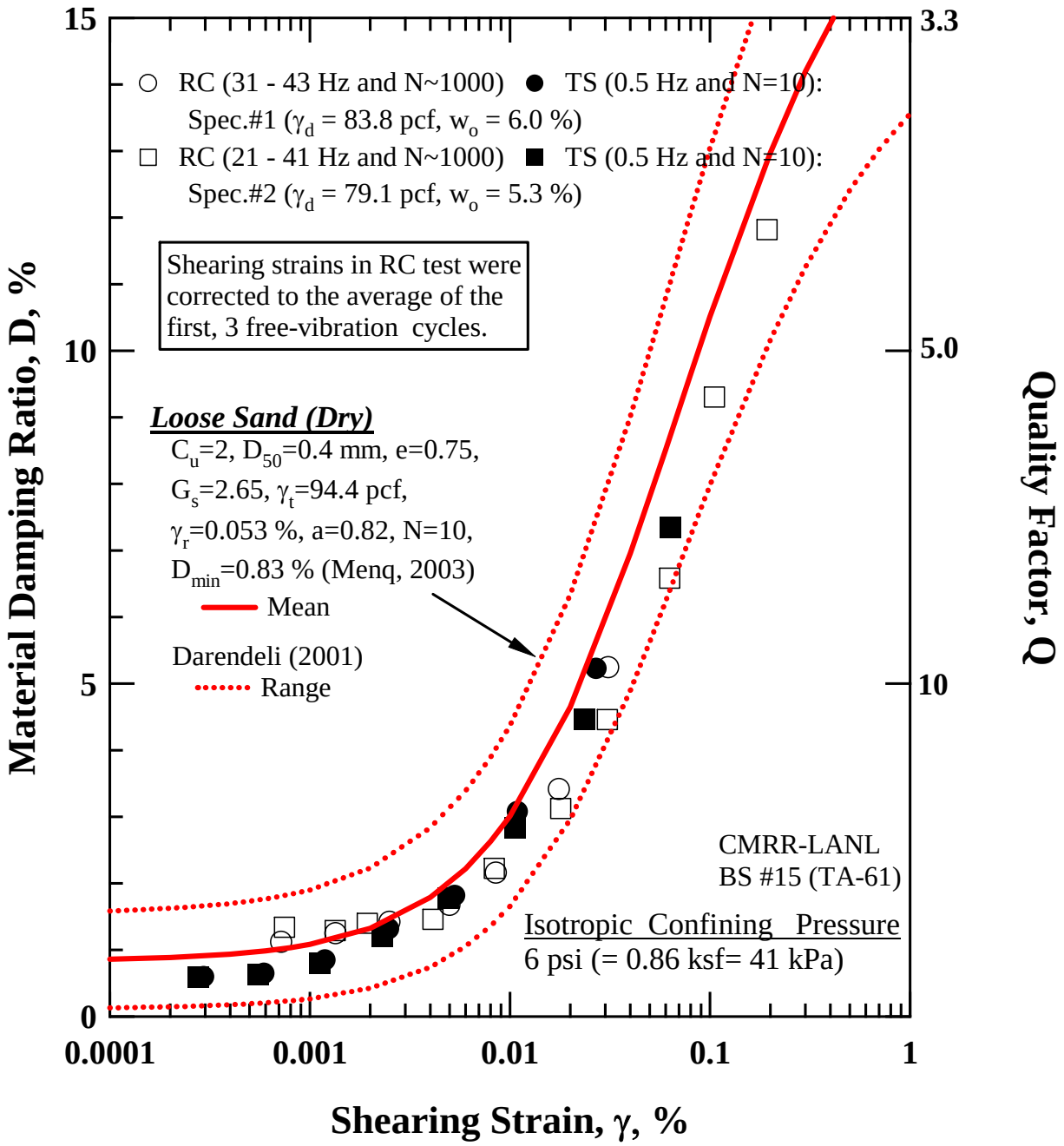

Figure 17 Comparison between the Trend Line for a Dry Loose Sand Predicted by Menq. (2003) and Darendeli (2001) and the Variation in Material Damping Ratio with Shearing Strain of the Two Intact Specimens from Block Sample #15 (Lower Unit 3, Bandelier Tuff (Qbt3L)) as Determined from Resonant Column (RC) Tests

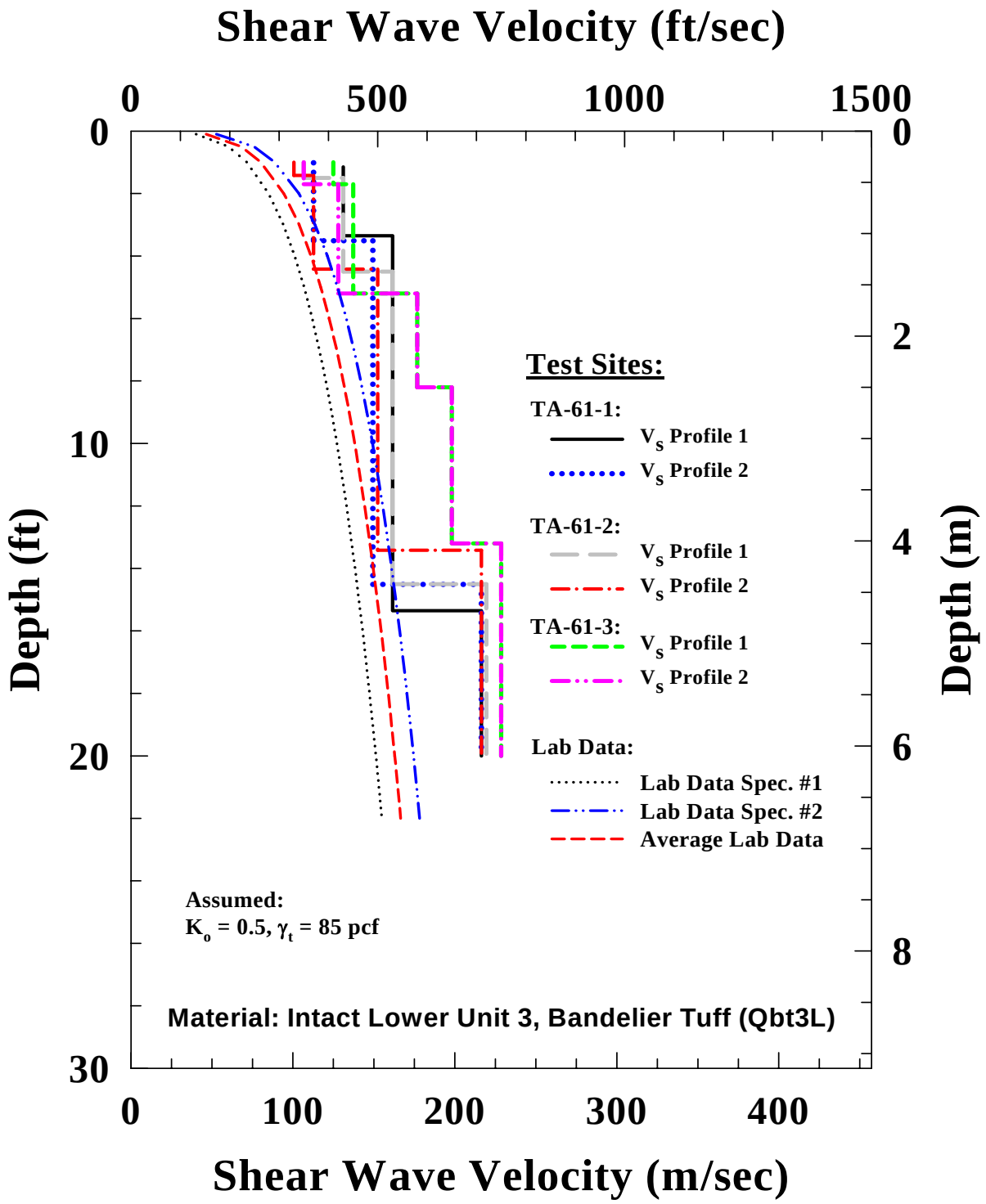

Figure 18 Comparison of Field-Measured V_s Profiles at the TA-61 Borrow Pit and Laboratory-Predicted V_s Profiles (K_o = 0.5, γ_t = 85 pcf) of the Qbt3L

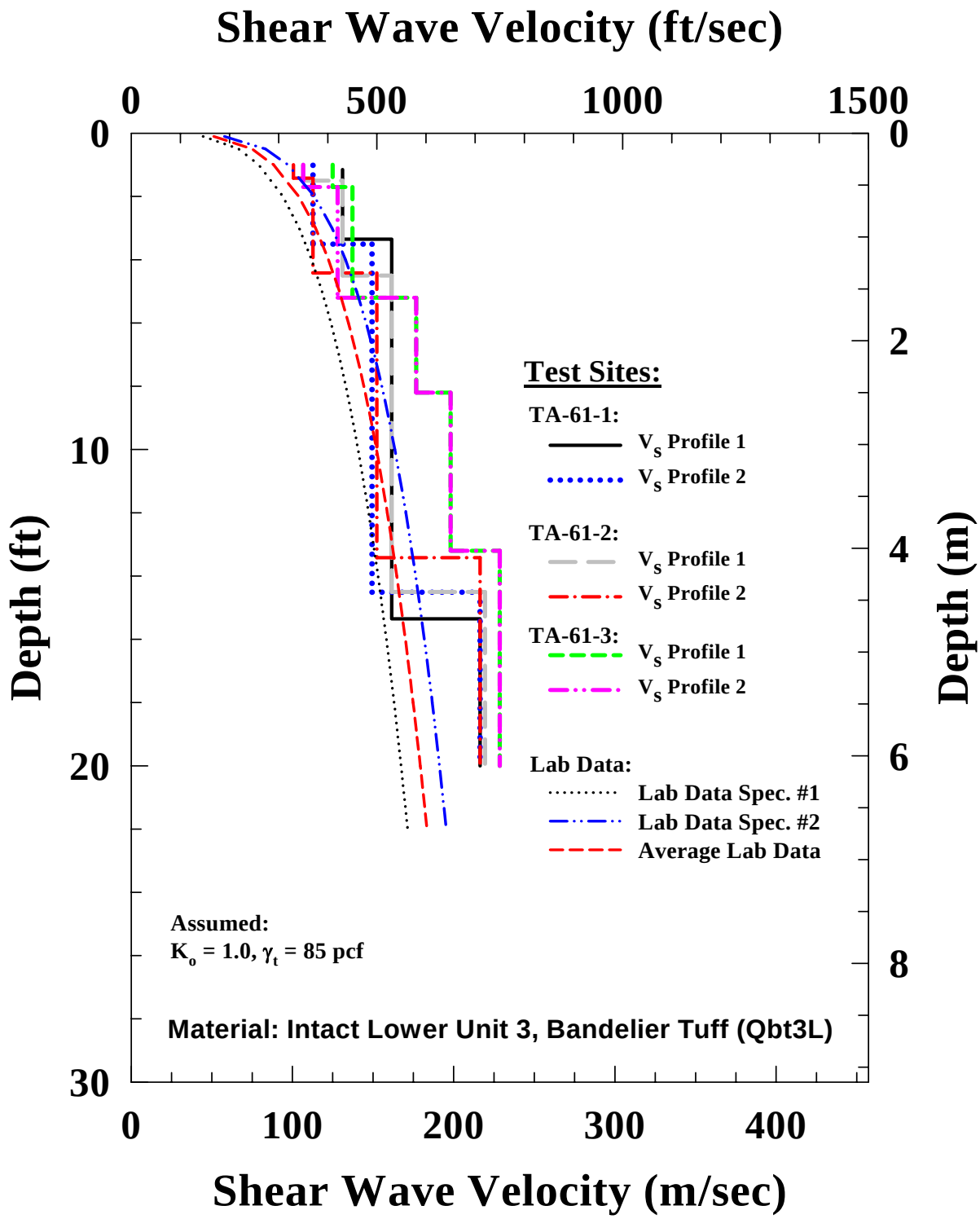

Figure 19 Comparison of Field-Measured V_s Profiles at the TA-61 Borrow Pit and Laboratory-Predicted V_s Profiles (K_o = 1.0, γ_t = 85 pcf) of the Qbt3L

5. COMPARISON OF V_S VALUES OF THE QBT3L MEASURED IN THE FIELD AND LABORATORY

The final comparison that should be made is to compare the in situ V_s profiles of the Qbt3L material (shown in Figure 3) with the profiles that would be predicted from the laboratory measurements (shown in Figure 5). The only field measurements used in this comparison are those that were performed in the vicinity of the block sample from which the intact laboratory specimens were hand carved. This comparison requires that the state of stress in the laboratory test and the depth in the field test be related. This relation can be expresses as:

$$\sigma_0 - (\sigma_v + 2\ \sigma_h)/3 \quad (1)$$

$$\sigma_v = \gamma_t * d \quad (2)$$

$$\sigma_h = K_0\ \sigma_v \quad (3)$$

where the field parameters are: σ_v = total vertical normal stress, σ_h = equals total horizontal normal stress, γ_t = total unit weight, d = depth below the ground surface, and K_0 = coefficient of earth pressure at rest.

By assuming γ_t = 85 pcf and a range in the values of K_0, the field V_s profiles can be compared with the laboratory-predicted profiles. These comparisons are shown in Figures 18 and 19 for K_0 = 0.5 and K_0 = 1.0, respectively. As noted above, only the field V_s profiles measured in the vicinity of the block sample (the three SASW sites in the TA-61 Borrow Pit) are used. The better comparison is found when K_0 = 1.0 is assumed. However, the laboratory-predicted V_s profiles still slightly underpredict the field V_s measurements. Laboratory V_s values underpredicting field values is typically found in the literature (Stokoe et al., 2004). However, the comparison shown in Figure 19 is quite close which indicates high-quality Qbt3L specimens.

6. REFERENCES

Darendeli, B. M. (2001). "Development of a New Family of Normalized Modulus Reduction and Material Damping Curves," Ph.D. Dissertation, University of Texas at Austin, 362 p.

Hardin, B.O. (1978), "Nature of Stress-Strain Behavior for Soils," Proceedings, Geotech. Eng. Div. Specialty Conference on Earthquake Eng. And Soil Dynamics, Vol. 1, ASCE, Pasadena, June, pp. 3-90.

Copyright 2007, Kleinfelder

Menq, F.-Y. (2003), "Dynamic Properties of Sandy and Gravelly Soils," Ph.D. Dissertation, University of Texas at Austin, 364 p.

Seed, H.B., R.T. Wong, I.M. Idriss, and K. Tokimatsu (1986), "Moduli and Damping Factors For Dynamic Analyses of Cohesionless Soils," Journal of the Soil Mechanics and Foundations Division, Vol. 112, No. SM11, pp. 1016-1032.

Stokoe, K.H., Joh, S.H., Woods, R.D. (2004). "Some Contributions on In Situ Geophysical Measurements to Solving Geotechnical Engineering Problems," 2nd International Conference on Geotechnical and Geophysical Site Characterization, Edited by A. Viana da Fonseca and P.W. Mayne, Vol. 1, September, pp. 97-132.

APPENDIX A

SEISMIC TESTING BY THE SPECTRAL-ANALYSIS-OF-SURFACE- WAVES (SASW) METHOD

APPENDIX A

SEISMIC TESTING BY THE SPECTRAL-ANALYSIS-OF-SURFACE-WAVES (SASW) METHOD

A.1 BACKGROUND ON SASW METHOD

The spectral-analysis-of-surface-waves (SASW) method is an in situ seismic method for determining shear wave velocity profiles at geotechnical sites. The test is non-invasive and non-destructive, with testing performed on the ground surface at strain levels in the elastic range ($\gamma <$ 0.001%). From the modeled shear wave velocity (V_S) profile, a small-strain shear modulus, G_{max}, profile can be determined using an estimated total mass density, ρ_t, as:

$$G_{max} = \rho_t * V_S^2 \quad (1)$$

SASW testing has been used for a variety of engineering applications requiring shear stiffness data, including studies of earthquake site response, liquefaction susceptibility analyses, soil compaction control and evaluation, and pavement testing (Nazarian and Stokoe, 1986; Stokoe et al., 1988; Andrus, 1994; Brown, 1998; Bueno, 1998; Stokoe et al., 2003; and Stokoe et al., 2004).

A.2 BASIS OF SASW METHOD

The basis of the SASW method is the dispersive characteristic of Rayleigh waves when propagating in a layered system. The phase velocity, V_R, depends primarily on the material properties (shear wave velocity, mass density, and Poisson's ratio or compression wave velocity) over a depth of approximately one wavelength. Waves of different wavelengths, λ, (or frequencies, f) sample different depths as illustrated in Figure A.1. As a result of the varying shear stiffnesses of the layers, waves with different wavelengths travel at different phase velocities. A surface wave dispersion curve, or dispersion curve for short, is the variation of V_R with λ or f, and it is the key characteristic of the site evaluated in the field for stiffness profiling.

Copyright 2007, Kleinfelder

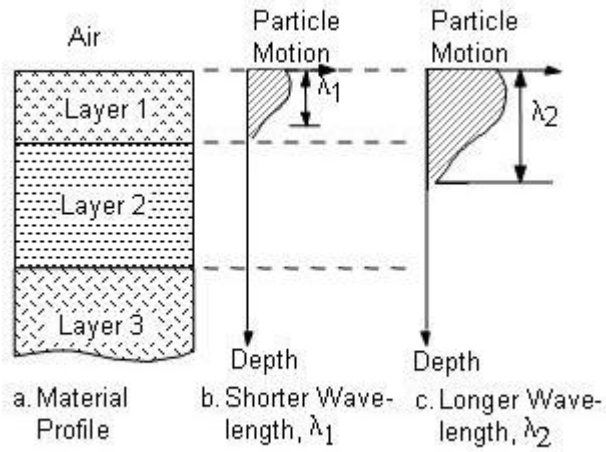

Figure A.1 Approximate Distribution of Vertical Particle Motion with Depth for Two Surface Waves with Different Wavelengths

A.2.1 FIELD TESTING

The test method involves actively exciting surface wave energy at one point and measuring the resulting vertical surface motions at various distances (receiver points) away from the source. Figure A.2a shows the typical field testing arrangement for one set-up of the source and two receivers. Measurements are performed along a linear array placed on the ground surface. Fourier transforms are performed on the recorded time records of two (or more) vertical receivers. The phase-difference relationship between the receivers as a function of frequency (ϕ vs. f) is found from the cross power spectrum, $G_{12}(f)$, defined by:

$$G_{12}(f)=S_1(f)\, S^*_2(f) \qquad (2)$$

where $S_1(f)$ is the Fourier transform of receiver 1 and $S^*_2(f)$ is the complex conjugate of the Fourier transform of receiver 2. A typical ϕ vs. f result is shown in Figure A.2b for one receiver pair. The ϕ vs. f plot in Figure A.2b is called a wrapped phase plot because of the "jumps" present in the plot. These "jumps" represent 360-degree phase shifts or full cycles of the wave. By properly counting these jumps, the phase plot can be unwrapped, as illustrated in Figures A.3a and A.3b. From the unwrapped phase and frequency values, the phase velocity can be found from:

$$V_R = f * (360/\phi)*d \quad (3)$$

where V_R is the phase velocity, f is the frequency, ϕ is the unwrapped phase angle and d is the receiver spacing. Therefore, a plot of phase velocity vs. wavelength can be determined as shown in Figure A.3c. In this particular test, the receiver spacing was 30.5 m, the source was a moving bulldozer, and the source was positioned slightly more than 30.5 m from the first receiver.

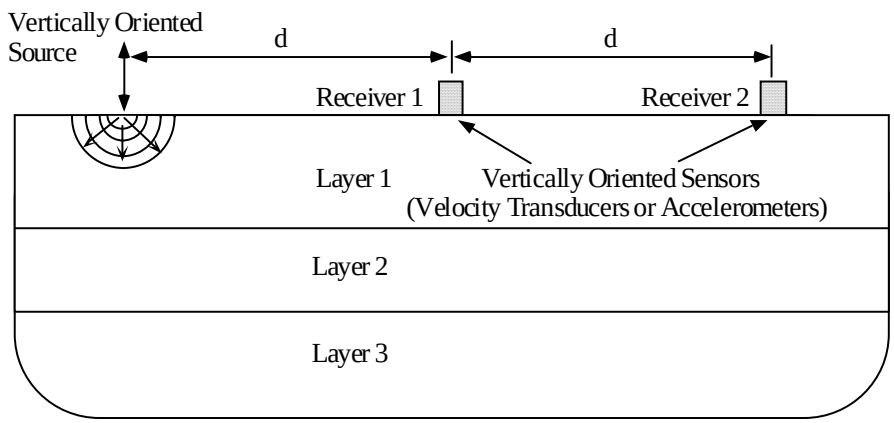

a. Field Arrangement of Source and Receivers for One Set-Up

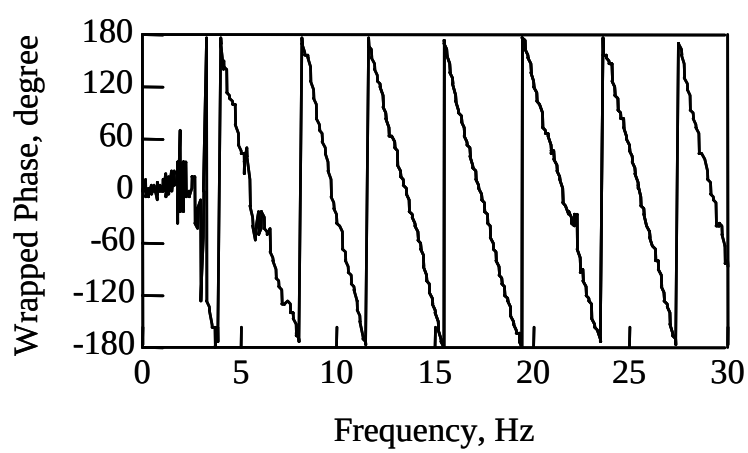

b. Wrapped Phase Spectrum Determined from Surface Waves Propagating between Receivers (30.5-m Receiver Spacing)

Figure A.2 Typical SASW Field Arrangement and Associated Phase Spectrum Measurement from One Source-Receivers Set-Up

Copyright 2007, Kleinfelder

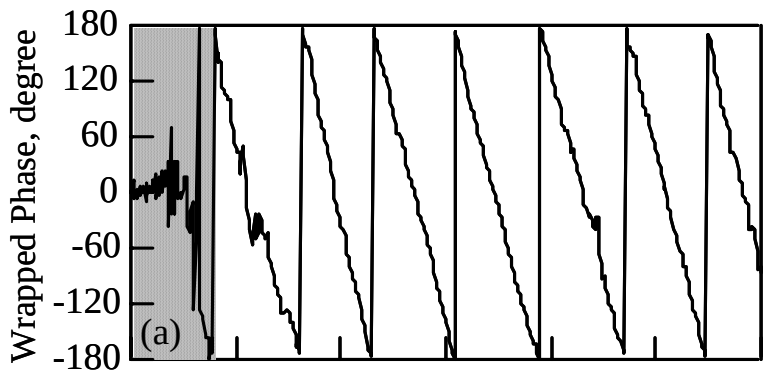

a. Wrapped Phase Spectrum (30.5-m Receiver Spacing)

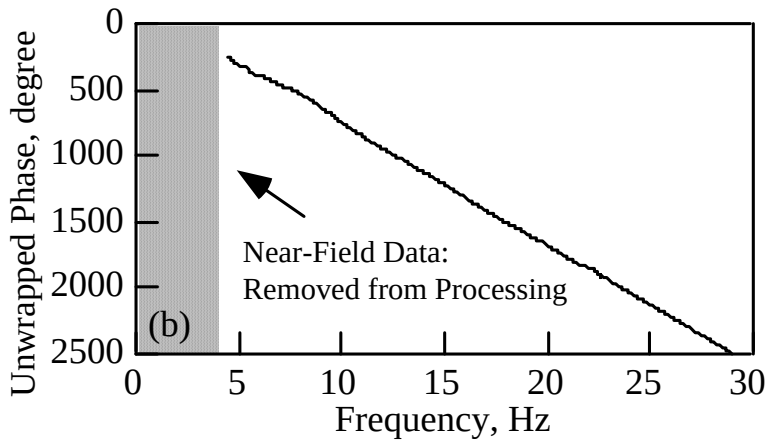

a. Unwrapped Phase Spectrum (30.5-m Receiver Spacing)

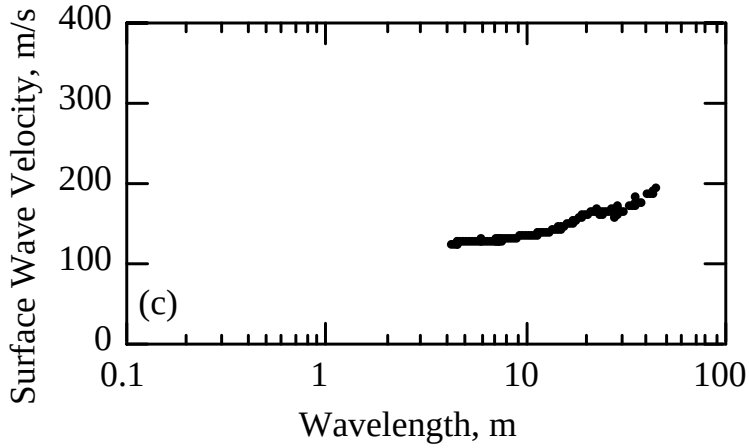

b. Phase Velocity Dispersion Curve Derived From Figure 3b.

Figure A.3 Unwrapped Phase Spectrum and Associated Dispersion Curve from Testing at One Receiver Spacing as Shown in Figure A.2a

The bulldozer simply moved back and forth over a distance of about 3 m. The bulldozer motion generated random noise which contained significant surface wave energy from about 4 Hz to above 30 Hz as shown in Figure A.2b by the continuity in the pattern of the wrapped phase.

The SASW test procedure is repeated with many receiver spacings which cover a broad range of wavelengths. For testing illustrated in this example, receiver spacings of 0.9, 1.8, 3.8, 7.6, 15.25, 30.5 and 61 m were employed. A sledge hammer was used at source spacings up to 3.8 m. The bulldozer was used as the source for the larger spacings. The process of collecting dispersion data at multiple receiver spacings is followed so that wavelengths are measured which cover the complete profile, ranging from shallow materials (high frequencies) to deep materials (low frequencies). Results from three receiver spacings with the bulldozer source are shown in Figure A.4.

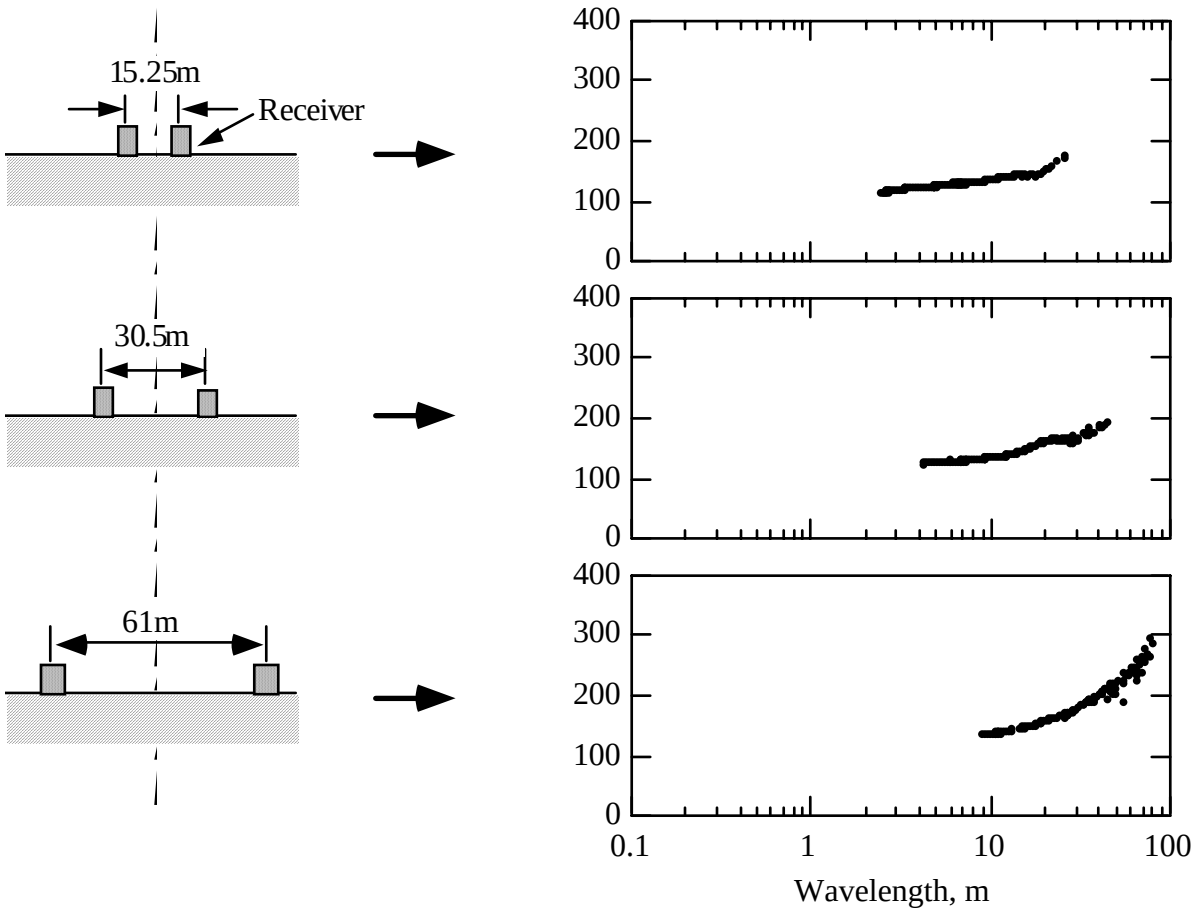

Figure A.4 Typical Receiver Arrangements and Associated Dispersion Curves

An important consideration in SASW data collection is that the spacing between the source and first receiver, d in Figure A.2a, is a significant fraction of the longest wavelength, λ_{max}, collected at that spacing for use in modeling the data.

In general, λ_{max} can be expressed as:

$$\lambda_{max} \leq 2d \tag{4}$$

In terms of unwrapped phase (or wrapped phase for that matter), Equation 4 represents $\phi = 180°$ in Figures A.3a and A.3b, and all data at longer wavelengths are deleted as shown by the darken zones in the figures. This criterion is used in an attempt to perform all data collection in the far field because forward modeling or inversion (Joh, 1996) of the dispersion curve is based on wave propagation in the far field. The source should never be located closer to the first receiver than d, a distance equal to the receiver spacing.

A.2.2 MODELING OF THE FIELD DISPERSION CURVE

A composite dispersion curve is created from field measurements at all receiver spacings, as illustrated in Figure A.5a. Due to the large number of data points in the composite field curve, an average dispersion curve with fewer points is calculated for the forward-modeling process, as shown in Figure A.5b. Through an iterative forward-modeling process of matching a theoretical dispersion curve with the average experimental dispersion curve, the shear wave velocity profile can be evaluated (Stokoe et al., 1994 and Joh, 1996). (This modeling is performed with the WinSASW computer program developed at the University of Texas at Austin.) A final match is shown in Figure A.5c, and the resulting stiffness profile, typically the final product of the SASW test, is shown in Figure A.6.

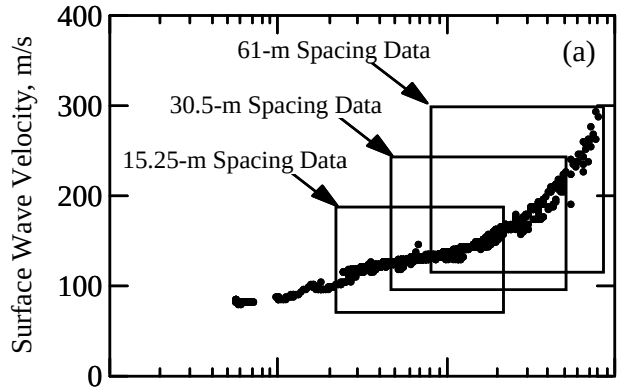

a. Composite Dispersion Curve from all Receiver Spacings

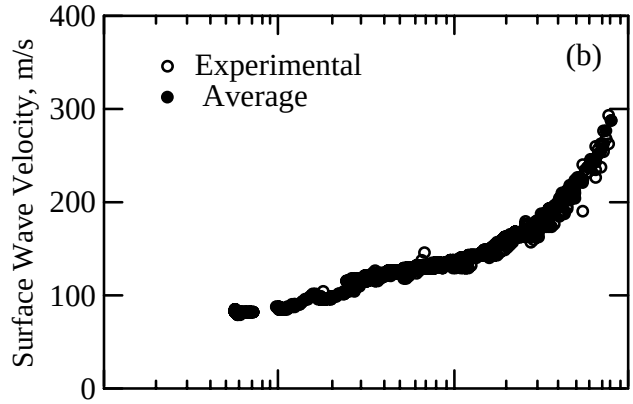

b. Average Dispersion Curve

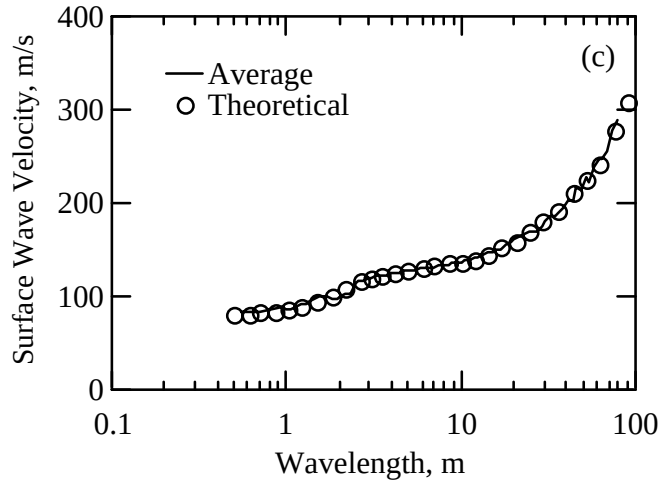

c. Matching the Theoretical Dispersion Curve with an Average Experimental Curve

Figure A.5 Developing the Field Dispersion Curve and Matching a Theoretical Curve to It

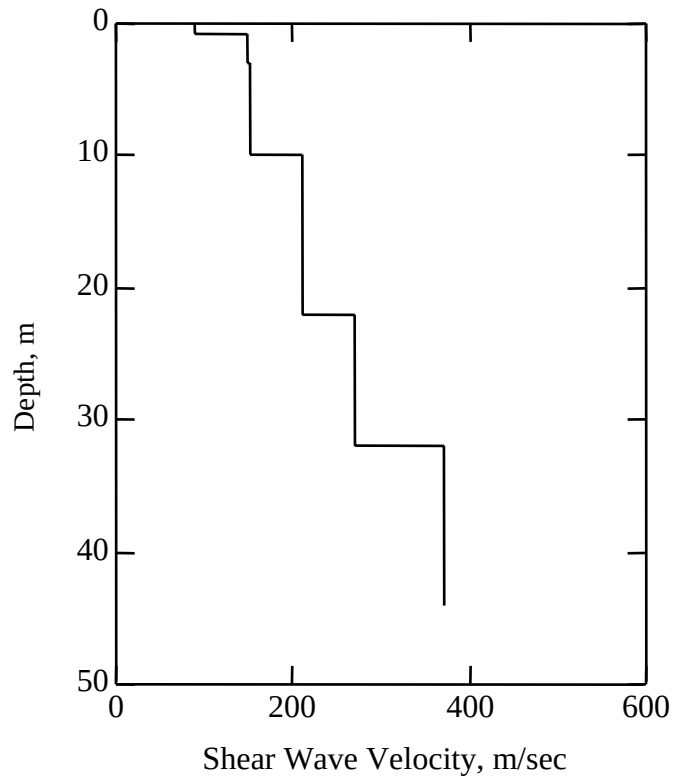

Figure A.6 Shear Wave Velocity Profile Determined from the Forward-Modeling Process Shown in Figure A.5c

A.3 REFERENCES

Andrus, Ronald D. (1994). "In Situ Characterization of Gravelly Soils That Liquefied in the 1983 Borah Peak Earthquake," Ph.D. Dissertation, University of Texas at Austin.

Brown, L.T. (1998). "Comparison of V_s Profiles from SASW and Borehole Measurements at Strong Motion Sites in Southern California," M.S. Thesis, University of Texas at Austin.

Bueno, J.L. (1998). "A Study on the Feasibility of Compacting Unbound Graded Aggregate Base Courses in Thicker Lifts than Presently Allowed by State Departments of Transportation," M.S. Thesis, University of Texas at Austin.

Joh, S.-H. (1996). "Advances in Interpretation and Analysis Techniques for Spectral-Analysis-of-Surface-Waves (SASW) Measurements," Ph.D. Dissertation, University of Texas at Austin.

Nazarian, S. and Stokoe, K.H., II. (1986). "Use of Surface Waves in Pavement Evaluation," Transportation Research Record 1070, pp. 132-144.

Copyright 2007, Kleinfelder

Stokoe, K.H., II, Roesset, J.M., Bierschwale, J.G. and Aouad, M., (1988). "Liquefaction Potential of Sands from Shear Wave Velocity," Proceedings of Ninth World Conference on Earthquake Engineering, Tokyo-Kyoto, Japan, Vol. III, pp. 213-218.

Stokoe, K.H., II, Rosenblad, B.L., Bay, J.A., Redpath, B., Diehl, J.G., Steller, R.A., Wong, I.G., Thomas, P.A. and Luebbers, M. (2003). "Comparison of V_s Profiles from Three Seismic Methods at Yucca Mountain," SARA 2003, 12th Panamerican Conference on Soil Mechanics and Geotechnical Engineering, Cambridge, MA, June 22-26.

Stokoe, K.H., II, Rosenblad, B.L., Wong, I.G., Bay, J.A., Thomas, P.A. and Silva, W.J. (2004). "Deep V_s Profiling Along the Top of Yucca Mountain Using a Vibroseis Source and Surface Waves," 13th World Conference on Earthquake Engineering, Vancouver, Canada, August (accepted for presentation and publication).

Stokoe, K.H., II, Wright, S.G., Bay, J.A. and Roesset, J.M. (1994). "Characterization of geotechnical sites by the SASW method," ISSMFE Technical Committee 10 for XIII ICSMFE, Geophysical Characteristics of Sites, A.A. Balkema Publishers/Rotterdam & Brookfield, Netherlands, pp. 785-816.

APPENDIX B

FIELD RESULTS AND SHEAR WAVE VELOCITY PROFILES FROM FOUR SASW TEST SITES

Copyright 2007, Kleinfelder

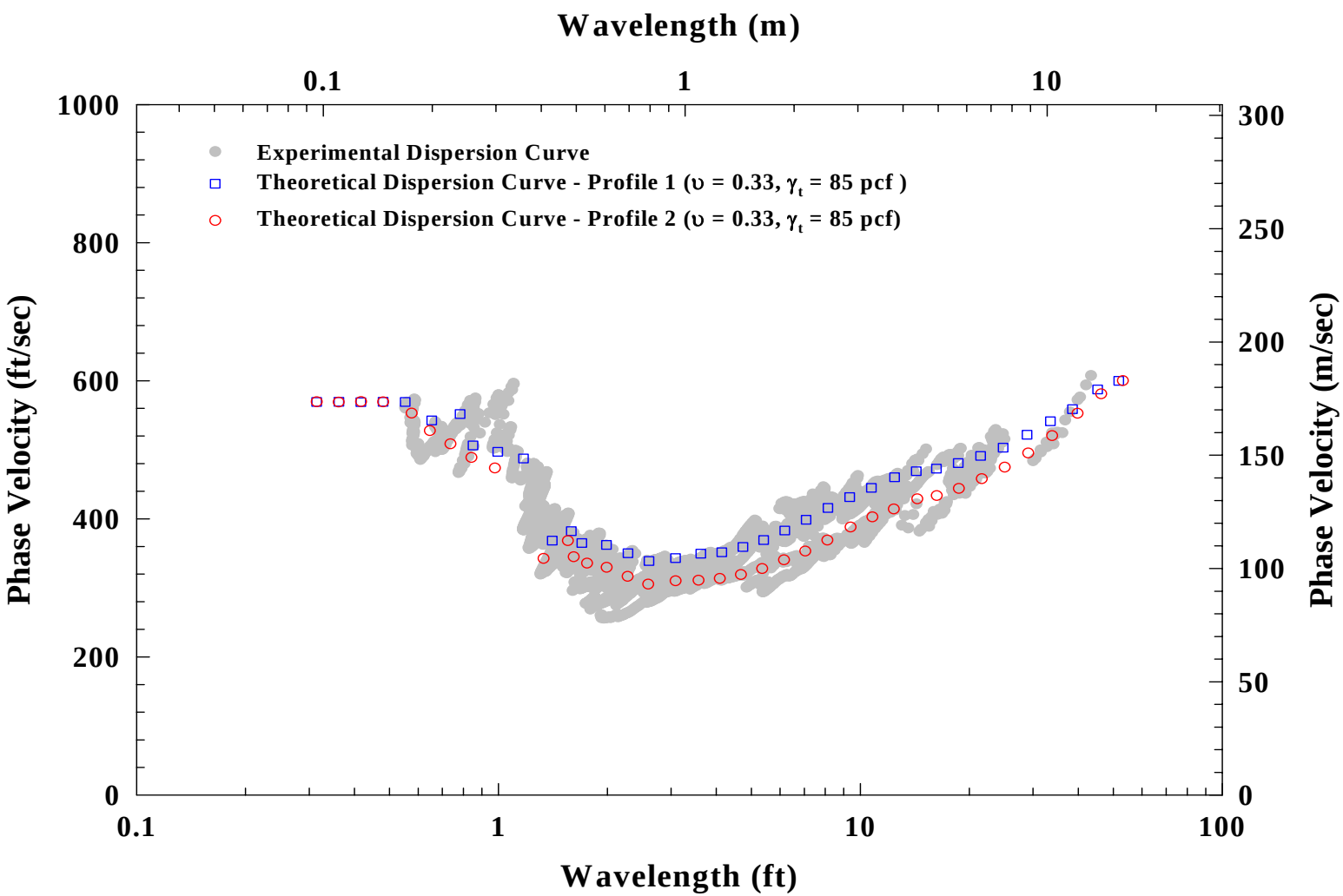

Figure B.1 Experimental and Theoretical Dispersion Curves for Site TA-61-1 at Los Alamos National Laboratory

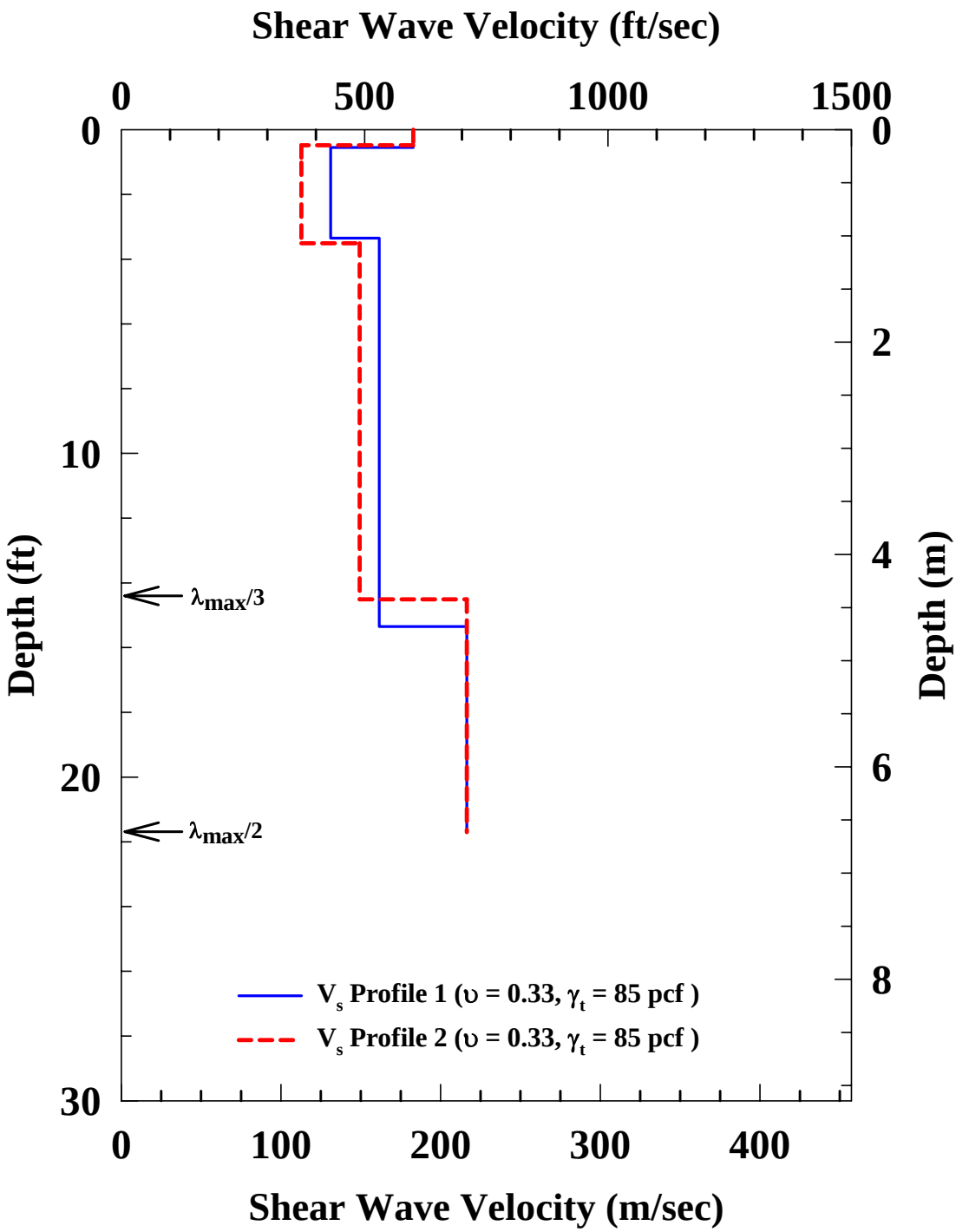

Figure B.2 Shear Wave Velocity Profiles of Site TA-61-1 from Fitting the Experimental Dispersion Curve

Copyright 2007, Kleinfelder

Table B.1 Parameters Used to Develop the Theoretical Dispersion Curve at Site TA-61-1, Profile 1

Layer No.	Thickness, ft	Depth to the Top of the Layer, ft	S-Wave Velocity, ft/s	Assumed Poisson's Ratio	P-Wave Velocity, ft/s	Assumed Mass Density, pcf
1	0.55	0.00	600	0.33	1191	85
2	0.60	0.55	200	0.33	397	85
3	2.20	1.15	430	0.33	854	85
4	12.00	3.35	530	0.33	1052	85
5	6.35	15.35	710	0.33	1410	85
6*	Half Space	21.70	710	0.33	1410	85

* Layer below maximum depth of the V_s Profile

Table B.2 Parameters Used to Develop the Theoretical Dispersion Curve at Site TA-61-1, Profile 2

Layer No.	Thickness, ft	Depth to the Top of the Layer, ft	S-Wave Velocity, ft/s	Assumed Poisson's Ratio	P-Wave Velocity, ft/s	Assumed Mass Density, pcf
1	0.48	0.00	600	0.33	1191	85
2	0.53	0.48	170	0.33	338	85
3	2.50	1.01	370	0.33	735	85
4	11.00	3.51	490	0.33	973	85
5	7.19	14.51	710	0.33	1410	85
6*	Half Space	21.70	710	0.33	1410	85

* Layer below maximum depth of the V_s Profile

Copyright 2007, Kleinfelder

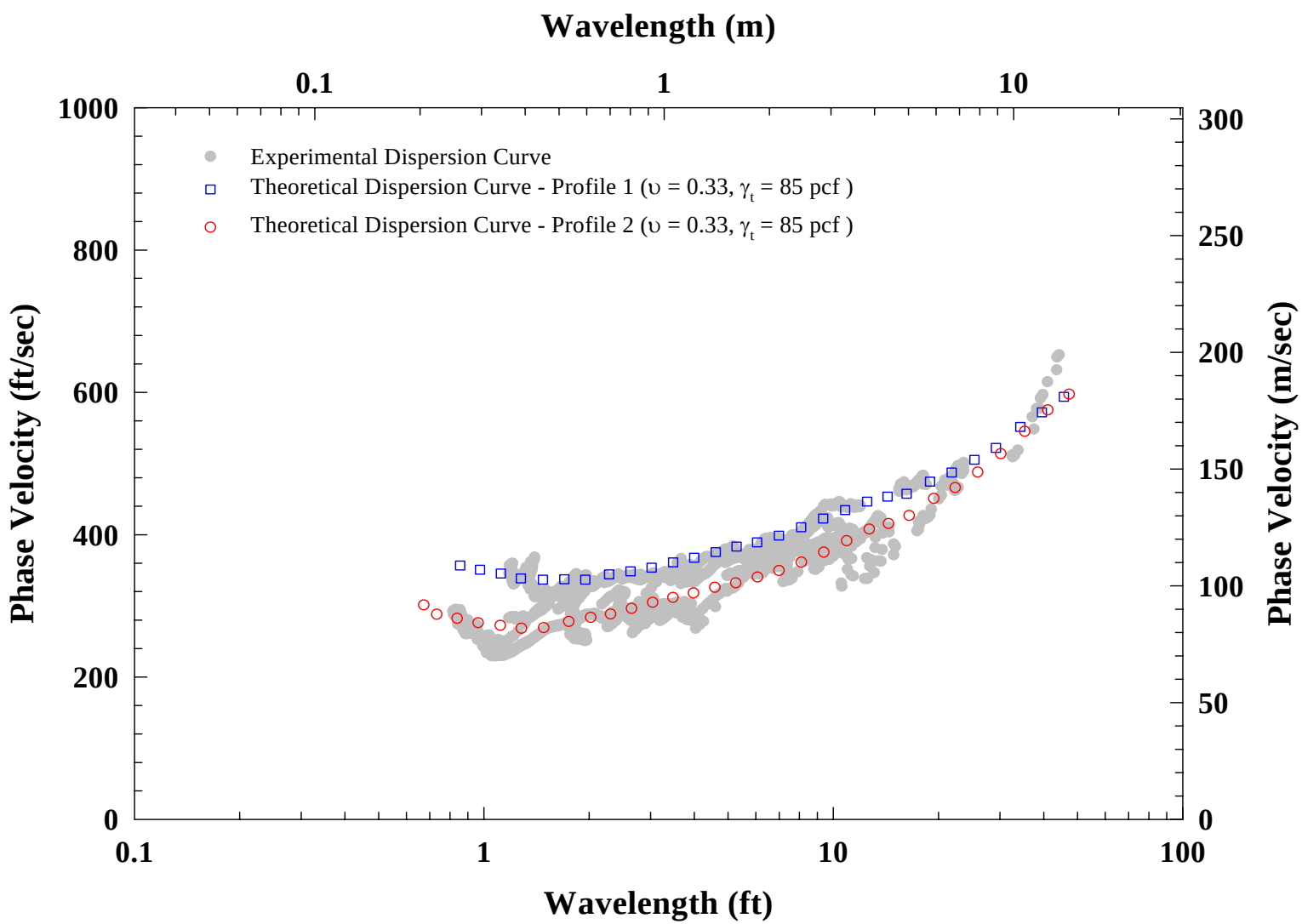

Figure B.3 Experimental and Theoretical Dispersion Curves for Site TA-61-2 at Los Alamos National Laboratory

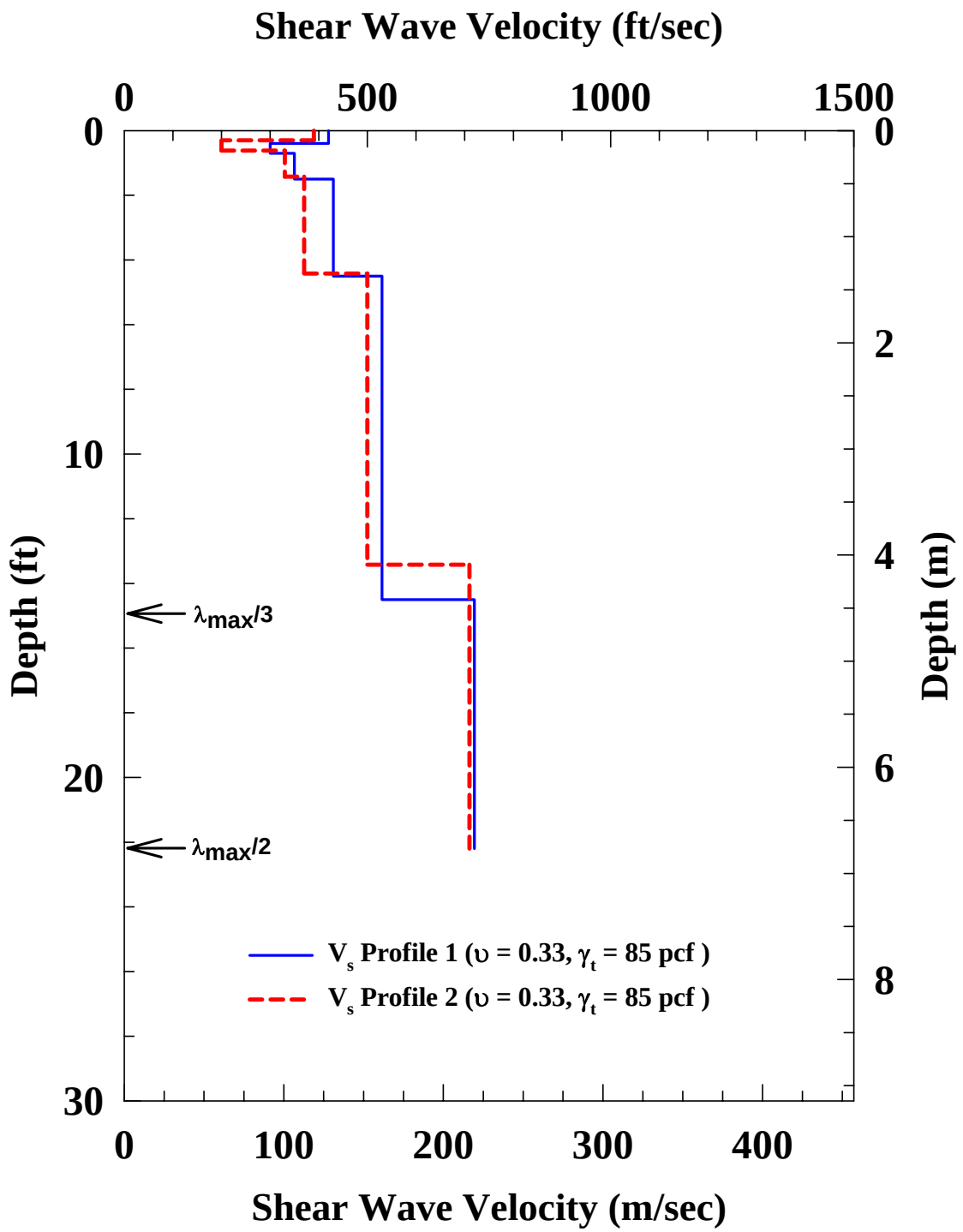

Figure B.4 Shear Wave Velocity Profiles of Site TA-61-2 from Fitting the Experimental Dispersion Curve

Copyright 2007, Kleinfelder

Table B.3 Parameters Used to Develop the Theoretical Dispersion Curve at Site TA-61-2, Profile 1

Layer No.	Thickness, ft	Depth to the Top of the Layer, ft	S-Wave Velocity, ft/s	Assumed Poisson's Ratio	P-Wave Velocity, ft/s	Assumed Mass Density, pcf
1	0.40	0.00	420	0.33	834	85
2	0.30	0.40	300	0.33	596	85
3	0.80	0.70	350	0.33	695	85
4	3.00	1.50	430	0.33	854	85
5	10.00	4.50	530	0.33	1052	85
6	7.70	14.50	720	0.33	1429	85
7*	Half Space	22.20	720	0.33	1429	85

* Layer below maximum depth of the V_s Profile

Table B.4 Parameters Used to Develop the Theoretical Dispersion Curve at Site TA-61-2, Profile 2

Layer No.	Thickness, ft	Depth to the Top of the Layer, ft	S-Wave Velocity, ft/s	Assumed Poisson's Ratio	P-Wave Velocity, ft/s	Assumed Mass Density, pcf
1	0.30	0.00	390	0.33	774	85
2	0.32	0.30	200	0.33	397	85
3	0.80	0.62	330	0.33	655	85
4	3.00	1.42	370	0.33	735	85
5	9.00	4.42	500	0.33	993	85
6	8.78	13.42	710	0.33	1410	85
7*	Half Space	22.20	710	0.33	1410	85

* Layer below maximum depth of the V_s Profile

Copyright 2007, Kleinfelder

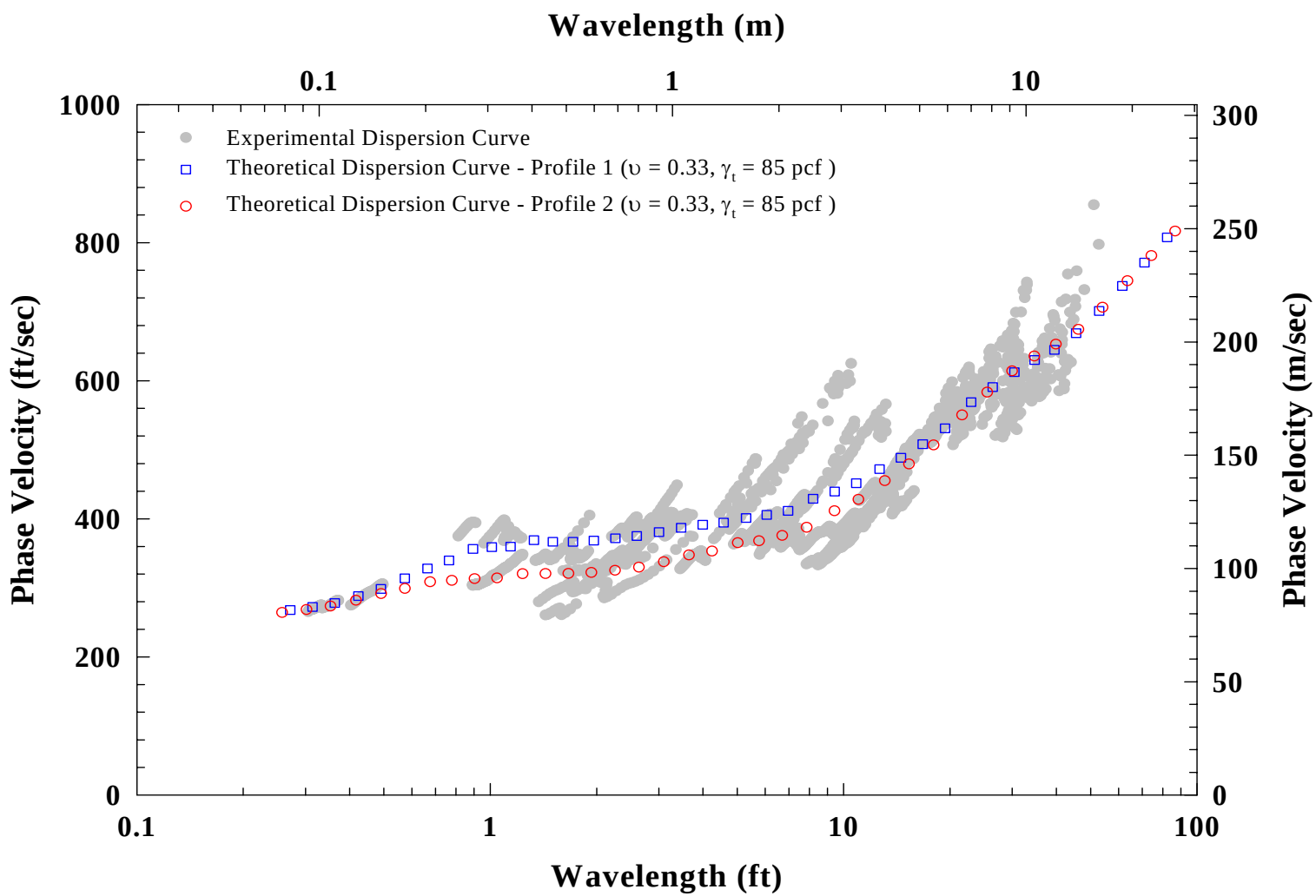

Figure B.5 Experimental and Theoretical Dispersion Curves for Site TA-61-3 at Los Alamos National Laboratory

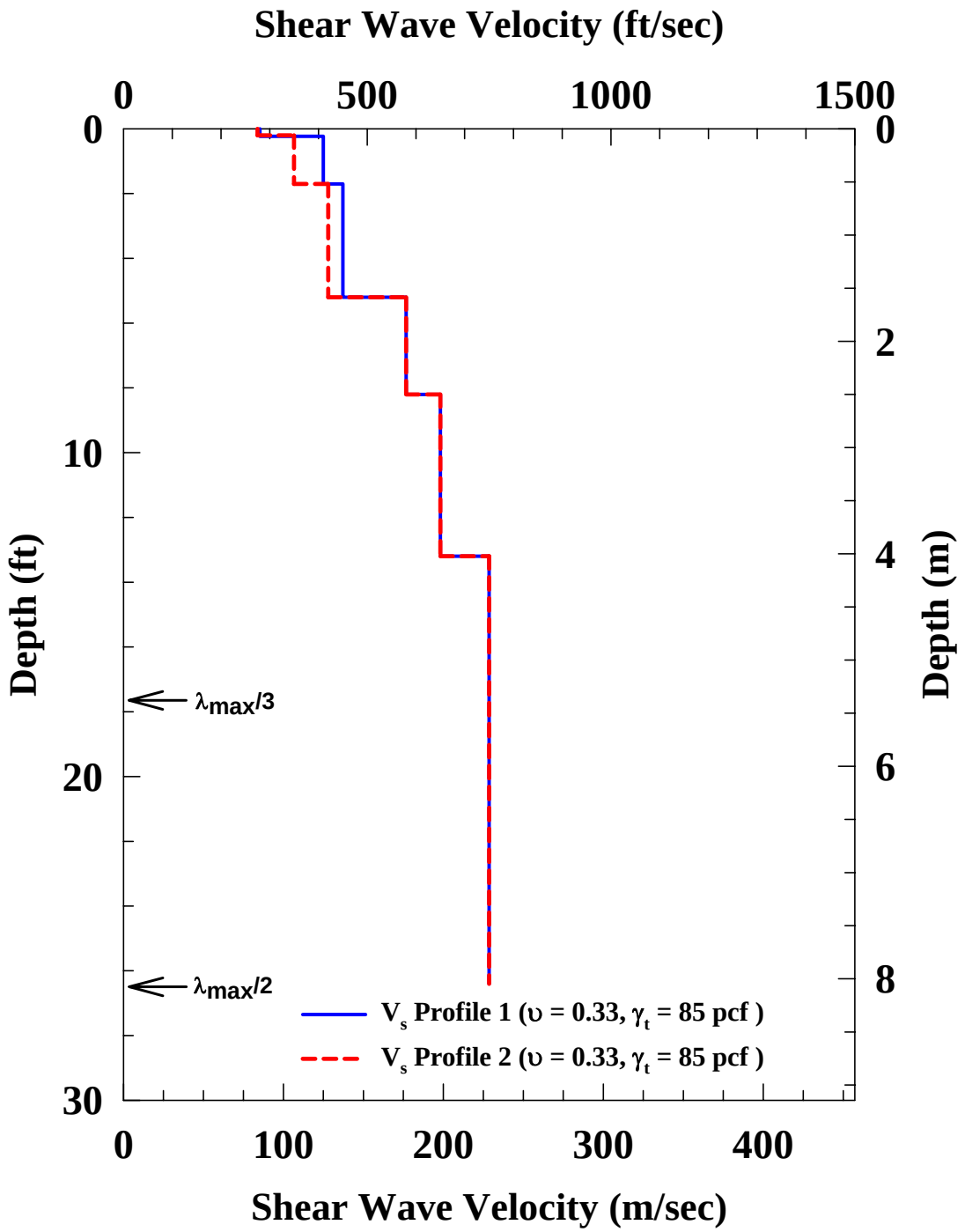

Figure B.6 Shear Wave Velocity Profiles of Site TA-61-3 from Fitting the Experimental Dispersion Curve

Copyright 2007, Kleinfelder

Table B.5 Parameters Used to Develop the Theoretical Dispersion Curve at Site TA-61-3, Profile 1

Layer No.	Thickness, ft	Depth to the Top of the Layer, ft	S-Wave Velocity, ft/s	Assumed Poisson's Ratio	P-Wave Velocity, ft/s	Assumed Mass Density, pcf
1	0.20	0.00	275	0.33	546	85
2	1.50	0.20	350	0.33	695	85
3	3.50	1.70	420	0.33	834	85
4	3.00	5.20	580	0.33	1151	85
5	5.00	8.20	650	0.33	1290	85
6	13.20	13.20	750	0.33	1489	85
7*	1.80	26.40	750	0.33	1489	85
8*	Half Space	28.20	1000	0.33	1985	85

* Layer below maximum depth of the V_s Profile

Table B.6 Parameters Used to Develop the Theoretical Dispersion Curve at Site TA-61-3, Profile 2

Layer No.	Thickness, ft	Depth to the Top of the Layer, ft	S-Wave Velocity, ft/s	Assumed Poisson's Ratio	P-Wave Velocity, ft/s	Assumed Mass Density, pcf
1	0.23	0.00	280	0.33	556	85
2	1.47	0.23	410	0.33	814	85
3	3.50	1.70	450	0.33	893	85
4	3.00	5.20	580	0.33	1151	85
5	5.00	8.20	650	0.33	1290	85
6	13.20	13.20	750	0.33	1489	85
7*	1.80	26.40	750	0.33	1489	85
8*	Half Space	28.20	1000	0.33	1985	85

* Layer below maximum depth of the V_s Profile

Copyright 2007, Kleinfelder

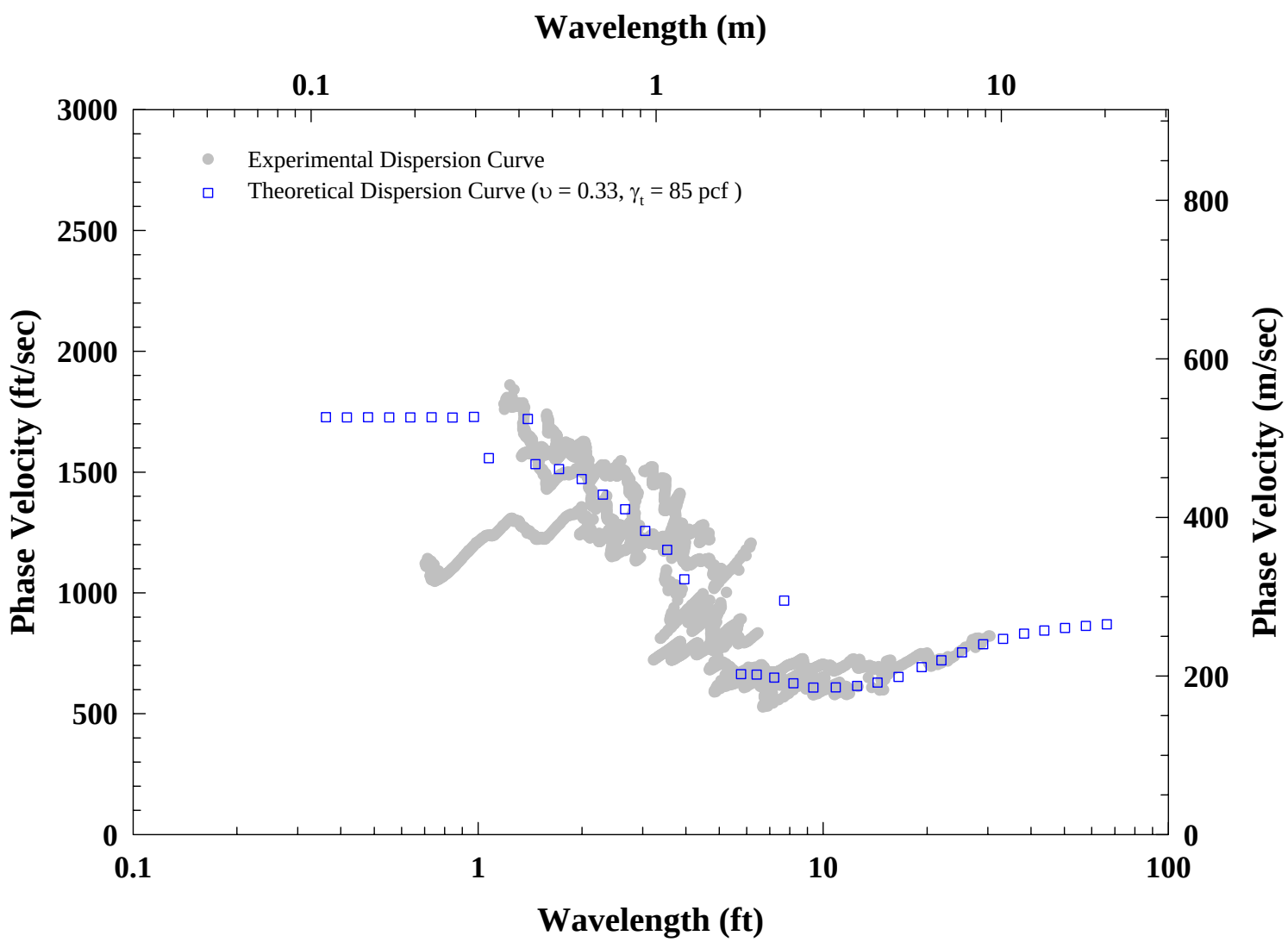

Figure B.7 Experimental and Theoretical Dispersion Curves for the Mortandad Canyon Site at Los Alamos National Laboratory

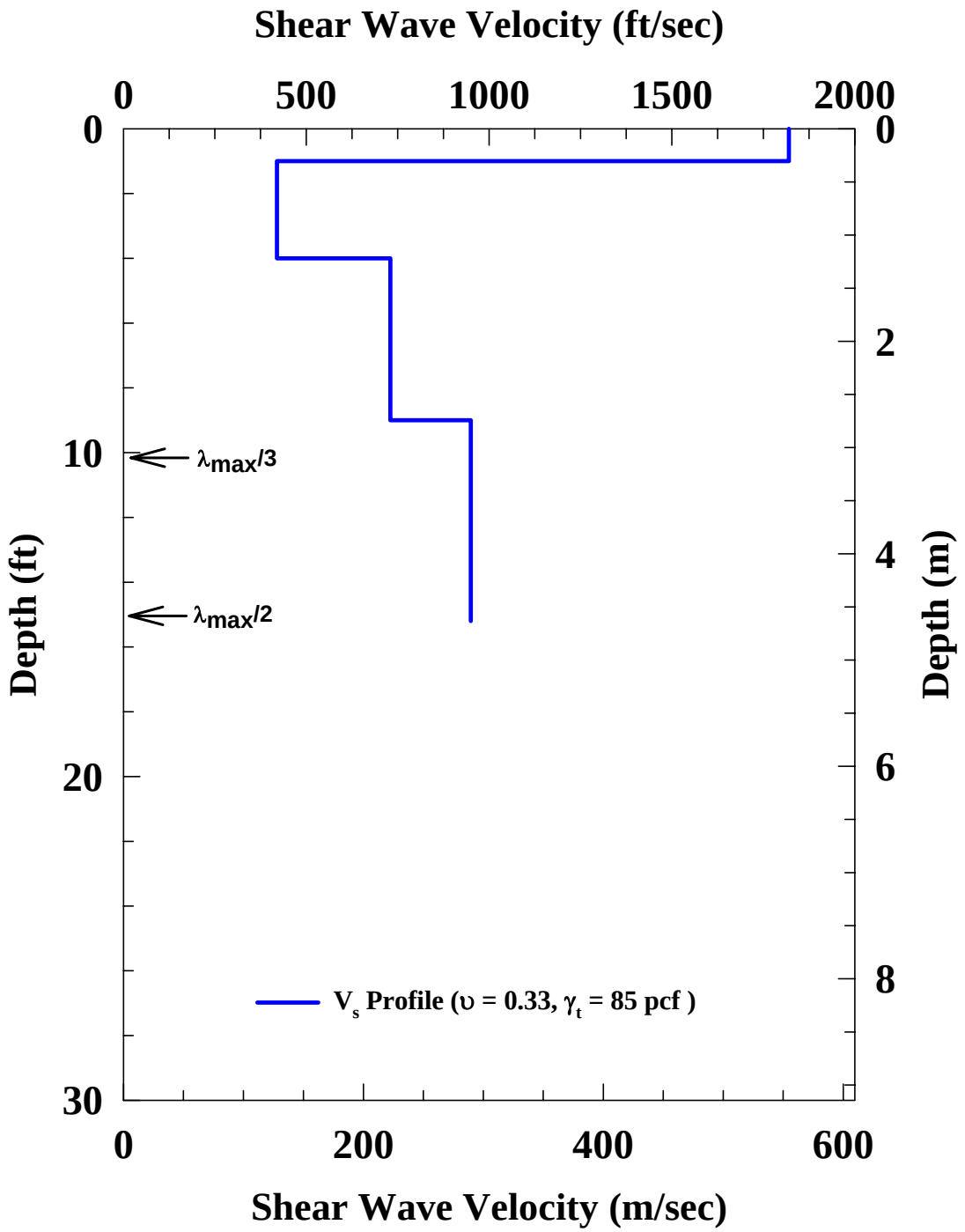

Figure B.8 Shear Wave Velocity Profile at the Mortandad Canyon Site from Fitting the Experimental Dispersion Curve

Copyright 2007, Kleinfelder

Table B.7 Parameters Used to Develop the Theoretical Dispersion Curve at the Mortandad Canyon Site

Layer No.	Thickness, ft	Depth to the Top of the Layer, ft	S-Wave Velocity, ft/s	Assumed Poisson's Ratio	P-Wave Velocity, ft/s	Assumed Mass Density, pcf
1	1.00	0.00	1820	0.33	3613	85
2	3.00	1.00	420	0.33	834	85
3	5.00	4.00	730	0.33	1449	85
4	6.20	9.00	950	0.33	1886	85
5*	Half Space	15.20	950	0.33	1886	85

* Layer below maximum depth of the V_s Profile

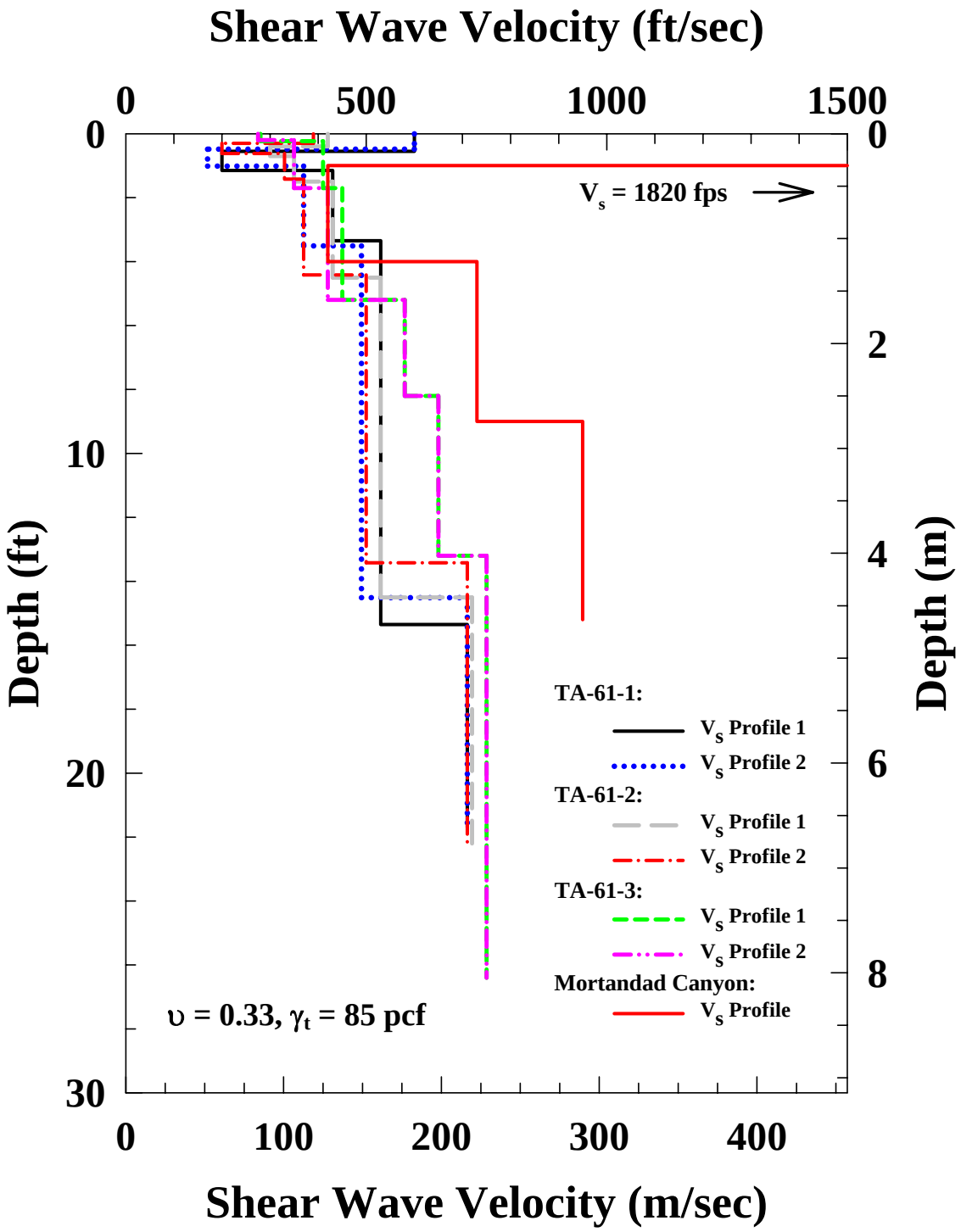

Figure B.9 Comparison of V_s Profiles of Sites TA-61-1, TA-61-2, TA-61-3 and Mortandad Canyon at Los Alamos National Laboratory

Copyright 2007, Kleinfelder

APPENDIX C

BACKGROUND ON THE COMBINED RESONANT COLUMN AND TORSIONAL SHEAR (RCTS) EQUIPMENT

Copyright 2007, Kleinfelder

APPENDIX C

Background on the Combined Resonant Column and Torsional Shear (RCTS) Equipment

C.1 BACKGROUND ON THE COMBINED RCTS EQUIPMENT

The effects of parameters such as soil type, particle size, plasticity, confining pressure, number of loading cycles, and shearing strain amplitude on the shear modulus, G, and the material damping ratio in shear, D, of soil are conveniently evaluated in the laboratory with combined resonant column and torsional shear (RCTS) equipment. This equipment and the results of parametric studies with it have been discussed by Stokoe, et al. (1994) and Stokoe, et al. (1999). The equipment is of the fixed-free type, with the bottom of the specimen fixed and torsional excitation applied to the top as illustrated in Figure C.1. The equipment has two important attributes. First, both resonant column (RC) and torsional shear (TS) tests can be performed with the same piece of equipment. Switching from one type of test to the other is simply done outside the confining chamber by changing: (1) the input excitation frequency used to drive the specimen, and (2) the motion monitoring devices used to record the specimen response. As a result, variability due to testing different specimens is eliminated so that results from both types of tests can be compared effectively. Second, the loading frequency in the torsional shear test can be easily changed from 0.01 to about 5 to 10 Hz. Therefore, the effect of frequency and number of loading cycles on the deformational characteristics (G and D) of intact specimens can be conveniently investigated.

C.2 OPERATION OF THE TORSIONAL RESONANT COLUMN (RC) DEVICE

The basic operational principle in the RC test is to vibrate a cylindrical specimen in first-mode torsional resonance. At the University of Texas (UT), this process is completely automated so that first-mode resonance can be quickly and accurately established as illustrated in Figure C.2 (Ni, 1987). Determinations of the resonant frequency and the amplitude of vibration are made from the response curve. These values are then combined with equipment

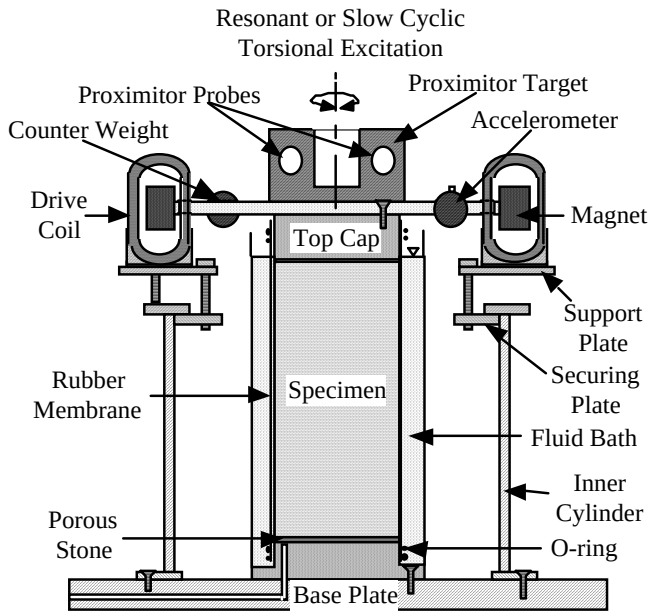

Figure C.1 Simplified Diagram of a Combined Resonant Column (RC) and Torsional Shear (TS) Device (Confining Chamber not Shown)

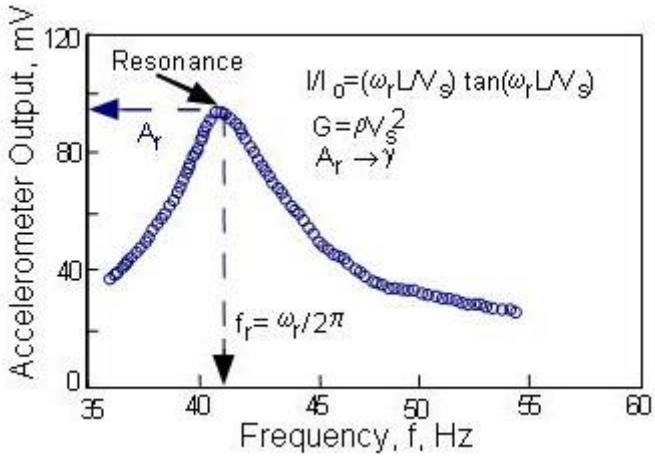

Figure C.2 An Example of the Dynamic Response Curve Measured in the RC Test

Copyright 2007, Kleinfelder

characteristics and specimen size to calculate shear wave velocity, V_s, shear modulus, G, and shearing strain amplitude, γ.

Material damping in the RC test is evaluated from the dynamic soil response using either the free-vibration decay curve or the half-power bandwidth method. The free-vibration decay curve is recorded by shutting off the driving force after the specimen is vibrating in steady-state motion at the resonant frequency. Figure C.3 shows an example of this process. The logarithmic decrement, δ, is defined from the decay curve as:

$$\delta = \ln(z_1/z_2) \qquad \text{(C.1)}$$

where z_1 and z_2 are the amplitudes of two successive cycles. The material damping ratio in shear, D, can then be determined from δ by:

$$D = [\delta^2/(4\pi^2+\delta^2)]^{1/2} \qquad \text{(C.2)}$$

Evaluation of material damping using the half-power bandwidth method is based on measurement of the width of the dynamic response curve around the resonance peak. For small values of material damping (D less than about 5%), one can approximate method damping as:

$$D \cong (f_2 - f_1)/2f_r \qquad \text{(C.3)}$$

where f_1 and f_2 are the two frequencies at which the amplitude of motion is 0.707 times the amplitude at the resonant frequency , f_r, as illustrated in Figure C.4.

For measurements at small strains ($\gamma<10^{-3}$ %), background noise can have a more adverse effect on the free-vibration decay curve than on the frequency response curve. On the other hand, at large strains, the assumption implied in the derivation of Equation C.3 is no longer valid, and serious errors can be introduced into values of D determined by the half-power bandwidth method (Ni, 1987). In this study, both methods were used at shearing strains less than about 0.002%, but only the free-vibration decay method was applied at larger strains. In addition, the strain at which the material damping measurement was assumed to occur was taken as the average of the first three cycles of free vibration. This procedure is not conventionally employed at γ > 0.002% but more correctly represents the strain associated with damping measurements from the free-vibration decay curve.

Copyright 2007, Kleinfelder

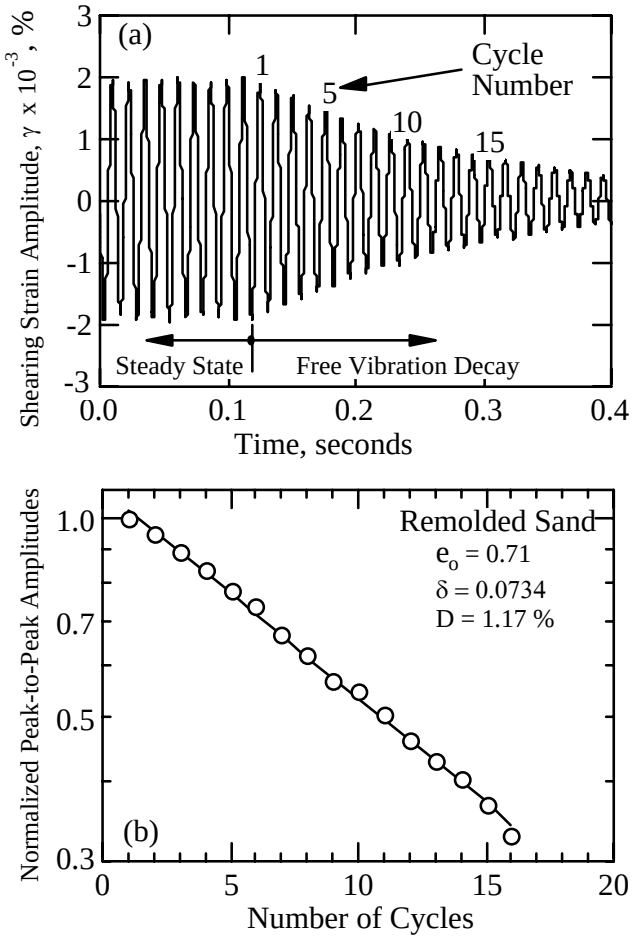

Figure C.3 Material Damping Measurement in the RC Test Using the Free-Vibration Decay Curve

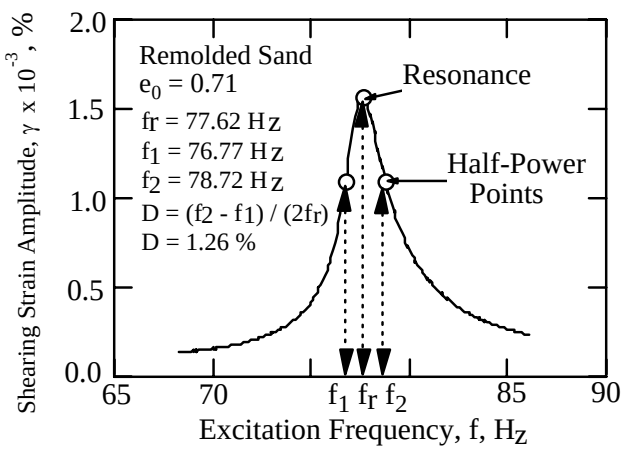

Figure C.4 Material Damping Measurement in the RC Test Using the Half-Power Bandwidth (Same Specimen as Shown in Figure C.3)

Copyright 2007, Kleinfelder

C.3 OPERATION OF THE TORSIONAL SHEAR (TS) DEVICE

In the TS test, shear modulus and material damping are measured using the same combined RCTS equipment, but the equipment is operated in slow cyclic torsional loading at a given frequency. Instead of determining the resonant frequency, the stress-strain hysteresis loop is determined from measuring the torque-twist response of the specimen as shown in Figure C.5. Proximitors are used to measure the angle of twist while the voltage applied to the coil is calibrated to yield torque. Shear modulus is calculated from the slope of a line through the end points of the hysteresis loop. Material damping is determined from the hysteresis loop as the ratio of the energy dissipated in one cycle of loading (A_L) to the peak strain energy stored during the cycle (A_T) times a factor of 4π as shown in Figure C.5.

C.4 CALIBRATION OF RCTS EQUIPMENT FOR EQUIPMENT-GENERATED DAMPING

As discussed by Stokoe, et al. (1994) and Stokoe, et al. (1999), the RCTS equipment at UT is calibrated so that equipment-generated damping can be subtracted from the measurements. Equipment-generated damping, D_{eq}, is measured along with material damping of the specimen when the damping measurements are performed following the procedures outlined in Figures C.2 through C.5. Equipment-generated damping results from the back-electromagnetic force generated by the magnets moving through the drive coils. It is important to calibrate the drive system of each RCTS device over the entire range of frequencies used in testing so that equipment-generated damping can be determined before testing any specimens. Typical results for D_{eq} in RC testing are shown in Figure C.6 (Hwang, 1997). This damping is then subtracted from the combined measurement to yield material damping of the specimen. In all results where material damping ratios of soil specimens are presented, these values have been corrected by subtracting D_{eq} from the combined measurement of D.

Copyright 2007, Kleinfelder

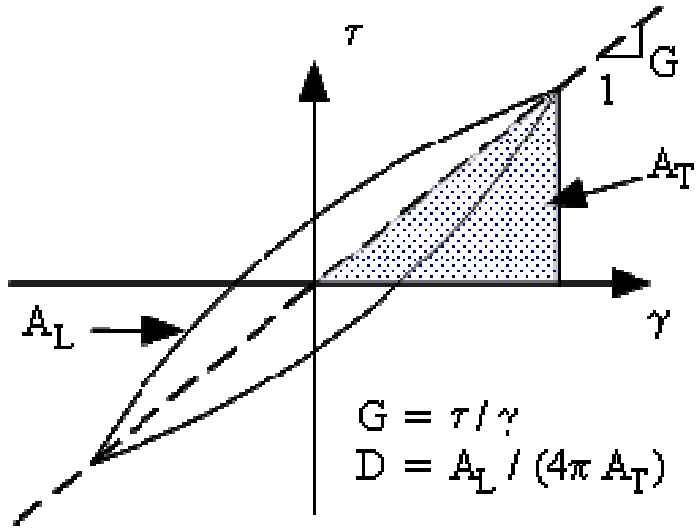

Figure C.5 An Example of a Hysteresis Loop Measured in the TS Test

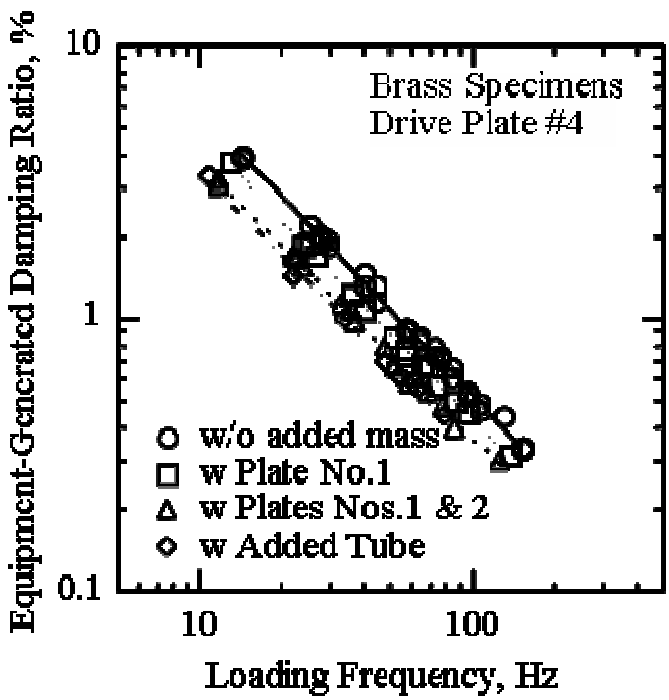

Figure C.6 Examples of Equipment-Generated Damping Measured in the Resonant Column Device Using Metal Specimens (from Hwang, 1997)

C.5 REFERENCES

Stokoe, K.H., II, Hwang, S.K., Lee J.N.K, and Andrus, R.D. (1994) "Effects of Various Parameters on the Stiffness and Damping of Soils at Small to Medium Strains," International Symposium on Pre-failure Deformation Characteristics of Geomaterials, Shibuya, Mitachi and Miura, eds., Sapporo, Japan, September, pp. 785-816.

Stokoe, K.H., II, Darendeli, M.B., Andrus, R.D. and Brown, L.T. (1999) "Dynamic Soil Properties: Laboratory, Field and Correlation Studies," Proceedings, Second International Conference on Earthquake Geotechnical Engineering, Sêco e Pinto, Editor, A.A. Balkema Publishers/Rotterdam & Brookfield, Netherlands, Vol. 3, pp. 811-845.

Ni, S.-H. (1987) "Dynamic Properties of Sand Under True Triaxial Stress States from Resonant Column/Torsional Shear tests," Ph.D. Dissertation, The University of Texas at Austin, 421 pp.

Hwang, S.K. (1997). "Investigation of the Dynamic Properties of Natural Soils," Ph.D. Dissertation, the University of Texas at Austin, 394 pp.

APPENDIX D

LABORATORY RESULTS OF COMBINED RESONANT COLUMN AND TORSIONAL SHEAR (RCTS) TESTS OF TWO SPECIMENS FROM BLOCK SAMPLE #15, TA-61

Copyright 2007, Kleinfelder

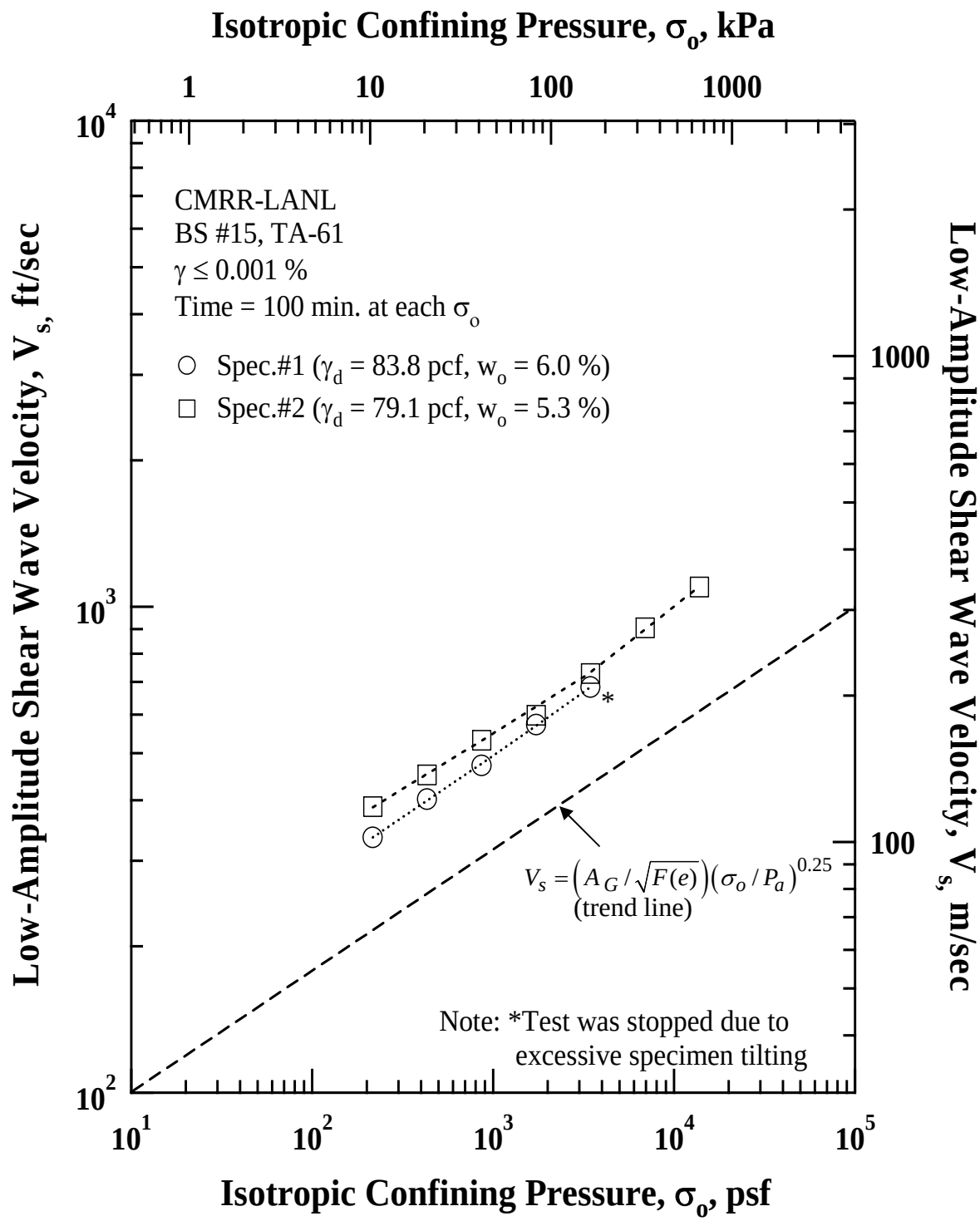

Figure D.1 Variation in Low-Amplitude Shear Wave Velocity with Isotropic Confining Pressure of the Two Intact Specimens from Block Sample #15 (Lower Unit 3, Bandelier Tuff (Qbt3L)) as Determined from Resonant Column (RC) Tests

Copyright 2007, Kleinfelder

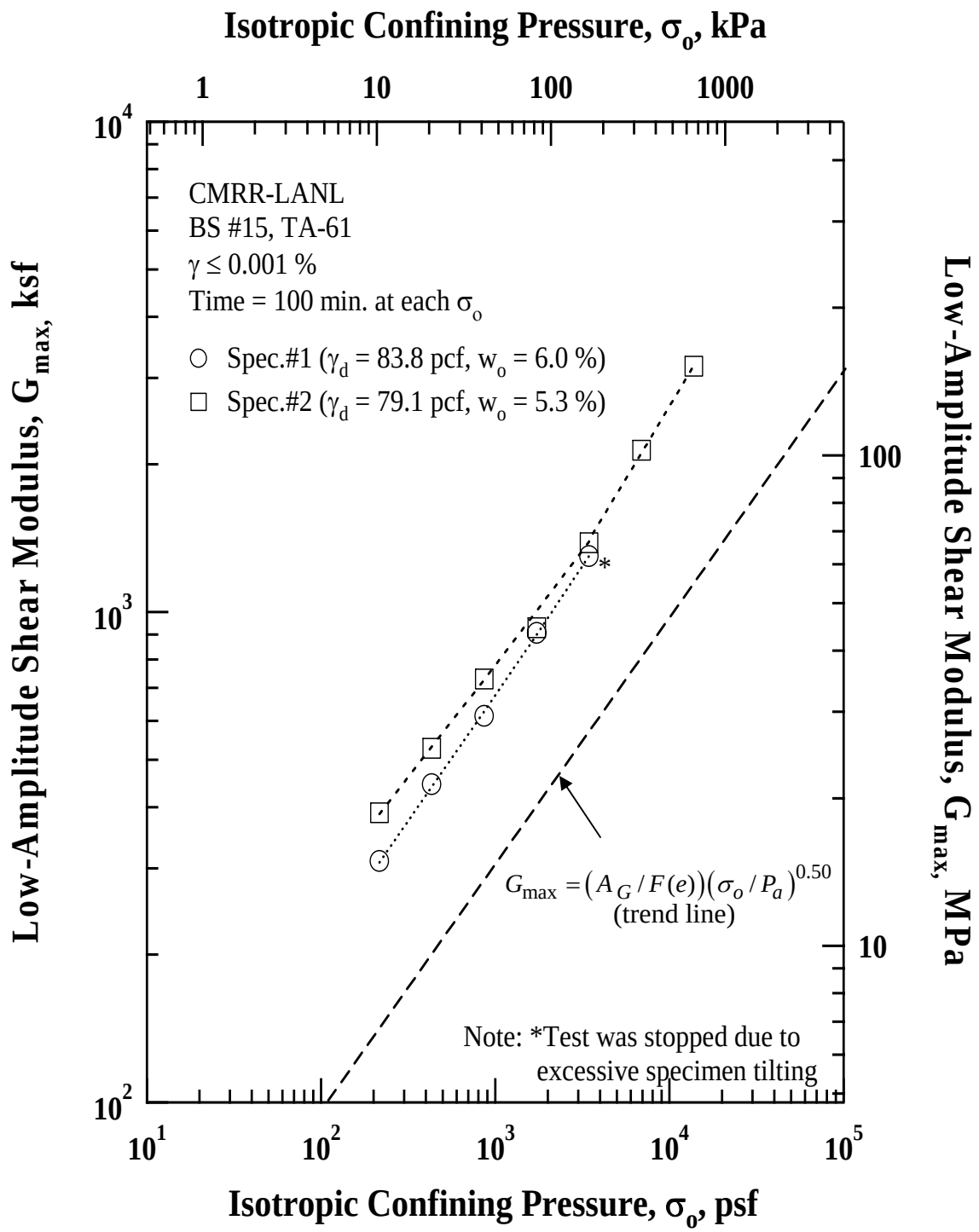

Figure D.2 Variation in Low-Amplitude Shear Modulus with Isotropic Confining Pressure of the Two Intact Specimens from Block Sample #15 (Lower Unit 3, Bandelier Tuff (Qbt3L)) as Determined from Resonant Column (RC) Tests

Copyright 2007, Kleinfelder

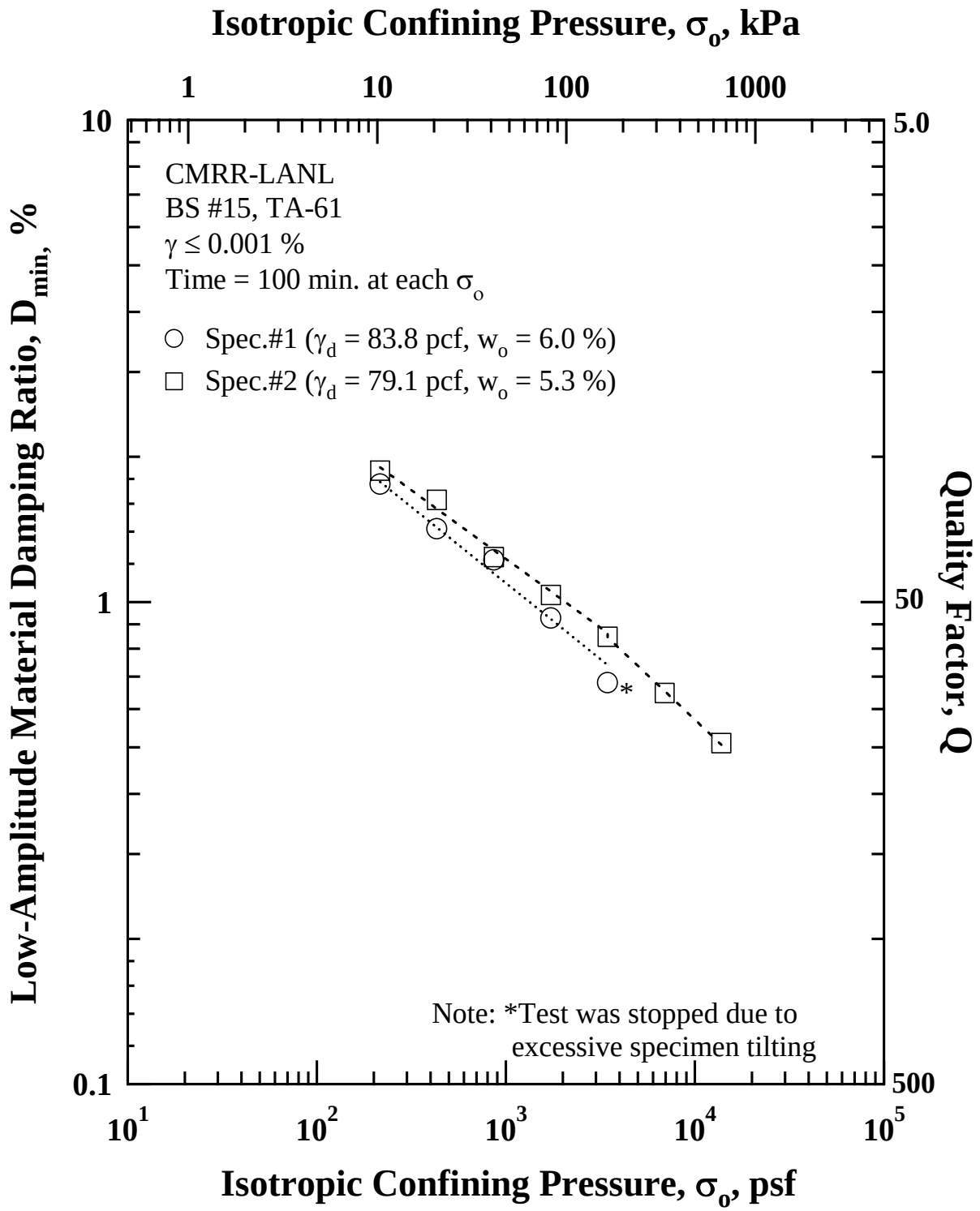

Figure D.3 Variation in Low-Amplitude Material Damping Ratio with Isotropic Confining Pressure of the Two Intact Specimens from Block Sample #15 (Lower Unit 3, Bandelier Tuff (Qbt3L)) as Determined from Resonant Column (RC) Tests

Copyright 2007, Kleinfelder

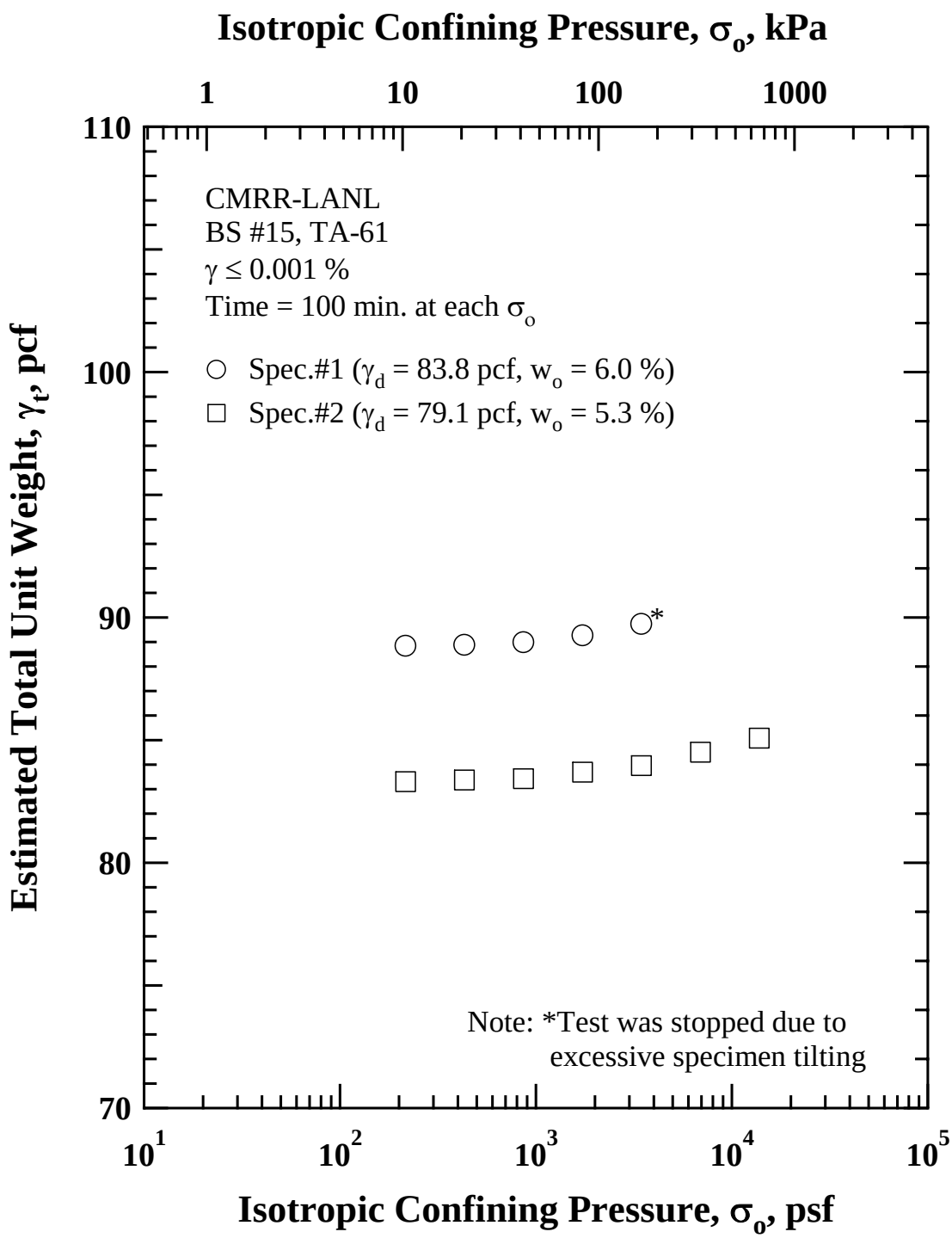

Figure D.4 Variation in Estimated Total Unit Weight with Isotropic Confining Pressure of the Two Intact Specimens from Block Sample #15 (Lower Unit 3, Bandelier Tuff (Qbt3L)) as Determined from Resonant Column (RC) Tests

Copyright 2007, Kleinfelder

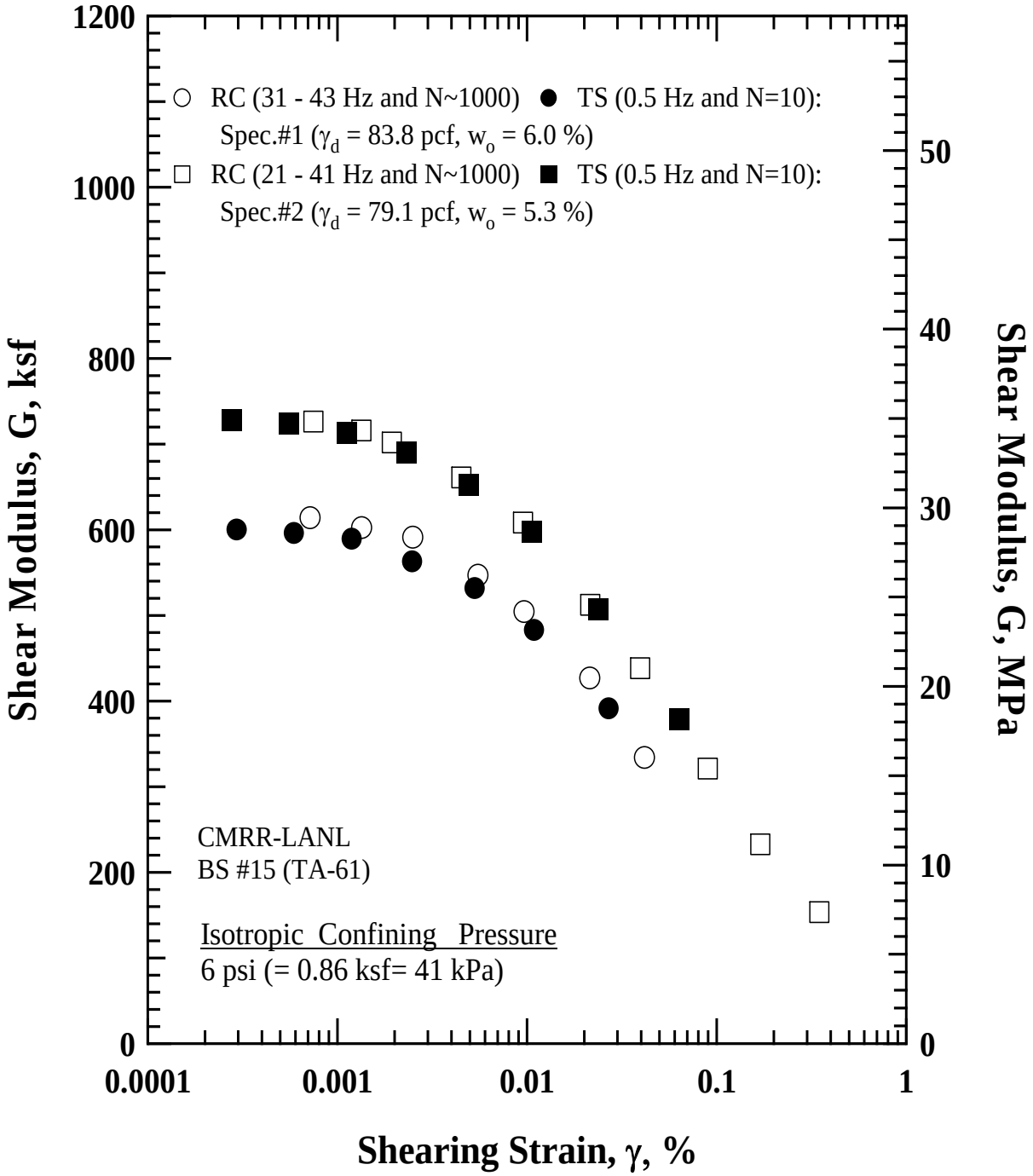

Figure D.5 Variation in Shear Modulus with Shearing Strain of the Two Intact Specimens from Block Sample #15 (Lower Unit 3, Bandelier Tuff (Qbt3L)) at an Isotropic Confining Pressure of 0.86 ksf (41 kPa) from Resonant Column (RC) and Torsional Shear (TS) Tests

Copyright 2007, Kleinfelder

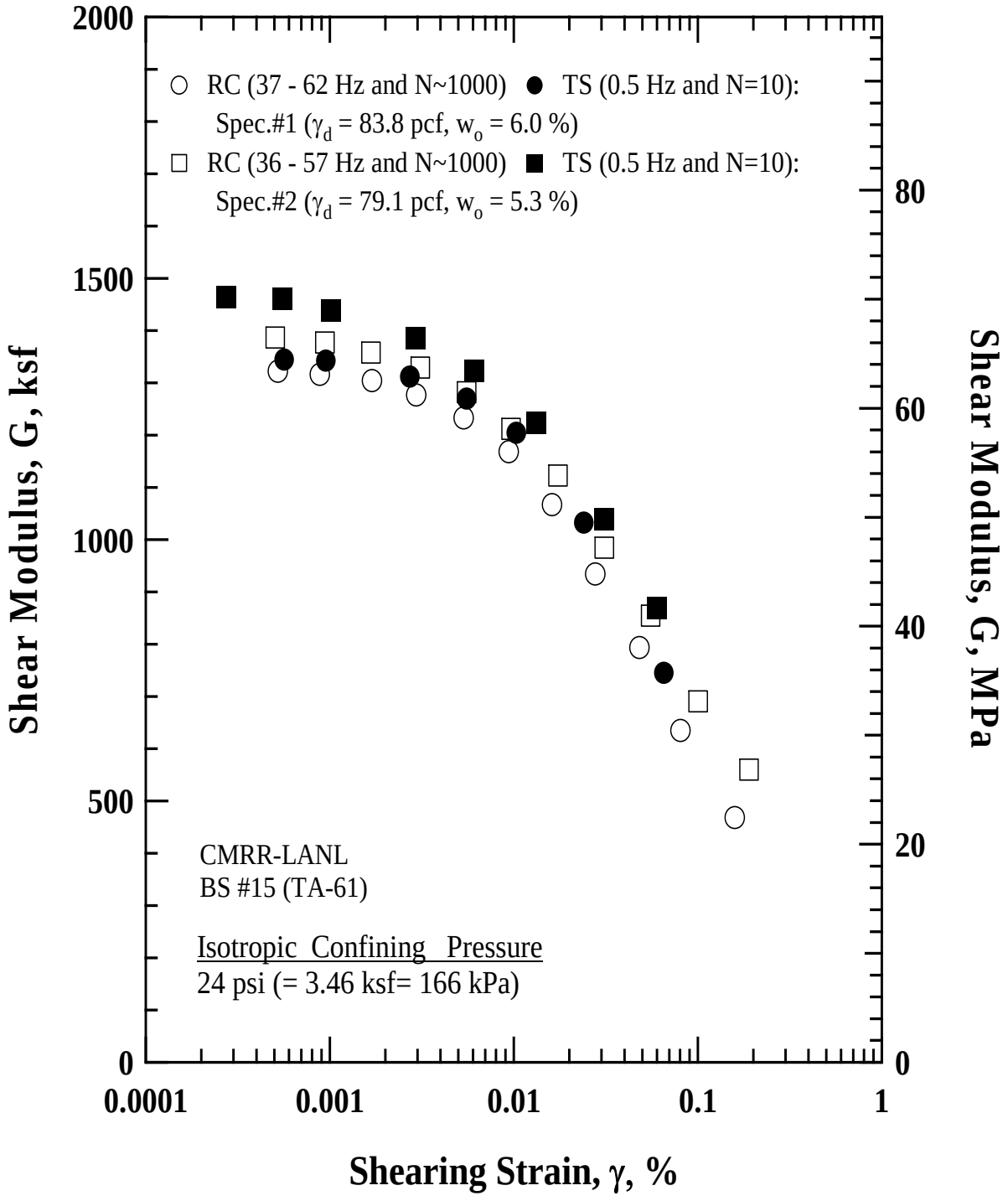

Figure D.6 Variation in Shear Modulus with Shearing Strain of the Two Intact Specimens from Block Sample #15 (Lower Unit 3, Bandelier Tuff (Qbt3L)) at an Isotropic Confining Pressure of 3.46 ksf (166 kPa) from Resonant Column (RC) and Torsional Shear (TS) Tests

Copyright 2007, Kleinfelder

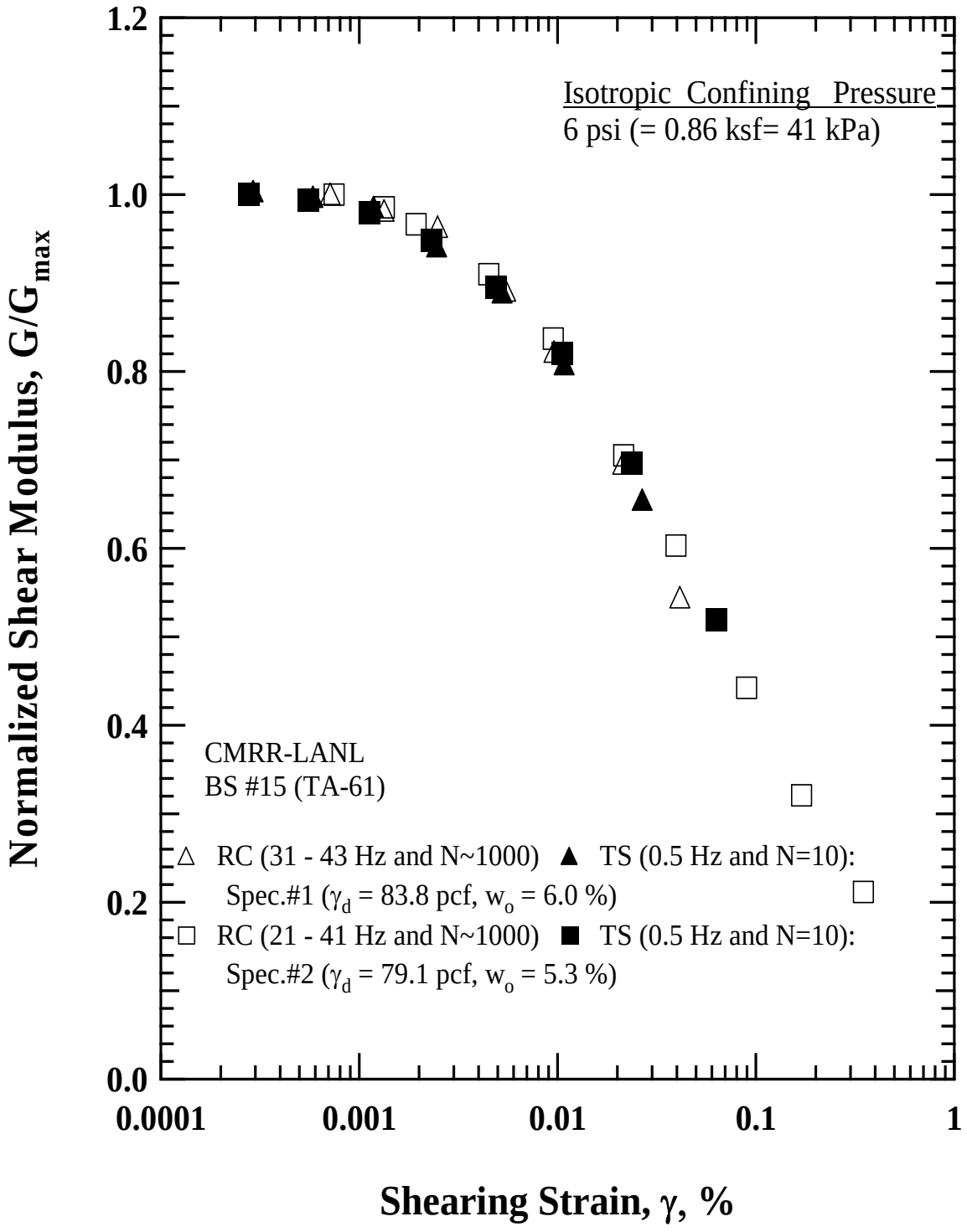

Figure D.7 Variation in Normalized Shear Modulus with Shearing Strain of the Two Intact Specimens from Block Sample #15 (Lower Unit 3, Bandelier Tuff (Qbt3L)) at an Isotropic Confining Pressure of 0.86 ksf (41 kPa) from Resonant Column (RC) and Torsional Shear (TS) Tests

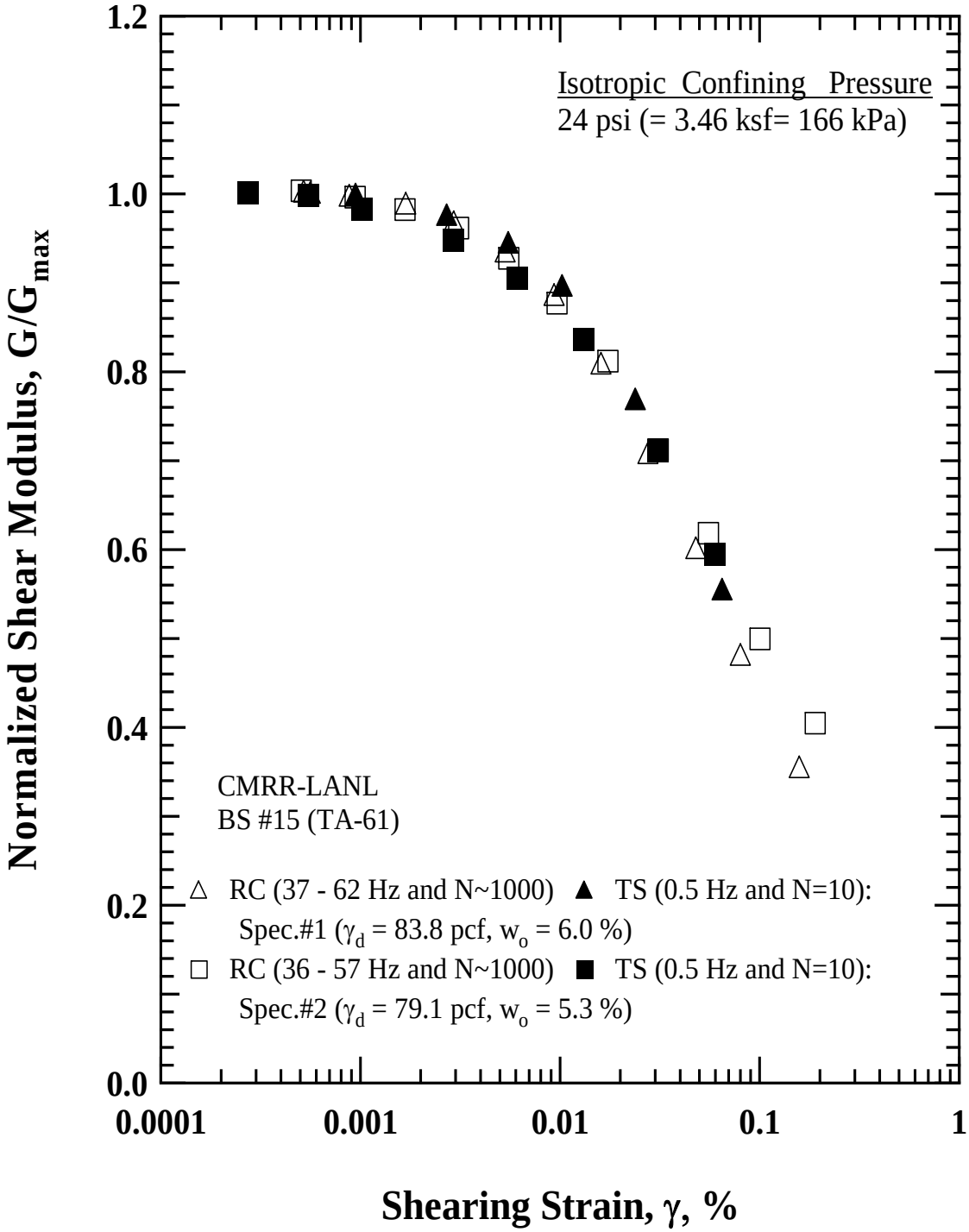

Figure D.8 Variation in Normalized Shear Modulus with Shearing Strain of the Two Intact Specimens from Block Sample #15 (Lower Unit 3, Bandelier Tuff (Qbt3L)) at an Isotropic Confining Pressure of 3.46 ksf (166 kPa) from Resonant Column (RC) and Torsional Shear (TS) Tests

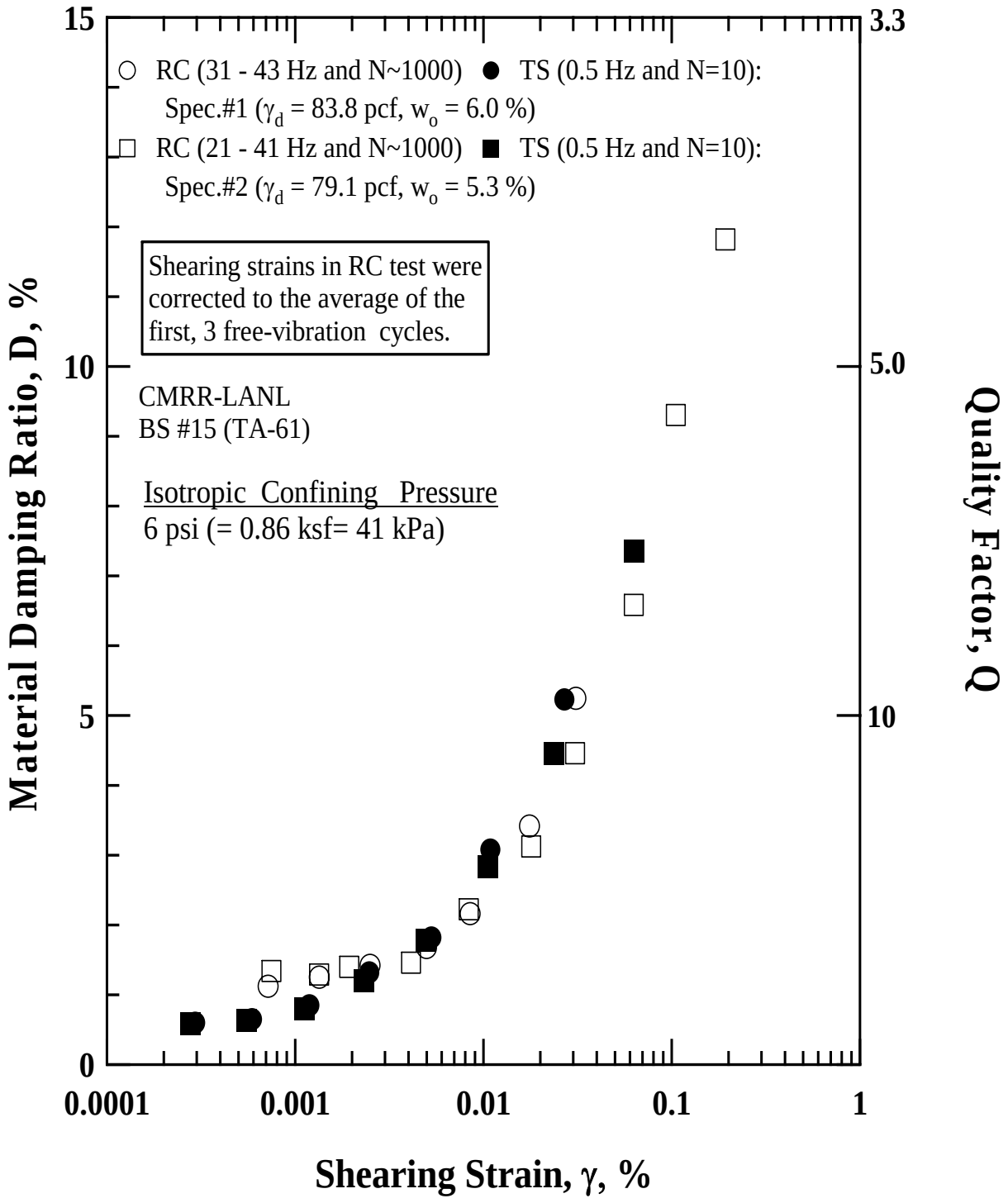

Figure D.9 Variation in Material Damping Ratio with Shearing Strain of the Two Intact Specimens from Block Sample #15 (Lower Unit 3, Bandelier Tuff (Qbt3L)) at an Isotropic Confining Pressure of 0.86 ksf (41 kPa) from Resonant Column (RC) and Torsional Shear (TS) Tests

Copyright 2007, Kleinfelder

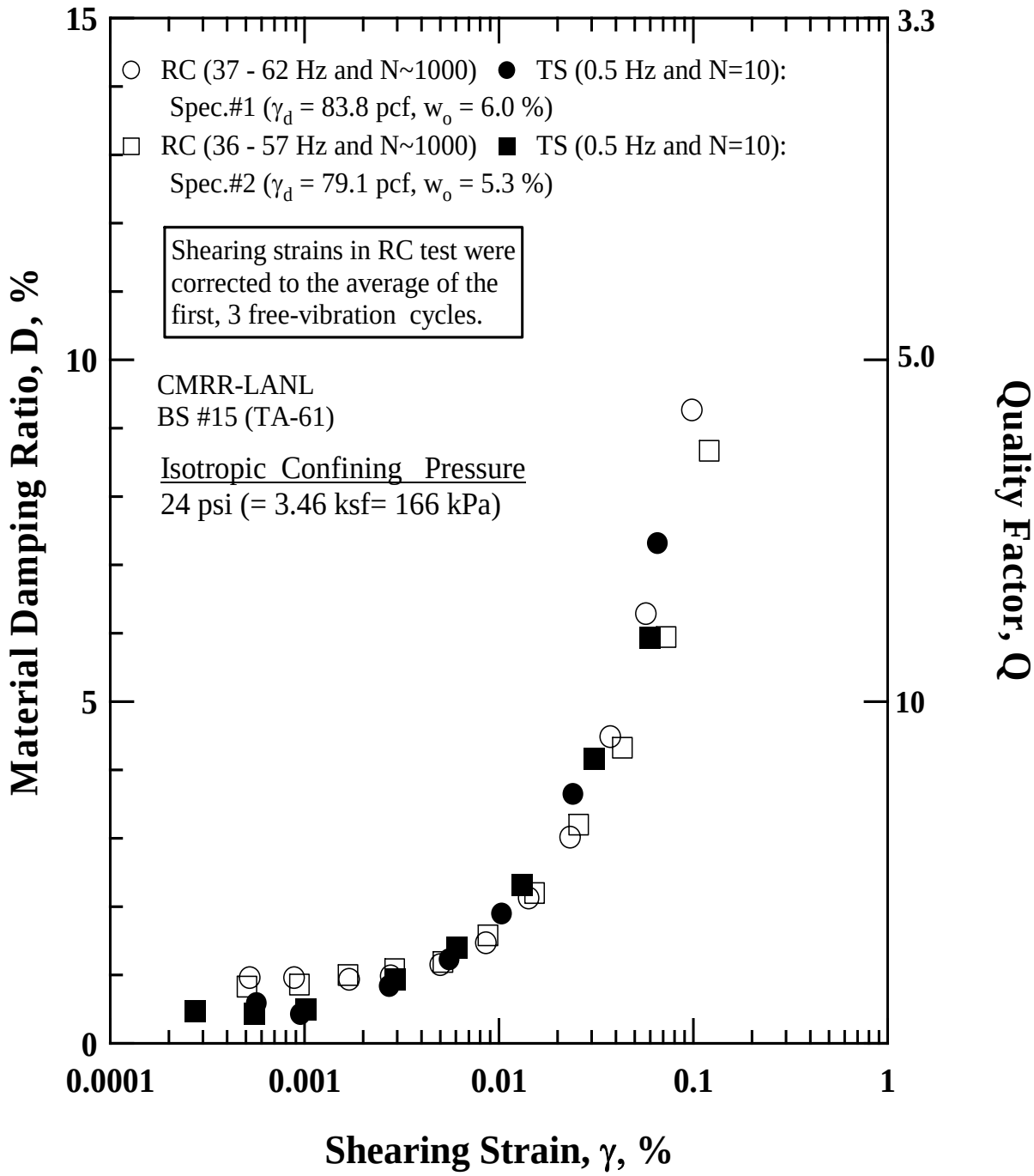

Figure D.10 Variation in Material Damping Ratio with Shearing Strain of the Two Intact Specimens from Block Sample #15 (Lower Unit 3, Bandelier Tuff (Qbt3L)) at an Isotropic Confining Pressure of 3.46 ksf (166 kPa) from Resonant Column (RC) and Torsional Shear (TS) Tests

Copyright 2007, Kleinfelder

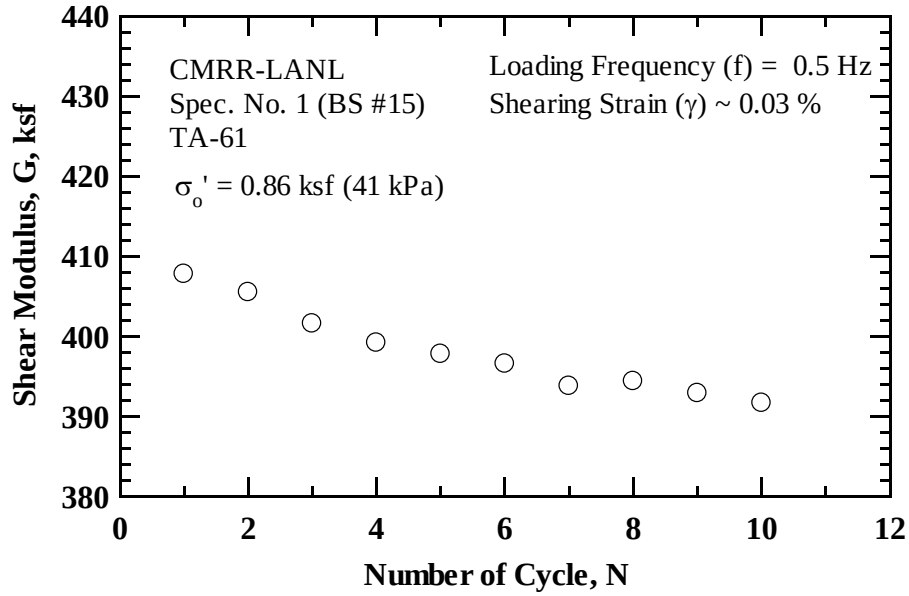

(a) Shear Modulus, G

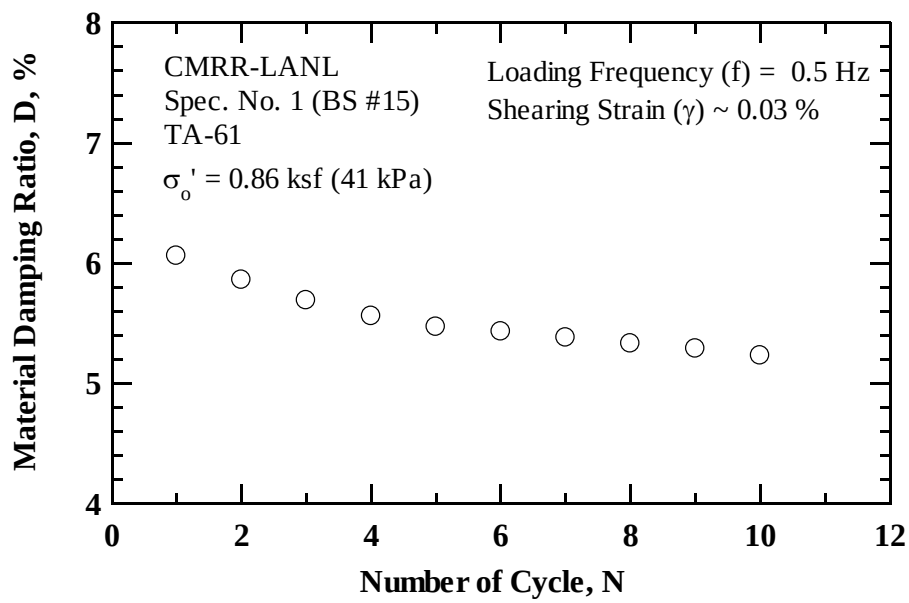

(b) Material Damping Ratio, D

Figure D.11 Variation of (a) Shear Modulus and (b) Material Damping Ratio with Number of Cycles for Spec. No. 1 from Block Sample #15 (Lower Unit 3, Bandelier Tuff (Qbt3L)) at an Isotropic Confining Pressure of 0.86 ksf (41 kPa) from Torsional Shear (TS) Tests

Copyright 2007, Kleinfelder

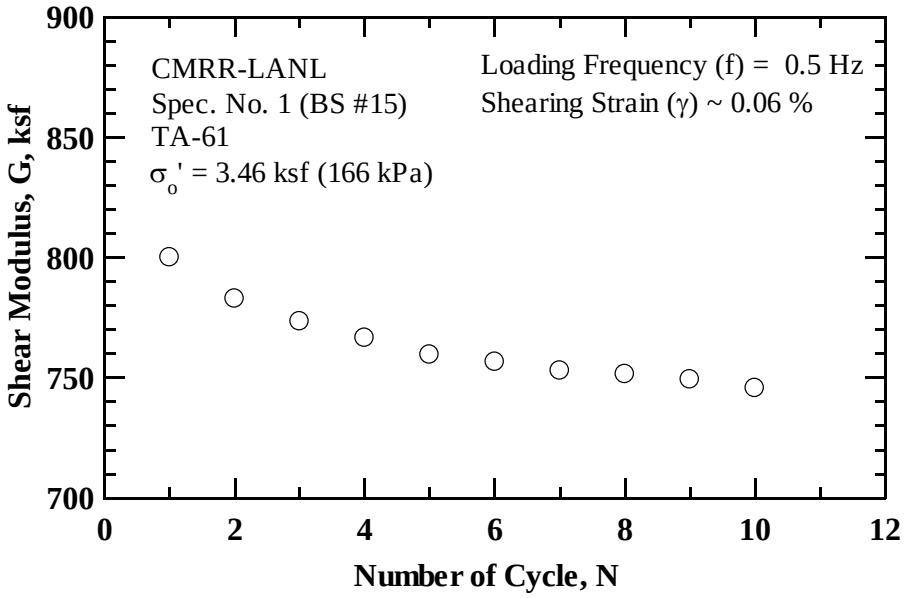

(a) Shear Modulus, G

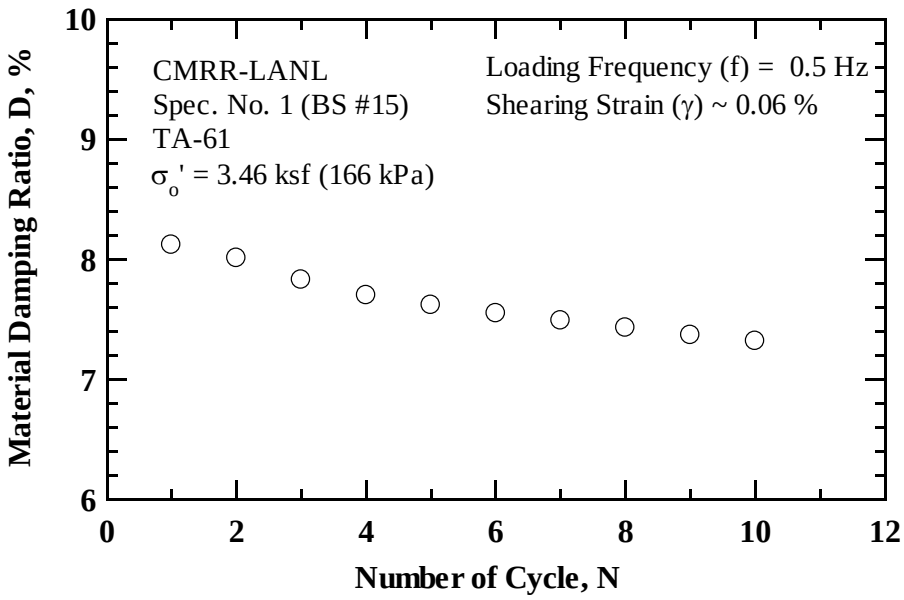

(b) Material Damping Ratio, D

Figure D.12 Variation of (a) Shear Modulus and (b) Material Damping Ratio with Number of Cycles for Spec. No. 1 from Block Sample #15 (Lower Unit 3, Bandelier Tuff (Qbt3L)) at an Isotropic Confining Pressure of 3.46 ksf (166 kPa) from Torsional Shear (TS) Tests

Copyright 2007, Kleinfelder

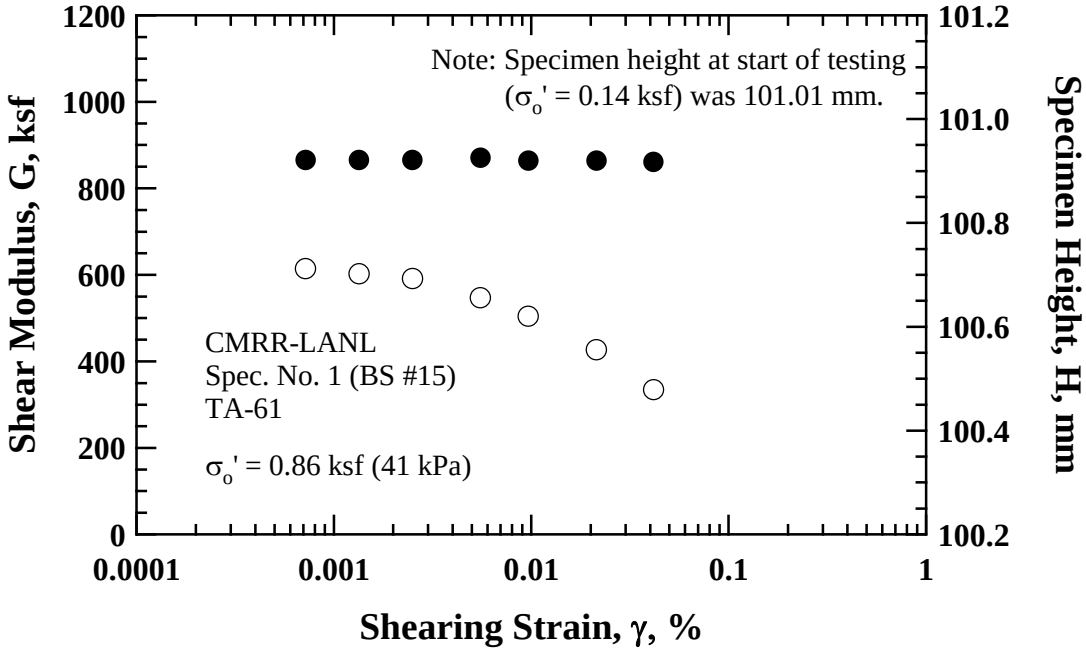

(a) σ_o' = 0.86 ksf (41 kPa)

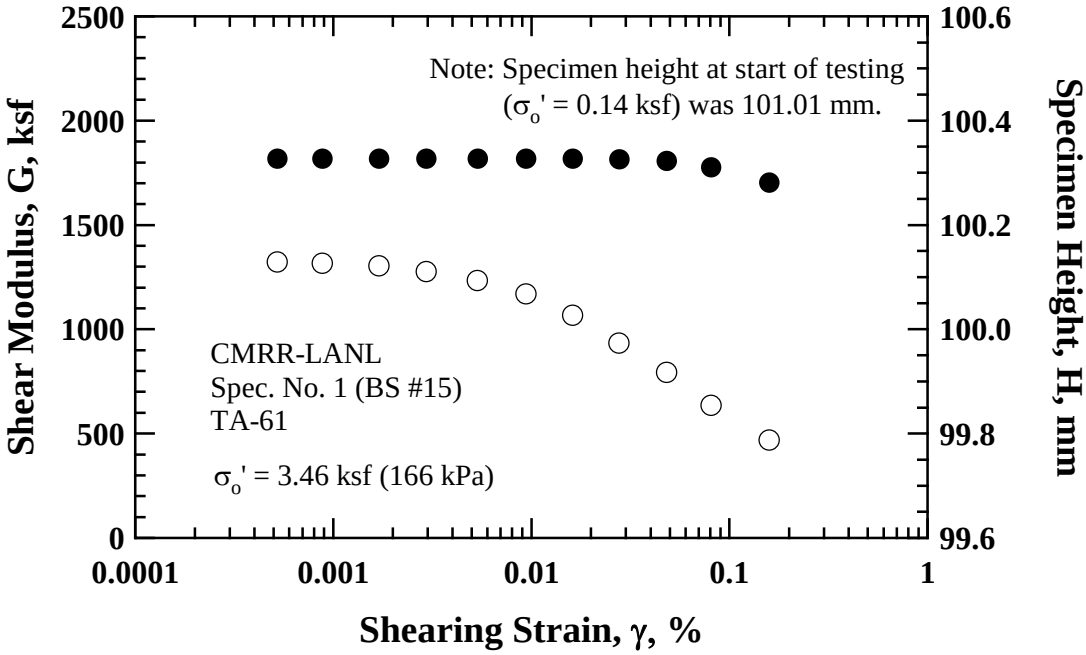

(b) σ_o' = 3.46 ksf (166 kPa)

Figure D.13 Variation in Shear Modulus and Specimen Height with Shearing Strain of Spec. No. 1 from Block Sample #15 (Lower Unit 3, Bandelier Tuff (Qbt3L)) as Determined from Resonant Column (RC) Tests at Two Different Isotropic Confining Pressures: (a) 0.86 ksf (41 kPa) and (b) 3.46 ksf (166 kPa)

Copyright 2007, Kleinfelder

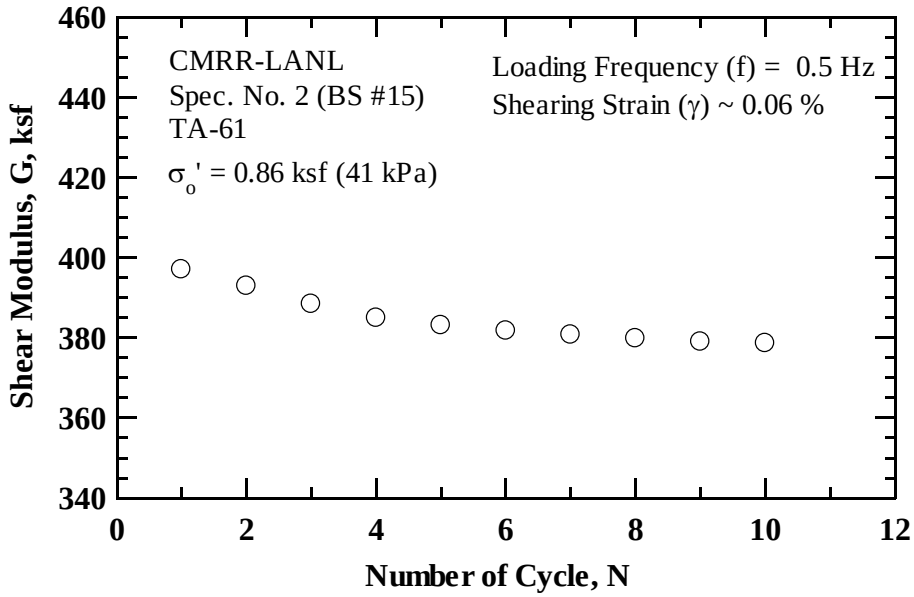

(a) Shear Modulus, G

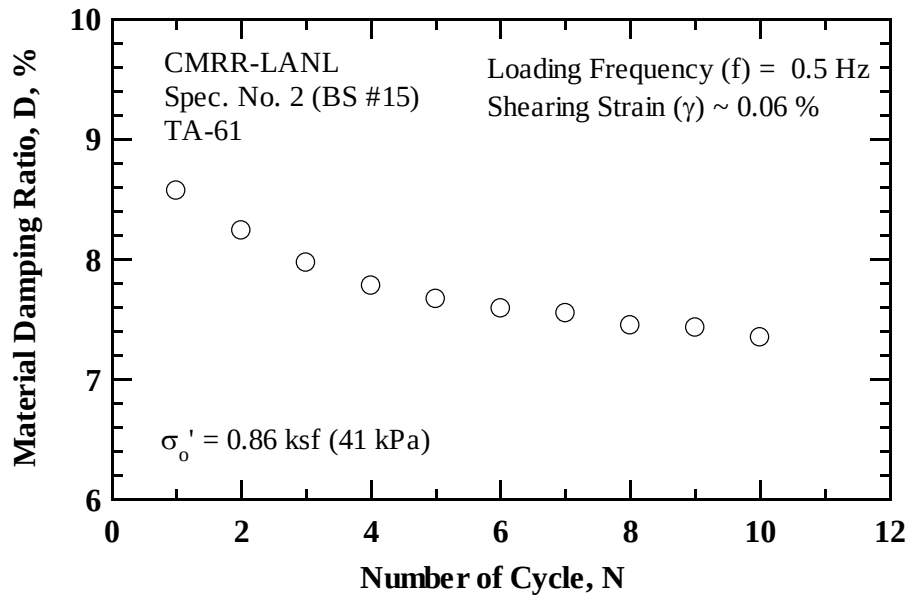

(b) Material Damping Ratio, D

Figure D.14 Variation of (a) Shear Modulus and (b) Material Damping Ratio with Number of Cycles for Spec. No. 2 from Block Sample #15 (Lower Unit 3, Bandelier Tuff (Qbt3L)) at an Isotropic Confining Pressure of 0.86 ksf (41 kPa) from Torsional Shear (TS) Tests

Copyright 2007, Kleinfelder

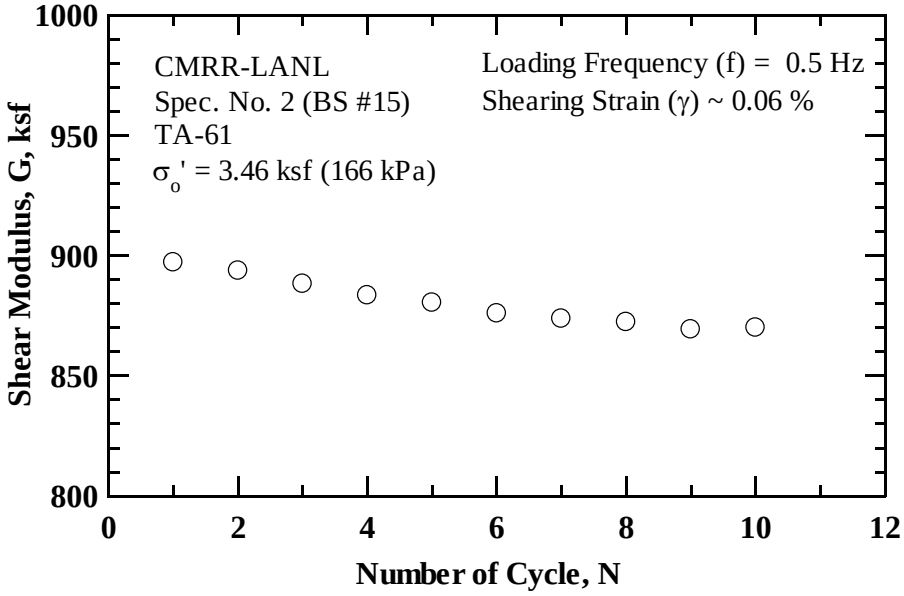

(a) Shear Modulus, G

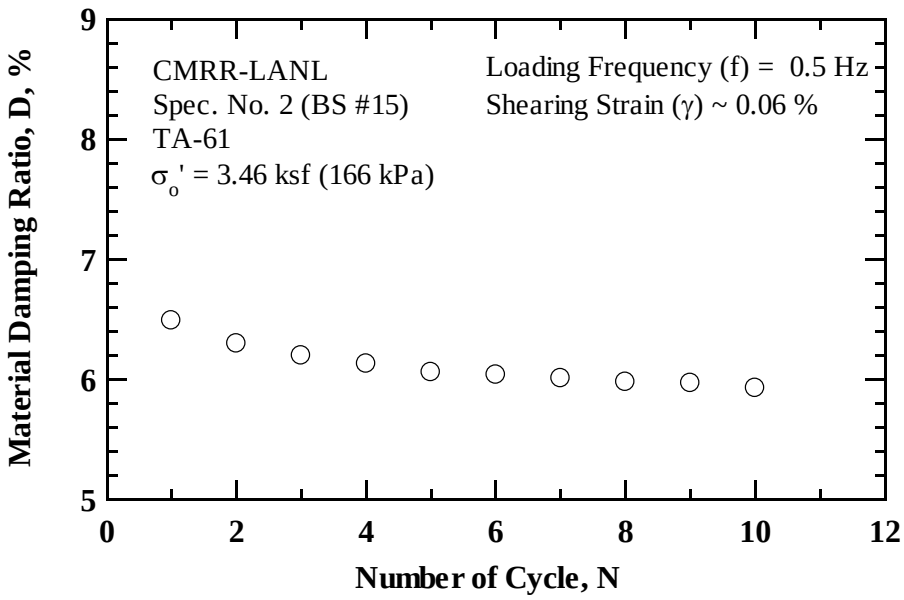

(b) Material Damping Ratio, D

Figure D.15 Variation of (a) Shear Modulus and (b) Material Damping Ratio with Number of Cycles for Spec. No. 2 from Block Sample #15 (Lower Unit 3, Bandelier Tuff (Qbt3L)) at an Isotropic Confining Pressure of 3.46 ksf (166 kPa) from Torsional Shear (TS) Tests

Copyright 2007, Kleinfelder

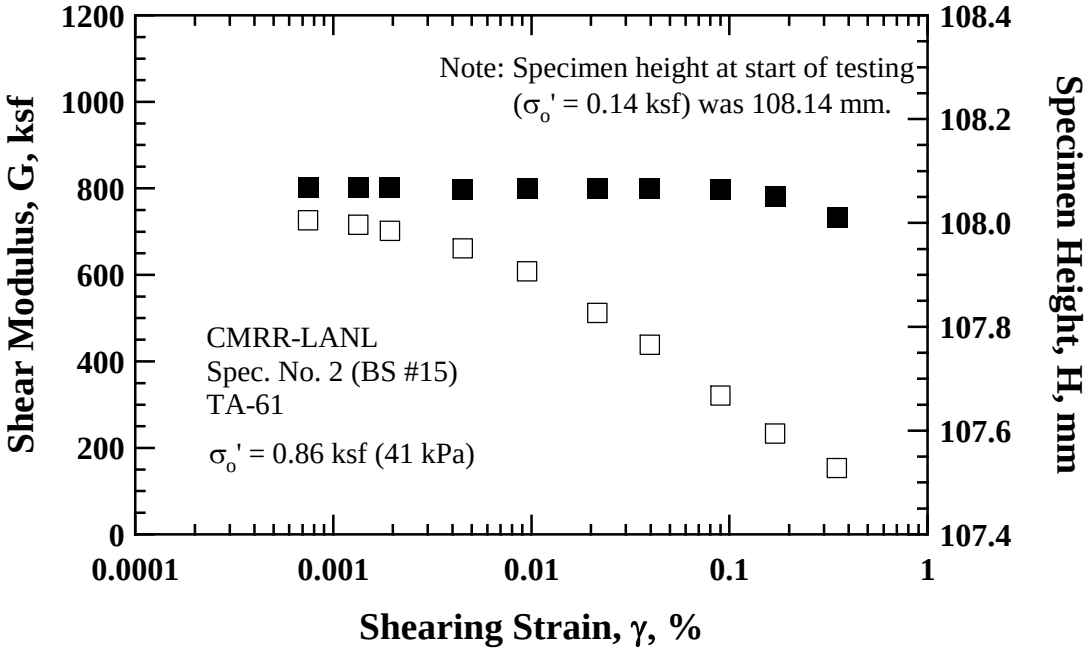

(a) σ_o' = 0.86 ksf (41 kPa)

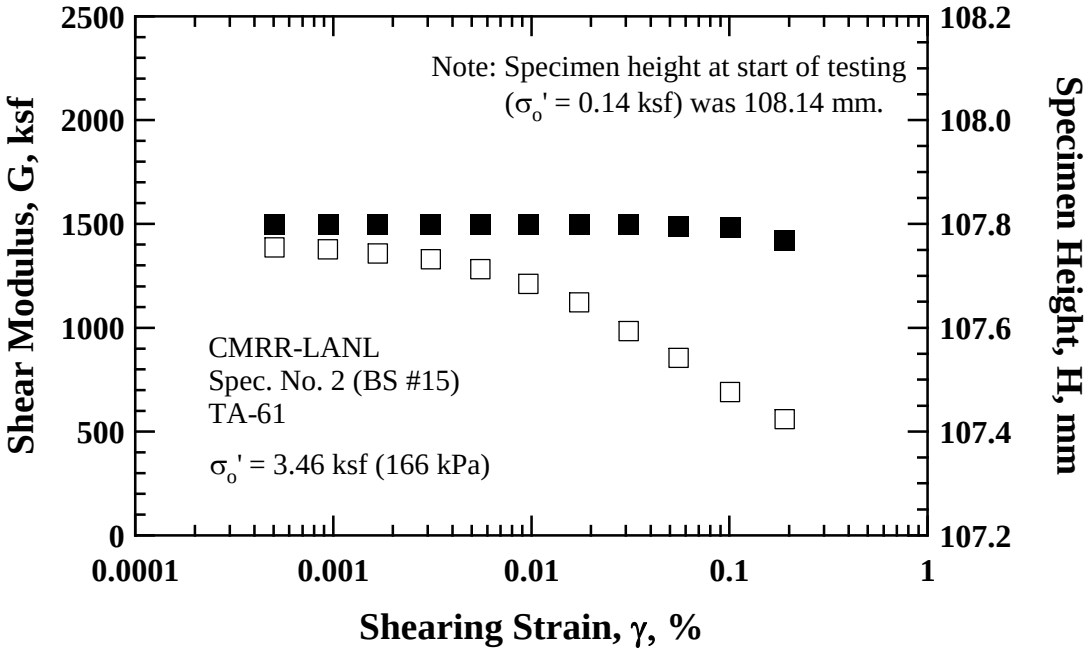

(b) σ_o' = 3.46 ksf (166 kPa)

Figure D.16 Variation in Shear Modulus and Specimen Height Change with Shearing Strain for Spec. No. 2 from Block Sample #15 (Lower Unit 3, Bandelier Tuff (Qbt3L)) as Determined from Resonant Column (RC) Tests at Two Different Isotropic Confining Pressures: (a) 0.86 ksf (41 kPa) and (b) 3.46 ksf (166 kPa)

Copyright 2007, Kleinfelder

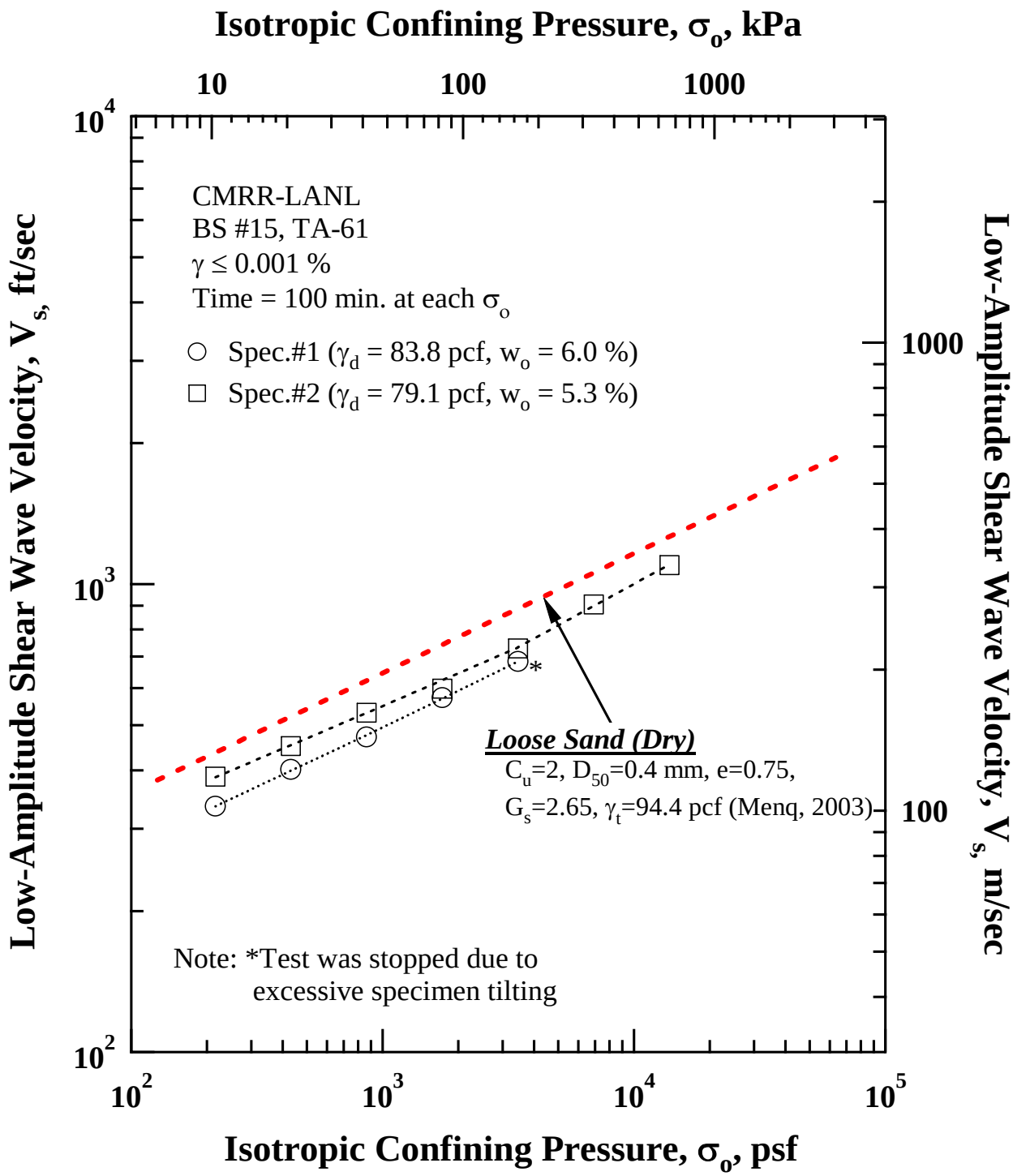

Figure D.17 Comparison between the Trend Line for a Dry Loose Sand Predicted by Menq (2003) and the Variation in Low-Amplitude Shear Wave Velocity with Isotropic Confining Pressure of the Two Intact Specimens from Block Sample #15 (Lower Unit 3, Bandelier Tuff (Qbt3L)) as Determined from Resonant Column (RC) Tests

Copyright 2007, Kleinfelder

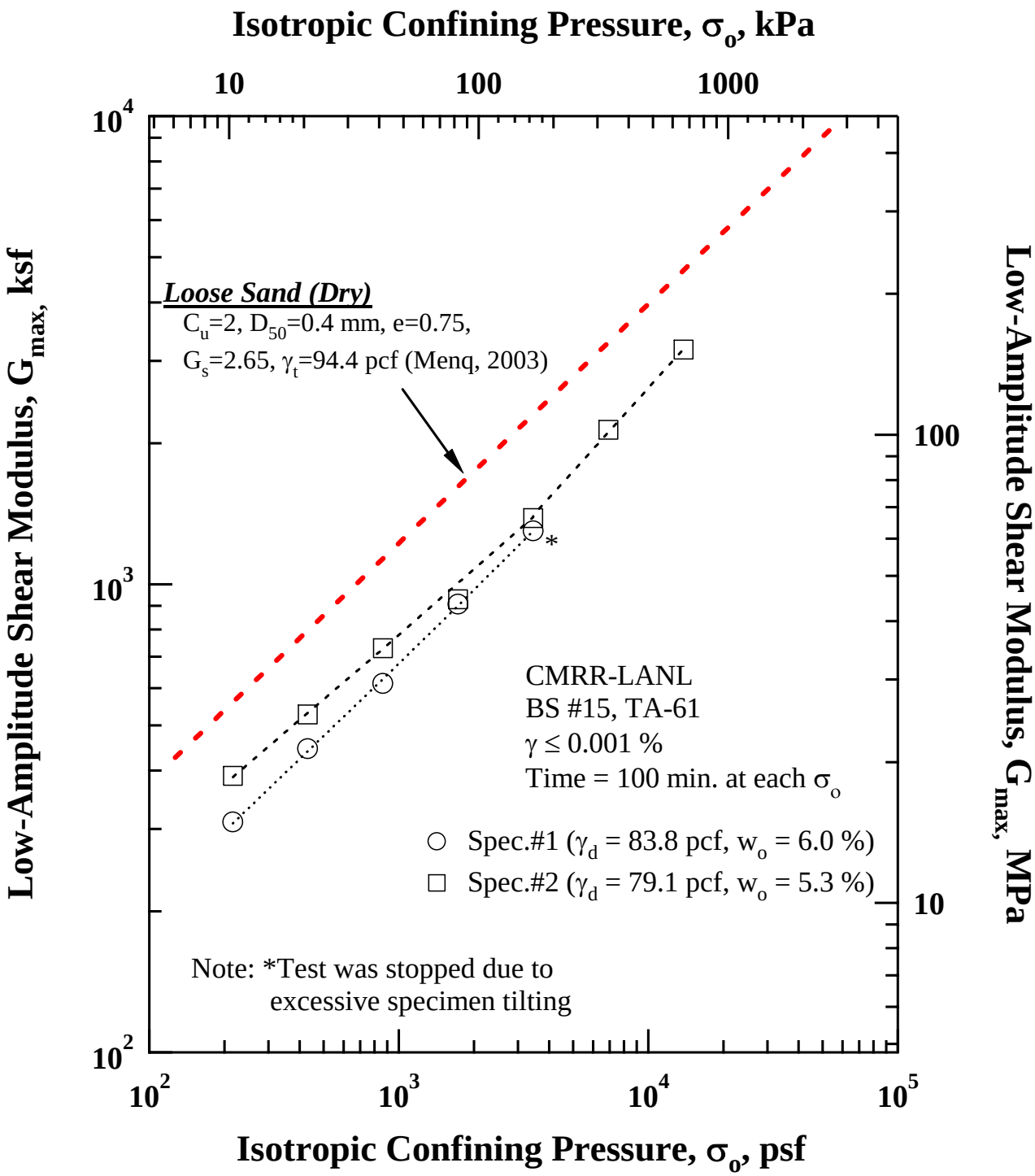

Figure D.18 Comparison between the Trend Line for a Dry Loose Sand Predicted by Menq (2003) and the Variation in Low-Amplitude Shear Modulus with Isotropic Confining Pressure of the Two Intact Specimens from Block Sample #15 (Lower Unit 3, Bandelier Tuff (Qbt3L)) as Determined from Resonant Column (RC) Tests

Copyright 2007, Kleinfelder

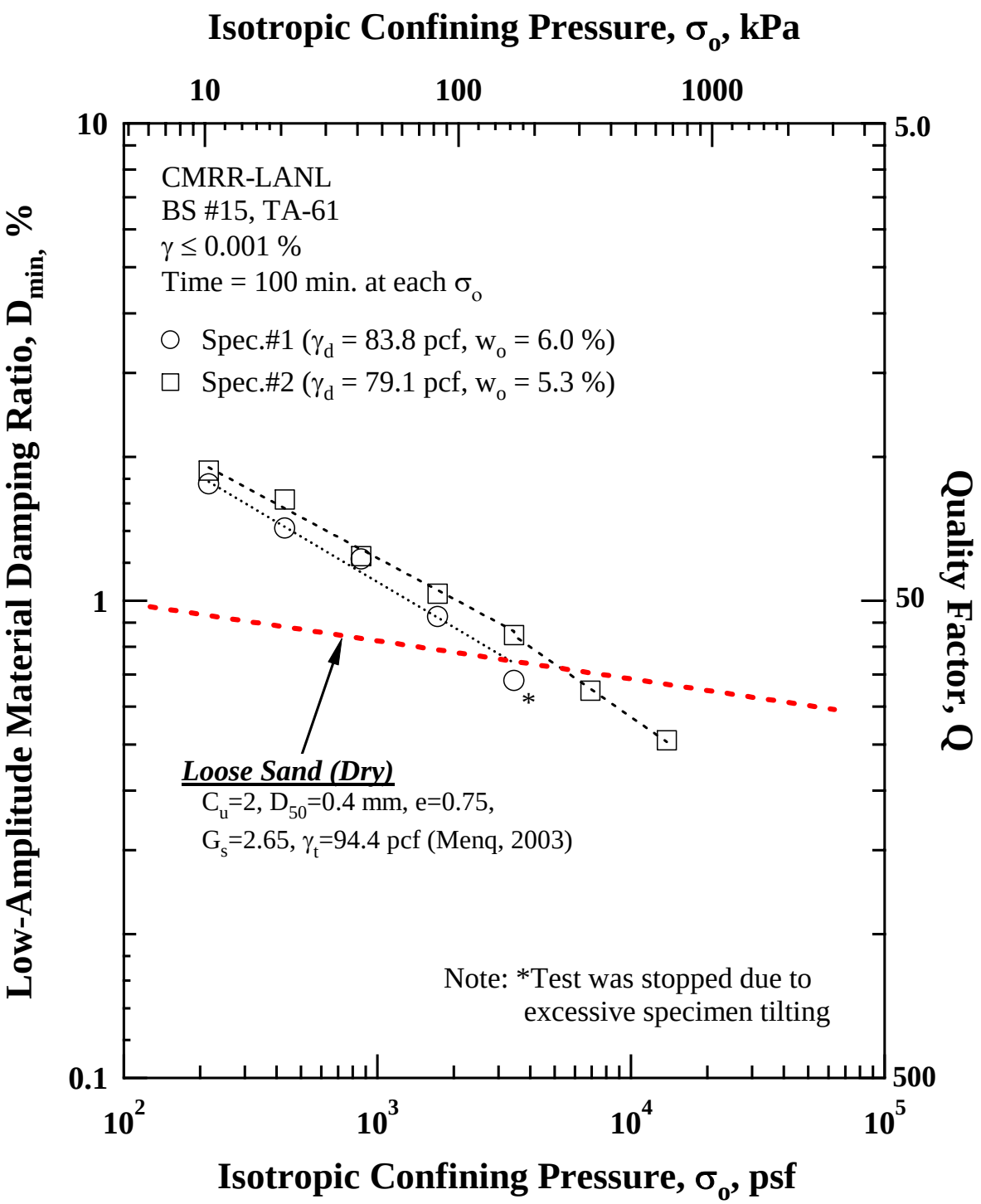

Figure D.19 Comparison between the Trend Line for a Dry Loose Sand Predicted by Menq (2003) and the Variation in Low-Amplitude Material Damping Ratio with Isotropic Confining Pressure of the Two Intact Specimens from Block Sample #15 (Lower Unit 3, Bandelier Tuff (Qbt3L)) as Determined from Resonant Column (RC) Tests

Copyright 2007, Kleinfelder

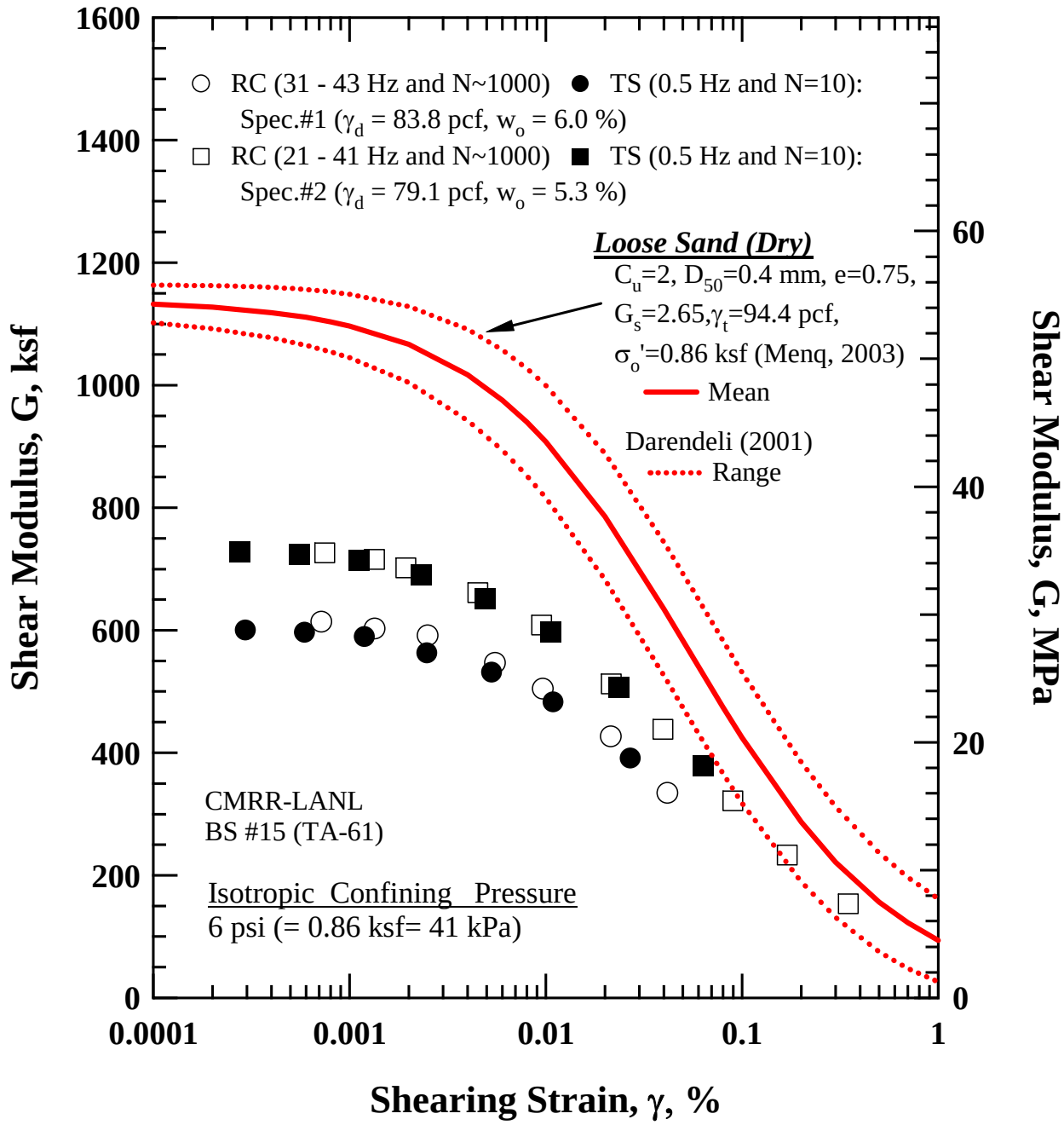

Figure D.20 Comparison between the Trend Line for a Dry Loose Sand Predicted by Menq (2003) and Darendeli (2001) and the Variation in Shear Modulus with Shearing Strain of the Two Intact Specimens from Block Sample #15 (Lower Unit 3, Bandelier Tuff (Qbt3L)) as Determined from Resonant Column (RC) Tests

Copyright 2007, Kleinfelder

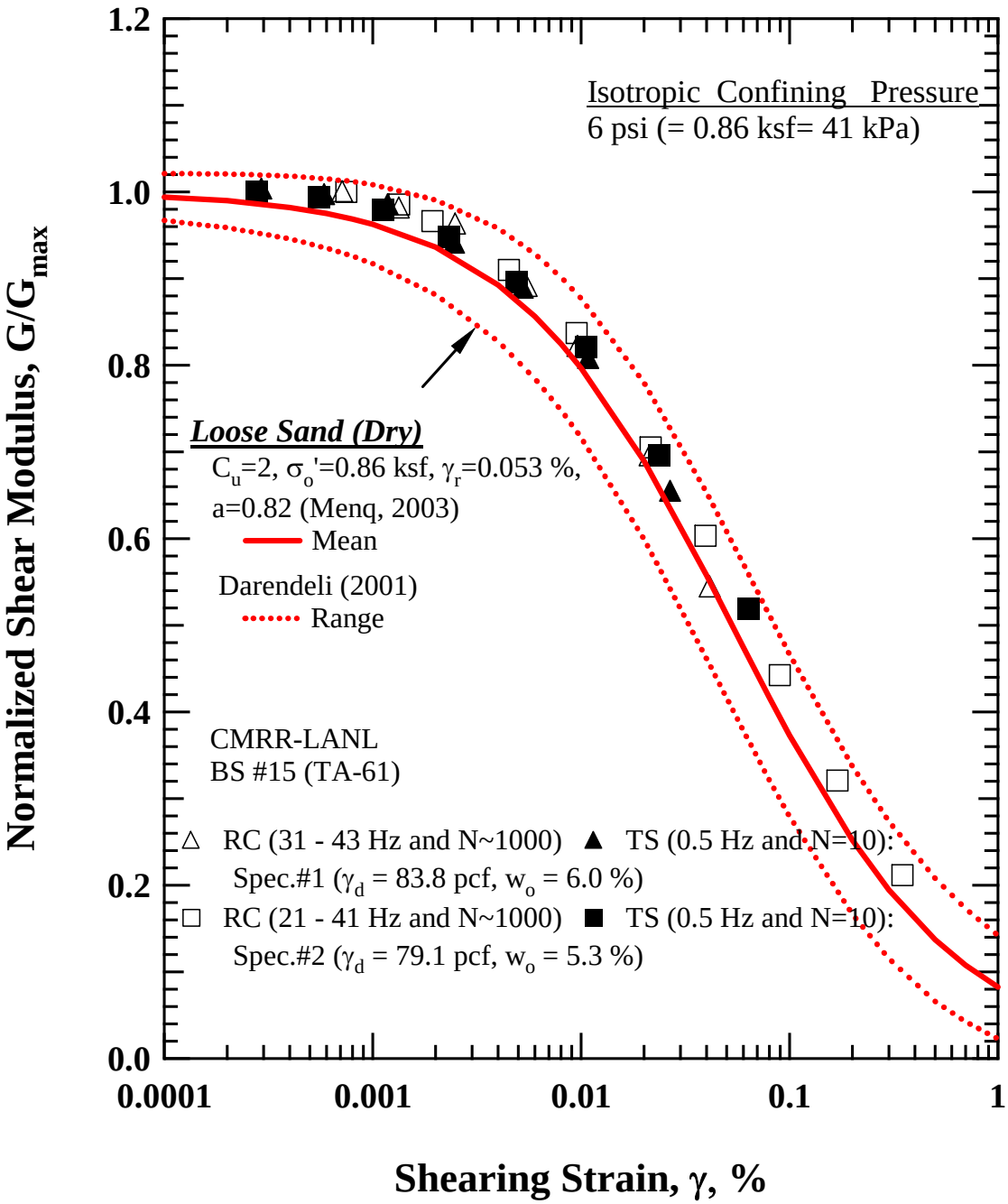

Figure D.21 Comparison between the Trend Line for a Dry Loose Sand Predicted by Menq (2003) and Darendeli (2001) and the Variation in Normalized Shear Modulus with Shearing Strain of the Two Intact Specimens from Block Sample #15 (Lower Unit 3, Bandelier Tuff (Qbt3L)) as Determined from Resonant Column (RC) Tests

Copyright 2007, Kleinfelder

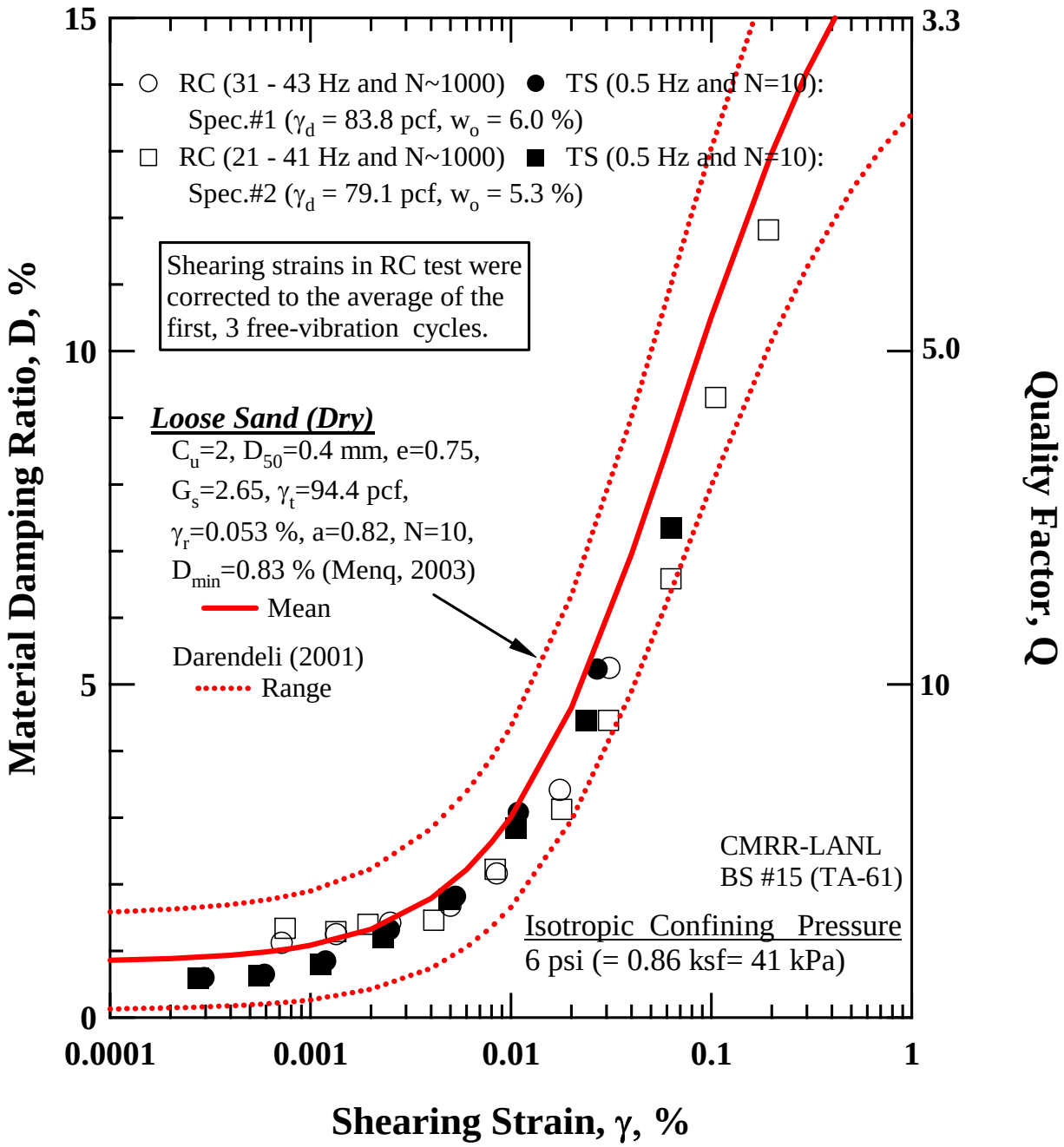

Figure D.22 Comparison between the Trend Line for a Dry Loose Sand Predicted by Menq. (2003) and Darendeli (2001) and the Variation in Material Damping Ratio with Shearing Strain of the Two Intact Specimens from Block Sample #15 (Lower Unit 3, Bandelier Tuff (Qbt3L)) as Determined from Resonant Column (RC) Tests

Copyright 2007, Kleinfelder

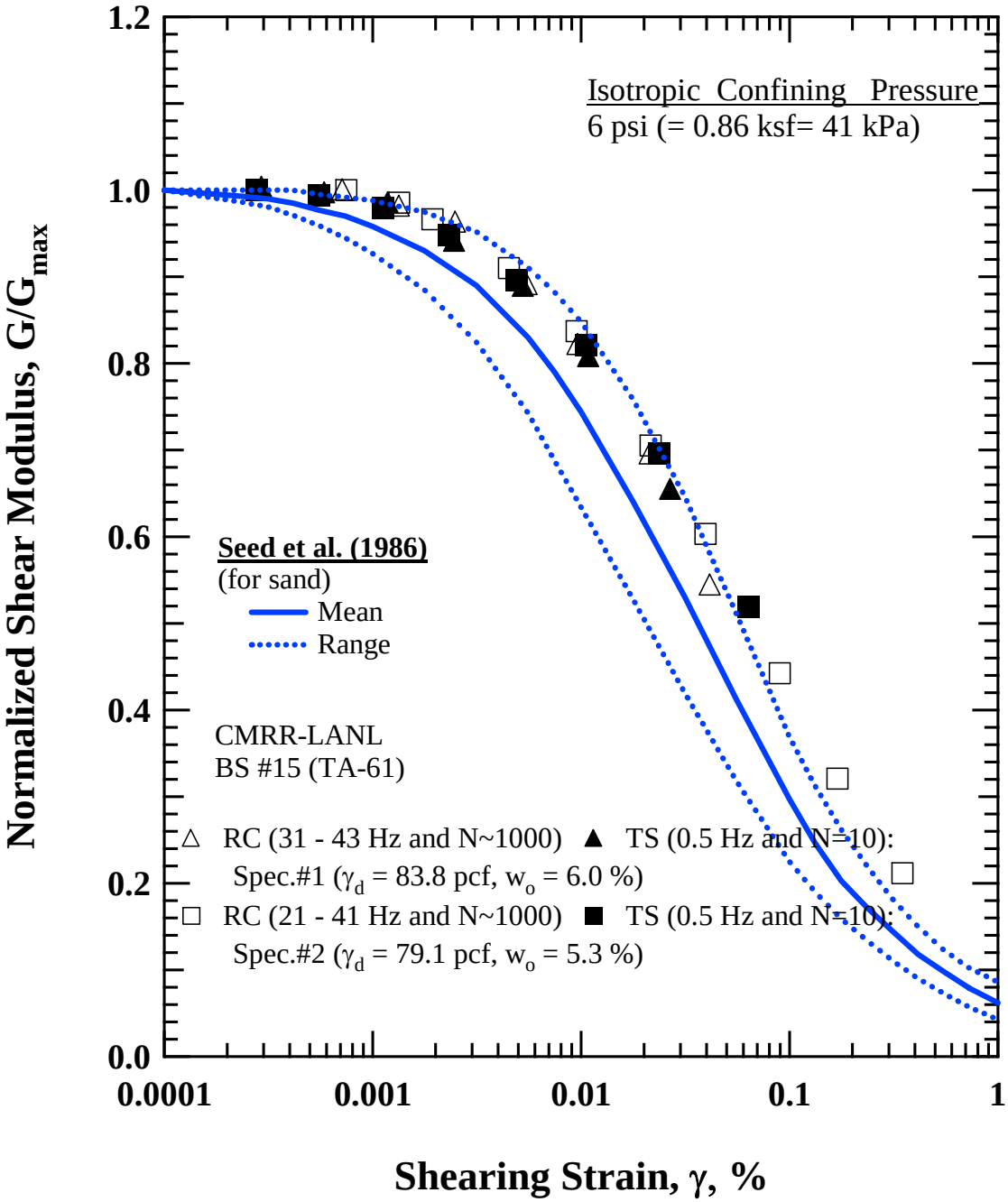

Figure D.23 Comparison between the Trend Line for a Dry Loose Sand Predicted by Seed et al. (1986) and the Variation in Shear Modulus with Shearing Strain of the Two Intact Specimens from Block Sample #15 (Lower Unit 3, Bandelier Tuff (Qbt3L)) as Determined from Resonant Column (RC) Tests

Copyright 2007, Kleinfelder

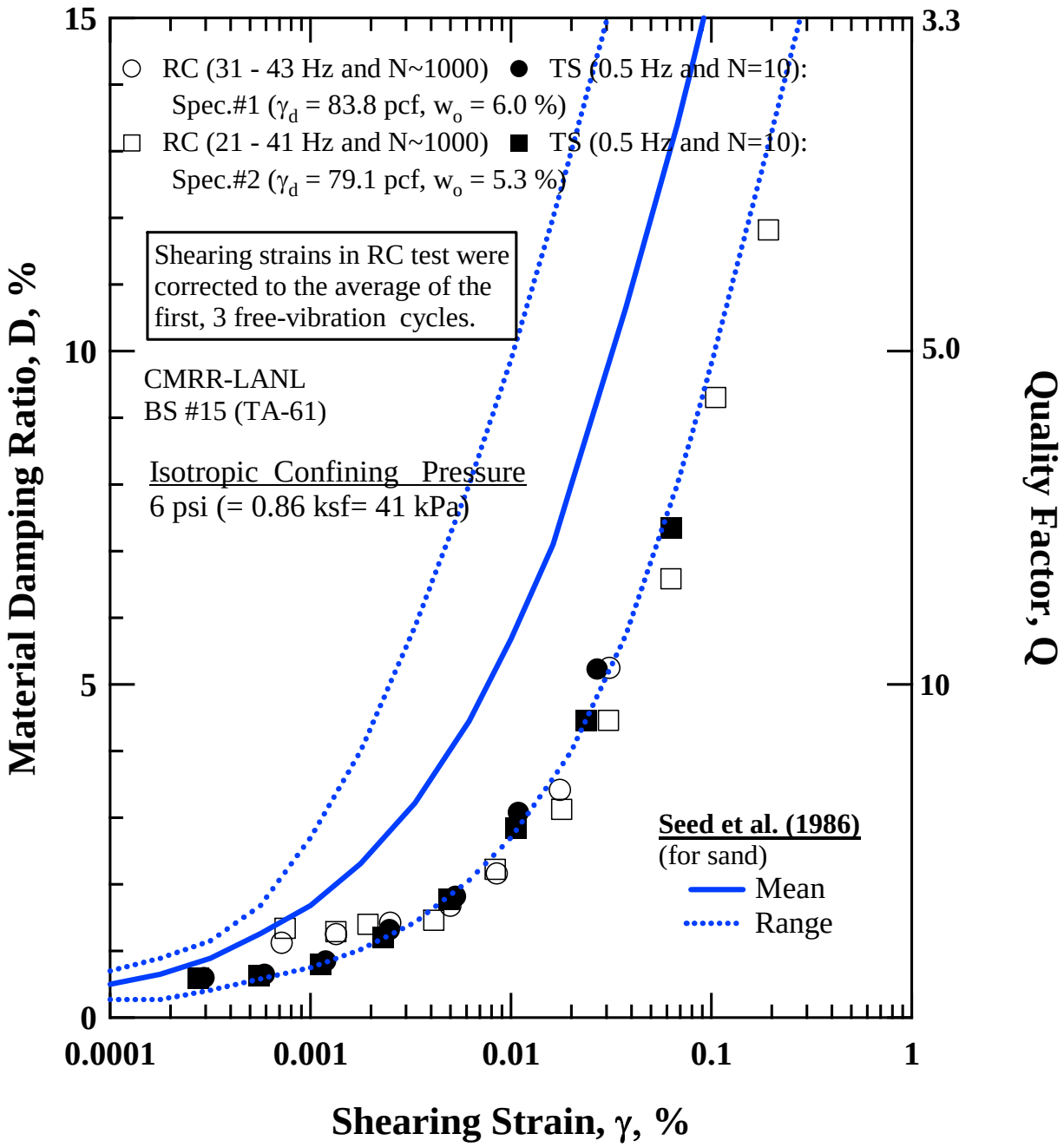

Figure D.24 Comparison between the Trend Line for a Dry Loose Sand Predicted by Seed et al. (1986) and the Variation in Material Damping Ratio with Shearing Strain of the Two Intact Specimens from Block Sample #15 (Lower Unit 3, Bandelier Tuff (Qbt3L)) as Determined from Resonant Column (RC) Tests

Copyright 2007, Kleinfelder

Table D.1 Variation in Low-Amplitude Shear Wave Velocity, Low-Amplitude Shear Modulus, Low-Amplitude Material Damping Ratio and Estimated Total Unit Weight with Isotropic Confining Pressure of Spec. No. 1 from Block Sample #15 (Lower Unit 3, Bandelier Tuff (Qbt3L)) as Determined from Resonant Column (RC) Tests

Isotropic Confining Pressure, σ_o'			Low-Amplitude Shear Modulus, G_{max}		Low-Amplitude Shear Wave Velocity, Vs	Low-Amplitude Material Damping Ratio, Dmin	Estimated Total Unit Weight, γ_t
(psi)	(psf)	(kPa)	(ksf)	(MPa)	(fps)	(%)	
1.5	216	10	311	14.9	335	1.76	88.8
3.0	432	21	445	21.4	402	1.42	88.9
6	864	41	614	29.4	471	1.22	89.0
12	1728	83	907	43.5	572	0.93	89.3
24	3456	166	1299	62.3	683	0.68	89.7

Table D.2 Variation in Low-Amplitude Shear Wave Velocity, Low-Amplitude Shear Modulus, Low-Amplitude Material Damping Ratio and Estimated Total Unit Weight with Isotropic Confining Pressure of Spec. No. 2 from Block Sample #15 (Lower Unit 3, Bandelier Tuff (Qbt3L)) as Determined from Resonant Column (RC) Tests

Isotropic Confining Pressure, σ_o'			Low-Amplitude Shear Modulus, G_{max}		Low-Amplitude Shear Wave Velocity, Vs	Low-Amplitude Material Damping Ratio, Dmin	Estimated Total Unit Weight, γ_t
(psi)	(psf)	(kPa)	(ksf)	(MPa)	(fps)	(%)	
1.5	216	10	390	18.7	388	1.87	83.3
3.0	432	21	527	25.3	451	1.63	83.4
6	864	41	730	35.0	531	1.24	83.4
12	1728	83	929	44.5	598	1.03	83.7
24	3456	166	1385	66.4	729	0.85	84.0
48	6912	331	2139	102.6	905	0.65	84.5
96	13824	663	3172	152.1	1098	0.51	85.1

Copyright 2007, Kleinfelder

Table D.3 Variation in Shear Modulus, Normalized Shear Modulus, Material Damping Ratio and Specimen Height with Shearing Strain from RC Tests of Spec. No. 1 from Block Sample #15 (Lower Unit 3, Bandelier Tuff (Qbt3L)); Isotropic Confining Pressure , σ_o' = 0.86 ksf (41 kPa)

Peak Shearing Strain, %	Shear Modulus, G, ksf	Normalized Shear Modulus, G/G_{max}	Average[+] Shearing Strain, %	Material Damping Ratio[x], D, %	Specimen Height[#], mm
7.18E-04	614	1.00	7.18E-04	1.12	100.92
1.34E-03	603	0.98	1.34E-03	1.25	100.92
2.50E-03	591	0.96	2.50E-03	1.42	100.92
5.52E-03	547	0.89	4.99E-03	1.67	100.93
9.68E-03	504	0.82	8.50E-03	2.16	100.92
2.14E-02	427	0.70	1.76E-02	3.41	100.92
4.16E-02	334	0.54	3.10E-02	5.25	100.92

Notes: [+]Average Shearing Strain from the First Three Cycles of the Free Vibration Decay Curve
[x]Average Damping Ratio from the First Three Cycles of the Free Vibration Decay Curve
[#]Specimen height at start of testing (σ_o' = 0.14 ksf) was 101.01 mm.

Table D.4 Variation in Shear Modulus, Normalized Shear Modulus and Material Damping Ratio with Shearing Strain from TS Tests of Spec. No. 1 from Block Sample #15 (Lower Unit 3, Bandelier Tuff (Qbt3L)); Isotropic Confining Pressure , σ_o' = 0.86 ksf (41 kPa)

First Cycle				Tenth Cycle			
Peak Shearing Strain, %	Shear Modulus, G, ksf	Normalized Shear Modulus, G/G_{max}	Material Damping Ratio, D, %	Peak Shearing Strain, %	Shear Modulus, G, ksf	Normalized Shear Modulus, G/G_{max}	Material Damping Ratio, D, %
2.95E-04	602	1.01	0.74	2.94E-04	601	1.00	0.60
5.87E-04	594	0.99	0.78	5.89E-04	597	1.00	0.65
1.18E-03	589	0.98	0.86	1.19E-03	590	0.99	0.85
2.47E-03	567	0.95	1.39	2.47E-03	563	0.94	1.32
5.24E-03	543	0.91	2.01	5.28E-03	532	0.89	1.82
1.07E-02	493	0.82	3.56	1.09E-02	483	0.81	3.08
2.58E-02	408	0.68	6.06	2.69E-02	392	0.65	5.23

Copyright 2007, Kleinfelder

Table D.5 Variation in Shear Modulus, Normalized Shear Modulus, Material Damping Ratio and Specimen Height with Shearing Strain from RC Tests of Spec. No. 1 from Block Sample #15 (Lower Unit 3, Bandelier Tuff (Qbt3L)); Isotropic Confining Pressure , σ_o' = 3.46 ksf (166 kPa)

Peak Shearing Strain, %	Shear Modulus, G, ksf	Normalized Shear Modulus, G/G_{max}	Average[+] Shearing Strain, %	Material Damping Ratio[x], D, %	Specimen Height[#], mm
5.23E-04	1322	1.00	5.23E-04	0.96	100.33
8.83E-04	1316	1.00	8.83E-04	0.96	100.33
1.70E-03	1304	0.99	1.70E-03	0.93	100.33
2.95E-03	1277	0.97	2.78E-03	0.99	100.33
5.36E-03	1233	0.93	4.99E-03	1.15	100.33
9.39E-03	1168	0.89	8.59E-03	1.47	100.33
1.62E-02	1067	0.81	1.42E-02	2.12	100.33
2.78E-02	934	0.71	2.32E-02	3.02	100.33
4.83E-02	793	0.60	3.74E-02	4.49	100.32
8.07E-02	634	0.48	5.72E-02	6.29	100.31
1.59E-01	468	0.35	9.86E-02	9.27	100.28

Notes: [+]Average Shearing Strain from the First Three Cycles of the Free Vibration Decay Curve
[x]Average Damping Ratio from the First Three Cycles of the Free Vibration Decay Curve
[#]Specimen height at start of testing (σ_o' = 0.14 ksf) was 101.01 mm.

Table D.6 Variation in Shear Modulus, Normalized Shear Modulus and Material Damping Ratio with Shearing Strain from TS Tests of Spec. No. 1 from Block Sample #15 (Lower Unit 3, Bandelier Tuff (Qbt3L)); Isotropic Confining Pressure , σ_o' = 3.46 ksf (166 kPa)

First Cycle				Tenth Cycle			
Peak Shearing Strain, %	Shear Modulus, G, ksf	Normalized Shear Modulus, G/G_{max}	Material Damping Ratio, D, %	Peak Shearing Strain, %	Shear Modulus, G, ksf	Normalized Shear Modulus, G/G_{max}	Material Damping Ratio, D, %
5.84E-04	1342	1.00	0.56	5.65E-04	1345	1.00	0.59
9.83E-04	1345	1.00	0.49	9.51E-04	1343	1.00	0.43
2.73E-03	1326	0.99	0.76	2.72E-03	1312	0.98	0.84
5.50E-03	1287	0.96	1.25	5.53E-03	1270	0.94	1.23
1.01E-02	1226	0.91	2.10	1.03E-02	1205	0.90	1.90
2.32E-02	1070	0.80	3.91	2.40E-02	1033	0.77	3.65
6.10E-02	800	0.60	8.12	6.53E-02	746	0.55	7.32

Copyright 2007, Kleinfelder

Table D.7 Variation in Shear Modulus, Normalized Shear Modulus, Material Damping Ratio and Specimen Height with Shearing Strain from RC Tests of Spec. No. 2 from Block Sample #15 (Lower Unit 3, Bandelier Tuff (Qbt3L)); Isotropic Confining Pressure , σ_o' = 0.86 ksf (41 kPa)

Peak Shearing Strain, %	Shear Modulus, G, ksf	Normalized Shear Modulus, G/G_{max}	Average[+] Shearing Strain, %	Material Damping Ratio[x], D, %	Specimen Height[#], mm
7.47E-04	727	1.00	7.47E-04	1.34	108.07
1.34E-03	716	0.99	1.34E-03	1.29	108.07
1.93E-03	702	0.97	1.93E-03	1.40	108.07
4.50E-03	661	0.91	4.12E-03	1.46	108.06
9.52E-03	608	0.84	8.33E-03	2.23	108.07
2.15E-02	512	0.71	1.79E-02	3.13	108.07
3.96E-02	438	0.60	3.07E-02	4.46	108.07
8.99E-02	321	0.44	6.28E-02	6.58	108.06
1.70E-01	233	0.32	1.05E-01	9.31	108.05
3.49E-01	154	0.21	1.93E-01	11.82	108.01

Notes: [+]Average Shearing Strain from the First Three Cycles of the Free Vibration Decay Curve
[x]Average Damping Ratio from the First Three Cycles of the Free Vibration Decay Curve
[#]Specimen height at start of testing (σ_o' = 0.14 ksf) was 108.14 mm.

Table D.8 Variation in Shear Modulus, Normalized Shear Modulus and Material Damping Ratio with Shearing Strain from TS Tests of Spec. No. 2 from Block Sample #15 (Lower Unit 3, Bandelier Tuff (Qbt3L)); Isotropic Confining Pressure , σ_o' = 0.86 ksf (41 kPa)

First Cycle				Tenth Cycle			
Peak Shearing Strain, %	Shear Modulus, G, ksf	Normalized Shear Modulus, G/G_{max}	Material Damping Ratio, D, %	Peak Shearing Strain, %	Shear Modulus, G, ksf	Normalized Shear Modulus, G/G_{max}	Material Damping Ratio, D, %
2.76E-04	727	1.00	0.69	2.76E-04	728	1.00	0.59
5.52E-04	722	0.99	0.70	5.53E-04	724	0.99	0.63
1.12E-03	714	0.98	0.90	1.12E-03	714	0.98	0.80
2.31E-03	689	0.95	1.22	2.31E-03	691	0.95	1.20
4.86E-03	660	0.91	1.93	4.91E-03	652	0.90	1.78
1.04E-02	610	0.84	3.17	1.06E-02	598	0.82	2.84
2.29E-02	522	0.72	4.85	2.36E-02	507	0.70	4.46
6.08E-02	397	0.55	8.57	6.33E-02	379	0.52	7.35

Copyright 2007, Kleinfelder

Table D.9. Variation in Shear Modulus, Normalized Shear Modulus, Material Damping Ratio and Specimen Height with Shearing Strain from RC Tests of Spec. No. 2 from Block Sample #15 (Lower Unit 3, Bandelier Tuff (Qbt3L)); Isotropic Confining Pressure , σ_o' = 3.46 ksf (166 kPa)

Peak Shearing Strain, %	Shear Modulus, G, ksf	Normalized Shear Modulus, G/G_{max}	Average[+] Shearing Strain, %	Material Damping Ratio[x], D, %	Specimen Height[#], mm
5.05E-04	1387	1.00	5.05E-04	0.83	107.80
9.41E-04	1377	1.00	9.41E-04	0.86	107.80
1.68E-03	1358	0.98	1.68E-03	1.00	107.80
3.11E-03	1329	0.96	2.91E-03	1.08	107.80
5.54E-03	1282	0.93	5.15E-03	1.19	107.80
9.67E-03	1212	0.88	8.79E-03	1.58	107.80
1.74E-02	1122	0.81	1.53E-02	2.20	107.80
3.10E-02	985	0.71	2.57E-02	3.20	107.80
5.53E-02	855	0.62	4.32E-02	4.33	107.80
1.01E-01	691	0.50	7.23E-02	5.95	107.79
1.90E-01	560	0.40	1.20E-01	8.67	107.77

Notes: [+]Average Shearing Strain from the First Three Cycles of the Free Vibration Decay Curve
[x]Average Damping Ratio from the First Three Cycles of the Free Vibration Decay Curve
[#]Specimen height at start of testing (σ_o' = 0.14 ksf) was 108.14 mm.

Table D.10 Variation in Shear Modulus, Normalized Shear Modulus and Material Damping Ratio with Shearing Strain from TS Tests of Spec. No. 2 from Block Sample #15 (Lower Unit 3, Bandelier Tuff (Qbt3L)); Isotropic Confining Pressure , σ_o' = 3.46 ksf (166 kPa)

First Cycle				Tenth Cycle			
Peak Shearing Strain, %	Shear Modulus, G, ksf	Normalized Shear Modulus, G/G_{max}	Material Damping Ratio, D, %	Peak Shearing Strain, %	Shear Modulus, G, ksf	Normalized Shear Modulus, G/G_{max}	Material Damping Ratio, D, %
2.75E-04	1461	1.00	0.36	2.74E-04	1464	1.00	0.47
5.50E-04	1461	1.00	0.46	5.50E-04	1461	1.00	0.44
1.01E-03	1430	0.98	0.50	1.01E-03	1438	0.98	0.50
2.93E-03	1384	0.95	1.04	2.92E-03	1386	0.95	0.93
6.05E-03	1326	0.91	1.59	6.08E-03	1323	0.90	1.40
1.30E-02	1242	0.85	2.73	1.32E-02	1224	0.84	2.32
3.02E-02	1069	0.73	4.79	3.10E-02	1040	0.71	4.16
5.80E-02	897	0.61	6.49	5.98E-02	870	0.59	5.93

Copyright 2007, Kleinfelder

Table D.11 Variation of Shear Modulus and Material Damping Ratio with Number of Cycles for Spec. No. 1 from Block Sample #15 (Lower Unit 3, Bandelier Tuff (Qbt3L)) at Isotropic Confining Pressures of 0.86 ksf (41 kPa) and 3.46 ksf (166 kPa) from Torsional Shear (TS) Tests

σ_o' = 0.86 ksf (41 kPa)			σ_o' = 3.46 ksf (166 kPa)		
Number of Cycles, N	Shear Modulus, G, ksf	Material Damping Ratio, D, %	Number of Cycles, N	Shear Modulus, G, ksf	Material Damping Ratio, D, %
1	408	6.06	1	800	8.12
2	406	5.86	2	783	8.01
3	402	5.69	3	773	7.83
4	399	5.56	4	767	7.70
5	398	5.47	5	760	7.62
6	397	5.43	6	757	7.55
7	394	5.38	7	753	7.49
8	394	5.33	8	752	7.43
9	393	5.29	9	749	7.37
10	392	5.23	10	746	7.32

Table D.12 Variation of Shear Modulus and Material Damping Ratio with Number of Cycles for Spec. No. 2 from Block Sample #15 (Lower Unit 3, Bandelier Tuff (Qbt3L)) at Isotropic Confining Pressures of 0.86 ksf (41 kPa) and 3.46 ksf (166 kPa) from Torsional Shear (TS) Tests

σ_o' = 0.86 ksf (41 kPa)			σ_o' = 3.46 ksf (166 kPa)		
Number of Cycles, N	Shear Modulus, G, ksf	Material Damping Ratio, D, %	Number of Cycles, N	Shear Modulus, G, ksf	Material Damping Ratio, D, %
1	397	8.57	1	897	6.49
2	393	8.24	2	894	6.30
3	388	7.97	3	888	6.20
4	385	7.78	4	883	6.13
5	383	7.67	5	880	6.06
6	382	7.59	6	876	6.04
7	381	7.55	7	874	6.01
8	380	7.45	8	872	5.98
9	379	7.43	9	869	5.97
10	379	7.35	10	870	5.93

Copyright 2007, Kleinfelder

Appendix D

Results of Laboratory Testing Performed by Advanced Terra Testing

ADVANCED TERRA TESTING, Inc.
ATT
833 Parfet Street • Lakewood, Colorado 80215 • (303) 232-8308 • Fax: (303) 232-1579

Copyright 2007, Kleinfelder

TRIAXIAL SHEAR TESTS
ASTM D 2664 and ASTM D 5407 Modified

Copyright 2007, Kleinfelder

TRIAXIAL COMPRESSION TEST DATA
ASTM D 2664 and ASTM D 5407 Modified

CLIENT	Kleinfelder	JOB NO.	2304-67
BORING NO.	Site A, TA61	SAMPLED	
DEPTH	Elev. 7125.4	DATE TESTED	03/18/05 CAL
SAMPLE NO.	BS-4	CELL NUMBER	3N
SOIL DESCR.	#19435 SBT	SATURATED TEST	No
LOCATION	East1628885.19, West 1772225.33	AT FIELD MOIST.	Yes
TEST TYPE	TX/UU	CONF. PRES. PSF	6300

MOISTURE/DENSITY DATA	BEFORE TEST
Wt. Soil + Moisture (g)	839.0
Wt. Wet Soil & Pan (g)	869.7
Wt. Dry Soil & Pan (g)	849.2
Wt. Lost Moisture (g)	20.5
Wt. of Pan Only (g)	30.7
Wt. of Dry Soil (g)	818.5
Moisture Content %	2.5
Wet Density PCF	82.0
Dry Density PCF	80.0

Init. Diameter (in)	2.892
Init. Area (sq in)	6.569
Init. Height (in)	5.931
Volume cu Ft.	0.02254

Notes & Comments:

Young's Modulus (Calculated from the elastic portion of the load-displacement curve) = 5.9 x 10E03 psi
Not possible to obtain Poisson's ratio

Data entered by: CJW Date: 03/22/2005
Data checked by: Cae Date: 3/22/05
FileName: KITCSB04

ADVANCED TERRA TESTING, INC.

Copyright 2007, Kleinfelder

TRIAXIAL COMPRESSION TEST DATA

CLIENT	Kleinfelder	JOB NO.	2304-67
BORING NO.	Site A, TA61	SAMPLED	
DEPTH	Elev. 7125.4	DATE TESTED	03/18/05 CAL
SAMPLE NO.	BS-4	SETUP NO.	3N
SOIL DESCR.	#19435 SBT	SATURATED TEST	No
LOCATION	East1628885.19, West 1772225.33	AT FIELD MOIST.	Yes
TEST TYPE	TX/UU	CONF. PRES. PSF	6300

Init. Ht. (in)	5.931	Init. Area (sq in)	6.569
		Strain Rate (in/min)	0.060

Axial Load Lbs.	Axial Load PSF	Delta Ht. In.	Axial % Strain	Area Final Sq In.	Dev. Stress PSF	Pore Pres. PSI	Delta Pres. PSF	Sigma 3 PSF	Sigma 1 PSF	Prin. Stress Ratio
0.0	0	0.000	0.00	6.569	0	0.00	0.0	6300	0	0.00
210.0	4604	0.050	0.84	6.625	4565	0.00	0.0	6300	10865	1.72
500.0	10961	0.100	1.69	6.681	10776	0.00	0.0	6300	17076	2.71
670.0	14688	0.150	2.53	6.739	14316	0.00	0.0	6300	20616	3.27
768.0	16836	0.200	3.37	6.798	16268	0.00	0.0	6300	22568	3.58
830.0	18195	0.250	4.22	6.858	17428	0.00	0.0	6300	23728	3.77
873.0	19138	0.300	5.06	6.919	18170	0.00	0.0	6300	24470	3.88
903.0	19795	0.350	5.90	6.981	18627	0.00	0.0	6300	24927	3.96
924.0	20256	0.400	6.74	7.044	18890	0.00	0.0	6300	25190	4.00
938.0	20563	0.450	7.59	7.108	19002	0.00	0.0	6300	25302	4.02
946.0	20738	0.500	8.43	7.174	18990	0.00	0.0	6300	25290	4.01
954.0	20913	0.550	9.27	7.240	18974	0.00	0.0	6300	25274	4.01
960.0	21045	0.600	10.12	7.308	18916	0.00	0.0	6300	25216	4.00
965.0	21155	0.650	10.96	7.377	18836	0.00	0.0	6300	25136	3.99
968.0	21220	0.700	11.80	7.448	18716	0.00	0.0	6300	25016	3.97
970.0	21264	0.750	12.65	7.520	18575	0.00	0.0	6300	24875	3.95
970.0	21264	0.800	13.49	7.593	18396	0.00	0.0	6300	24696	3.92
965.0	21155	0.850	14.33	7.668	18123	0.00	0.0	6300	24423	3.88
958.0	21001	0.900	15.18	7.744	17814	0.00	0.0	6300	24114	3.83

Data entered by: CJW Date: 03/22/2005
Data checked by: [illegible] Date: 3/22/05
FileName: KITCSB04

ADVANCED TERRA TESTING, INC.

Copyright 2007, Kleinfelder

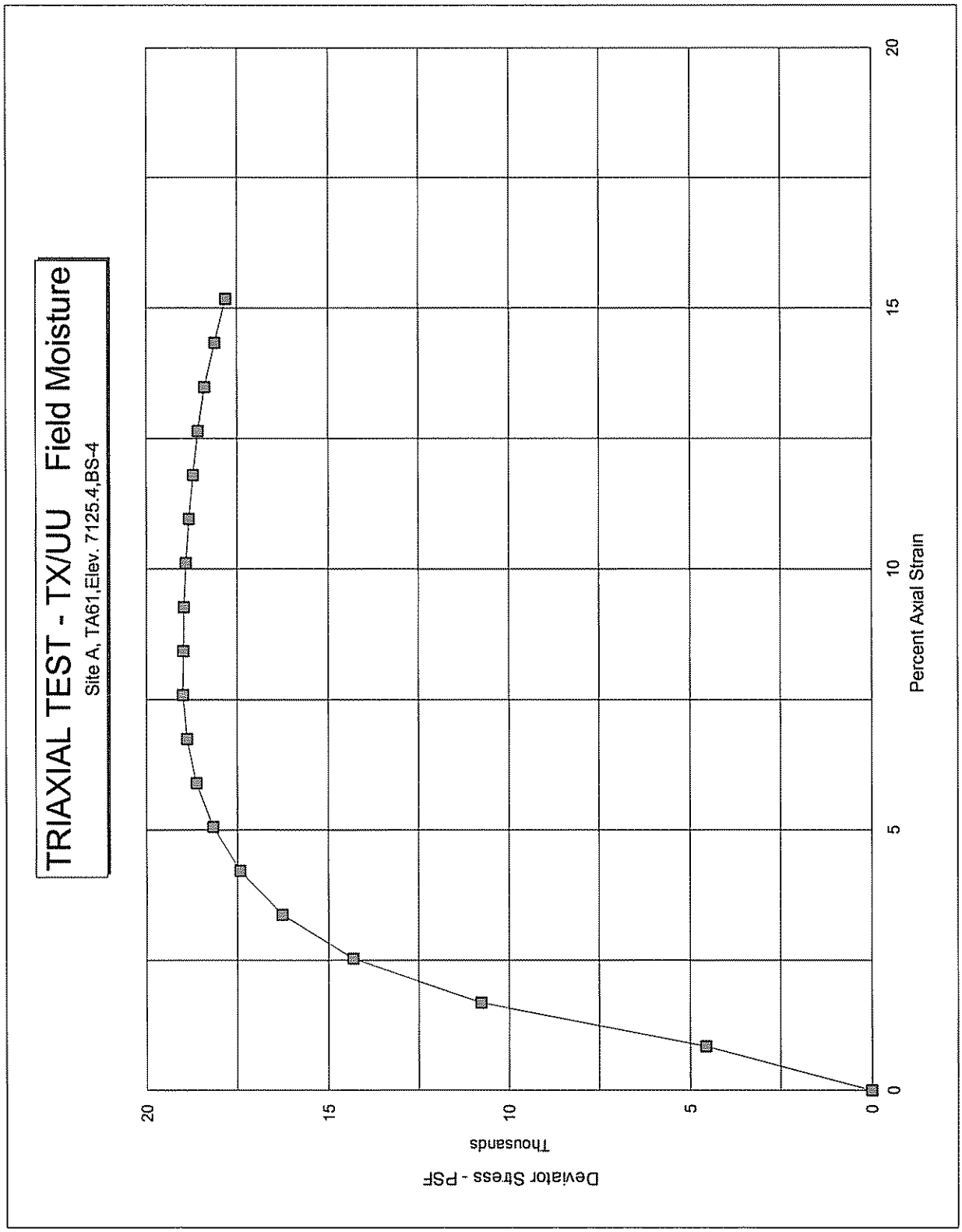
TRIAXIAL TEST - TX/UU Field Moisture
Site A, TA61,Elev. 7125.4,BS-4
Deviator Stress - PSF
Thousands
20
15
10
5
0
0
5
10
15
20
Percent Axial Strain

Client Kleinfelder
Job No. 2304-67
Boring No. TA61 BS-4
Depth Elev. 7788.4
Sample No. 4
Project SITE A
Sampled / / by
Prepped 9/18/05 by
Project No.
Before Test
KI2304/KISBT/KIDPTA6B.JPG
03-19-05

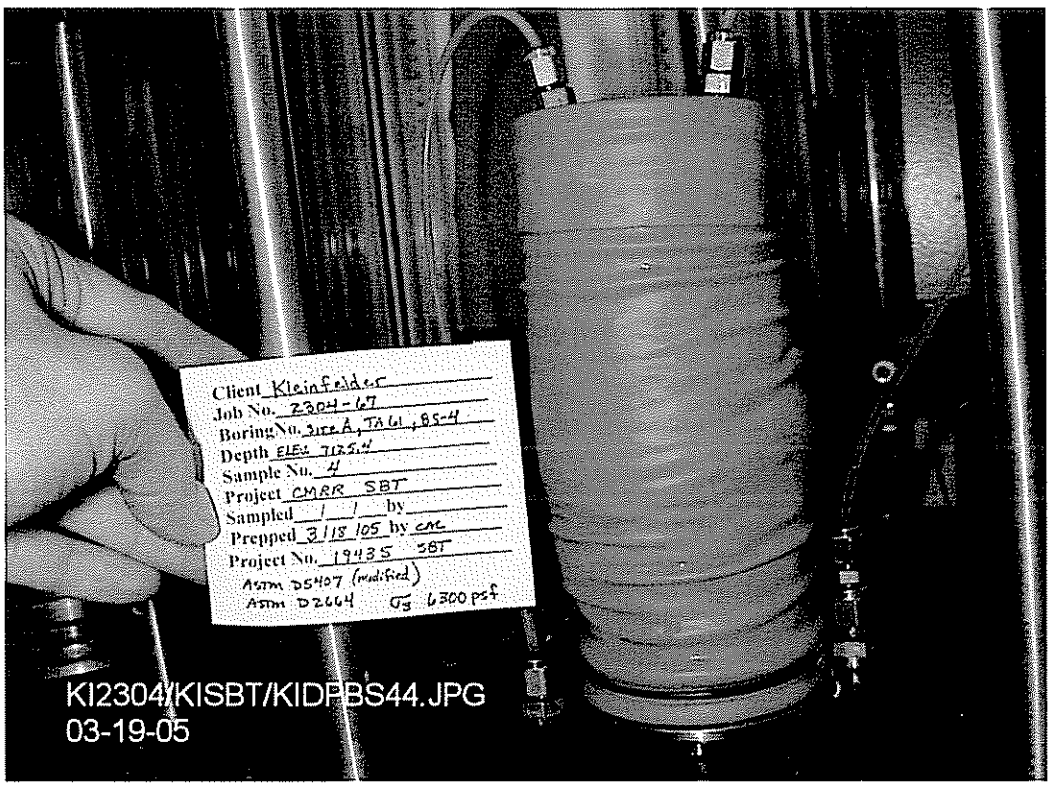

Copyright 2007, Kleinfelder

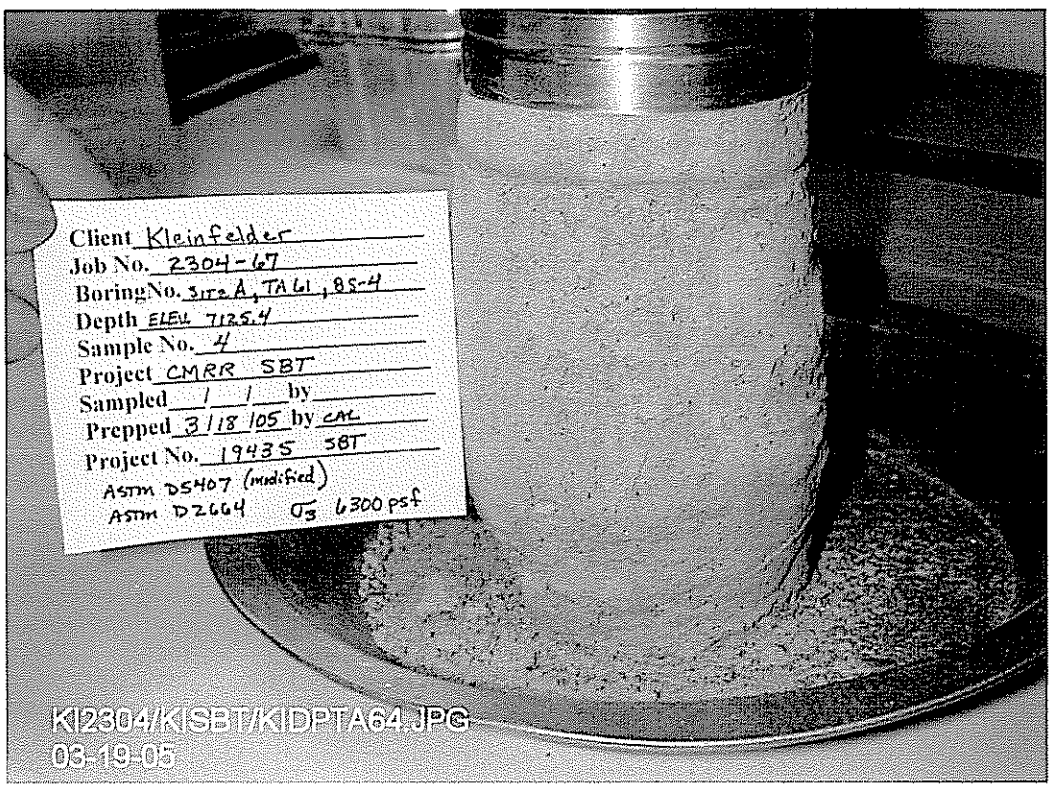

Copyright 2007, Kleinfelder

TRIAXIAL COMPRESSION TEST DATA
ASTM D 2664 and ASTM D 5407 Modified

CLIENT	Kleinfelder	JOB NO.	2304-67
BORING NO.	Site A, TA61	SAMPLED	
DEPTH	Elev. 7127.4	DATE TESTED	03/18/05 CAL
SAMPLE NO.	BS-14	CELL NUMBER	3N
SOIL DESCR.	#19435 SBT	SATURATED TEST	No
LOCATION	East1628908.58, West 1772225.88	AT FIELD MOIST.	Yes
TEST TYPE	TX/UU	CONF. PRES. PSF	9400

MOISTURE/DENSITY DATA	BEFORE TEST
Wt. Soil + Moisture (g)	885.4
Wt. Wet Soil & Pan (g)	1000.1
Wt. Dry Soil & Pan (g)	964.4
Wt. Lost Moisture (g)	35.7
Wt. of Pan Only (g)	114.7
Wt. of Dry Soil (g)	849.7
Moisture Content %	4.2
Wet Density PCF	87.1
Dry Density PCF	83.6
Init. Diameter (in)	2.816
Init. Area (sq in)	6.228
Init. Height (in)	6.216
Volume cu Ft.	0.02240

Notes & Comments:
Young's Modulus (Calculated from the elastic portion of the load-displacement curve) = 7.9 x 10E03 psi
Not possible to obtain Poisson's Ratio

Data entered by: CJW Date: 03/22/2005
Data checked by: cal Date: 3/22/05
FileName: KITCSB14

ADVANCED TERRA TESTING, INC.

Copyright 2007, Kleinfelder

TRIAXIAL COMPRESSION TEST DATA

CLIENT	Kleinfelder	JOB NO.	2304-67
BORING NO.	Site A, TA61	SAMPLED	
DEPTH	Elev. 7127.4	DATE TESTED	03/18/05 CAL
SAMPLE NO.	BS-14	SETUP NO.	3N
SOIL DESCR.	#19435 SBT	SATURATED TEST	No
LOCATION	East1628908.58, West 1772225.88	AT FIELD MOIST.	Yes
TEST TYPE	TX/UU	CONF. PRES. PSF	9400

Init. Ht. (in)	6.216	Init. Area (sq in)	6.228
		Strain Rate (in/min)	0.060

Axial Load Lbs.	Axial Load PSF	Delta Ht. In.	Axial % Strain	Area Final Sq In.	Dev. Stress PSF	Pore Pres. PSI	Delta Pres. PSF	Sigma 3 PSF	Sigma 1 PSF	Prin. Stress Ratio
0.0	0	0.000	0.00	6.228	0	0.00	0.0	9400	0	0.00
413.0	9549	0.050	0.80	6.279	9472	0.00	0.0	9400	18872	2.01
685.0	15838	0.100	1.61	6.330	15583	0.00	0.0	9400	24983	2.66
845.0	19537	0.150	2.41	6.382	19066	0.00	0.0	9400	28466	3.03
950.0	21965	0.200	3.22	6.435	21258	0.00	0.0	9400	30658	3.26
1025.0	23699	0.250	4.02	6.489	22746	0.00	0.0	9400	32146	3.42
1080.0	24971	0.300	4.83	6.544	23766	0.00	0.0	9400	33166	3.53
1125.0	26011	0.350	5.63	6.600	24547	0.00	0.0	9400	33947	3.61
1163.0	26890	0.400	6.44	6.656	25159	0.00	0.0	9400	34559	3.68
1195.0	27630	0.450	7.24	6.714	25629	0.00	0.0	9400	35029	3.73
1220.0	28208	0.500	8.04	6.773	25939	0.00	0.0	9400	35339	3.76
1235.0	28554	0.550	8.85	6.833	26028	0.00	0.0	9400	35428	3.77
1255.0	29017	0.600	9.65	6.893	26216	0.00	0.0	9400	35616	3.79
1270.0	29364	0.650	10.46	6.955	26293	0.00	0.0	9400	35693	3.80
1275.0	29479	0.700	11.26	7.018	26160	0.00	0.0	9400	35560	3.78
1273.0	29433	0.750	12.07	7.083	25882	0.00	0.0	9400	35282	3.75
1265.0	29248	0.800	12.87	7.148	25484	0.00	0.0	9400	34884	3.71
1255.0	29017	0.850	13.67	7.215	25049	0.00	0.0	9400	34449	3.66
1253.0	28971	0.900	14.48	7.283	24776	0.00	0.0	9400	34176	3.64
1250.0	28901	0.950	15.28	7.352	24484	0.00	0.0	9400	33884	3.60

Data entered by: CJW Date: 03/22/2005
Data checked by: cal Date: 3/22/05
FileName: KITCSB14

ADVANCED TERRA TESTING, INC.

Copyright 2007, Kleinfelder

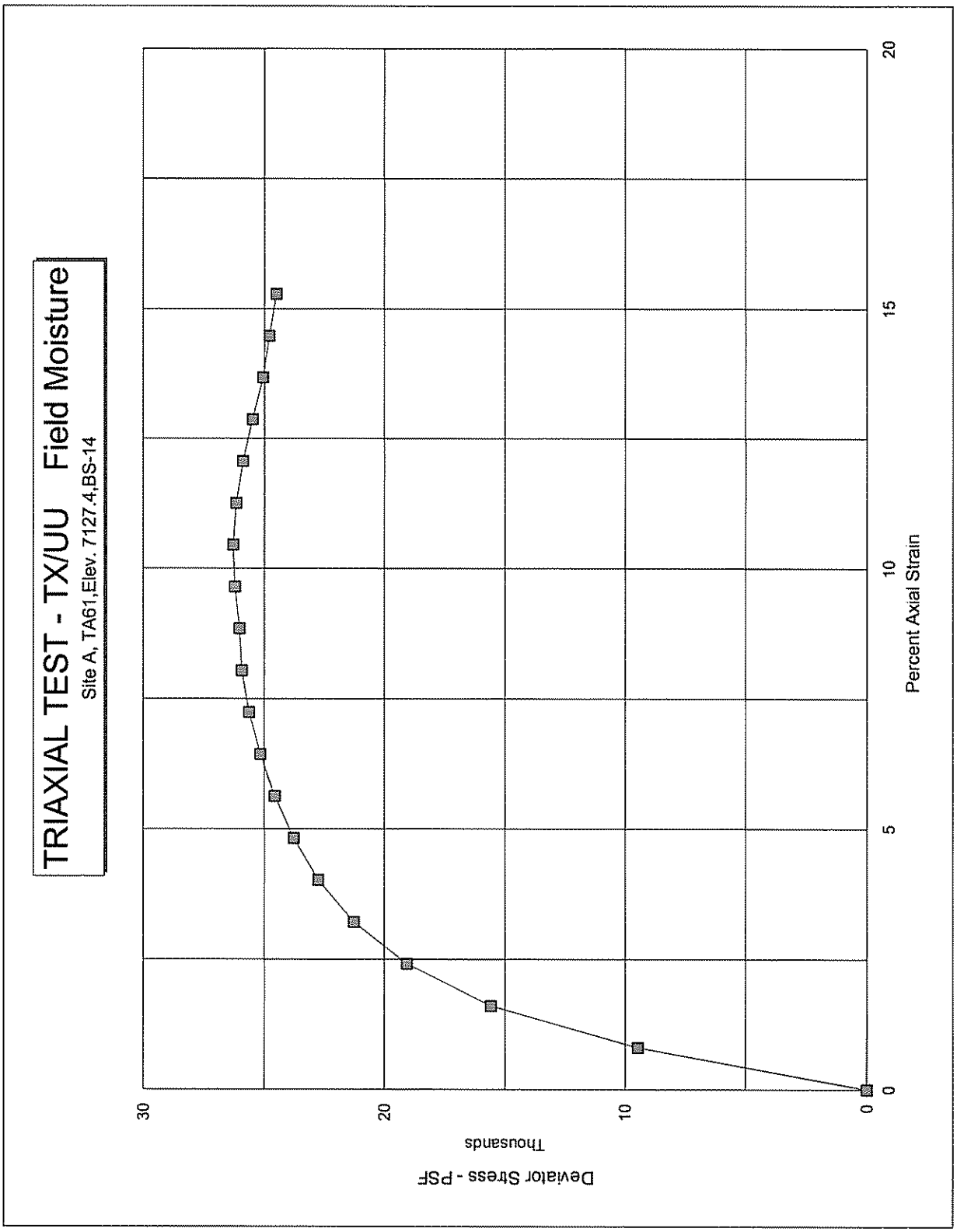
TRIAXIAL TEST - TX/UU Field Moisture
Site A, TA61,Elev. 7127.4,BS-14
Deviator Stress - PSF
Thousands
30
20
10
0
0
5
10
15
20
Percent Axial Strain

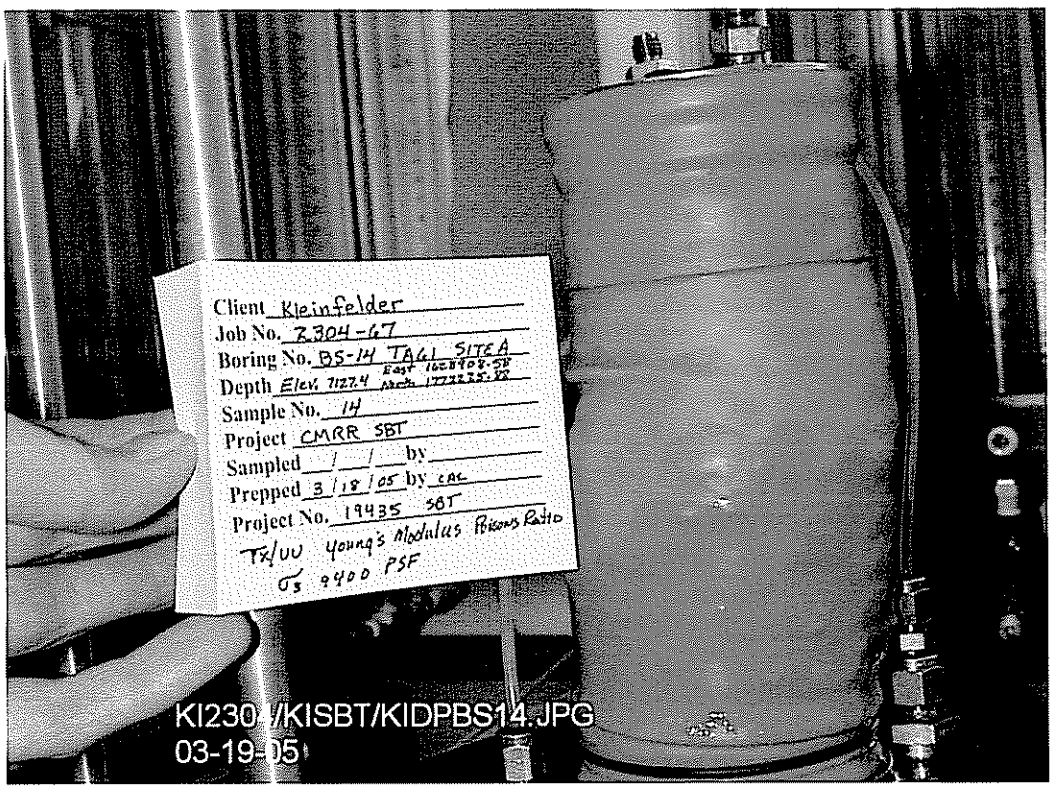
Client Kleinfelder
Job No. 3304-67
Boring No. BS-14 TA61 SITE A
Depth Elev. 7127.4
Sample No. 14
Project CMRR SBT
Sampled / / by
Prepped 3 / 18 / 05 by CAC
Project No. 19435 SBT
TX/UU Young's Modulus Poisons Ratio
σ3 9400 PSF
KI2304/KISBT/KIDPBS14.JPG
03-19-05

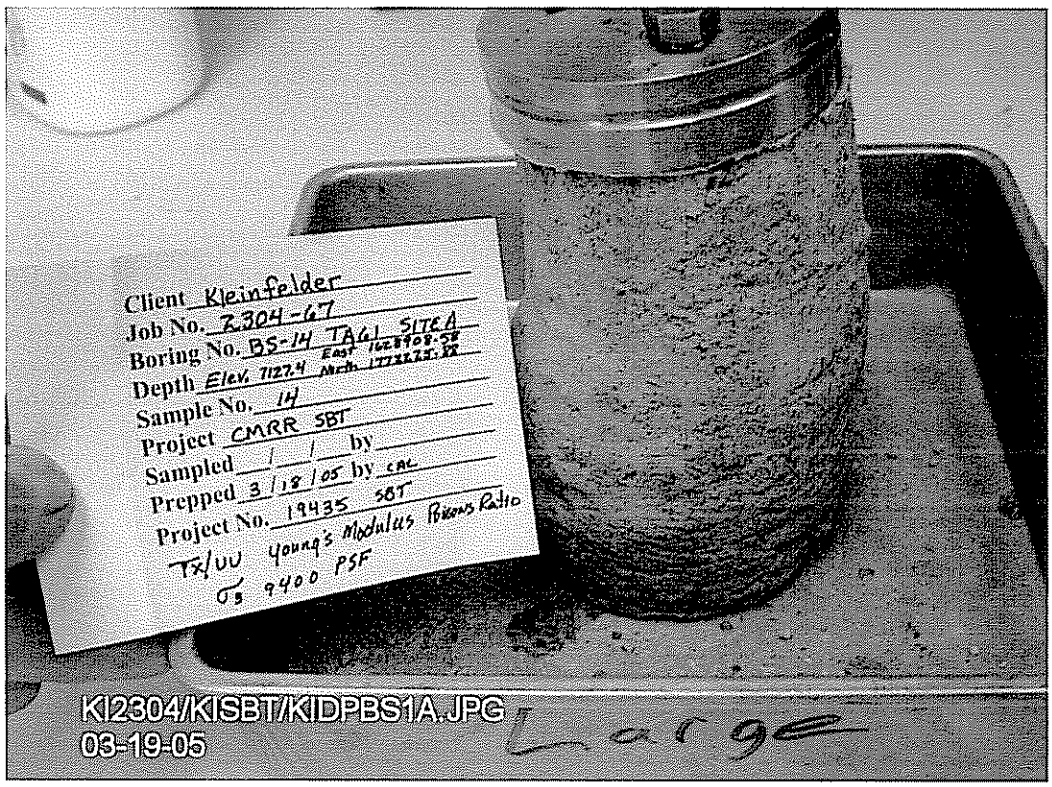

Copyright 2007, Kleinfelder

SPECIFIC GRAVITY TEST

ASTM D 854

Copyright 2007, Kleinfelder

SPECIFIC GRAVITY TESTS ASTM D 854

CLIENT:	Kleinfelder	JOB NO.	2304-67
SOIL DESCR.		LOCATION	Site A

BORING NO.	BS-4	BS-14
DEPTH	7125.4 elevation	7127.4 elevation
SAMPLE NO.	TA61	TA61
DATE SAMPLED		
DATE TESTED	3/21/05 RS	3/21/05 RS
Pycnometer #	Big3	Big4
Weight of oven dry soil (g) (Wo)	99.707	101.807
Weight of flask, soil, and water. (g) (Wb)	720.730	733.690
Temperature (deg. C) (Tx)	22.9	22.9
Weight of water & flask at Tx (from cal. curve)(Wa)	659.704	671.881
Specific Gravity*	2.58	2.55

*Specific Gravity = Wo/[Wo+(Wa-Wb)]

Data entry by: RS Date: 03/21/2005
Data checked by: CJ Date: 03/21/05
FileName: KISATA61

ADVANCED TERRA TESTING, INC.

Copyright 2007, Kleinfelder

Appendix E

Report of Cyclic Simple Shear Testing Performed by the University of California, Berkeley

Final Report

Feasibility Study of Cyclic Simple Shear Testing of Volcanic Tuff at UC Berkeley

Prepared for: Kleinfelder, Inc.
CMRR Project (# 19435)

Prepared by: Dr. Michael Riemer
University of California, Berkeley

Date: April 30, 2007

Document Control #: UCB/EERC – 20053687 Rev. 2

Copyright 2007, Kleinfelder

Feasibility Study of Cyclic Simple Shear Testing of Volcanic Tuff at UC Berkeley

History of Revisions

Revision #	Date	Description	Type
0	September 16, 2005	Original submittal of report	
1	September 29, 2005	Address all comments made on draft report	Editorial/corrections
2	April 30, 2007	Add revision history and signature	Editorial

Report Prepared and Revised by:

Michael Riemer, Principal Investigator	April 30, 2007 Date:

Copyright 2007, Kleinfelder

Feasibility Study of Cyclic Simple Shear Testing of Volcanic Tuff at UC Berkeley

Contents

1.0 Introduction 1

2.0 Scope 1

3.0 Materials 1

4.0 Preparation Procedures 2

4.1 Trimming Block Samples 2

4.2 Trimming Pitcher Tube Samples 2

4.3 Membranes 3

4.4 Epoxy Application 3

4.5 Specimen Measurements 4

4.6 Elastomer Gauges 4

5.0 Testing Conditions and Procedures 5

5.1 Vertical Deformations 5

5.2 Testing Stresses 5

6.0 Test Results 9

7.0 Conclusions 11

8.0 References 11

Appendix A: Testing Procedures 018420-PROC-04; Rev 1 A1

Appendix B: Summary Test Results B1

Copyright 2007, Kleinfelder

Feasibility Study of Cyclic Simple Shear Testing of Volcanic Tuff at UC Berkeley

1.0 Introduction

This report describes the results of experimental research conducted in the UC Berkeley Geotechnical laboratories to investigate the feasibility of evaluating the likely seismic response of a lightly welded volcanic tuff using the Cyclic Simple Shear device. The project was sponsored by Kleinfelder Inc.(Project # 19435), in conjunction with the CMRR project at the Los Alamos National Laboratory, and the primary parameter of interest was the vertical strain induced in the specimens in response to different levels of cyclic loading, as an indicator of potential levels of ground surface settlement.

2.0 Scope

Due to the nature of this project as a feasibility study, the scope of work included development and refinement of appropriate specimen preparation and testing procedures, in addition to the performance of the tests themselves. Stringent QA/QC requirements included a formal QA audit by representatives of DMJM H+N, focusing on both calibration and procedural issues. The proper functioning of the ATS testing software was confirmed by acquiring data as each instrument was exercised under controlled conditions, and the testing system as a whole was validated through the performance of "check" tests on standard Ottawa sand. Results of these tests showed that the system reported vertical settlement consistent with expectations when the standard material was tested. Following initial exploratory efforts, a total of eight specimens of the tuff were successfully prepared and tested as part of this phase of the project, with each specimen subjected to a series of three cyclic tests.

In the first phase of testing, a flexible (unreinforced) membrane was used, and tuff specimens extracted from block samples were consolidated both isotropically and anisotropically. These tests clearly identified the importance of the stress ratio on the observed vertical deformations, highlighting the need for a better understanding of the K_0 stress conditions. In response, a second phase of testing was performed, utilizing the recently developed Elastomer Gauges to assess radial strains under a variety of stress conditions in both "standard" specimens of Ottawa sand, and additional specimens of tuff retrieved from Pitcher samples at the site.

In addition, a final specimen was tested using a conventional wire-reinforced membrane, by under reaming the tuff specimen and backfilling the annular gap between the tuff and the membrane with densely deposited Ottawa sand, to investigate this approach to maintaining the appropriate strain conditions in the specimens.

3.0 Materials

The tuff tested in this phase was obtained from two different locations: block samples were hand carved from a borrow pit some 3,500 feet from the CMRR site, while large diameter Pitcher tube samples were recovered from depth at the CMRR site itself. Due to the fragile nature of the material, both types of samples were carefully packed, instrumented and transported.

Of the 14 block samples obtained, three were delivered to UC Berkeley (BS-3, BS-13, and BS-16). Each block was approximately cubical, with 12" sides. More detail on the source location,

Copyright 2007, Kleinfelder

sampling and transport of these materials is provided in Kleinfelder's "Block Sample Testing Plan" (19435-SBT16.2-TPL).

A total of ten Pitcher tube samples were delivered to Berkeley for possible testing. The two designated for this feasibility phase were R-27 and R-28, from DSC-1, from depths of 96-98 feet, and 98-100 feet, respectively.

4.0 Preparation Procedures

In general terms, the cyclic simple shear testing was performed on specimens that were nominally 10 cm in diameter, approximately 2.5 cm in height, and were conducted under drained conditions at ambient moisture content, under nominally constant vertical stresses. The most challenging aspect of the program, and the reason it was considered a feasibility study, was the potential difficulty of trimming and preparing a sufficiently "undisturbed" specimen of the lightly welded material. The preparation and testing procedures utilized are presented in detail in Appendix A, while background and discussion of various aspects are discussed in this section.

4.1 Trimming Block Samples

The character of the tuff in the block samples observed during trimming was very variable, with zones of little to no cementation only a few centimeters from more competent material. The gradation and mineralogy also visually appear to vary over a similar scale. Throughout the material, there are also substantially stiffer chunks or clasts that are more strongly cemented, commonly ranging in size between ¼ to a full centimeter, which typically cannot be divided or cut without damage to the surrounding material fabric. During the trimming process it was also observed that while the existing moisture content was relatively low, surfaces of the tuff that seemed reasonably well cemented when freshly exposed would apparently lose cementation over time, resulting in a surface layer of uncemented particles or powder as the surface dried. Whether this was simply a loss of capillary suction, or also involved other processes was not investigated during this project, though a general shift in color of the material toward a pink or red tone during trimming and drying suggests oxidation may also take place.

The combination of a brittle, friable matrix containing stiffer clasts precluded the use of directly cutting the specimen surfaces, or coring the entire specimen to its final geometry. Instead, a "mini-block" (roughly 6" diameter by 2 inches tall) of the tuff was excavated from the Block Sample in much the same way that the Block Sample was itself obtained in the field: by essentially trenching around the edges of the desired material (see Figure 1), then breaking off the block from its remaining pedestal. Because the tuff is very sensitive to any tensile stresses, it was necessary to place a specimen cap directly on the exposed surface of the mini-block prior to removing it from the Block Sample, to minimize subsequent handling. The over-sized specimen could then be inverted onto the cap on the laboratory bench (Figure 2), then trimmed down to the appropriate size (Figure 3) by carefully abrading away the excess material with scrapers, paintbrushes and other hand tools.

4.2 Trimming Pitcher Tube Samples

The tube samples were retrieved from roughly 100 foot depth at the CMMR site, and are nominally 6 inches in diameter. To prepare a specimen from these samples, a 6.5 cm tall slice of the steel tube was cut circumferentially, using a tube cutter, while the tube was strapped to a work table on both sides of the cut. Once the tube was cut through, a wire was pulled through

Copyright 2007, Kleinfelder

the gap in the tube to cut through the tuff within (Figure 4). The tuff was observed to be firmly attached to the tube apparently due to a thin annular cake of residual drilling mud around the perimeter of the tuff, which had corroded the inside wall of the tube (Figure 5). This outer layer was removed during the initial stages of trimming the specimen down to the required diameter of 10 cm, and was discarded prior to saving trimmings for evaluation of water content. As with the block samples, the oversized slice of the tuff was trimmed down to the desired size by hand. Compared to the block sample material, the tuff from the Pitcher tubes seemed to be somewhat moister, to be even more variable in the degree of cementation, and included significantly larger clasts (up to 5 cm) of strongly cemented material, which could not be effectively trimmed, and which therefore caused the abandonment of a number of potential specimens when such clasts were discovered spanning the intended boundary of the specimen.

4.3 Membranes

Simple shear tests are commonly performed using inextensible, wire-reinforced membranes which provide the desired K_0 conditions by passively resisting lateral strains induced by vertical loading. Unfortunately, the brittle and variable nature of the tuff, and the impossibility of trimming the specimen to a smooth, uniform diameter meant that the traditional use of a wire reinforced membrane would have resulted in large radial strains, and substantial damage to the specimen's structure, before significant radial stresses could be mobilized.

For this reason, for seven of the specimens tested a plain latex membrane (0.025" thick) was applied to the specimen and sealed to each cap, and a drain line from the base cap was attached to provide control of the internal specimen pressure. The flexible membrane was slightly undersized, and thus was able to conform to the shape of the trimmed specimen. A lucite chamber could then be sealed to the rest of the simple shear device, and chamber pressures could be applied to control the lateral confining stress on the specimen, while vertical loads could still be applied to independently control the vertical deviatoric stress.

For one specimen (LANL-9), a different approach was used: the tuff specimen was trimmed down to a slightly smaller diameter, and a 10 cm wire reinforced membrane was loosely placed around the specimen, and sealed to the base cap. Ottawa standard sand was then deposited in the annular space between the tuff and membrane, and densified with a thin metal rod, to ensure that the fine sand fully occupied the irregular voids in the surface of the tuff, and made good contact with the membrane surface, prior to placing and sealing the top cap. This test was conducted to investigate whether such a system could effectively mobilize lateral stresses in the membrane while the tuff remained intact.

4.4 Epoxy Application

The surface roughness, and tendency for the tuff to lose cementation after trimming, prompted the need for a modification to the usual procedure: the use of epoxy to physically attach the specimen to the top and bottom platens (as alluded to in Attachment A, Step III-6). This attachment had two major benefits: it prevented any tendency for the block to slip at the cap interface under the applied horizontal load, rather than shearing; and it eliminated any vertical compliance due to densification of loose material at the cap interfaces. A layer about 2 mm thick of viscous, slow setting epoxy was used to ensure that the adhesive did not penetrate far into the voids of the tuff, but instead acted as a capping compound. Use of the epoxy prompted the design and fabrication of new, 2 part specimen end caps, since the epoxy could not be removed following testing.

Copyright 2007, Kleinfelder

4.5 Specimen Measurements

The variability of the material also led to having a very rough vertical surface around the circumference of the specimen. This makes precise measurement of the equivalent diameter (and therefore the area, volume, density, and vertical stress) rather difficult, since measurement devices such as calipers, Pi-tapes and such rest on the outermost protrusions, and cannot reflect the degree of "pitting" in the edge voids. Because of this, the measurements of diameter using the Pi-tape made prior to testing are necessarily biased toward the high side. To provide an alternate (and I believe more accurate) measure of the equivalent diameter and specimen area, an additional step was taken at the conclusion of testing, whereby the entire specimen, still encased within its membrane and between its platens, and under a small degree of vacuum confinement, was submerged in a basin of water, and the volume of displaced water was measured. By conducting a similar process with just the end platens and no specimen, the difference between the two volumes represented the volume of the specimen, and by tracking the height of the specimen, its equivalent area was determined. This area based on the displaced volume is the value that has been used in reducing the data for this report.

The specimen height was determined using a fixed dial gauge to measure the full height of the specimen, including the caps and epoxy, relative to an initial dial gauge reading with a known thickness spacer between the caps. This height was used in conjunction with the displaced volume measurements (described above) to assess the average cross-sectional area of the specimen. However, since a portion of this height consisted of rigidly epoxied material, the thickness of these two interface layers was measured after the specimen was disassembled, and subtracted from the full height to obtain an "effective height" of the specimen for use in calculating shear and vertical strains during the tests.

Due to the need for the epoxy to cure, specimens were left overnight after being installed in the Bi-directional Simple Shear device, under small levels of vacuum confinement and a nominal vertical load to ensure parallel caps. The following day, specimens were "consolidated" to the desired stress state for testing, then a sequence of three cyclic tests were performed at increasing amplitudes of loading.

4.6 Elastomer Gauges

Following the first four simple shear tests on the tuff, it became clear that a technique for evaluating the radial strains occurring in the specimen during both static and cyclic loading would provide valuable insight into the appropriate stress state to test at. Toward this end, the simple shear device was modified to accommodate the use of two newly developed deformation sensors referred to at "Elastomer Gauges", which are thin urethane strips encapsulating a fine capillary of liquid metal alloy. The strip itself is very flexible, and therefore can be attached to a flexible strip of membrane, which conforms to the perimeter of the specimen. Electrically, the EGs respond like a very low resistance strain gauge, and therefore are conditioned using a Wheatstone bridge amplifier outside the device.

The EGs used in this application were approximately 5.0 cm in length, and placed on opposite sides of the tuff specimens, at approximately mid-height. Because the gauges are pressed up against the rough specimen surface, they should be considered truly local gauges, reflecting the degree of radial expansion or contraction where they are mounted, rather than an average response of the entire circumference. More detailed information on the function and validation of the Elastomer Gauges is presented by Safaqah and Riemer (2005).

Copyright 2007, Kleinfelder

5.0 Testing Conditions and Procedures

5.1 Vertical Deformations

Careful monitoring of the vertical displacements was performed throughout the stress application and cyclic loading of the specimens. This was accomplished using three internal LVDTs that are mounted vertically between the rigid vertical table and the horizontal surface of the base table, and distributed around the perimeter of the specimen. Due to their locations, the three LVDTs provide both an accurate average measure of vertical displacement, and the means to identify whether there is significant rotation or rocking of the platens relative to one another.

5.2 Testing Stresses

Identification of the appropriate stress state was a major issue in the planning for the testing program, as it was difficult to assess the most appropriate ratio of vertical to lateral stress. In addition to having little information about the lateral stresses at depth at the CMRR site, it was also pointed out that seismically induced settlements in the field would probably take place under whatever stress state resulted from one-dimensional compression – which could be different from the current stress state.

During the first phase of testing, using only the flexible membranes, it was decided to run two specimens at either end of the range of anticipated stress conditions, to investigate whether the stress ratio was important to the resulting vertical strains observed. Specimens LANL-3 and LANL-4 were therefore run under isotropic stress conditions (lateral = vertical), while specimens LANL-2 and LANL-5 were run under a stress ratio of 1:2 (lateral: vertical). These stress levels were specified in the "Block Sample Testing Plan" developed and distributed by Kleinfelder, and are shown in Table 1, in addition to other preparation data for each test, as well as the summarized results. The target values of Cyclic Stress Ratio (CSR = $\tau_{h,max} / \sigma'_{v,con}$) were also specified in the Testing Plan, and represent approximately 0.5, 1.0, and 2.0 times the CSR identified for the site. Values of CSR in the table represent those achieved in each specific test, which varied somewhat from the target values due to initial uncertainties in the specimen area.

As discussed further in the 'Results' section, there was a clear tendency from the first four tests for the isotropically consolidated specimens to undergo less vertical deformation - both under application of the consolidation stresses, and during cyclic loading - than those specimens tested under larger vertical stresses. This confirmed the importance of applying the correct state of stress in order to estimate the likely vertical response in the field. Two approaches were identified to further investigate how the "correct" stress state might be applied: (1) a pair of Elastomer Gauges (described in Section 4.6) were used to monitor the radial strains in the specimen during both isotropically (LANL-6) and anisotropically consolidated tests (LANL-7 and LANL-8); and a wire reinforced membrane was utilized on a final specimen (LANL-9), which had a thin annular ring of Ottawa sand to bridge between the tuff and the inextensible membrane (Section 4.3). The stresses applied to these specimens are summarized in Table 1. All cyclic loading was applied at a frequency of 0.25 Hz, in order to allow good control of the loading to the large shear values required at the higher stress ratios.

Following completion of the cyclic loading, vertical deformation data was again measured as the consolidation stresses were removed from each specimen (Appendix B, Consolidation plots). This consistently showed rebound of a small portion of the vertical deformations observed during the consolidation phase, suggesting that some of the deformation was recoverable, and

Copyright 2007, Kleinfelder

may have included compliance of the track systems of the device under the large vertical loads applied. As a result, the column in Table 1 labeled as "Vert. Strain" under Preparation Conditions reflects the net vertical deformation, where the rebound has been subtracted from the total vertical deformations observed during load application.

Figure 1: Preparing "mini-block" for separation from large Block Sample.

Figure 2: Trimming down to specimen size.

Figure 3: Trimmed specimen between base and top caps.

Figure 4: Separation of slice from Pitcher tube, following cutting of tube and tuff.

Copyright 2007, Kleinfelder

Figure 5: Edges of sample against tube, showing drilling mud (white) and corrosion (orange).

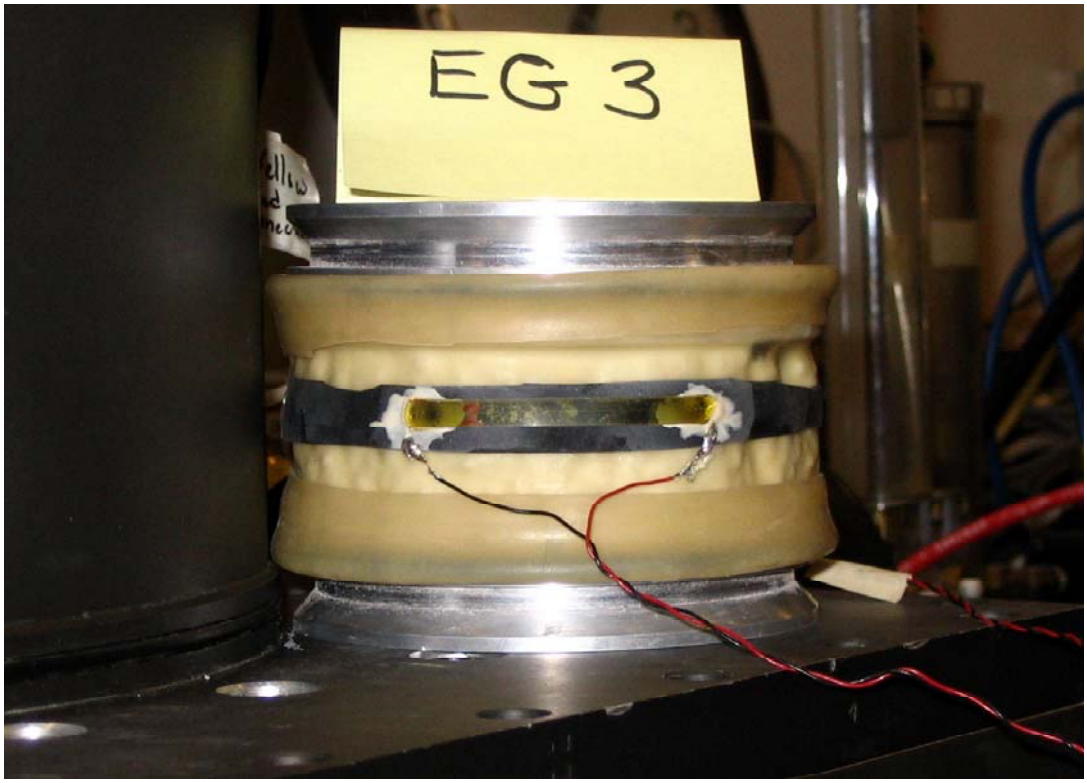

Figure 6: Elastomer Gauge, mounted on black latex "belt", positioned on perimeter of specimen

Copyright 2007, Kleinfelder

6.0 Test Results

Detailed test results for the three cyclic tests performed on each of the ten specimens (eight tuff and two Ottawa sand) are compiled in Appendix B. The first page for each specimen includes both a summary of the observed vertical strains during each segment or stage of testing, as well as a graph illustrating the compressive vertical strains experienced during the application of the static stresses, and the expansive vertical strains during the unloading, after all testing was completed on a given specimen. These are analogous to "consolidation" strains, though of course these are not saturated specimens. The table includes a summary of the observed test results for each of the cyclic tests as well, including the applied CSR, the number of cycles, the resulting single-amplitude shear strain (γ), the approximate shear modulus (G), and the observed incremental vertical strain during each cyclic test.

This initial page is followed by three pages each summarizing a cyclic test on the specimen, and consisting of two plots: the upper plot shows the time history of vertical strains and either the vertical loading or the radial strains, for tests in which the EGs were utilized. The lower plot shows selected hysteretic stress-strain ($\tau - \gamma$) loops during the cyclic test in question. These loops have not been corrected for potential track friction, and thus may slightly overestimate the shear modulus (G), and significantly overestimate the damping ratios.

It is important to remember that the vertical strains are not necessarily equal to the volumetric strains for most of the specimens – the exception is the final specimen tested, LANL-9, for which the wire reinforced membrane and dense sand backfill are assumed to maintain K_0 conditions. Also, it should be noted that the shear stresses (τ) reported are those on the horizontal plane, regardless of the degree of stress anisotropy, and therefore do not necessarily represent the maximum shear stress within the specimen.

The key preparation information, loading conditions and results for the tests are summarized in Table 1, which facilitates a direct comparison among the tests. The vertical strains measured in the cyclic tests are plotted graphically in Figure 7, including all of the tests on the tuff, and both tests on the Ottawa sand. Several clear points can be observed by making such a comparison:

- Overall, the degree of vertical strain, if interpreted as volumetric strain, is relatively low compared to similar testing performed in simple shear on clean, moderately dense sands, and compacted fills (Whang et al, 2000), including the Ottawa sand tested in this study.

- Despite some differences in appearance and texture, the tuff from the block samples and the Pitcher tubes show similar vertical strain response at comparable loads.

- Not surprisingly, the specimens prepared to essentially isotropic stress states (LANL-3, LANL-4, LANL-6 and EG-1) exhibited significantly less tendency for vertical strains, both during the application of static stresses and during cyclic testing, than comparable specimens prepared with the large deviatoric vertical stresses. This is consistent with the observations that under isotropic stresses, the radial strains are contractive, and may inhibit vertical deformations. In contrast, the specimens tested at stress states of approximately K = 0.5 showed a tendency for expansive radial strains, which could result in larger vertical strains than a "true" K_0 condition.

Copyright 2007, Kleinfelder

- Note however, that part of this discrepancy could also be due to higher vertical stress levels applied to the anisotropically loaded specimens (LANL-2, LANL-5, LANL-7 and LANL-8) – both directly, since the larger stresses could induce larger strains, and indirectly, since larger vertical stresses were used in the calculation of Cyclic Stress Ratio, thus larger shear stresses were applied to LANL-2 and LANL-5 for a given CSR.

- While implementation of the Elastomer Gauges proved to be challenging, and early tests are less clear than the later tests, the radial strain measurements recorded during the static load application suggest that to maintain K_0 conditions during consolidation, the vertical stresses need to be maintained significantly higher than the lateral stresses (K = 0.45, for test LANL-8). At these stress conditions, however, subsequent cyclic loading produced mildly dilative strains in the radial direction, suggesting that K_0 may be somewhat higher in dynamic loading. Combining results from multiple tests, the appropriate K_0 for the cyclic loading condition appears to be somewhat larger than 0.5, though well below 1.0.

- The wire-reinforced membrane was successfully used in conjunction with the backfilling of the annular space between the membrane and tuff with Ottawa sand (LANL-9). Vertical strains in this test were comparable to those observed in the other anisotropically consolidated specimens, indicating that the radial stress could be mobilized without excessive vertical straining. This approach may benefit from the similar shear stiffness of the tuff and the Ottawa sand, and suggests that the sand can be densified sufficiently into the voids of the trimmed tuff to effectively transmit the lateral stresses.

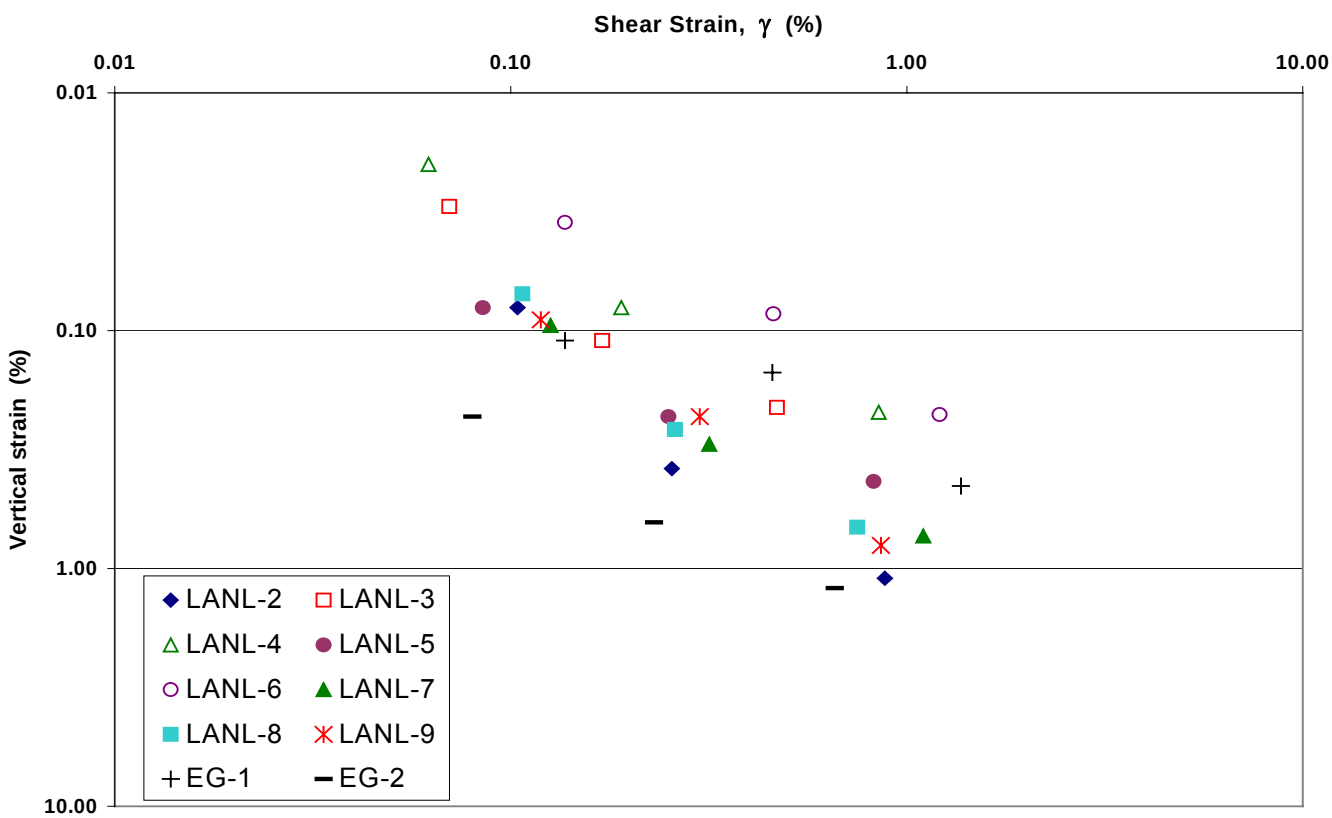

Figure 7: Summary plot showing vertical strains recorded in all cyclic tests from Table 1.

Copyright 2007, Kleinfelder

7.0 Conclusions

From the feasibility perspective, this study has demonstrated that testable specimens can indeed be prepared from both the Block Samples and the Pitcher tube samples of the tuff. The procedure developed, including the mounting of the specimens to the caps with epoxy, provided specimens that were free of the specimen/cap compliance that might have obscured the vertical strains in the tuff, and allowed testing over a range of stress conditions. While the trimming process proved to be a delicate and time consuming operation, the resulting specimens seemed to retain the cemented nature of the original material – which could in fact be observed following completion of each test, when the specimens were removed from the testing device and dismantled, and needed to be "broken" off the specimen caps, still in a cemented state.

The magnitude of vertical deformations in the tested specimens is not particularly large under the levels of cyclic loading anticipated. In fact, the vertical strains during the static application of stresses were larger prior to cyclic testing both for the shallow block samples from the borrow site, and the deeper Pitcher samples from the CMRR site.

The amplitude of vertical strains depended significantly on the ratio of stresses under which cyclic loading was conducted, likely due to accompanying (unwanted) radial strains. For this reason, it would appear advisable for production testing to either 1) use a flexible membrane, applying anisotropic stresses to mimic the K_0 condition as closely as possible, and use the EGs to monitor radial strains; or 2) use the wire reinforced membranes and densify Ottawa sand backfill around the perimeter of the tuff specimen.

8.0 References:

"Block Sample Testing Plan – Special Block Test" CMRR Project, 19435 SBT16.2-TPL, J. Laird, Kleinfelder, Inc., December 3, 2004.

"Characterization of Seismic Compression of Some Compacted Fills," D. Whang, M. Riemer, J. Bray, J. Stewart, P. Smith. *Advances in Unsaturated Geotechnics*, ASCE Geotechnical Special Publication #99, 2000, pp. 180-194.

Safaqah, O. and Riemer, M. , "The Elastomer Gauge for Local Strain Measurement in Monotonic and Cyclic Soil Testing," Submitted for publication in *ASTM Geotechnical Testing Journal*, Fall 2005.

Copyright 2007, Kleinfelder

Table 1: Summary of preparation conditions, stress conditions, and results from cyclic simple shear tests on tuff, and Ottawa sand.

		Preparation Conditions					Test Conditions			Cyclic Test Results		
Specimen	Sample	w (%)	Vert. Stress (kPa)	Lateral stress (kPa)	Vert. Strain (%) *	Dry density (g/cm3) **	Test	CSR	# cycles	shear strain (%)	Approx. G (kPa)	Vert. strain (%)
LANL-2	BS-13	2.9	457	223	2.15	1.38	Cyc 1	0.08	5	0.104	33,600	0.08
							Cyc 2	0.16	10	0.255	27,800	0.38
							Cyc 3	0.32	10	0.880	16,500	1.10
LANL-3	BS-13	2.8	340	330	1.05	1.34	Cyc 1	0.07	5	0.070	34,300	0.03
							Cyc 2	0.14	10	0.170	29,100	0.11
							Cyc 3	0.29	10	0.470	21,500	0.21
LANL-4	BS-16	5.8	352	336	0.8	1.32	Cyc 1	0.08	5	0.062	38,500	0.02
							Cyc 2	0.16	10	0.190	28,000	0.08
							Cyc 3	0.31	10	0.850	12,500	0.22
LANL-5	BS-16	4.9	455	223	1.33	1.38	Cyc 1	0.08	5	0.085	43,500	0.08
							Cyc 2	0.15	10	0.250	28,000	0.23
							Cyc 3	0.31	10	0.825	17,000	0.43
LANL-6	R-27	7.6	341	334	0.79	1.48	Cyc 1	0.08	5	0.137	20,700	0.04
							Cyc 2	0.17	10	0.460	12,700	0.09
							Cyc 3	0.35	10	1.210	9,600	0.23
LANL-7	R-27	8.3	450	225	1.43	1.34	Cyc 1	0.08	5	0.126	26,200	0.10
							Cyc 2	0.15	10	0.317	21,450	0.30
							Cyc 3	0.30	10	1.100	12,400	0.73
LANL-8	R-28	6.2	465	210	0.93	1.26	Cyc 1	0.07	5	0.107	31,200	0.07
							Cyc 2	0.15	10	0.260	26,100	0.26
							Cyc 3	0.29	10	0.750	17,900	0.67
LANL-9	R-28	5.7	402	$k^*(\sigma_v)$	1.54	1.44	Cyc 1	0.08	5	0.119	26,200	0.09
							Cyc 2	0.15	10	0.300	20,400	0.23
							Cyc 3	0.30	10	0.860	14,200	0.80
EG-1	Ottawa Sand	0	276	264	0.21	1.66	Cyc 1	0.11	5	0.137	21,100	0.11
							Cyc 2	0.22	10	0.458	12,750	0.15
							Cyc 3	0.41	10	1.370	7,800	0.45
EG-2	Ottawa Sand	0	350	175	0.96	1.65	Cyc 1	0.11	5	0.080	44,400	0.23
							Cyc 2	0.21	10	0.230	30,000	0.64
							Cyc 3	0.37	10	0.658	19,500	1.21

** the net vertical strain calculated from the observed vertical deformation during static stress application, less the rebound during unloading*
*** estimated values based on displaced volumes after testing, and including mass of epoxy, and Ottawa sand for LANL-9*

Appendix A:

Testing Procedures

018420-PROC-04; Rev 1

Copyright 2007, Kleinfelder

I. Sample Delivery, Storage and Handling

1) The Pitcher tube samples will be delivered to Davis Hall, on the UC Berkeley Campus, by representatives of Kleinfelder. The samples will be brought directly to Room 434 Davis.

2) The Kleinfelder chain of custody paperwork will be used; once received at Berkeley, copies of the custody paperwork will be forwarded to DMJMH&N. The original traveler will stay with the samples in Berkeley until the material is returned or disposed of.

3) The tubes, in their racks, will be placed in a separate and clearly identified area within this temperature controlled room, and remain there until trimmed for testing, or until the testing program is completed. Only those persons involved in the trimming and testing of the samples will be authorized to handle the samples.

4) The sample numbering system used during transport will continue to be used throughout the testing program, with smaller sections created during the cutting of the original samples carrying an additional letter designation (eg. slice A, B, C, etc.)

5) The tested material, and most of the material removed in trimming the specimens, will be bagged, labeled and stored in the same cabinets prior to further characterization. Labeling will be carried out with an indelible marker on the block container, whether it's a plastic bag or the original tube.

II. Equipment Calibration and Quality Assurance

1) The test data obtained in this program will be acquired using the Bidirectional Simple Shear Testing System. The instrumentation in this device consists of:

    a. electronic load cells, for measuring the vertical and shear stresses on the specimen, which will be calibrated against a NIST-traceable proving ring

    b. vertical and shear Linear Variable Differential Transformers (LVDTs), for measuring the shear displacement and vertical compression of the specimen, which will be calibrated using a purpose-built LVDT calibrator;

    c. differential pressure transducers, for electronically measuring the cell and effective pressures on the specimen, which will be calibrated against a NIST-traceable Heise reference pressure gauge.

2) This instrumentation is all powered and conditioned by electronic signal conditioners which provide DC voltage output signals, which are in turn recorded by PC computer through a data acquisition card.

Copyright 2007, Kleinfelder

3) Calibration of each instrument will be documented on an approved form, and submitted with the final report.

4) Validation of the computer software (ATS) consists of confirming that the values recorded in the data files accurately represent the values measured by the instrumentation. This will be done after all the instrumentation itself has been individually calibrated, by recording a "software verification" file, during which each instrument will be sequentially and systematically exercised, and the data file will subsequently be examined to confirm appropriate recording of the data.

5) Support equipment required for completion of the testing program includes a dial gauge (for measurement of specimen height), an electronic scale (for recording the specimen mass), and a "Pi tape" for measurement of specimen diameter. The calibration of these devices will also be documented and recorded as part of the calibration process.

III. Specimen preparation

1) Measurements and observations made throughout preparation and testing will be recorded on Form 018420-PREP-04. These will be included in the final report for each specimen tested.

2) The cylindrical specimens will be trimmed down from the larger tube samples to a nominal diameter of 10 cm, and a nominal height of 2.5 cm.

3) This will be carried out with the oversized sample placed on the specimen base cap, with the interface epoxied to preclude slippage during subsequent testing. It is anticipated that trimming will consist of progressive abrasion of the outer material down to the final specimen size, rather than direct coring.

4) Following trimming to the final dimensions, the top cap will be placed on the upper specimen surface, and this interface will also be epoxied.

5) Trimmings from the around the perimeter of the specimen will be recovered and used to measure the moisture content of the material (following ASTM D 2216)

6) For specimens tested with conventional latex membranes, these will be lowered around the specimen (expanded away from the soil surface), then gently released onto the specimen and caps. The membrane will be sealed against the top and bottom cap surfaces using O-rings.

7) For specimens on which a reinforced wire membrane is utilized, the specimen diameter will be trimmed sufficiently smaller such that the wire reinforced membrane fits easily around the tuff, after which the annular space between the tuff and the membrane will be back-filled with Ottawa standard sand, which will be densified by rodding to provide a bridging element between the specimen and these membranes.

Copyright 2007, Kleinfelder

8) The mass of the specimen will be determined by weighing on the electronic scale, and subtracting the weight of the caps, membrane, O-rings, and any adhesive applied.

9) A moderate isotropic confining stress (approximately 25 kPa) will be applied as vacuum to the interior of the specimen, to improve the specimen's durability during subsequent handling.

10) Specimen average height and diameter will be recorded using the dial gauge reference system, and Pi-tape, respectively.

11) The specimen will be placed in the Bidirectional Simple Shear device, and the bottom cap will be clamped to the lower loading table.

12) The vertical loading table will be lowered over the top cap of the specimen, and clamped into place.

13) The three vertical LVDTs will be placed around the specimen, to monitor subsequent changes in the specimen height.

14) The chamber will be lowered and sealed on the device.

15) Isotropic confinement will be switched over, replacing the internal vacuum with an equivalent chamber pressure.

16) The specimen will then be consolidated to the desired testing state, by gradually increasing the chamber pressure and vertical load (including accounting for piston uplift). Final values will be dictated by the approved Test Plan ("*Block Sample Testing Plan", 19435-SBT16.2-TPL Rev. 2*). A data file will be obtained throughout this process, recording the confining stress, vertical deviator stress, vertical deformation and shear deformation during consolidation.

IV) Cyclic Shearing

1) Shearing will be applied on a load controlled basis, to the desired level of Cyclic Stress Ratio (CSR), using the ATS testing software. The target value of CSR and the number of cycles of loading for each test will be based on the approved Test Plan (see Attachment 1). Cyclic loading will be conducted at a frequency of 0.25 Hz.

2) The software will record data from the test at a rate of at least 100 samples/cycle, with the acquired data consisting of: elapsed time; lateral confining stress; vertical deviatoric stress; shear stress; shear displacement; and 3 measures of vertical displacement.

Copyright 2007, Kleinfelder

3) If the loading level is sufficiently large to fail the specimen, very large strains will be recorded and the test may shut down prior to completing the full number of cycles specified.

4) If loading amplitude is relatively low, and comparatively small deformations are observed in the initial test, a subsequent cyclic loading test on the same specimen, with larger load amplitude can be performed. The specifications for such a follow-on test are specified in the Test Plan.

V) Post-test procedures

1) Following completion of testing, the device will be shut down, the pressures removed, the chamber will be unsealed, and the specimen will be removed. As much of the soil specimen as possible will be recovered and weighed (though use of the epoxy will preclude full recovery of soil solids).

2) Data files from the consolidation and cyclic testing phases will be transferred to disk, and the data will be reduced using a simple Excel spreadsheet to convert the loads and deformations into stresses and strains. Results will include plots of the time histories of the stresses and strains, as well as other forms as desired by Kleinfelder. Both the raw and post-processed files will be delivered with the final report.

3) In addition, the data recorded during the preparation and testing phases will be used to track the moist and dry densities of each specimen throughout the testing process, with particular attention paid to the levels of volumetric strain/densification experienced during cyclic loading.

4) Grain size distributions will also be determined by sieving the material from each specimen, though these will likely be performed at another location, by other parties, in order to insure uniform procedures are applied for the gradation testing of samples from all of the participating facilities in the larger testing program).

Copyright 2007, Kleinfelder

Appendix B:

Summary Test Results

- Tests EG1 and EG2 on Ottawa Sand, with radial strain measurements
- Tests LANL-2 through LANL-5 on tuff, with no radial strain measurements
- Tests LANL-6 through LANL-8 on tuff, with radial strain measurements
- Test LANL-9, using wire reinforced membrane and Ottawa sand backfill

Copyright 2007, Kleinfelder

TEST EG -1

Stage of testing					Incremental Vert. Strain (%)	Incremental Volumetric strain (%)	Incremental Radial Strain (%)
Consol. #1	Raise isotropic effective stress from 100 to 200 kPa				0.14	0.32	+0.09
							(eg2)
Consol. #2	Raise isotropic effective stress from 200 to 265 kPa				0.07	0.23	+0.06
							(eg2)
	CSR	***# of cycles***	***s.a. shear strain***	***Approx. G***			
			(%)	***(kPa)***			***(Average)***
Cyclic loading 1	0.11	5	0.137	21,100	0.11	0.08	0
Cyclic loading 2	0.22	10	0.458	12,750	0.15	0.23	+0.02
Cyclic loading 3	0.41	10	1.37	7,800	0.45	0.89	+0.03

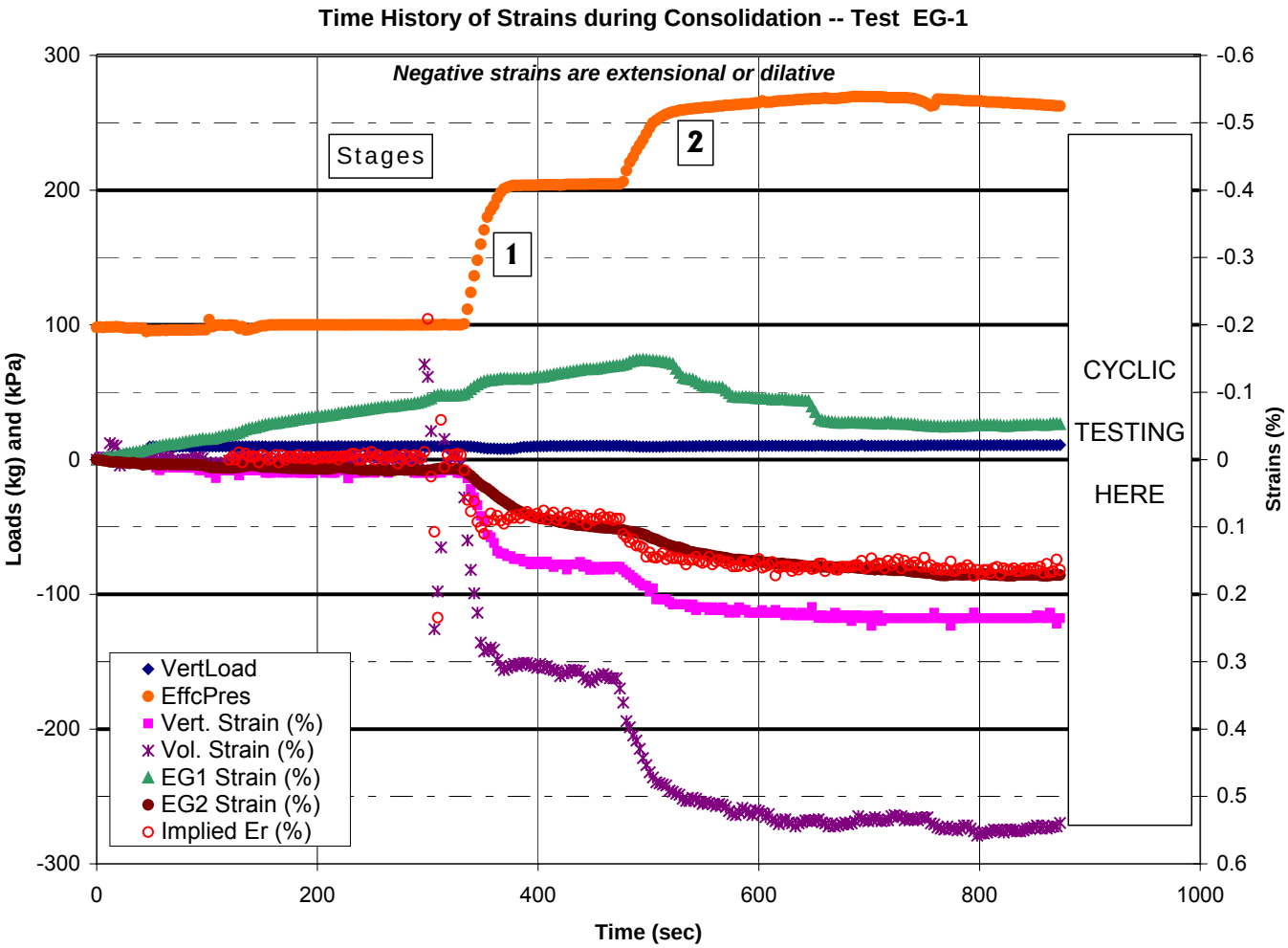

Copyright 2007, Kleinfelder

EG1 Cyc 1: Vertical , radial and volumetric strains, CSR ~ 0.11

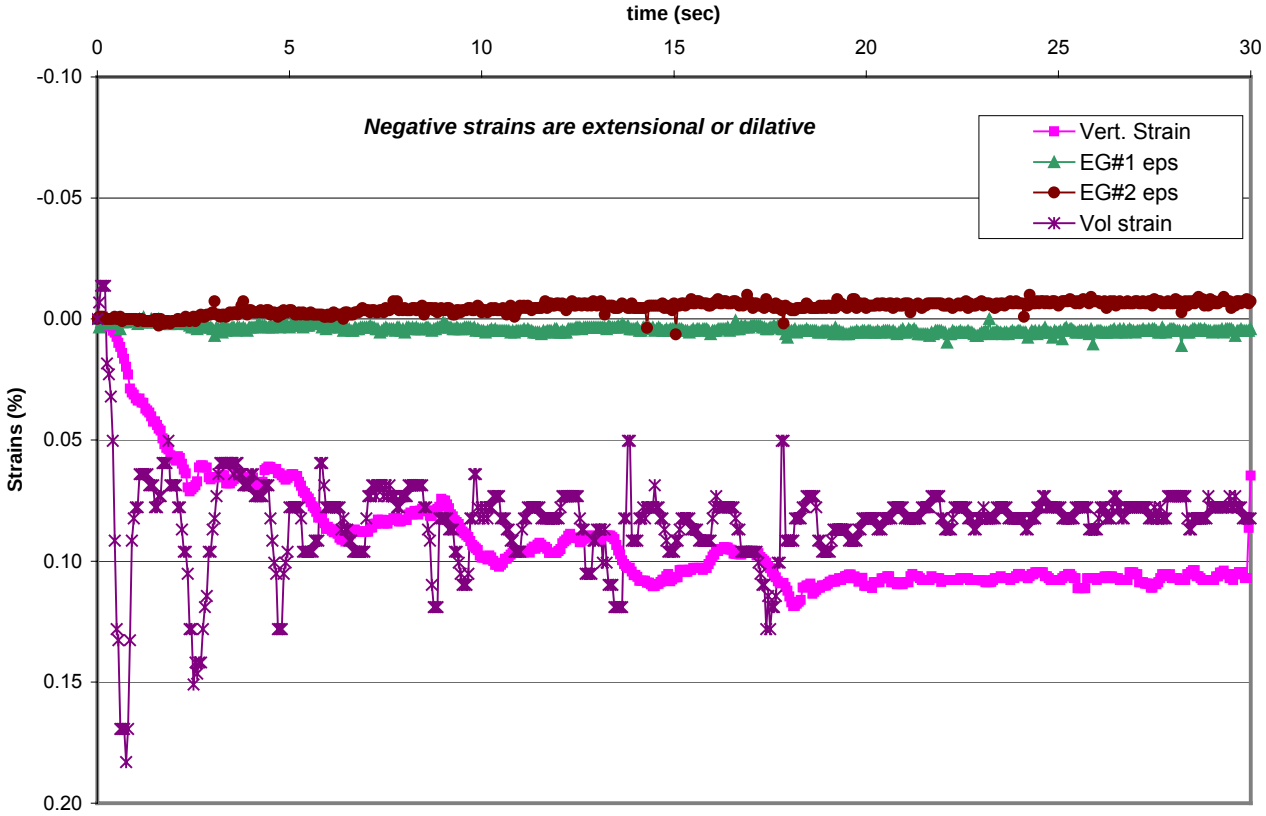

EG1 Cyc 1: Hysteresis Loops, CSR ~ 0.11

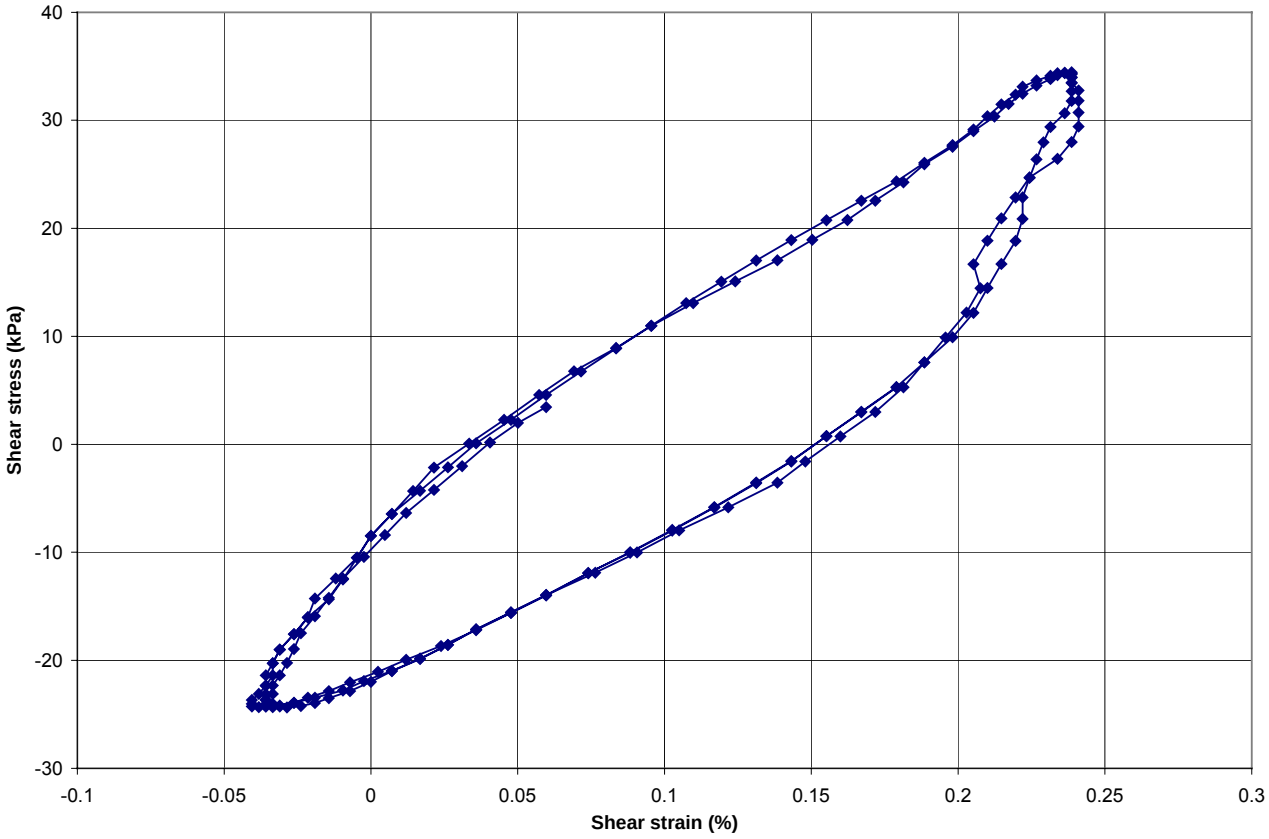

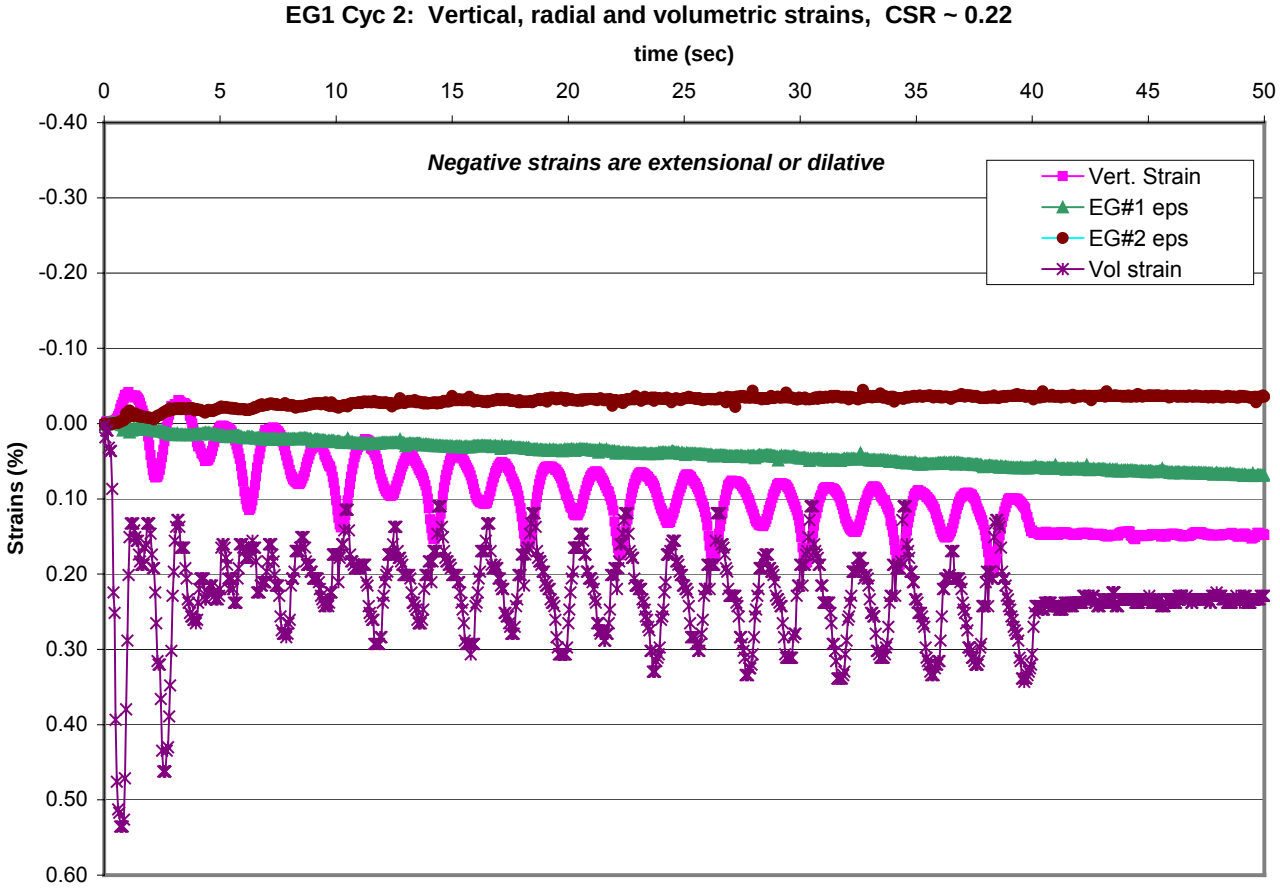
EG1 Cyc 2: Vertical, radial and volumetric strains, CSR ~ 0.22
time (sec)
0
5
10
15
20
25
30
35
40
45
50
-0.40
-0.30
-0.20
-0.10
0.00
0.10
0.20
0.30
0.40
0.50
0.60
Strains (%)
Negative strains are extensional or dilative
Vert. Strain
EG#1 eps
EG#2 eps
Vol strain

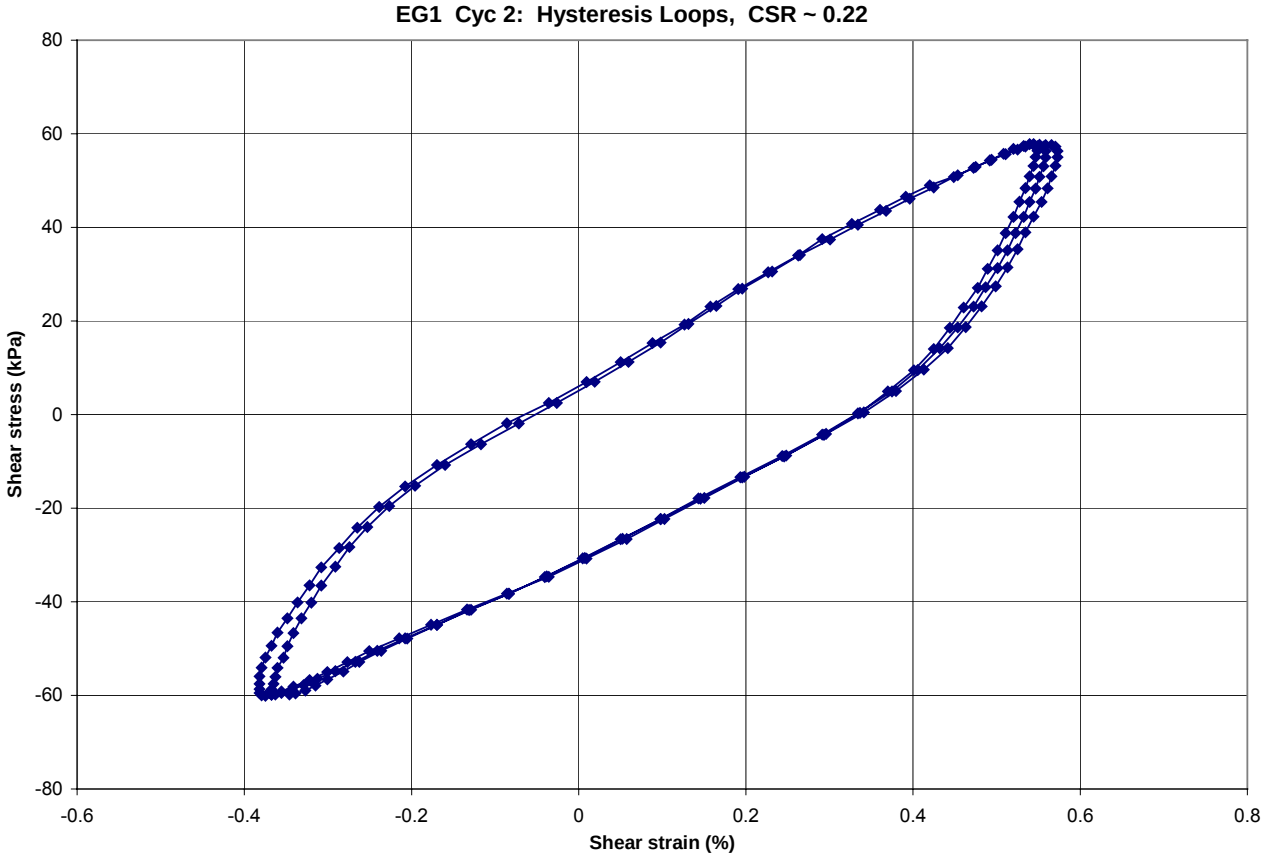
EG1 Cyc 2: Hysteresis Loops, CSR ~ 0.22
80
60
40
20
0
-20
-40
-60
-80
Shear stress (kPa)
-0.6
-0.4
-0.2
0
0.2
0.4
0.6
0.8
Shear strain (%)

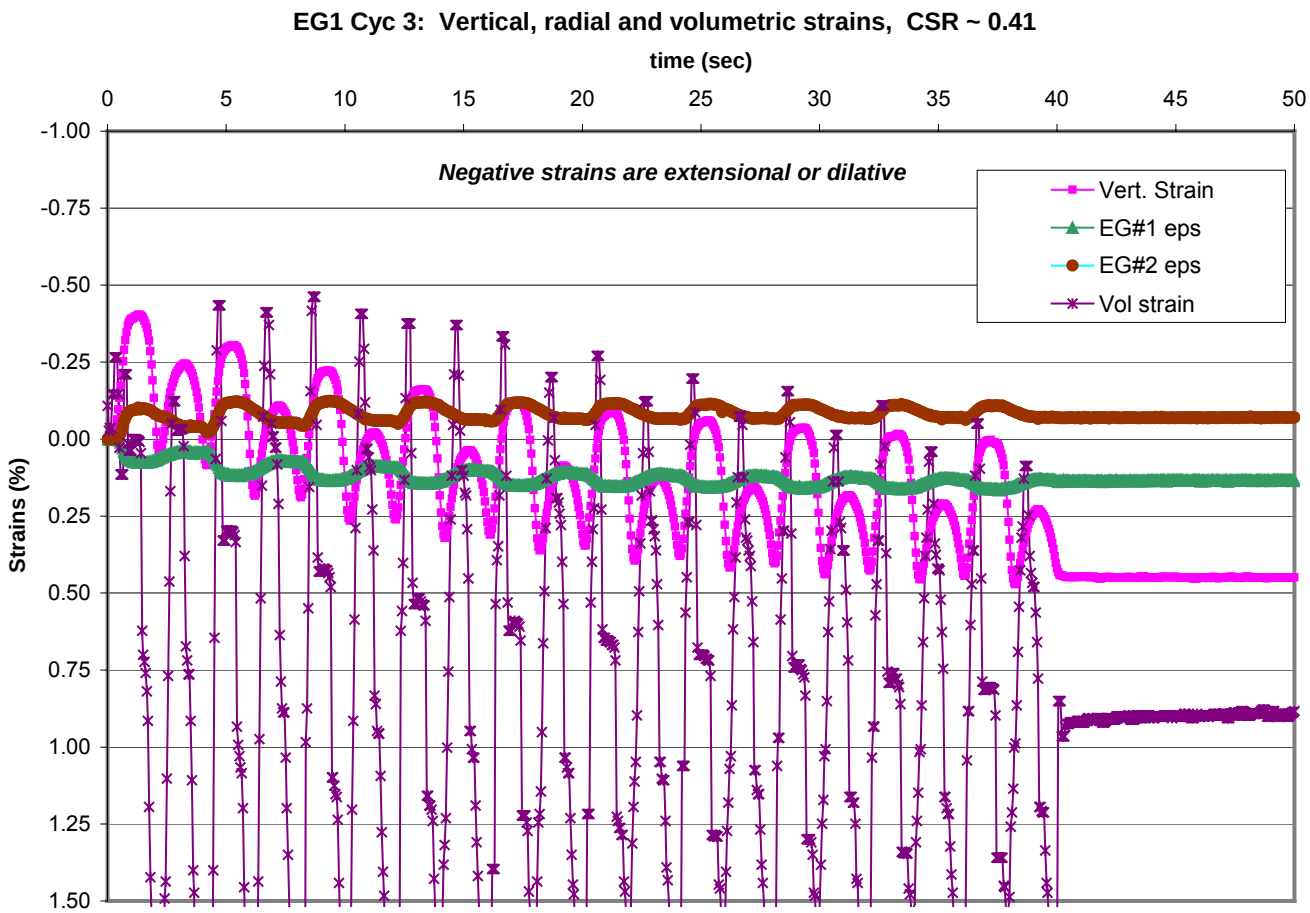
EG1 Cyc 3: Vertical, radial and volumetric strains, CSR ~ 0.41
time (sec)
0
5
10
15
20
25
30
35
40
45
50
-1.00
-0.75
-0.50
-0.25
0.00
0.25
0.50
0.75
1.00
1.25
1.50
Strains (%)
Negative strains are extensional or dilative
Vert. Strain
EG#1 eps
EG#2 eps
Vol strain

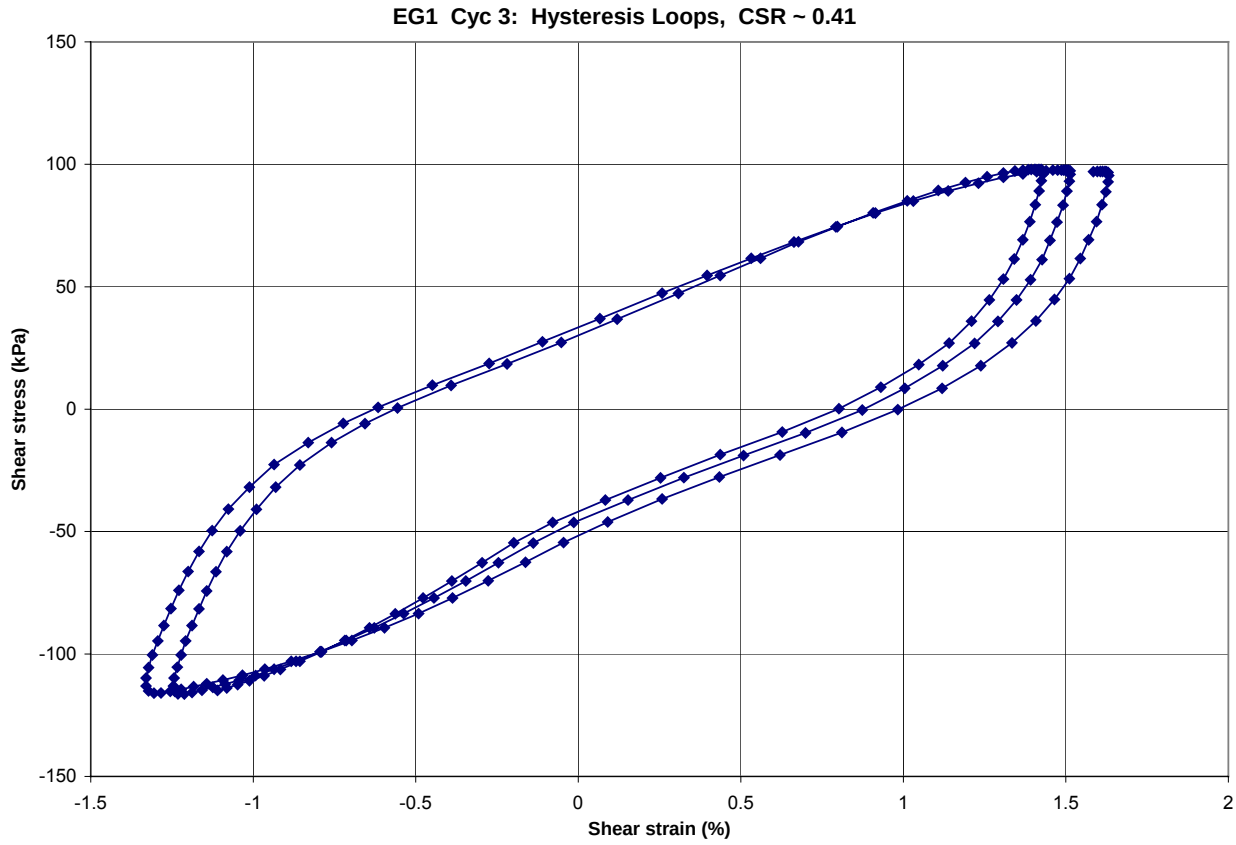
EG1 Cyc 3: Hysteresis Loops, CSR ~ 0.41
150
100
50
0
-50
-100
-150
Shear stress (kPa)
-1.5
-1
-0.5
0
0.5
1
1.5
2
Shear strain (%)

TEST EG -2

Stage of testing					*Incremental Vert. Strain (%)*	*Incremental Volumetric strain (%)*	*Incremental Radial Strain (%)*
Consol. #1	Keep lateral stress at 90 kPa, raise vertical stress to 180 kPa				0.46	0.11	-0.10
Consol. #2	Raise lateral to 125 kPa, vertical to 215 kPa				0.05	0.08	+0.01
Consol. #3	Raise vertical stress to 250 kPa				0.19	0.04	-0.03
Consol. #4	Raise lateral to 150 kPa, vertical to 275 kPa				0.04	0.045	+0.01
Consol. #5	Raise vertical stress to 300 kPa				0.08	0.02	-0.02
Consol #6	Raise lateral to 175 kPa, vertical stress to 350				0.14	0.07	~0
	CSR	***# of cycles***	***s.a. shear strain***	***Approx. G***			
			(%)	***(kPa)***			***(EG2)***
Cyclic loading 1	0.11	5	0.08	44,400	0.23	0.06	-0.08
Cyclic loading 2	0.21	10	0.23	30,000	0.64	0.18	-0.26
Cyclic loading 3	0.37	10	0.658	19,500	1.21	0.73	-0.42

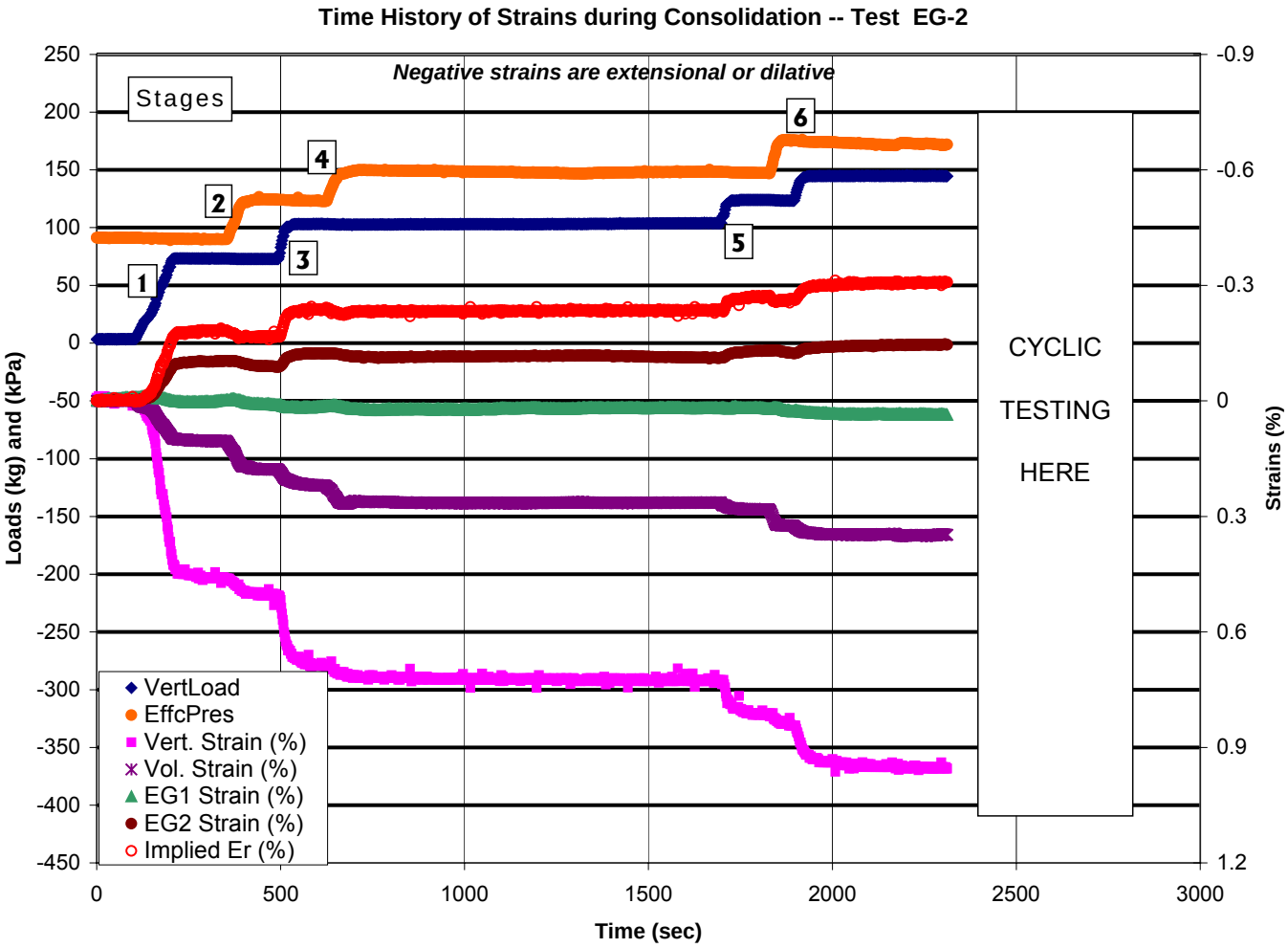

Copyright 2007, Kleinfelder

EG2 Cyc 1: Vertical , radial and volumetric strains, CSR ~ 0.11

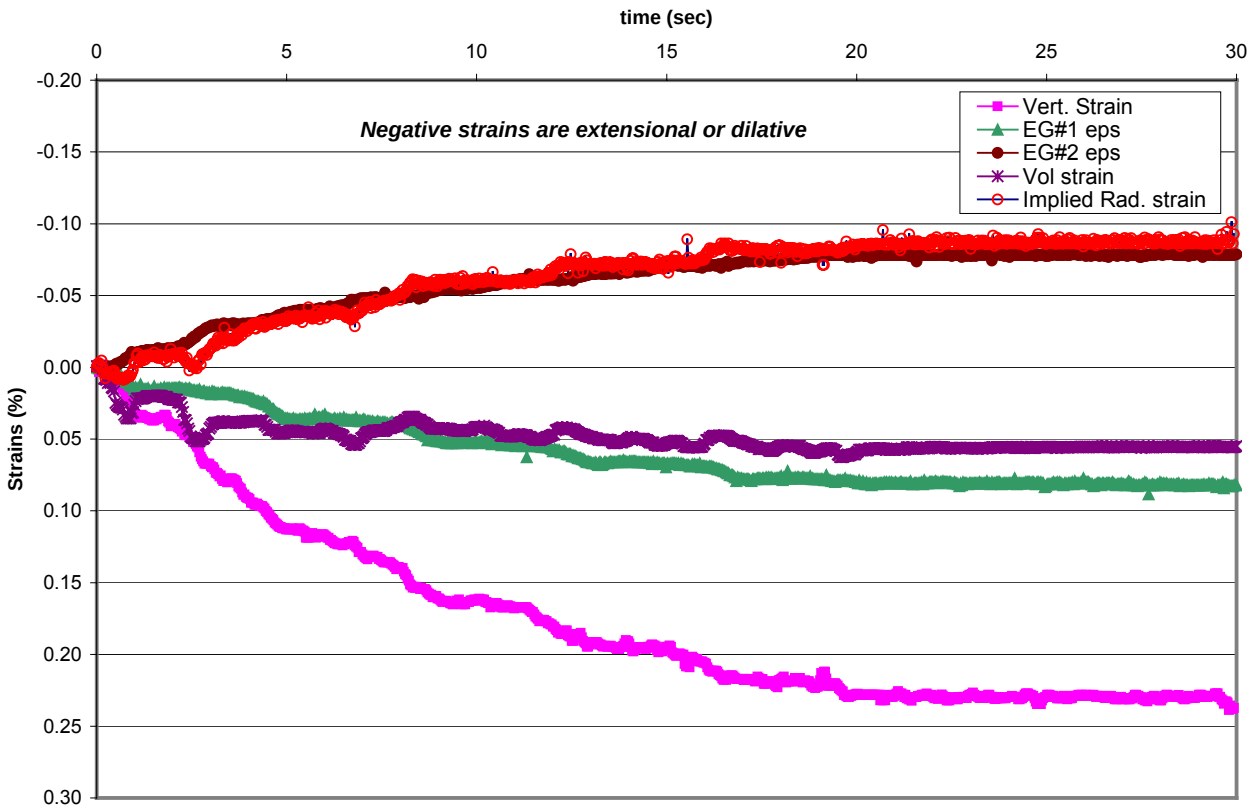

EG2 Cyc 1: Hysteresis Loops, CSR ~ 0.11

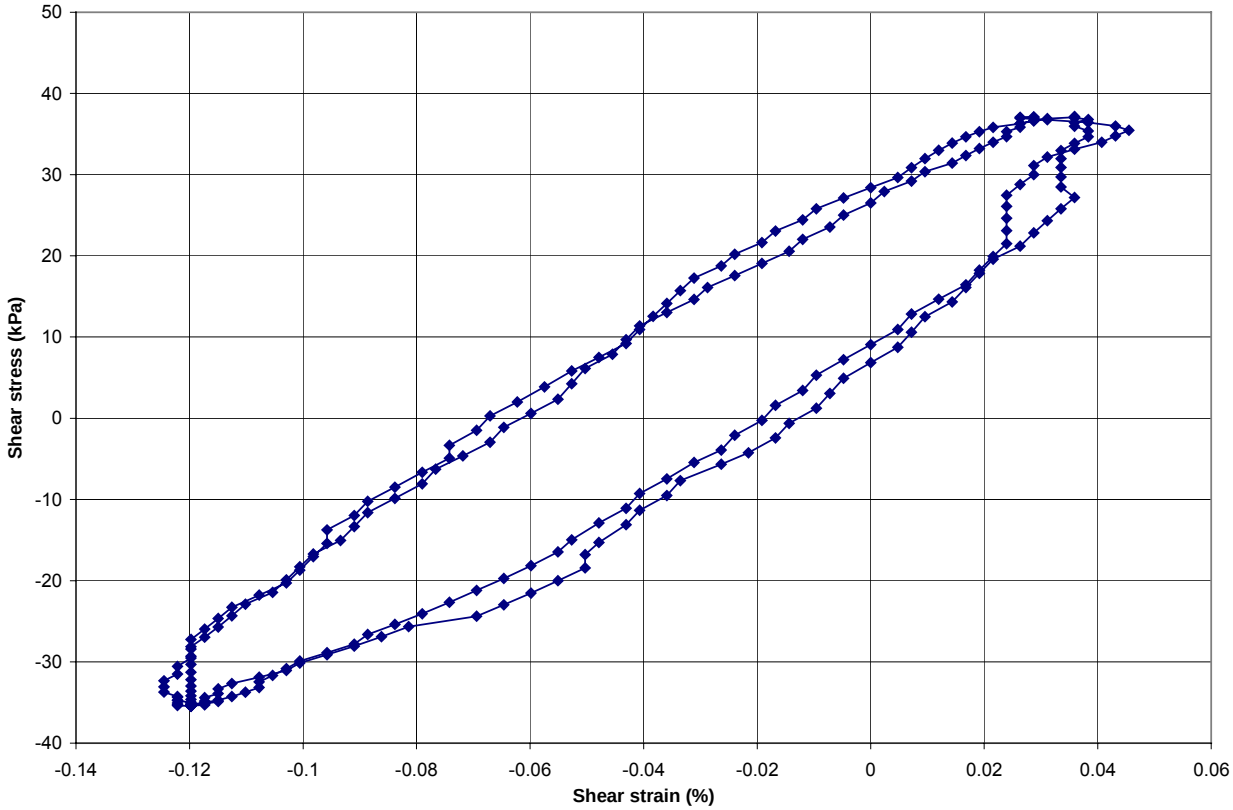

Copyright 2007, Kleinfelder

EG2 Cyc 2: Vertical , radial and volumetric strains, CSR ~ 0.21

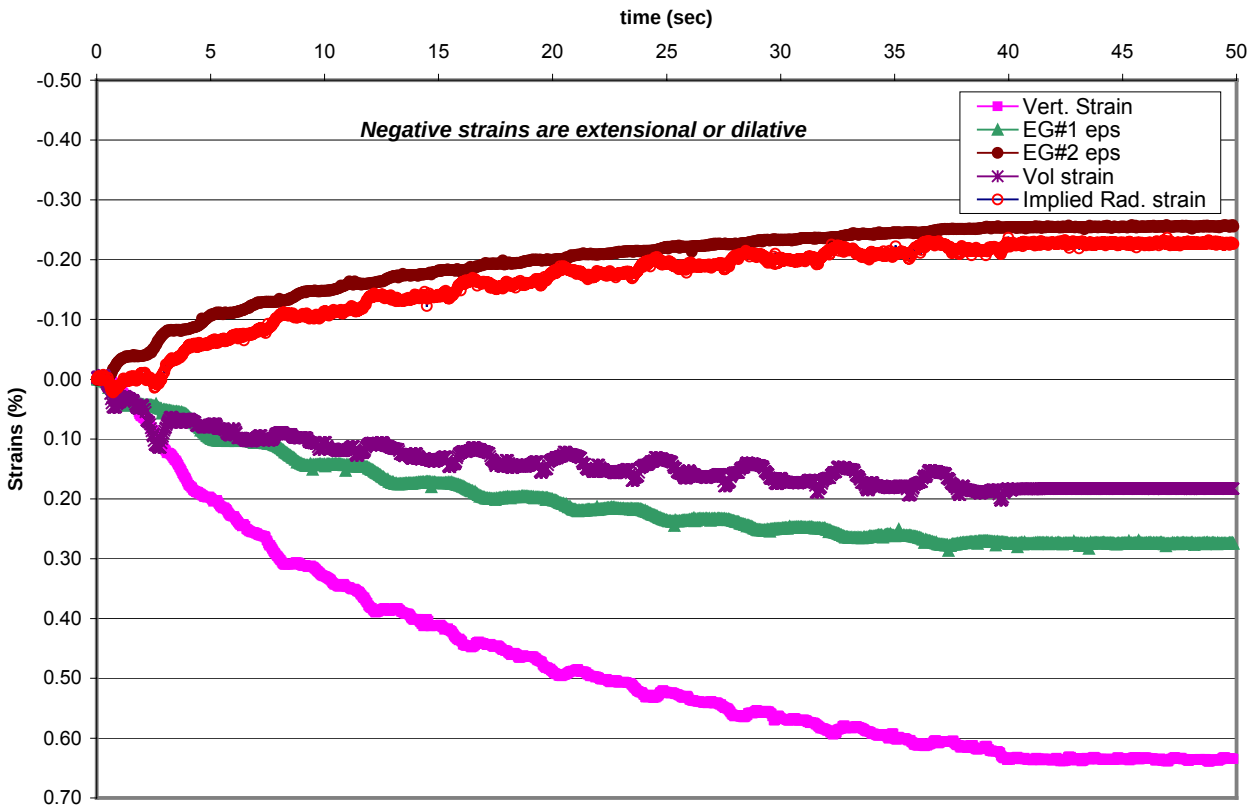

EG2 Cyc 2: Hysteresis Loops, CSR ~ 0.21

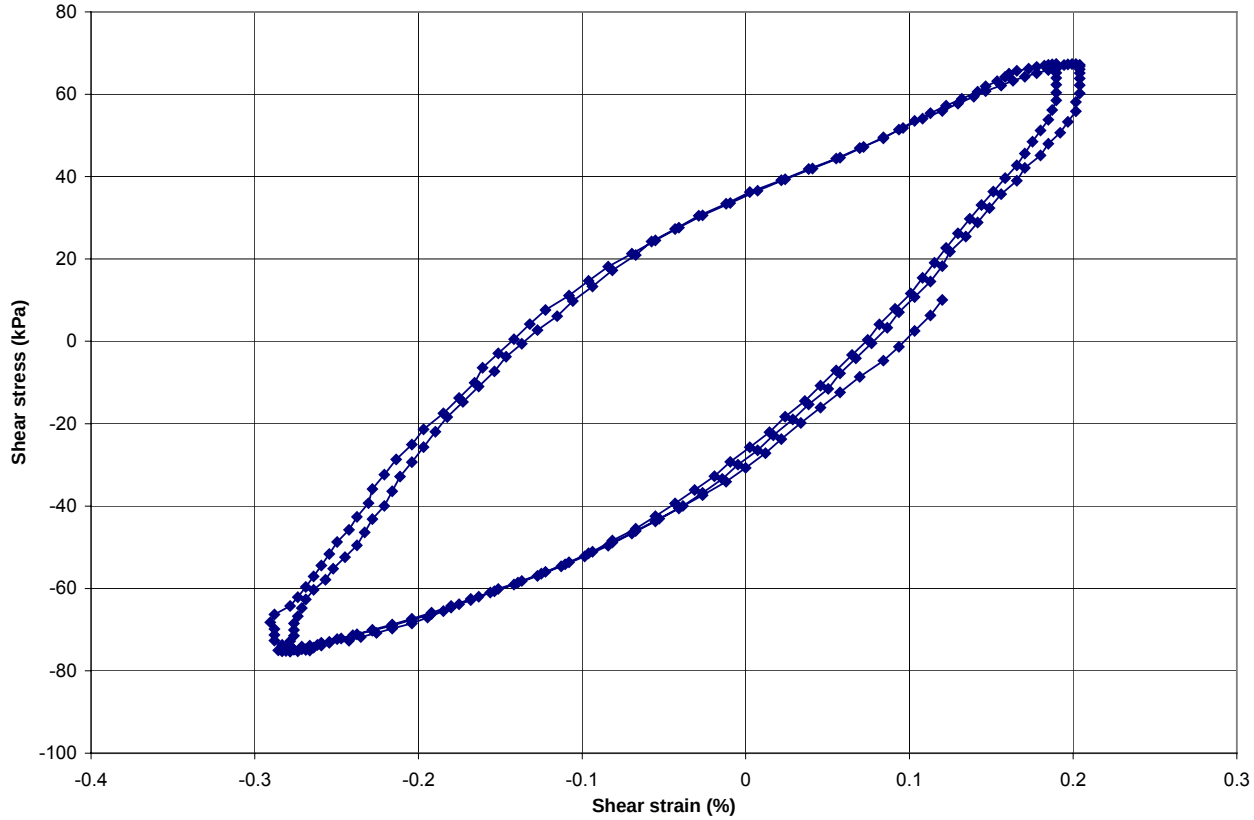

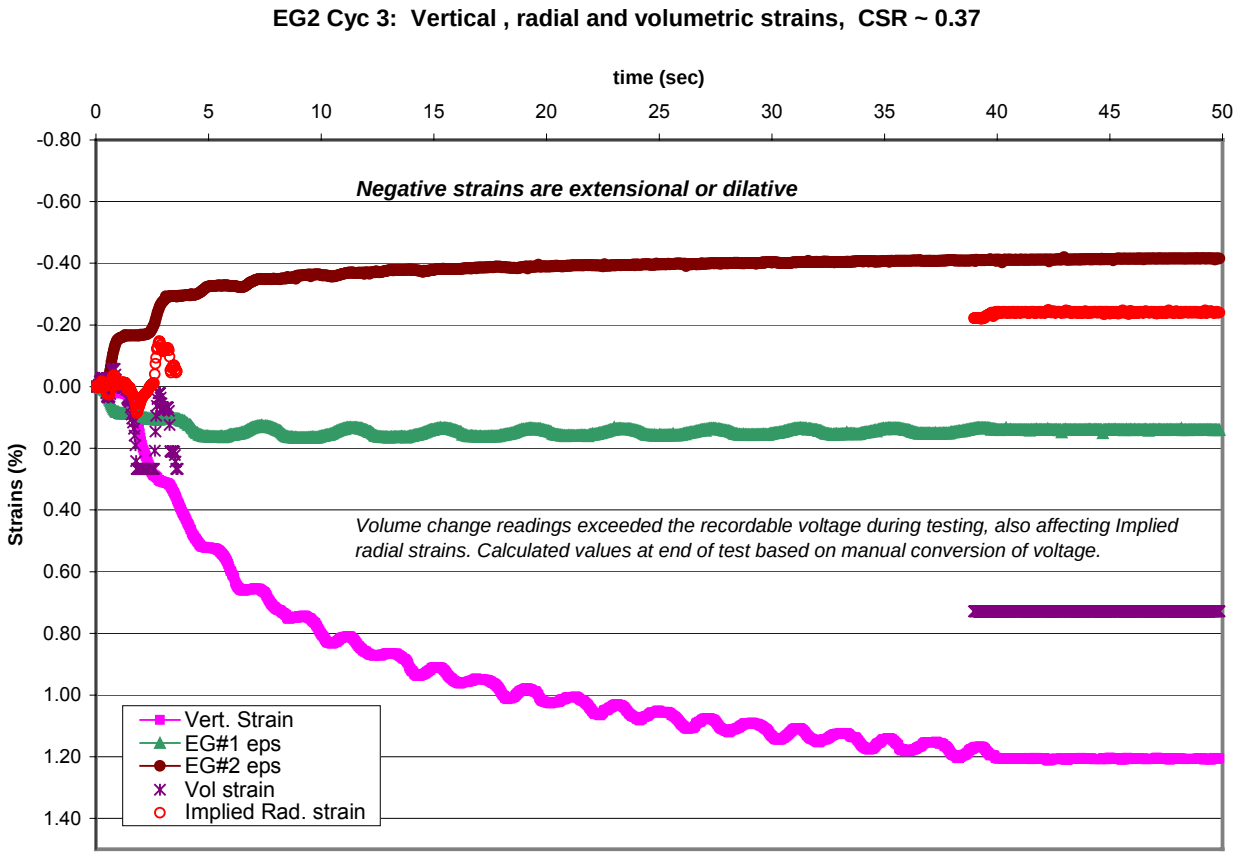
EG2 Cyc 3: Vertical , radial and volumetric strains, CSR ~ 0.37
time (sec)
0
5
10
15
20
25
30
35
40
45
50
-0.80
-0.60
-0.40
-0.20
0.00
0.20
0.40
0.60
0.80
1.00
1.20
1.40
Strains (%)
Negative strains are extensional or dilative
Volume change readings exceeded the recordable voltage during testing, also affecting Implied radial strains. Calculated values at end of test based on manual conversion of voltage.
Vert. Strain
EG#1 eps
EG#2 eps
Vol strain
Implied Rad. strain

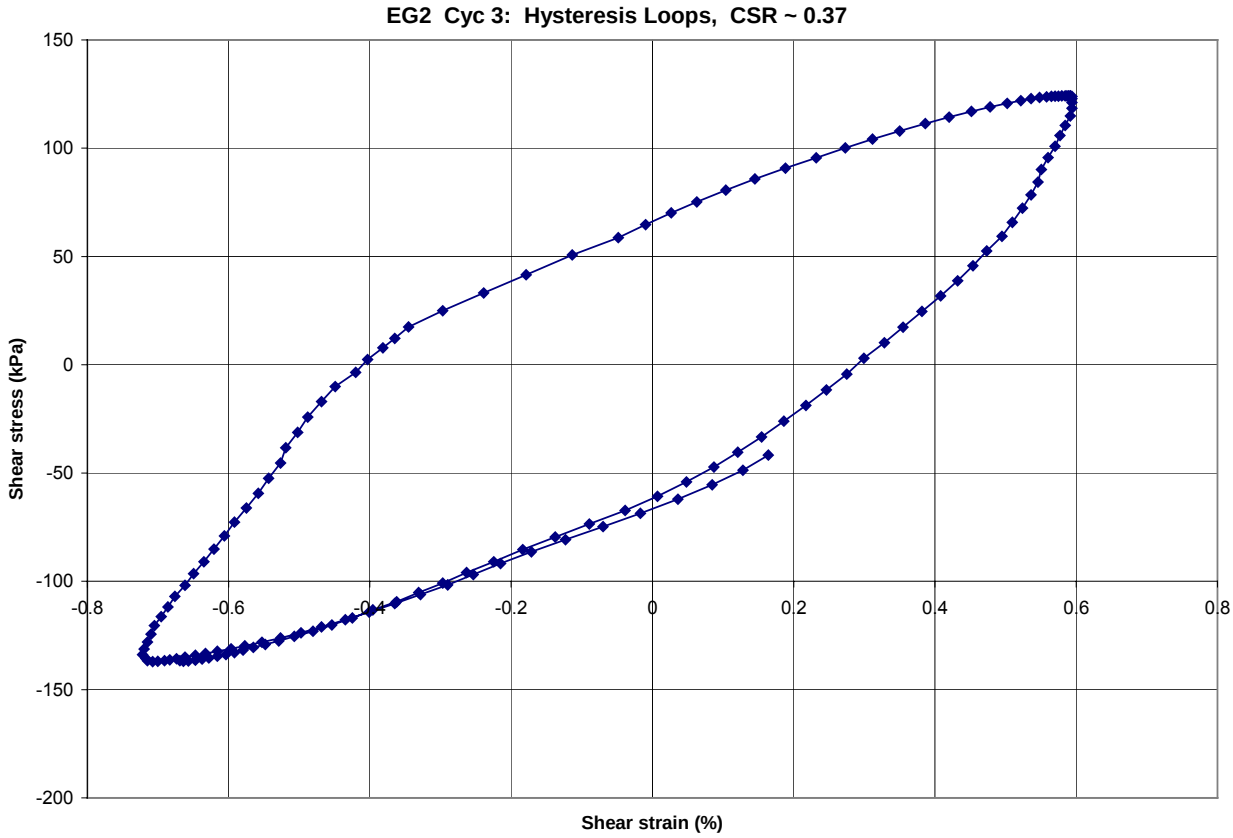
EG2 Cyc 3: Hysteresis Loops, CSR ~ 0.37
150
100
50
0
-50
-100
-150
-200
Shear stress (kPa)
-0.8
-0.6
-0.4
-0.2
0
0.2
0.4
0.6
0.8
Shear strain (%)

LANL-2

Stage of testing					***Incremental Vert. Strain (%)***
Consol. #1	Switch from ~33 kPa vacuum to ~33 kPa chamber pressure confinement				< 0.02
Consol. #2	Raise chamber pressure to isotropic stress of 100 kPa				0.26
Consol. #3	Raise deviatoric load to reach Ko ~ 0.5 condition				0.94
Consol. #4	Raise chamber pressure to isotropic stress of 225 kPa				0.5
Consol. #5	Raise deviatoric load to re-establish Ko ~ 0.5 condition				1.1
	CSR	***# of cycles***	***s.a. shear strain***	***Approx. G***	
			(%)	***(kPa)***	
Cyclic loading 1	0.077	5	0.104	33,600	0.08
Cyclic loading 2	0.155	10	0.255	27,800	0.38
Cyclic loading 3	0.315	10	0.88	16,500	1.1
Unloading	Reduce stresses thru same path, return to ~33 kPa vacuum confinement				-0.65

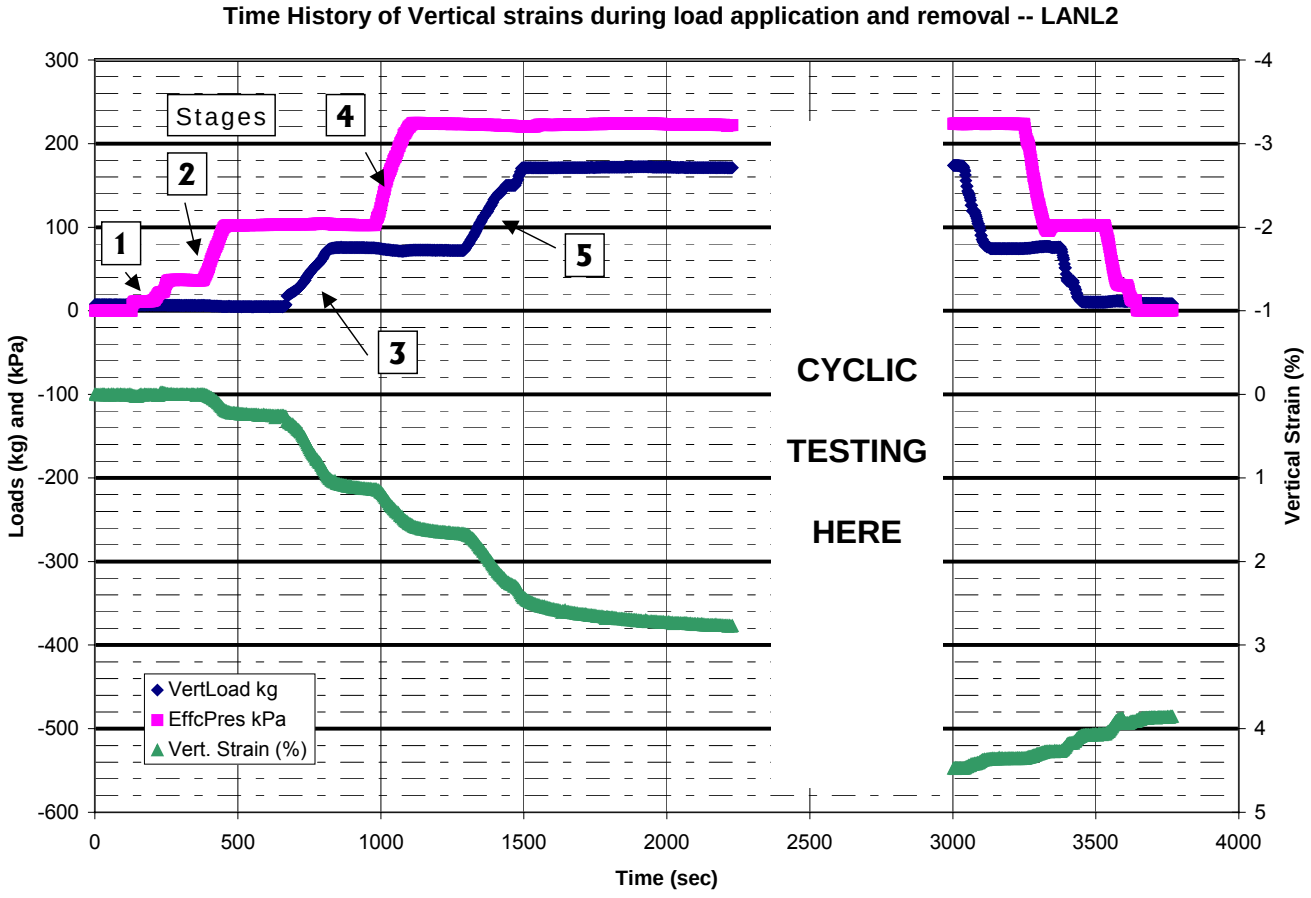

Copyright 2007, Kleinfelder

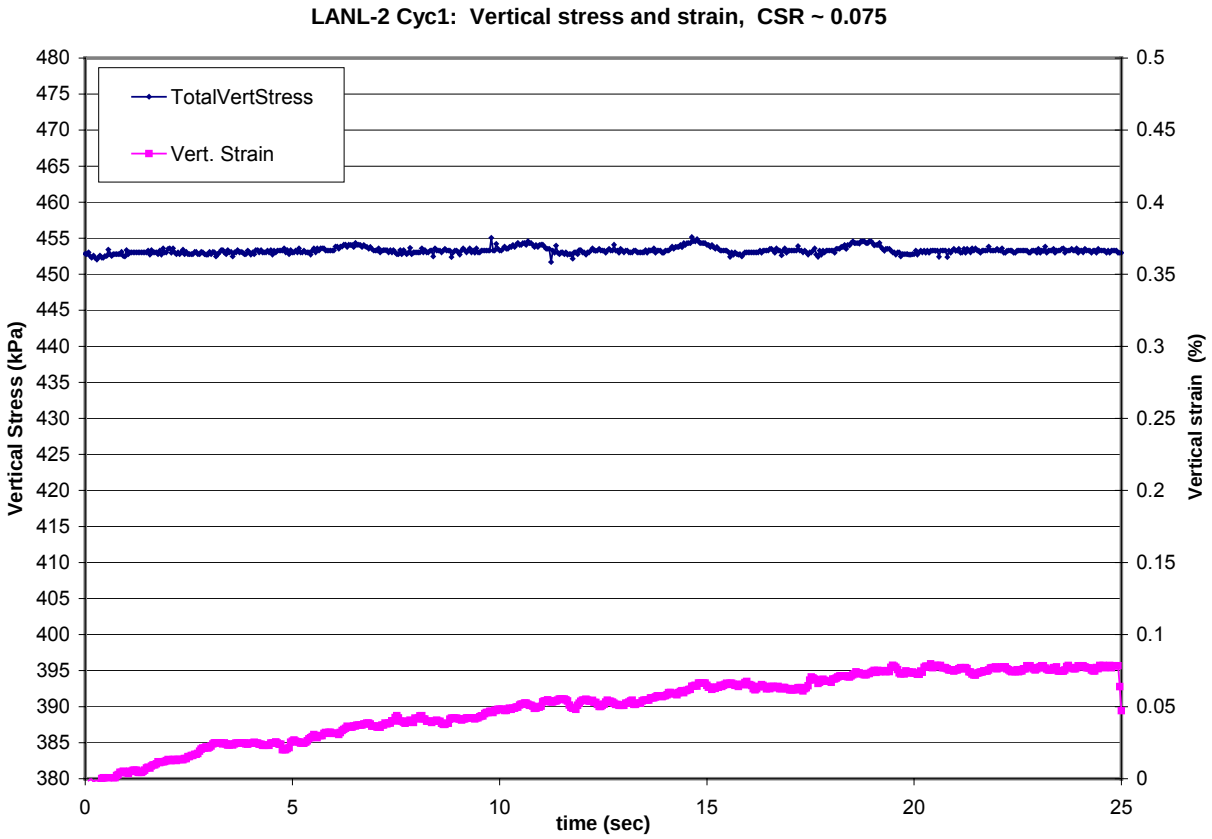
LANL-2 Cyc1: Vertical stress and strain, CSR ~ 0.075
TotalVertStress
Vert. Strain
Vertical Stress (kPa)
Vertical strain (%)
time (sec)
480
475
470
465
460
455
450
445
440
435
430
425
420
415
410
405
400
395
390
385
380
0.5
0.45
0.4
0.35
0.3
0.25
0.2
0.15
0.1
0.05
0
0
5
10
15
20
25

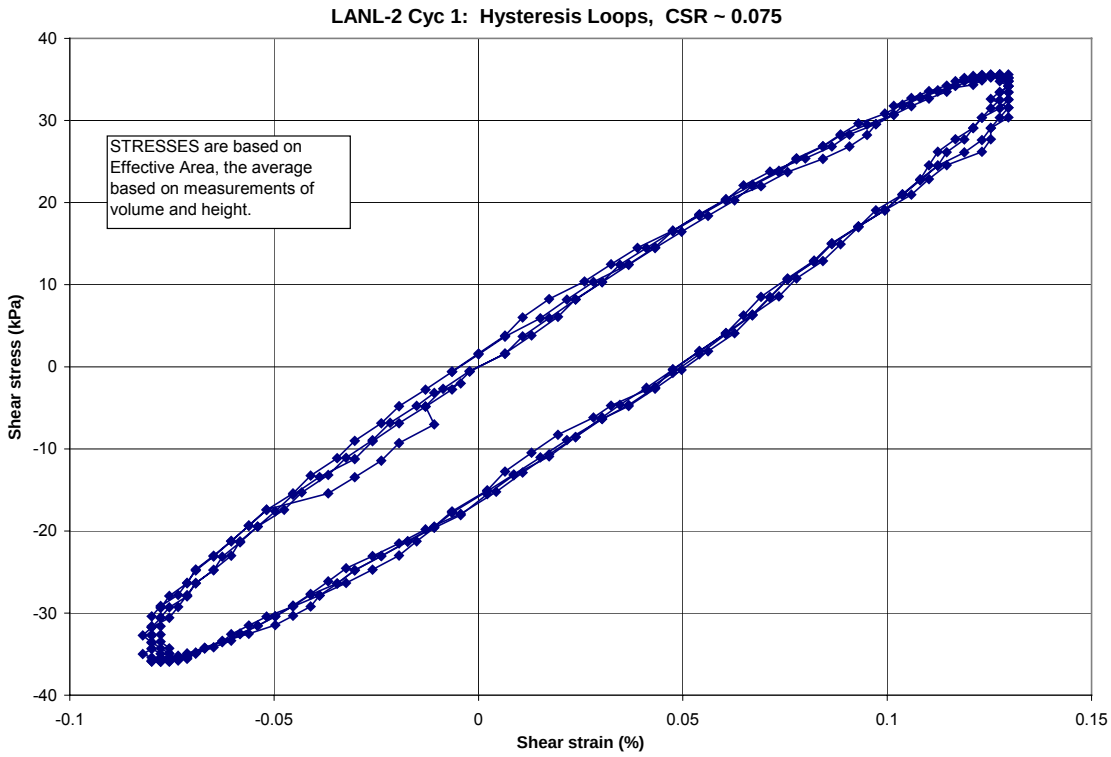
LANL-2 Cyc 1: Hysteresis Loops, CSR ~ 0.075
STRESSES are based on Effective Area, the average based on measurements of volume and height.
Shear stress (kPa)
Shear strain (%)
40
30
20
10
0
-10
-20
-30
-40
-0.1
-0.05
0
0.05
0.1
0.15

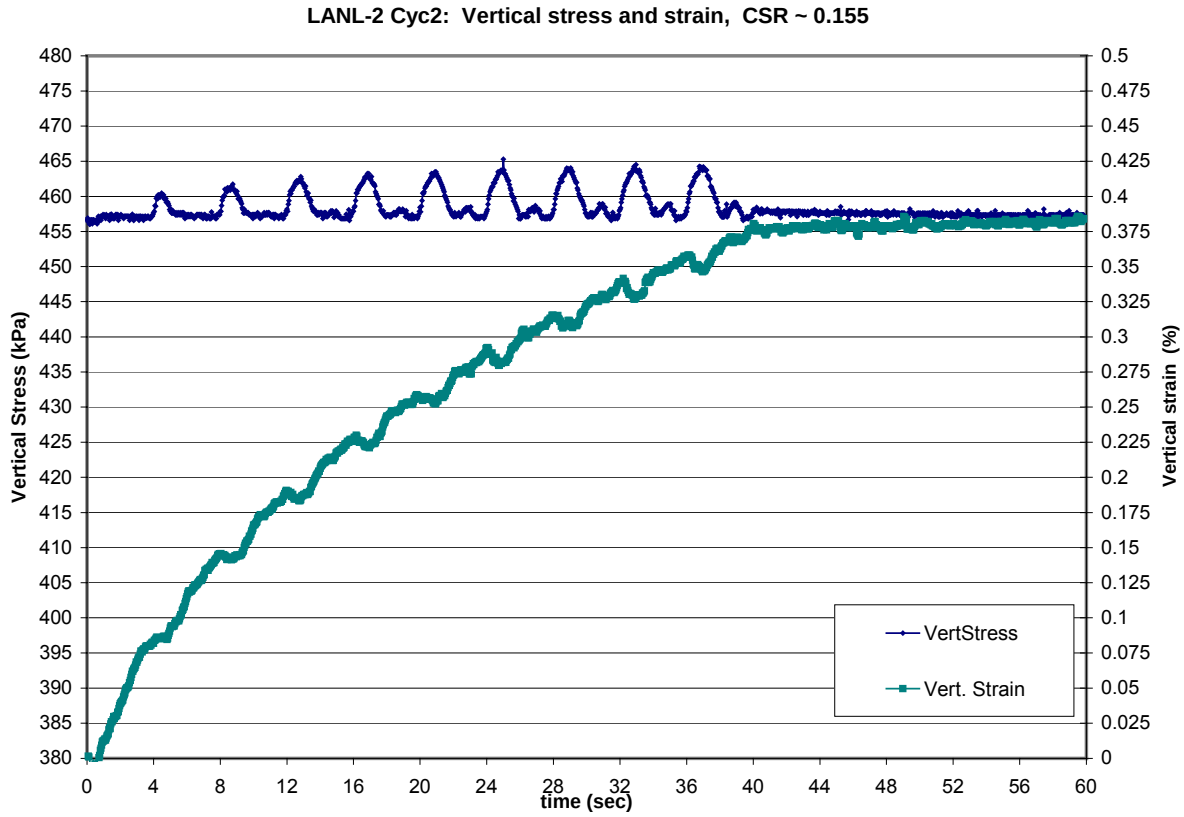
LANL-2 Cyc2: Vertical stress and strain, CSR ~ 0.155
Vertical Stress (kPa)
Vertical strain (%)
time (sec)
VertStress
Vert. Strain

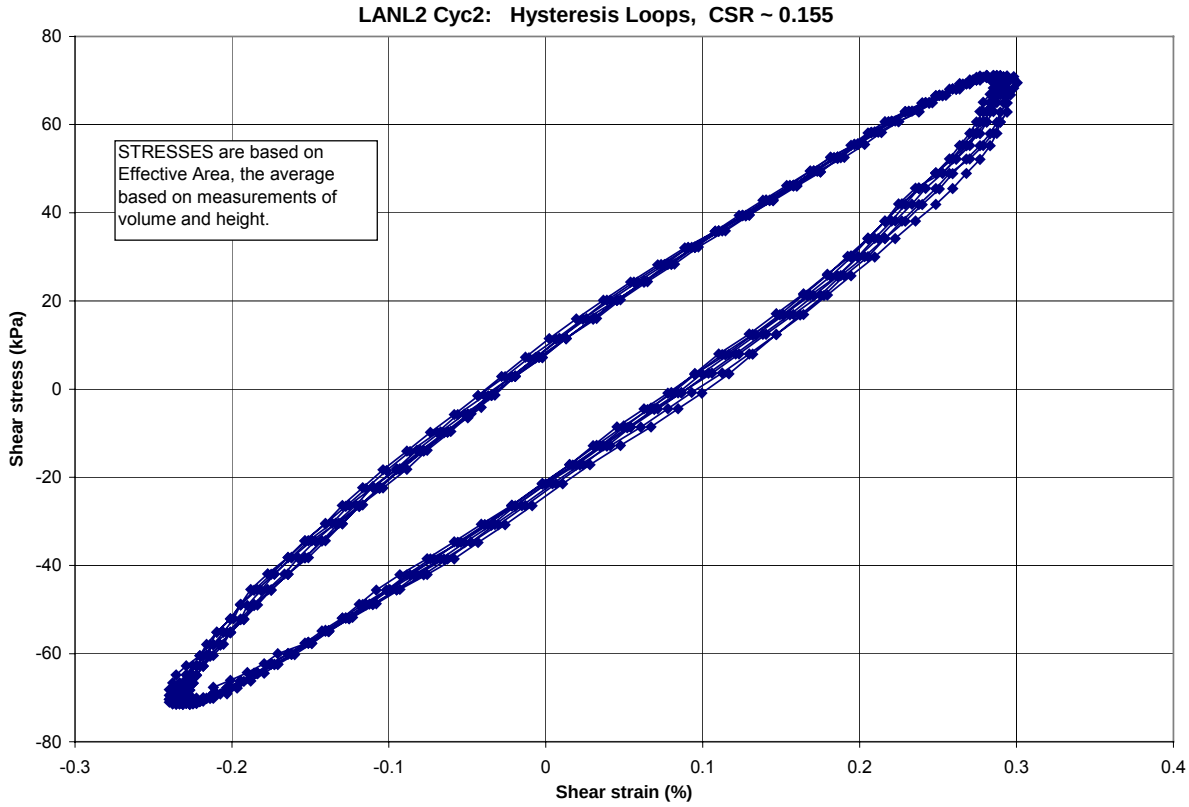
LANL2 Cyc2: Hysteresis Loops, CSR ~ 0.155
STRESSES are based on Effective Area, the average based on measurements of volume and height.
Shear stress (kPa)
Shear strain (%)

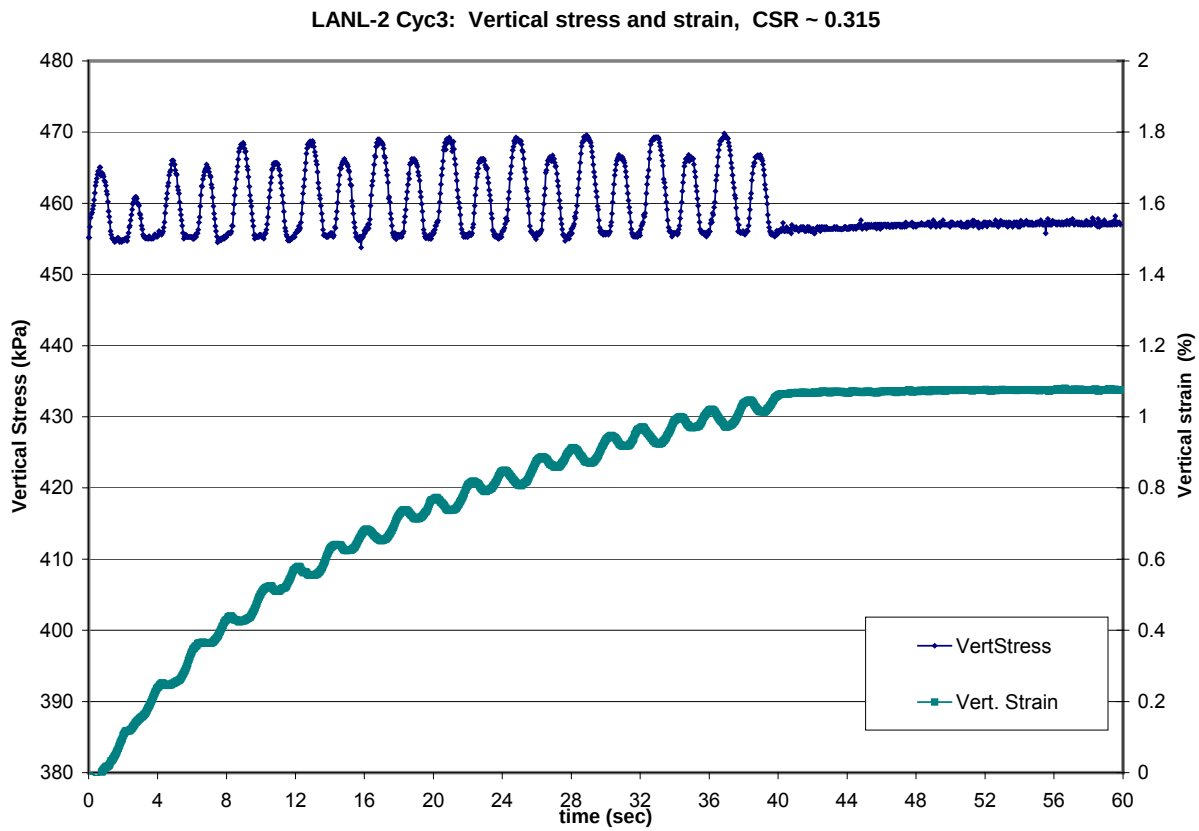
LANL-2 Cyc3: Vertical stress and strain, CSR ~ 0.315
Vertical Stress (kPa)
Vertical strain (%)
time (sec)
VertStress
Vert. Strain
480
470
460
450
440
430
420
410
400
390
380
2
1.8
1.6
1.4
1.2
1
0.8
0.6
0.4
0.2
0
0
4
8
12
16
20
24
28
32
36
40
44
48
52
56
60

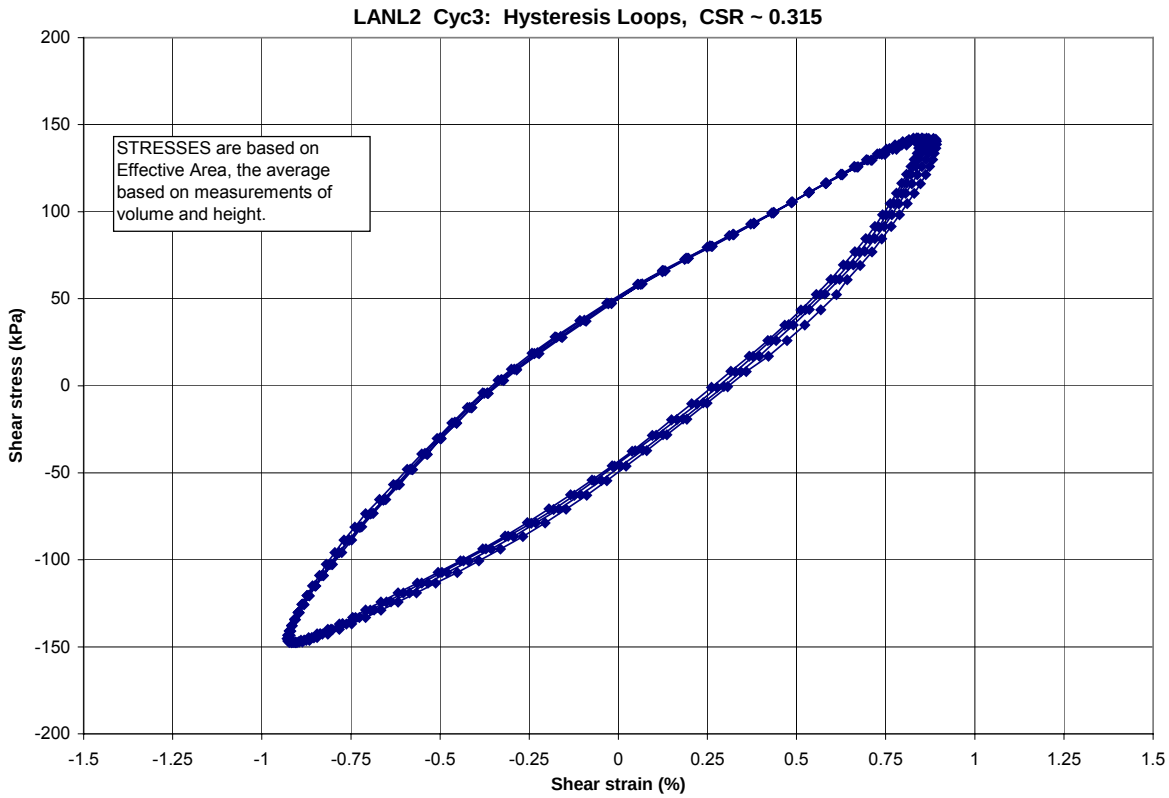
LANL2 Cyc3: Hysteresis Loops, CSR ~ 0.315
STRESSES are based on Effective Area, the average based on measurements of volume and height.
Shear stress (kPa)
Shear strain (%)
200
150
100
50
0
-50
-100
-150
-200
-1.5
-1.25
-1
-0.75
-0.5
-0.25
0
0.25
0.5
0.75
1
1.25
1.5

LANL-3

Stage of testing					***Incremental Vert. Strain (%)***
Consol. #1	Switch from ~20 kPa vacuum to ~20 kPa chamber pressure confinement				< 0.05
Consol. #2	Raise chamber pressure to isotropic stress of ~58 kPa				0.23
Consol. #3	Raise chamber pressure to isotropic stress of ~150 kPa				0.52
Consol. #4	Raise chamber pressure to isotropic stress of ~250 kPa				0.35
Consol. #5	Raise chamber pressure to isotropic stress of ~340 kPa				0.3
	CSR	***# of cycles***	***s.a. shear strain (%)***	***Approx. G (kPa)***	
Cyclic loading 1	0.07	5	0.07	34,300	0.025
Cyclic loading 2	0.14	10	0.17	29,100	0.107
Cyclic loading 3	0.29	10	0.47	21,500	0.21
Unloading	Reduce stresses thru same path, return to ~33 kPa vacuum confinement				-0.35

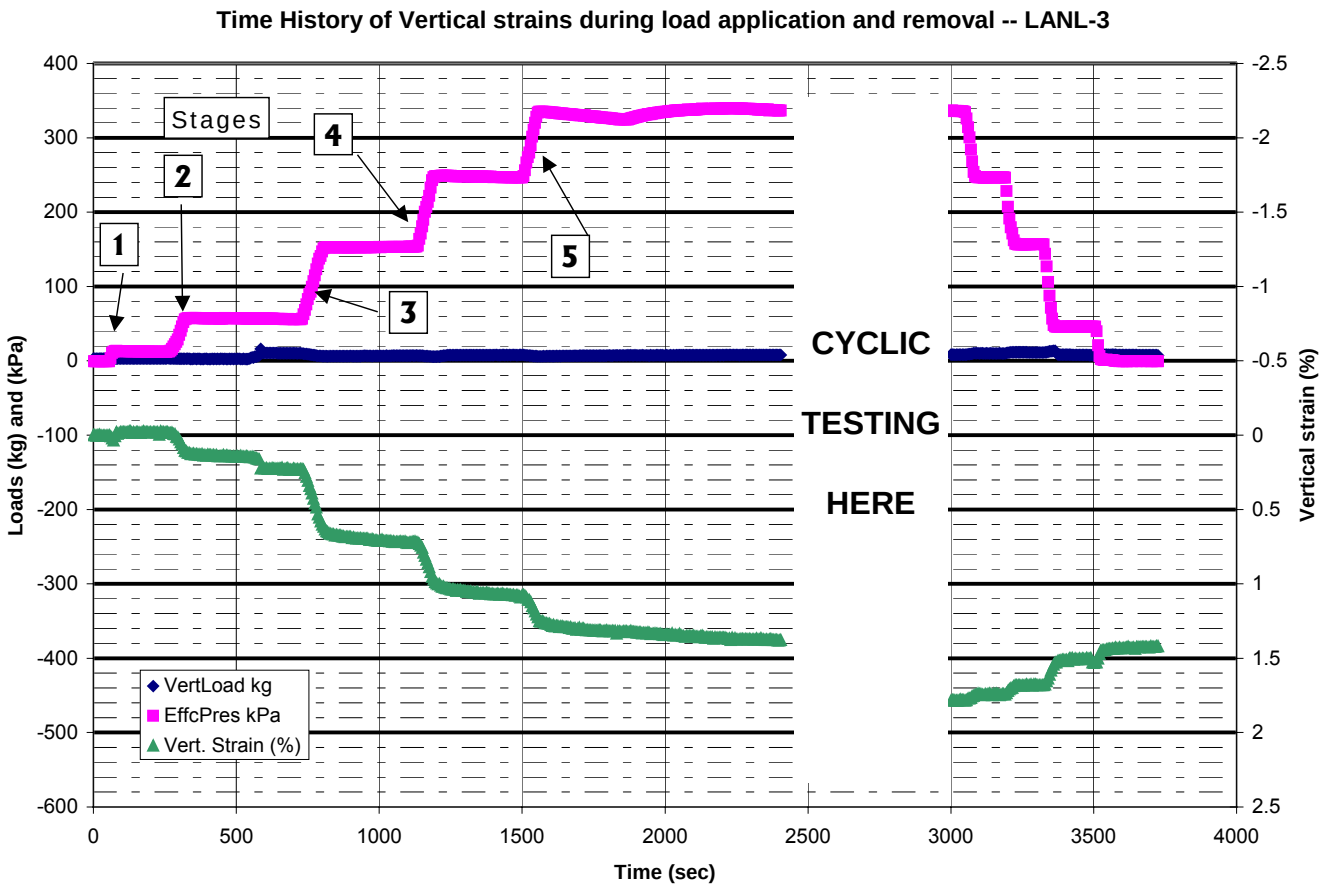

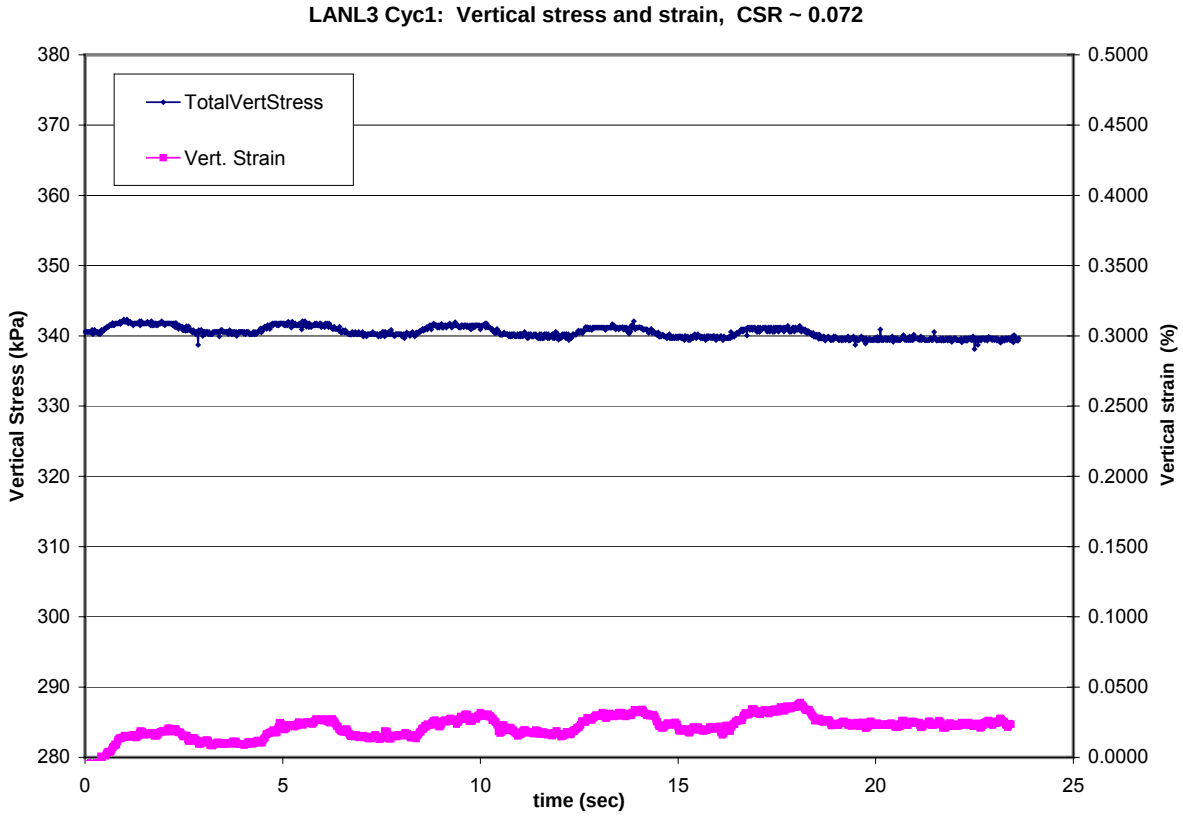
LANL3 Cyc1: Vertical stress and strain, CSR ~ 0.072
TotalVertStress
Vert. Strain
Vertical Stress (kPa)
Vertical strain (%)
time (sec)
380
370
360
350
340
330
320
310
300
290
280
0.5000
0.4500
0.4000
0.3500
0.3000
0.2500
0.2000
0.1500
0.1000
0.0500
0.0000
0
5
10
15
20
25

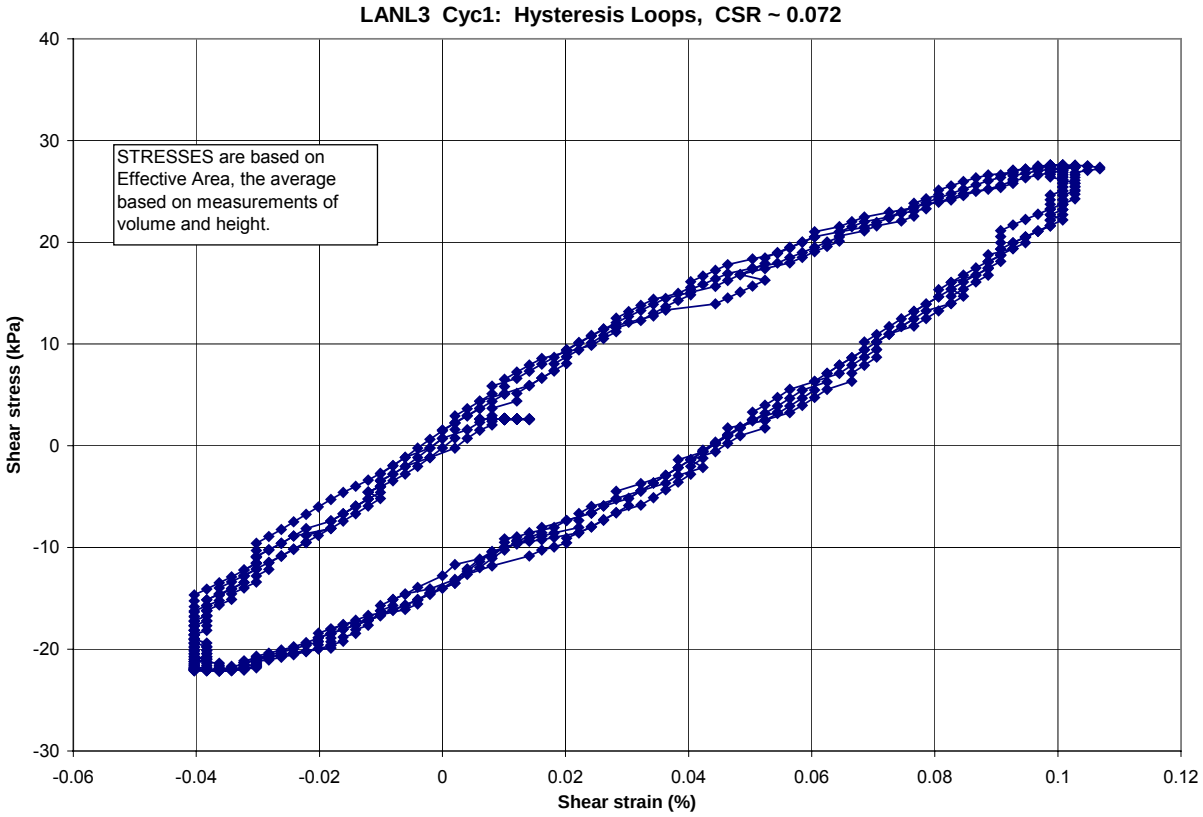
LANL3 Cyc1: Hysteresis Loops, CSR ~ 0.072
STRESSES are based on Effective Area, the average based on measurements of volume and height.
Shear stress (kPa)
Shear strain (%)
40
30
20
10
0
-10
-20
-30
-0.06
-0.04
-0.02
0
0.02
0.04
0.06
0.08
0.1
0.12

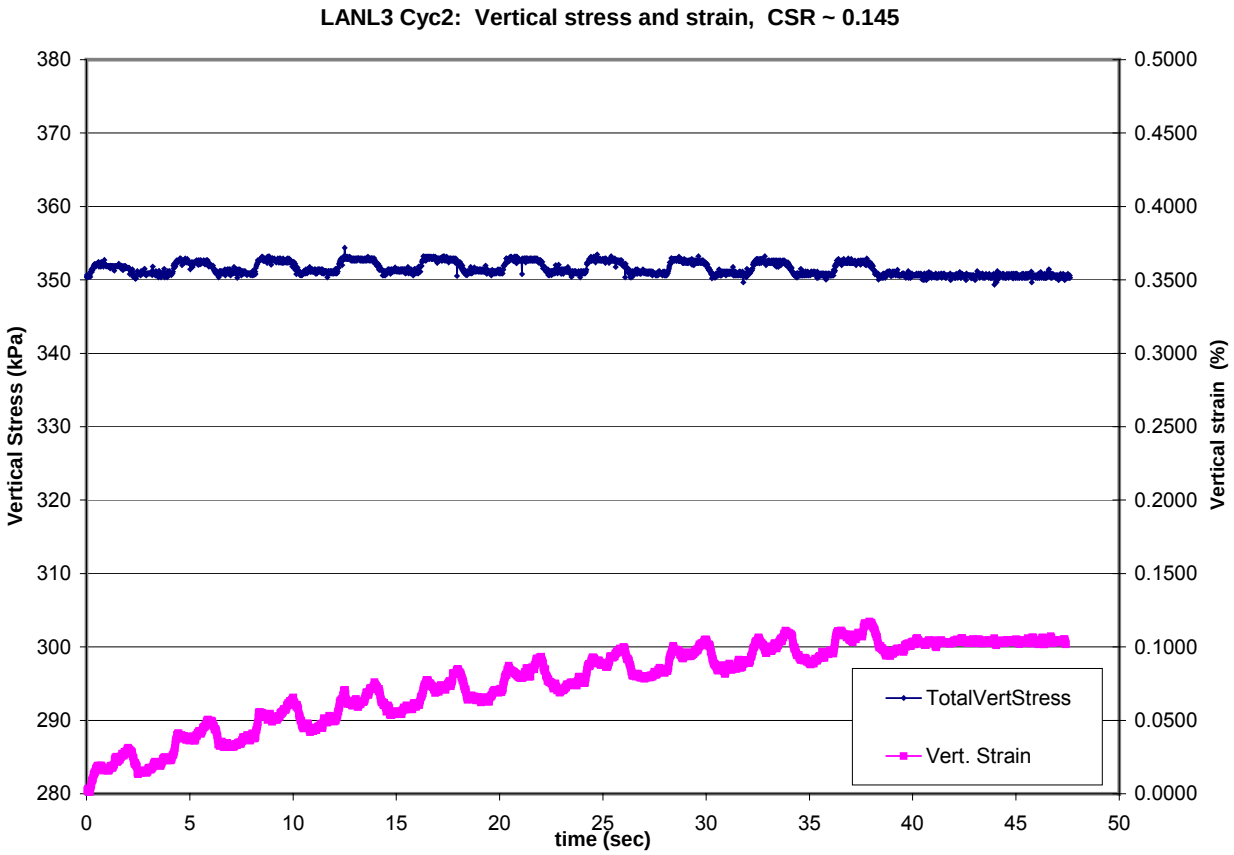
LANL3 Cyc2: Vertical stress and strain, CSR ~ 0.145
Vertical Stress (kPa)
Vertical strain (%)
time (sec)
TotalVertStress
Vert. Strain
380
370
360
350
340
330
320
310
300
290
280
0.5000
0.4500
0.4000
0.3500
0.3000
0.2500
0.2000
0.1500
0.1000
0.0500
0.0000
0
5
10
15
20
25
30
35
40
45
50

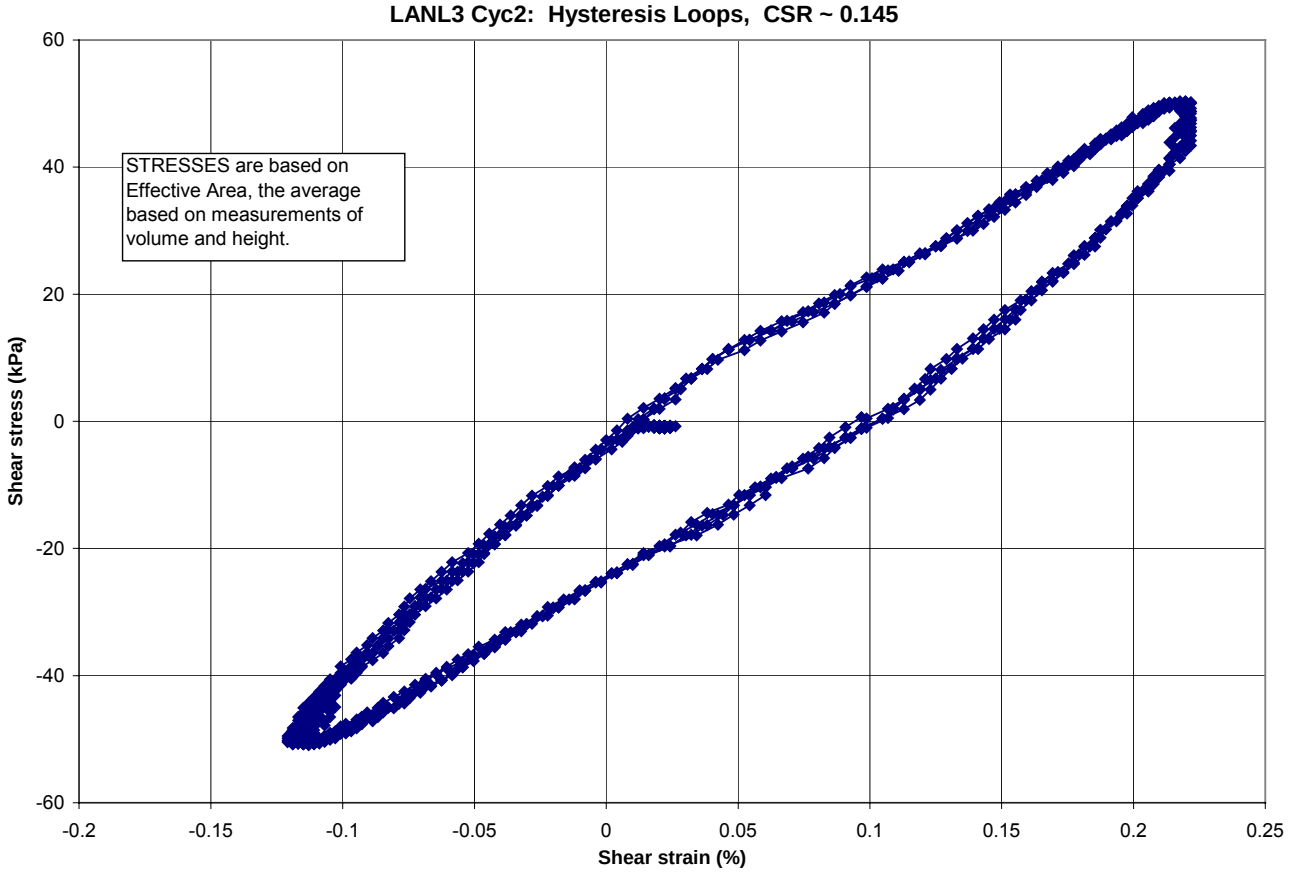
LANL3 Cyc2: Hysteresis Loops, CSR ~ 0.145
STRESSES are based on Effective Area, the average based on measurements of volume and height.
Shear stress (kPa)
Shear strain (%)
60
40
20
0
-20
-40
-60
-0.2
-0.15
-0.1
-0.05
0
0.05
0.1
0.15
0.2
0.25

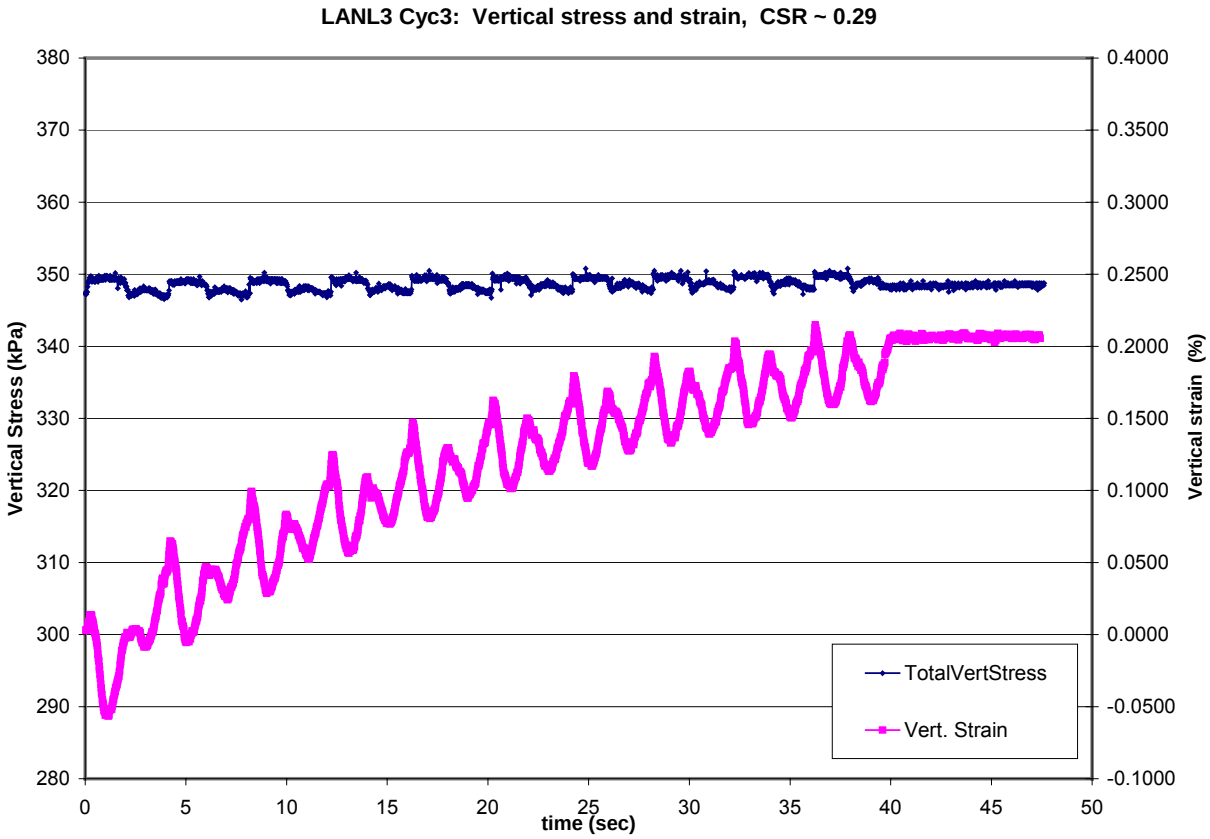
LANL3 Cyc3: Vertical stress and strain, CSR ~ 0.29
Vertical Stress (kPa)
Vertical strain (%)
time (sec)
TotalVertStress
Vert. Strain
380
370
360
350
340
330
320
310
300
290
280
0.4000
0.3500
0.3000
0.2500
0.2000
0.1500
0.1000
0.0500
0.0000
-0.0500
-0.1000
0
5
10
15
20
25
30
35
40
45
50

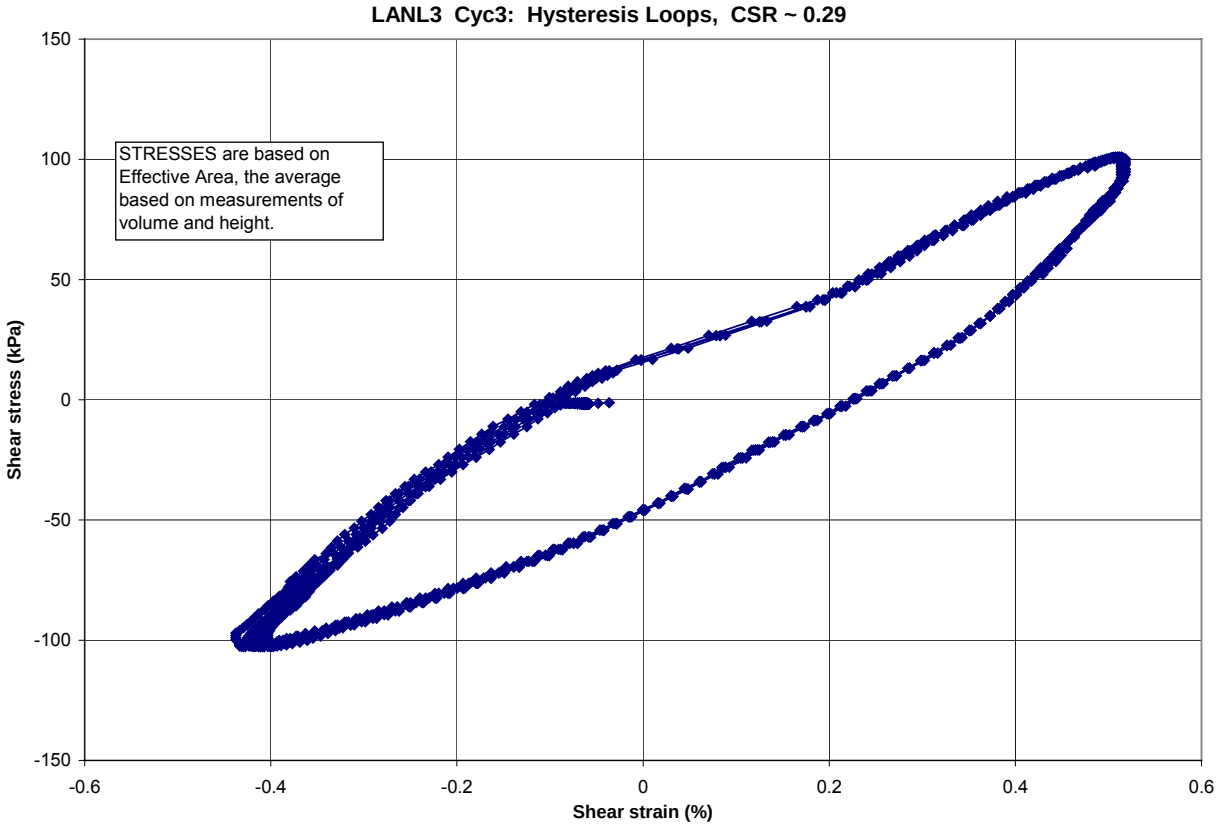
LANL3 Cyc3: Hysteresis Loops, CSR ~ 0.29
STRESSES are based on Effective Area, the average based on measurements of volume and height.
Shear stress (kPa)
Shear strain (%)
150
100
50
0
-50
-100
-150
-0.6
-0.4
-0.2
0
0.2
0.4
0.6

LANL-4

Stage of testing					Incremental Vert. Strain (%)
Consol. #1	Switch from ~15 kPa vacuum to ~15 kPa chamber pressure confinement				< 0.05
Consol. #2	Raise chamber pressure to isotropic stress of ~50 kPa				0.06
Consol. #3	Raise chamber pressure to isotropic stress of ~100 kPa				0.25
Consol. #4	Raise chamber pressure to isotropic stress of ~200 kPa				0.45
Consol. #5	Raise chamber pressure to isotropic stress of ~335 kPa				0.4
	CSR	***# of cycles***	***s.a. shear strain (%)***	***Approx. G (kPa)***	
Cyclic loading 1	0.076	5	0.062	38,500	0.02
Cyclic loading 2	0.158	10	0.19	28,000	0.08
Cyclic loading 3	0.31	10	0.85	12,500 (odd loops)	0.22
Unloading	Reduce stresses thru same path, return to ~15 kPa vacuum confinement				-0.36

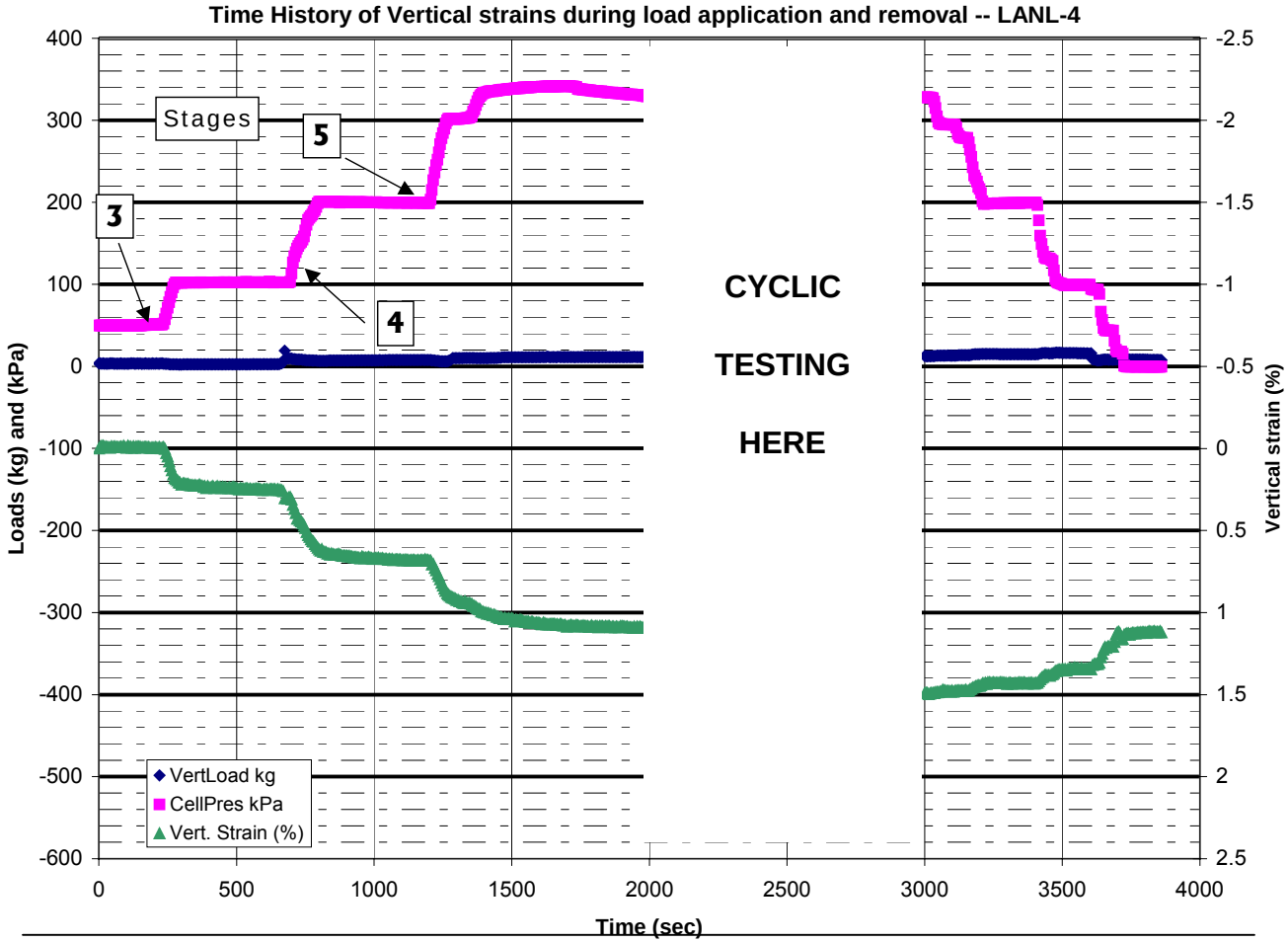

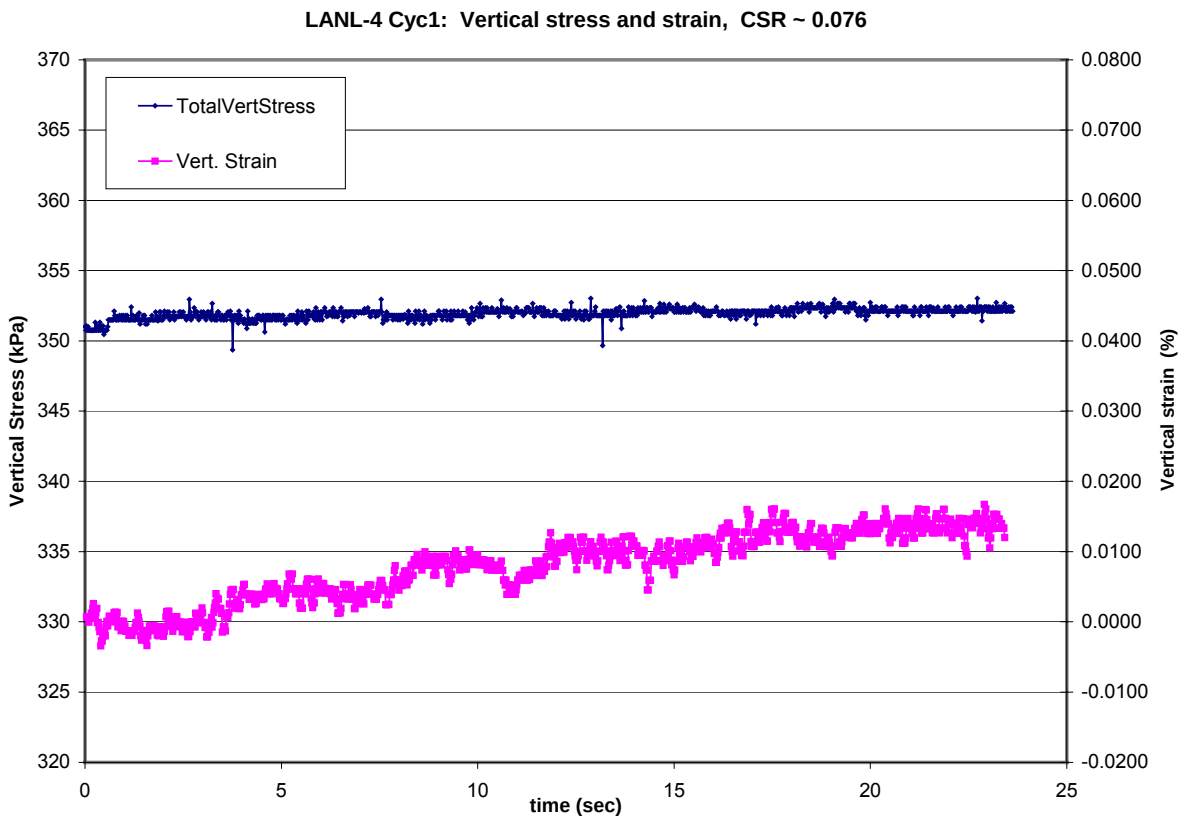
LANL-4 Cyc1: Vertical stress and strain, CSR ~ 0.076
TotalVertStress
Vert. Strain
Vertical Stress (kPa)
Vertical strain (%)
time (sec)
370
365
360
355
350
345
340
335
330
325
320
0.0800
0.0700
0.0600
0.0500
0.0400
0.0300
0.0200
0.0100
0.0000
-0.0100
-0.0200
0
5
10
15
20
25

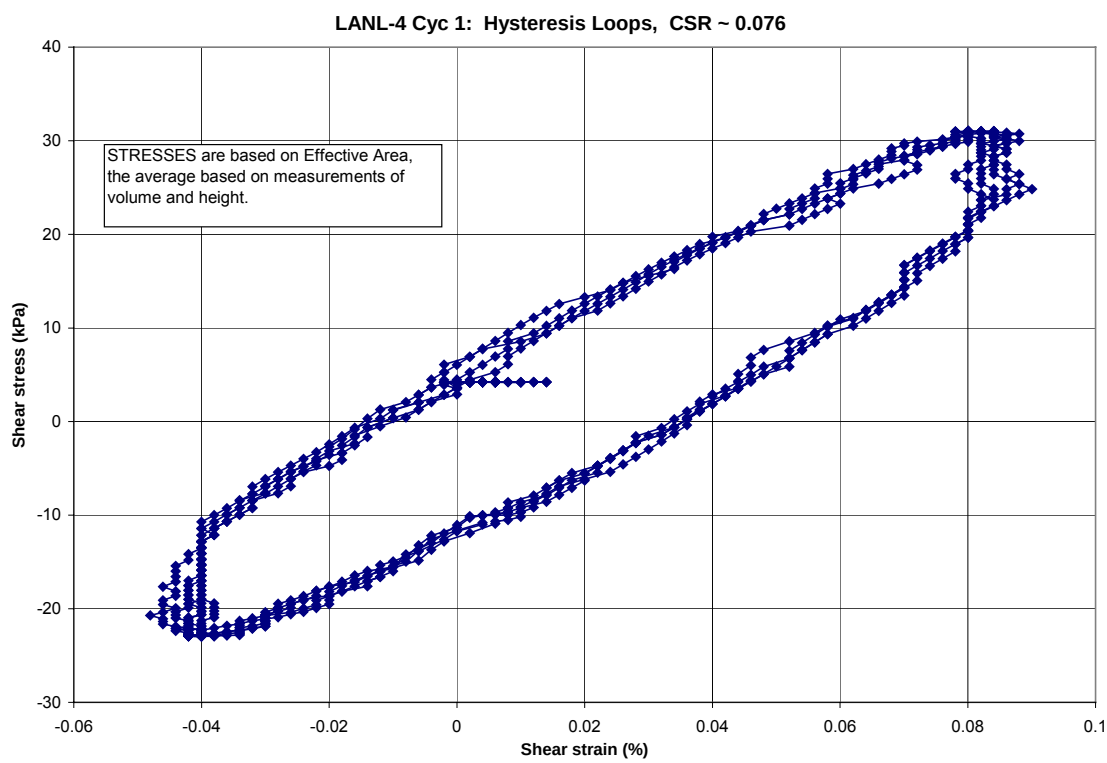
LANL-4 Cyc 1: Hysteresis Loops, CSR ~ 0.076
STRESSES are based on Effective Area, the average based on measurements of volume and height.
Shear stress (kPa)
Shear strain (%)
40
30
20
10
0
-10
-20
-30
-0.06
-0.04
-0.02
0
0.02
0.04
0.06
0.08
0.1

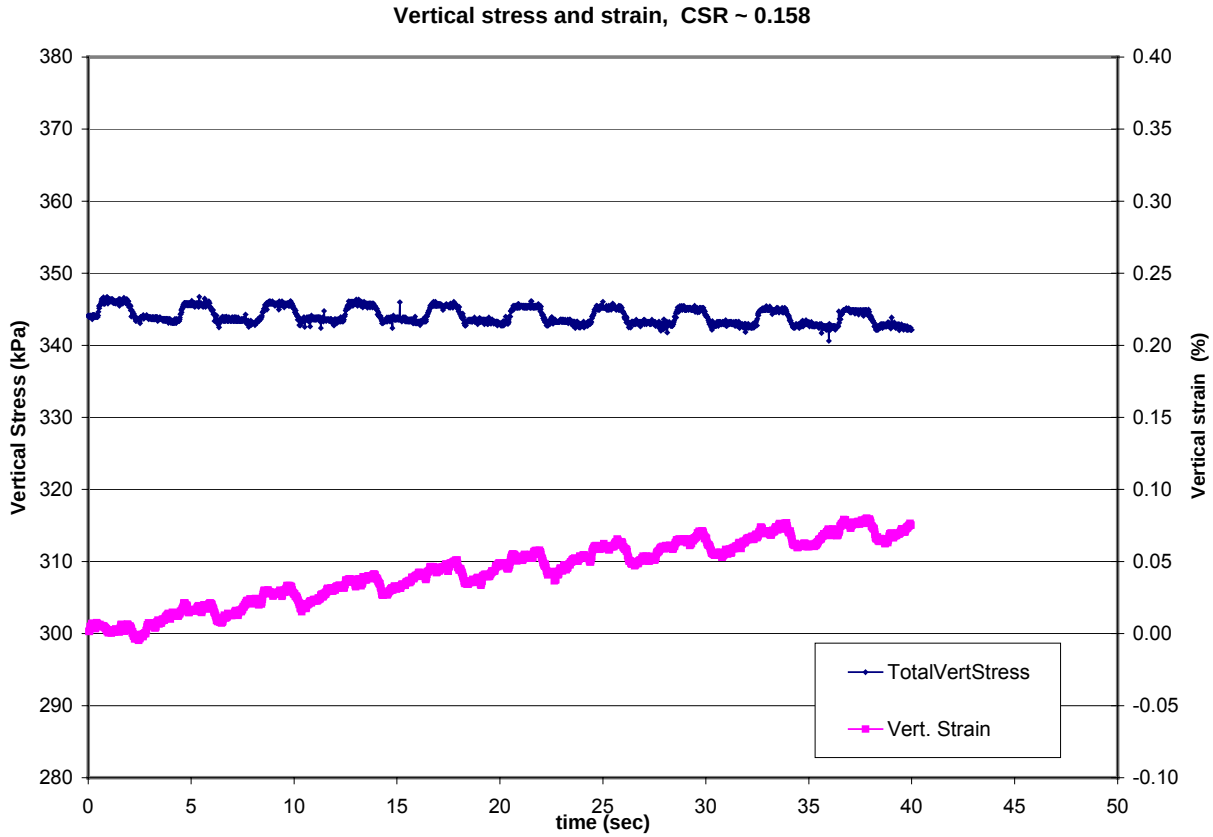
Vertical stress and strain, CSR ~ 0.158
Vertical Stress (kPa)
Vertical strain (%)
time (sec)
TotalVertStress
Vert. Strain
380
370
360
350
340
330
320
310
300
290
280
0.40
0.35
0.30
0.25
0.20
0.15
0.10
0.05
0.00
-0.05
-0.10
0
5
10
15
20
25
30
35
40
45
50

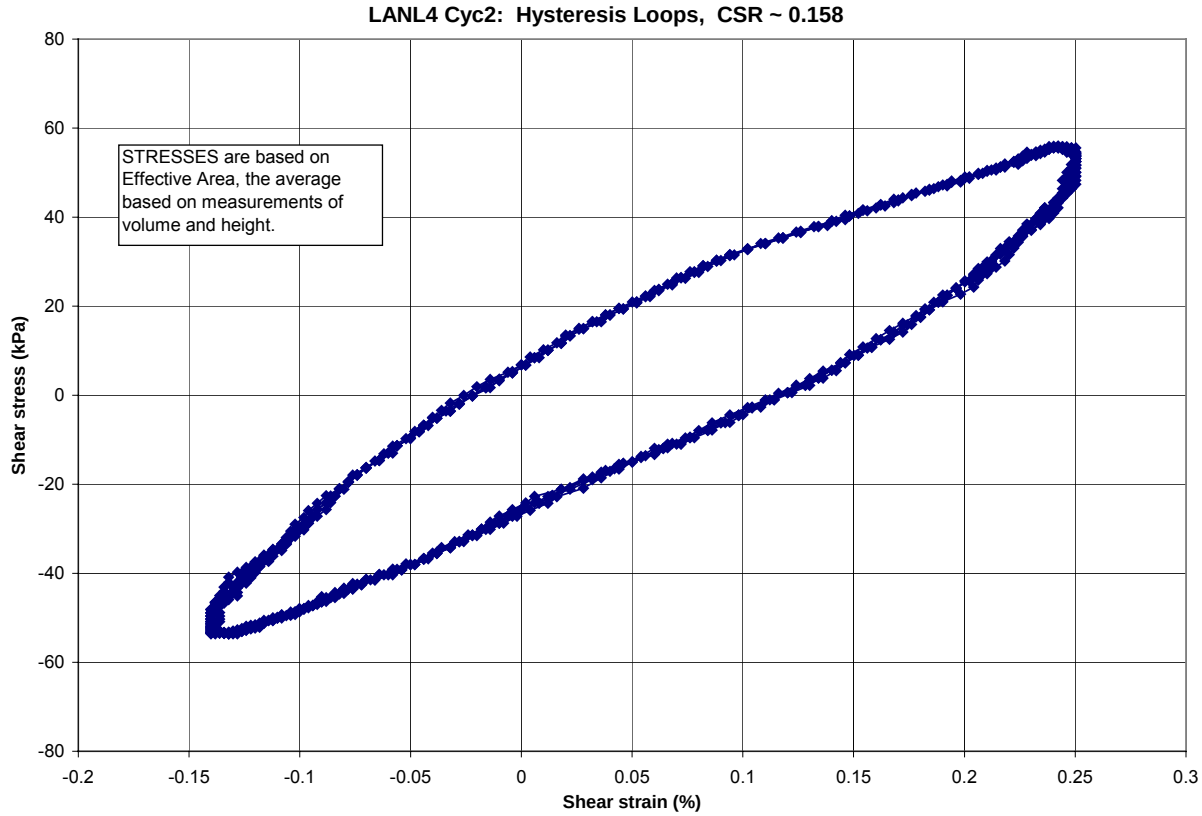
LANL4 Cyc2: Hysteresis Loops, CSR ~ 0.158
STRESSES are based on Effective Area, the average based on measurements of volume and height.
Shear stress (kPa)
Shear strain (%)
80
60
40
20
0
-20
-40
-60
-80
-0.2
-0.15
-0.1
-0.05
0
0.05
0.1
0.15
0.2
0.25
0.3

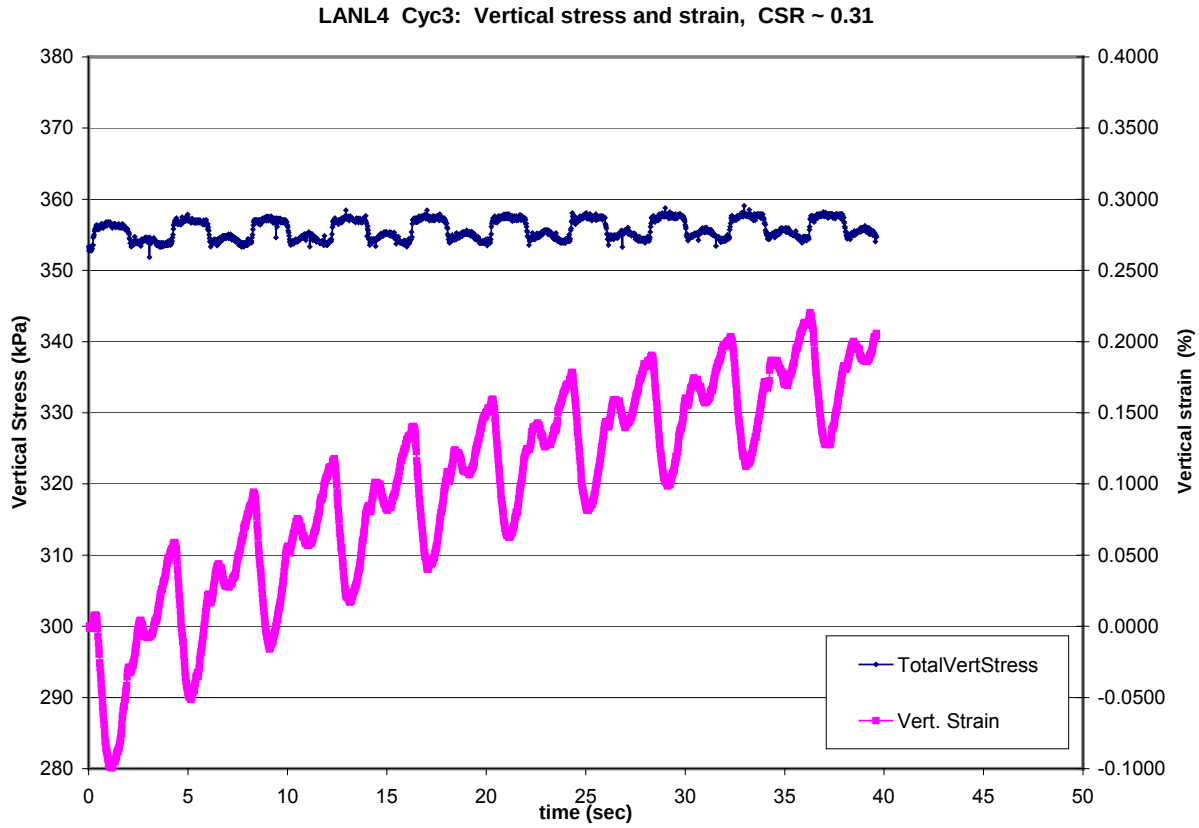
LANL4 Cyc3: Vertical stress and strain, CSR ~ 0.31
Vertical Stress (kPa)
Vertical strain (%)
time (sec)
TotalVertStress
Vert. Strain
380
370
360
350
340
330
320
310
300
290
280
0.4000
0.3500
0.3000
0.2500
0.2000
0.1500
0.1000
0.0500
0.0000
-0.0500
-0.1000
0
5
10
15
20
25
30
35
40
45
50

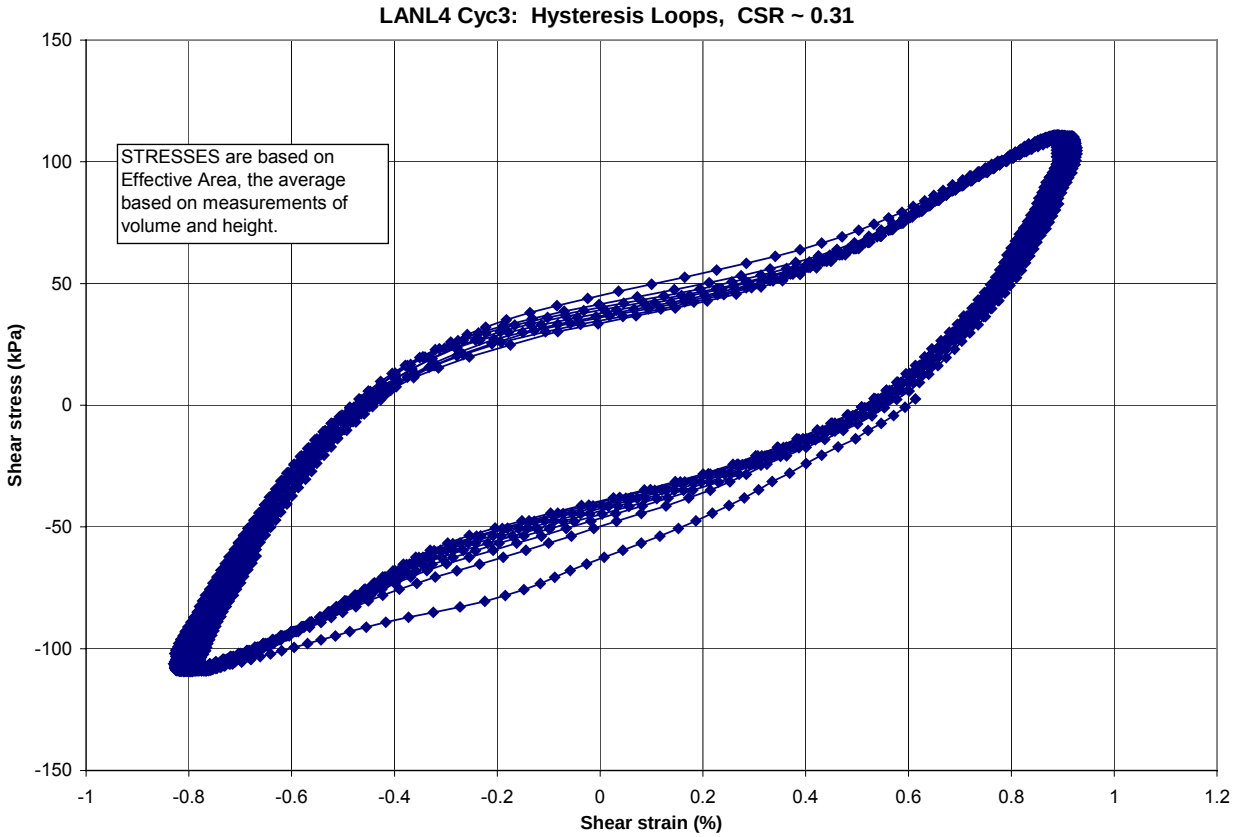
LANL4 Cyc3: Hysteresis Loops, CSR ~ 0.31
STRESSES are based on Effective Area, the average based on measurements of volume and height.
Shear stress (kPa)
Shear strain (%)
150
100
50
0
-50
-100
-150
-1
-0.8
-0.6
-0.4
-0.2
0
0.2
0.4
0.6
0.8
1
1.2

LANL #5

Stage of testing					***Incremental Vert. Strain (%)***
Consol. #1	Raise chamber pressure from isotropic stress of ~15 kPa to ~100 kPa				0.38
Consol. #2	Raise deviator stress to ~100 kPa				0.7
Consol. #3	Raise chamber pressure to 225 kPa				0.3
Consol. #4	Raise deviator stress to ~225 kPa				0.5
	CSR	***# of cycles***	***s.a. shear strain (%)***	***Approx. G (kPa)***	
Cyclic loading 1	0.079	5	0.085	43,500	0.08
Cyclic loading 2	0.152	10	0.25	28,000	0.23
Cyclic loading 3	0.305	10	0.825	17,000 (odd loops)	0.43
Unloading	Reduce stresses thru same path, return to ~15 kPa vacuum confinement				-0.55

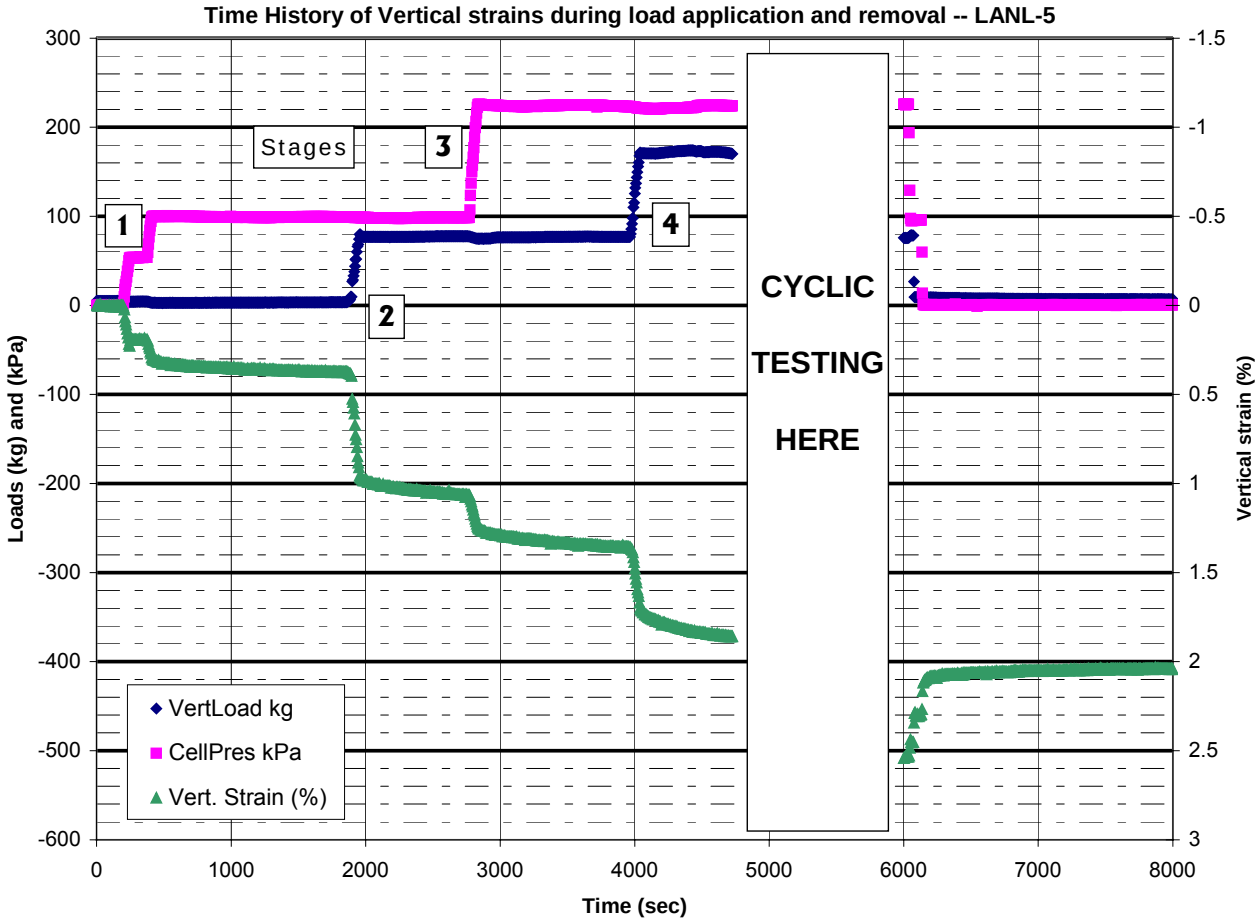

Copyright 2007, Kleinfelder

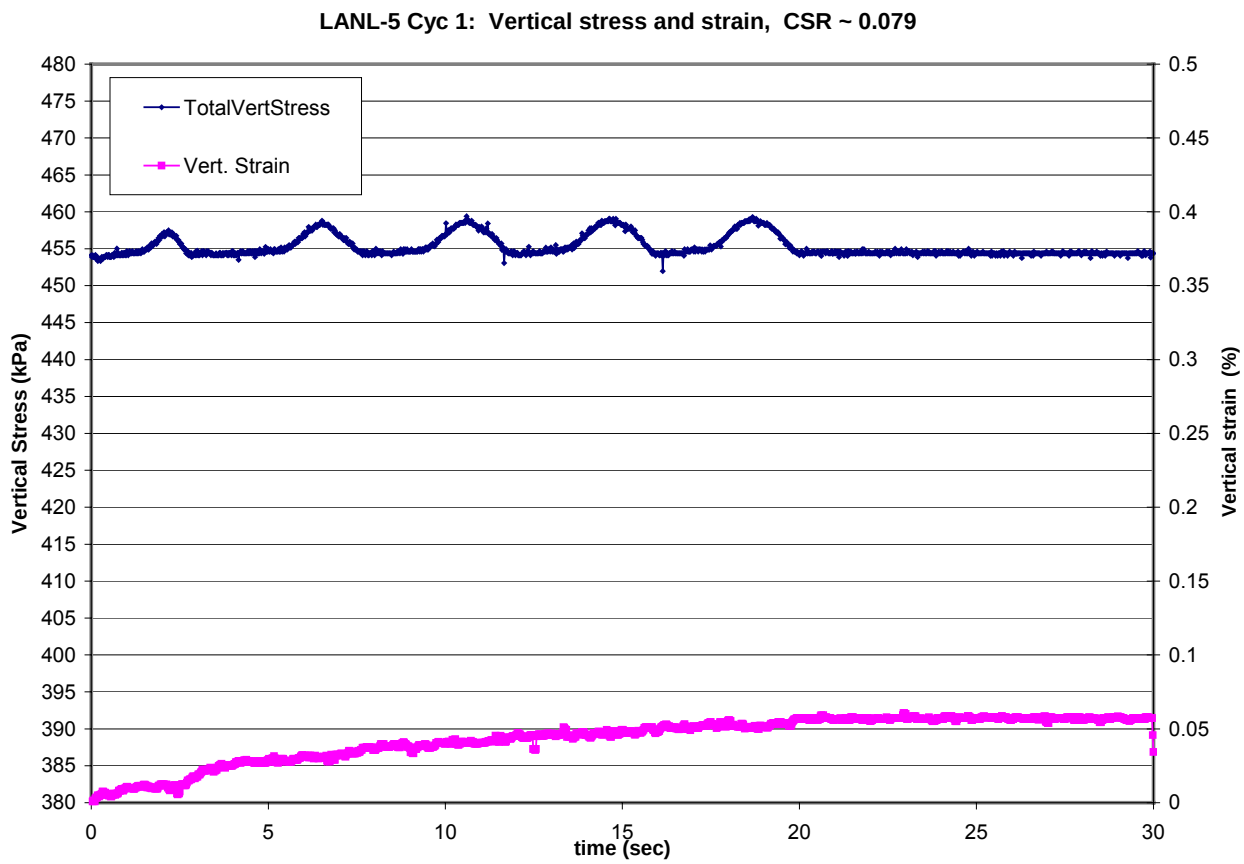
LANL-5 Cyc 1: Vertical stress and strain, CSR ~ 0.079
TotalVertStress
Vert. Strain
Vertical Stress (kPa)
Vertical strain (%)
time (sec)
480
475
470
465
460
455
450
445
440
435
430
425
420
415
410
405
400
395
390
385
380
0.5
0.45
0.4
0.35
0.3
0.25
0.2
0.15
0.1
0.05
0
0
5
10
15
20
25
30

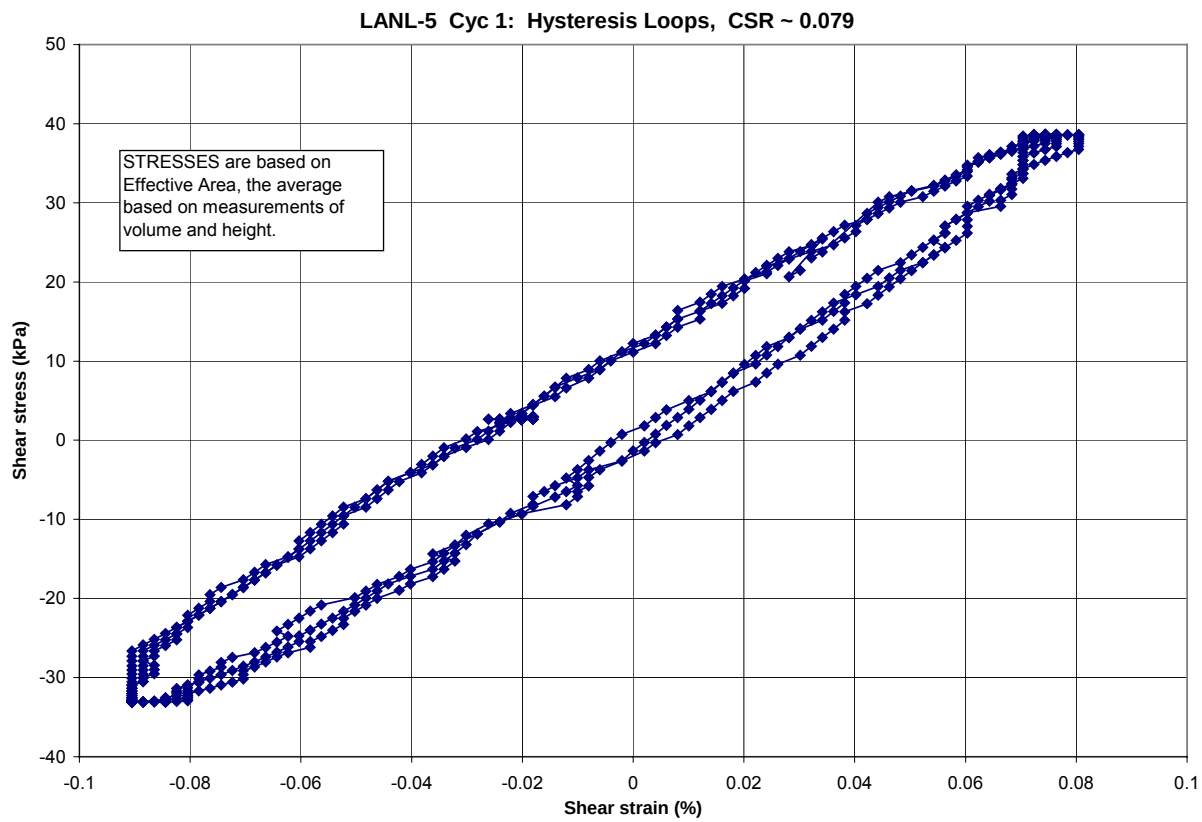
LANL-5 Cyc 1: Hysteresis Loops, CSR ~ 0.079
STRESSES are based on Effective Area, the average based on measurements of volume and height.
Shear stress (kPa)
Shear strain (%)
50
40
30
20
10
0
-10
-20
-30
-40
-0.1
-0.08
-0.06
-0.04
-0.02
0
0.02
0.04
0.06
0.08
0.1

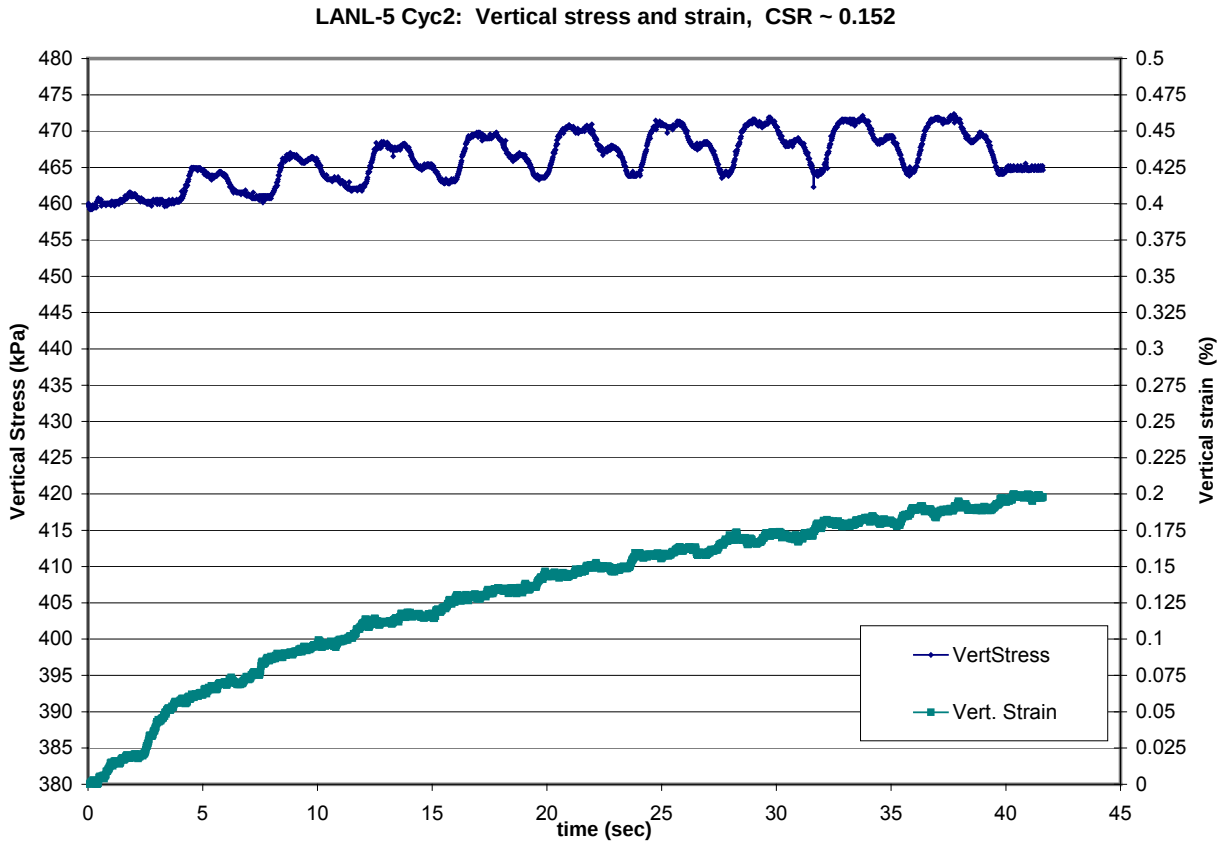
LANL-5 Cyc2: Vertical stress and strain, CSR ~ 0.152
Vertical Stress (kPa)
Vertical strain (%)
time (sec)
VertStress
Vert. Strain

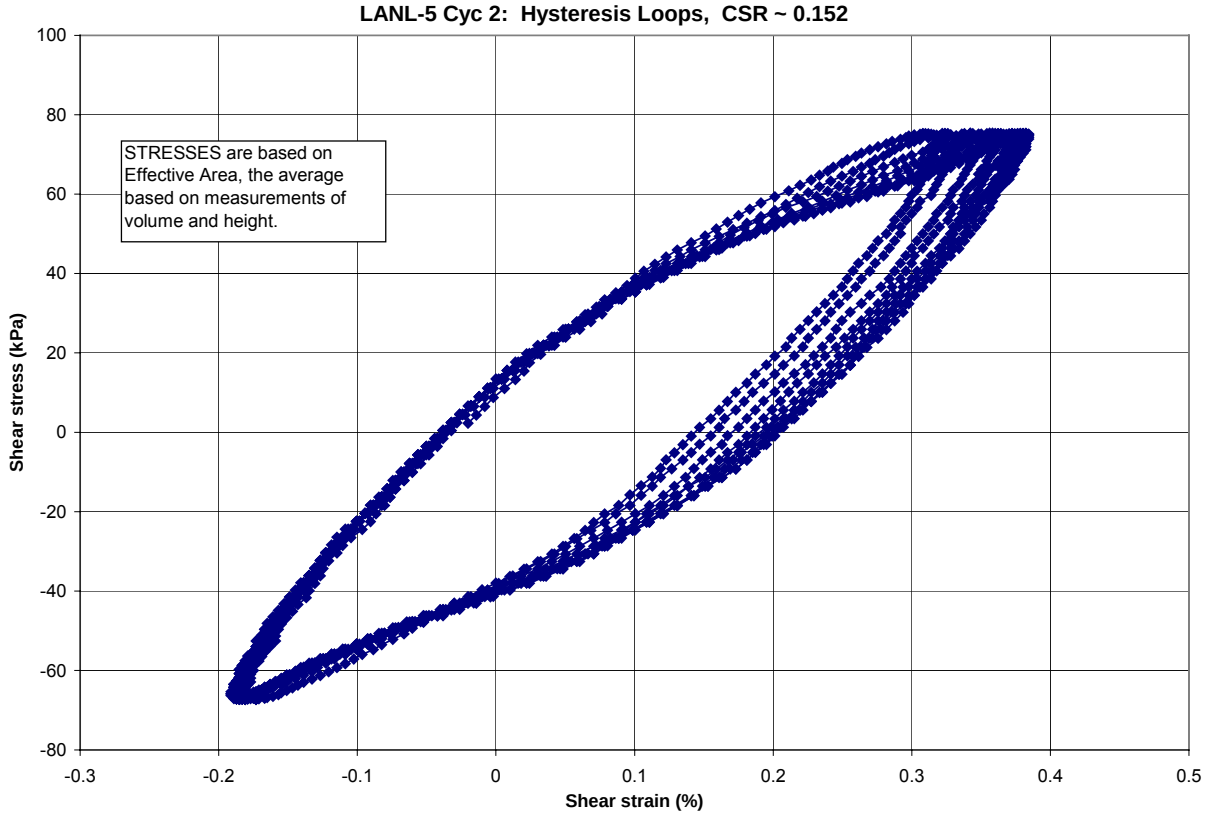
LANL-5 Cyc 2: Hysteresis Loops, CSR ~ 0.152
STRESSES are based on Effective Area, the average based on measurements of volume and height.
Shear stress (kPa)
Shear strain (%)

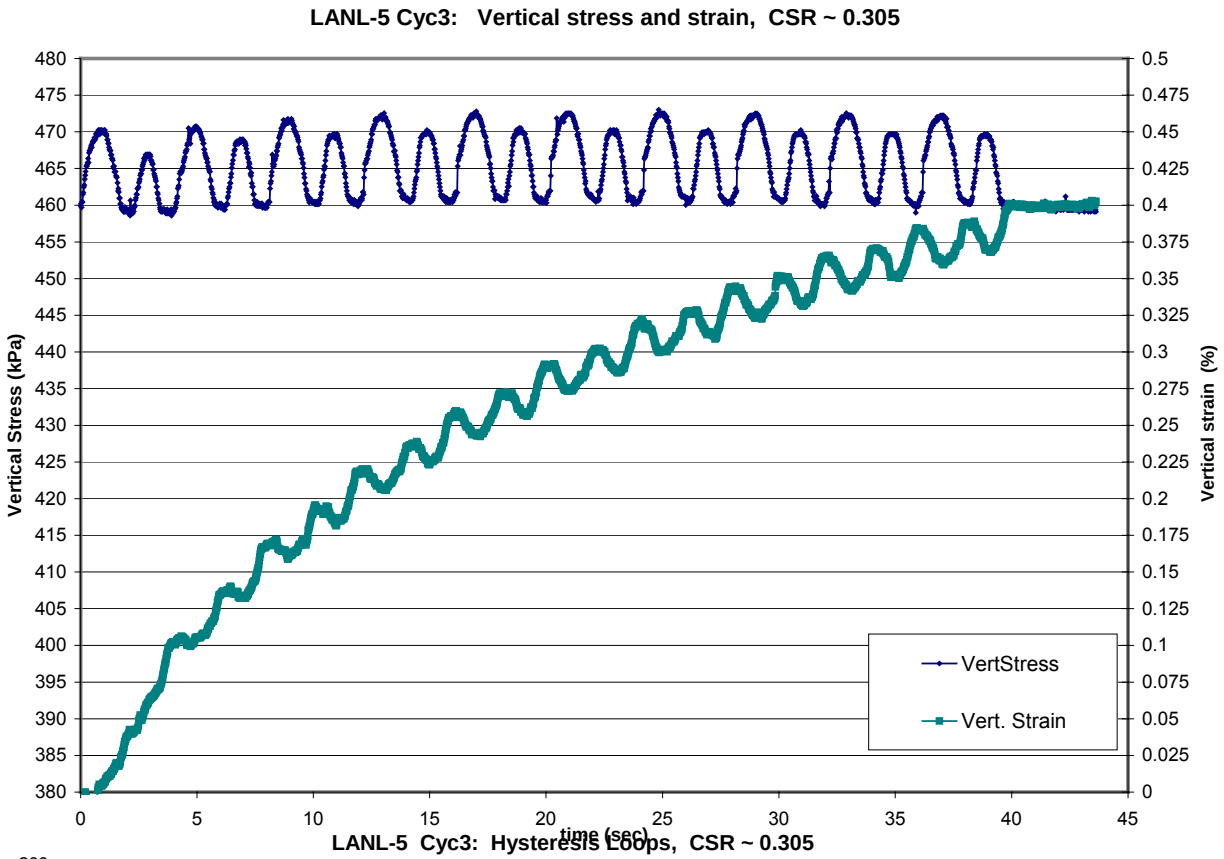
LANL-5 Cyc3: Vertical stress and strain, CSR ~ 0.305
Vertical Stress (kPa)
Vertical strain (%)
time (sec)
VertStress
Vert. Strain

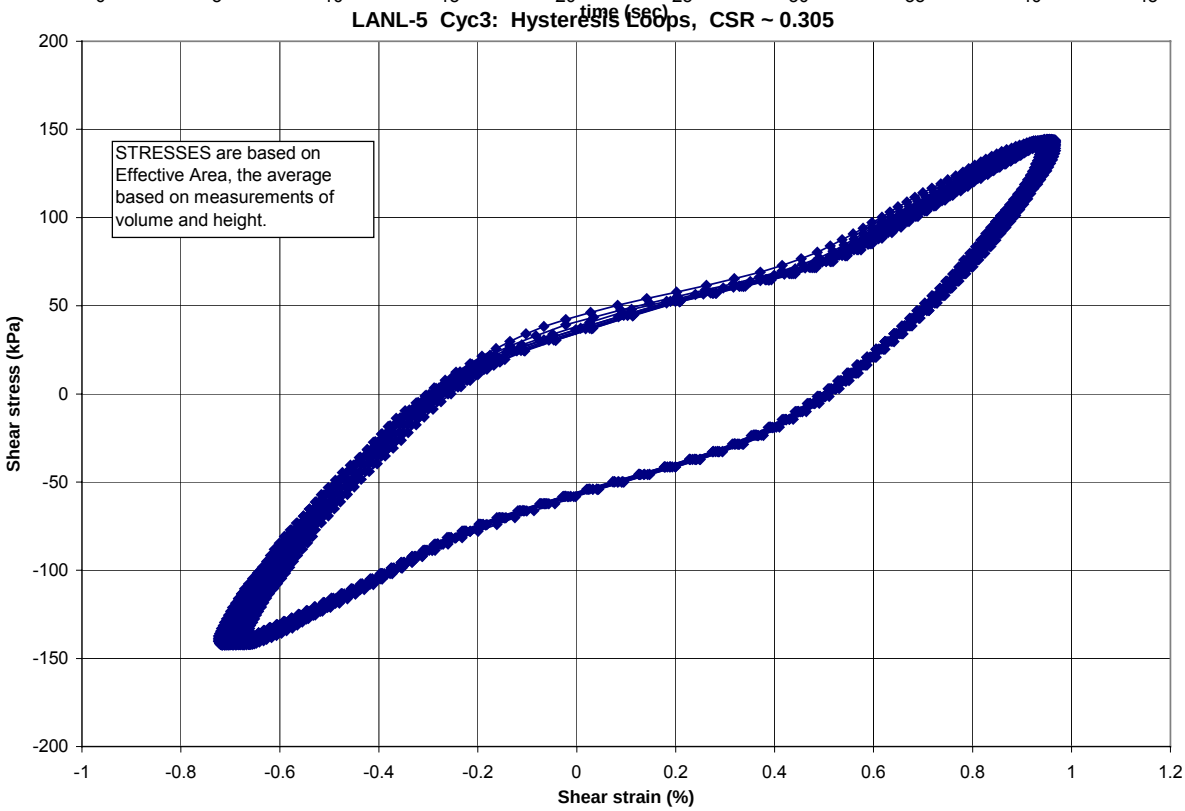
LANL-5 Cyc3: Hysteresis Loops, CSR ~ 0.305
STRESSES are based on Effective Area, the average based on measurements of volume and height.
Shear stress (kPa)
Shear strain (%)

LANL # 6

Stage of testing					Incremental Vert. Strain (%)
Consol. #1	Raise isotropic effective stress from ~15 kPa to ~50 kPa				0.2
Consol. #2	Raise isotropic effective stress to ~100 kPa				0.28
Consol. #3	Raise isotropic effective stress to ~200 kPa				0.33
Consol. #4	Raise isotropic effective stress to ~300 kPa				0.19
Consol. #5	Raise isotropic effective stress to ~325 kPa				0.06
	CSR	***# of cycles***	***s.a. shear strain (%)***	***Approx. G (kPa)***	
Cyclic loading 1	0.08	5	0.137	20,700	0.035
Cyclic loading 2	0.17	10	0.46	12,700	0.085
Cyclic loading 3	0.35	10	1.21	9,600	0.225
Unloading	Reduce stresses thru same path, return to ~15 kPa vacuum confinement				-0.27

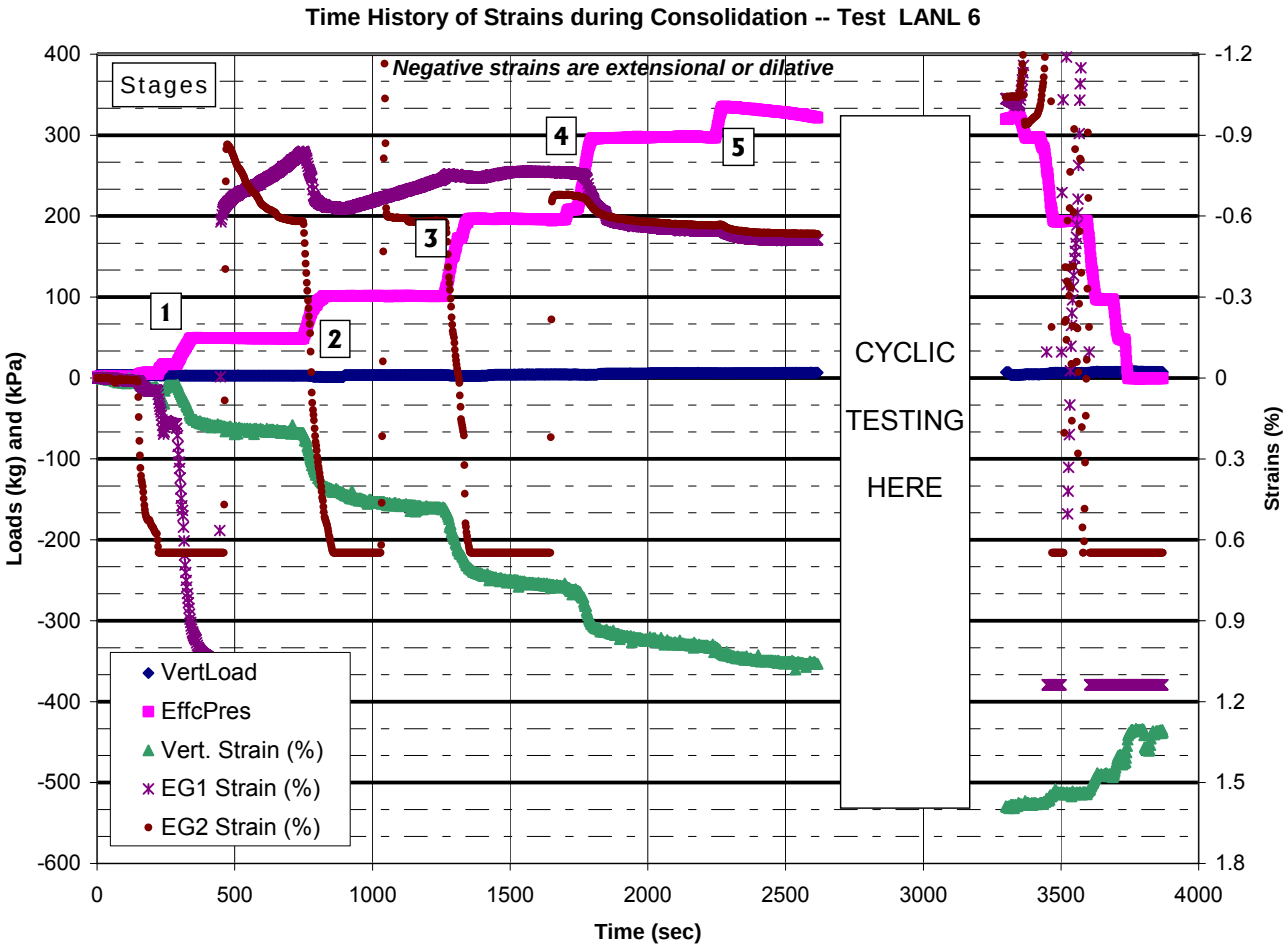

LANL6 Cyc 1: Vertical , radial and volumetric strains, CSR ~ 0.08

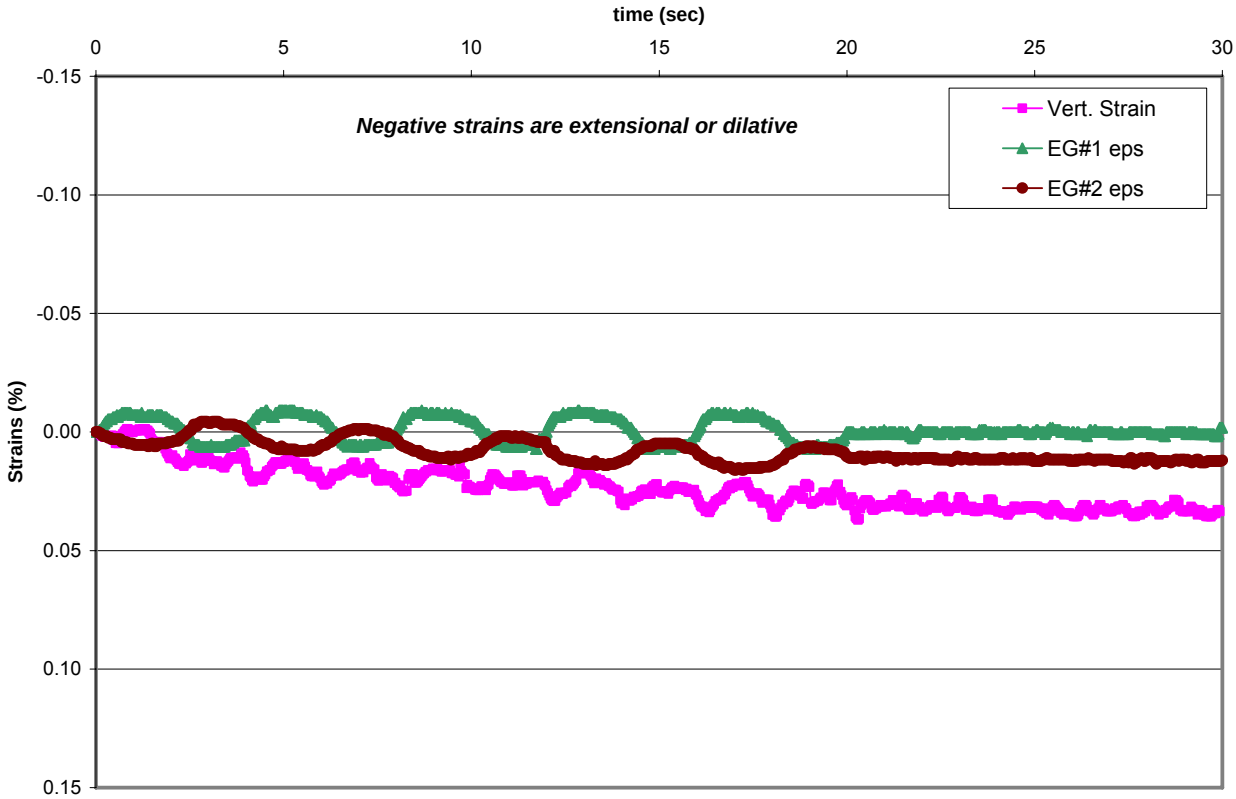

LANL6 Cyc 1: Hysteresis Loops, CSR ~ 0.08

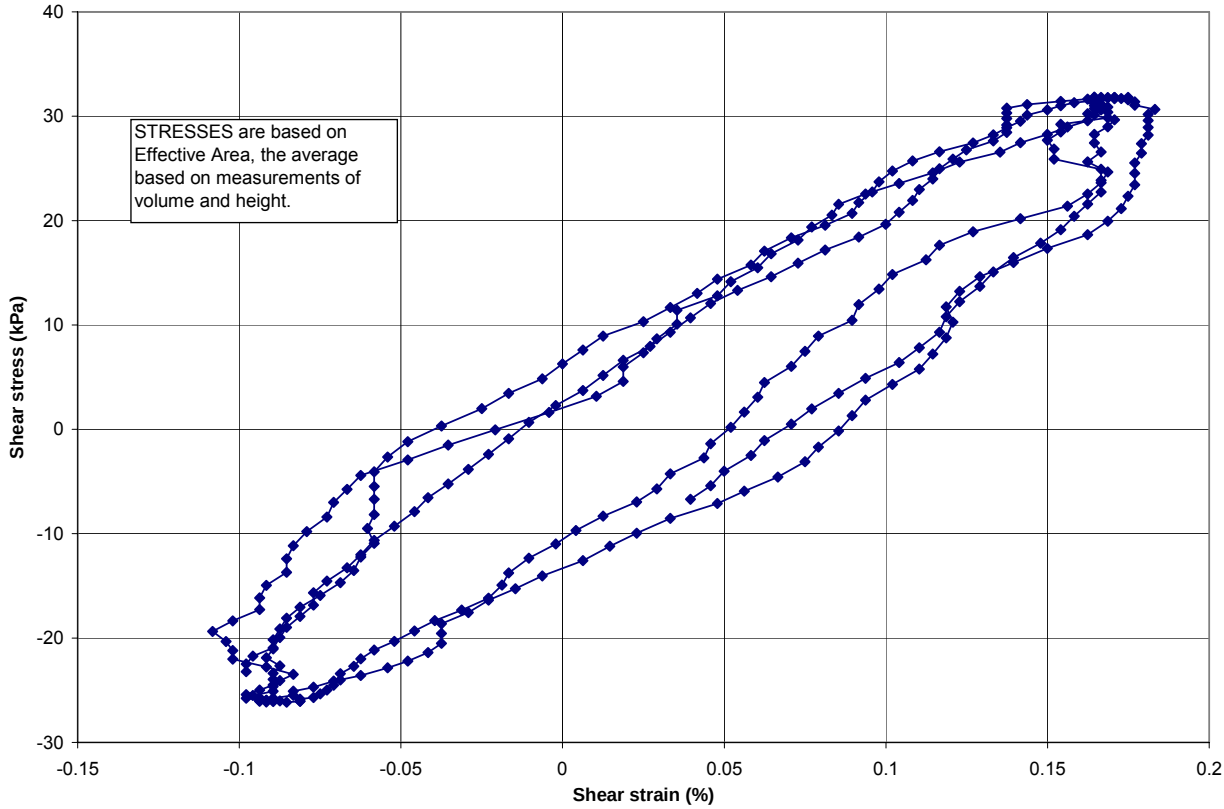

Copyright 2007, Kleinfelder

LANL6 Cyc 2: Vertical , radial and volumetric strains, CSR ~ 0.17

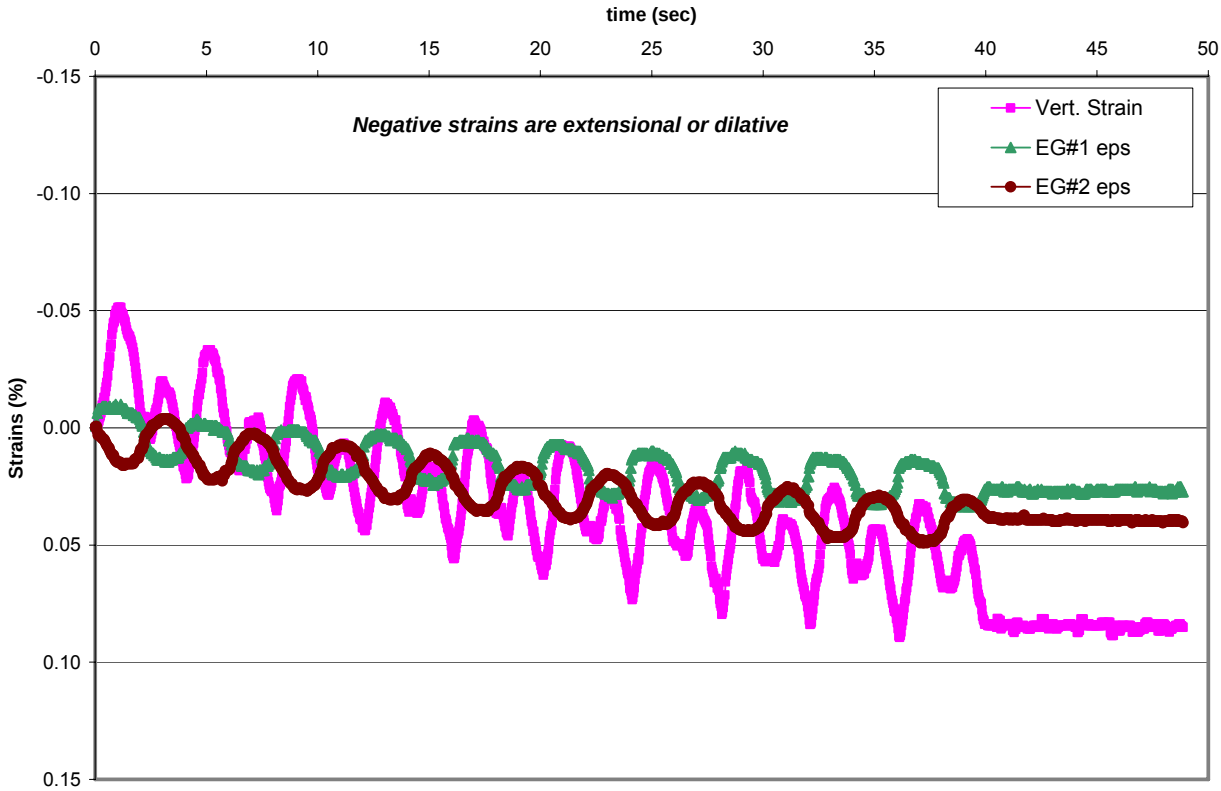

LANL6 Cyc 2: Hysteresis Loops, CSR ~ 0.17

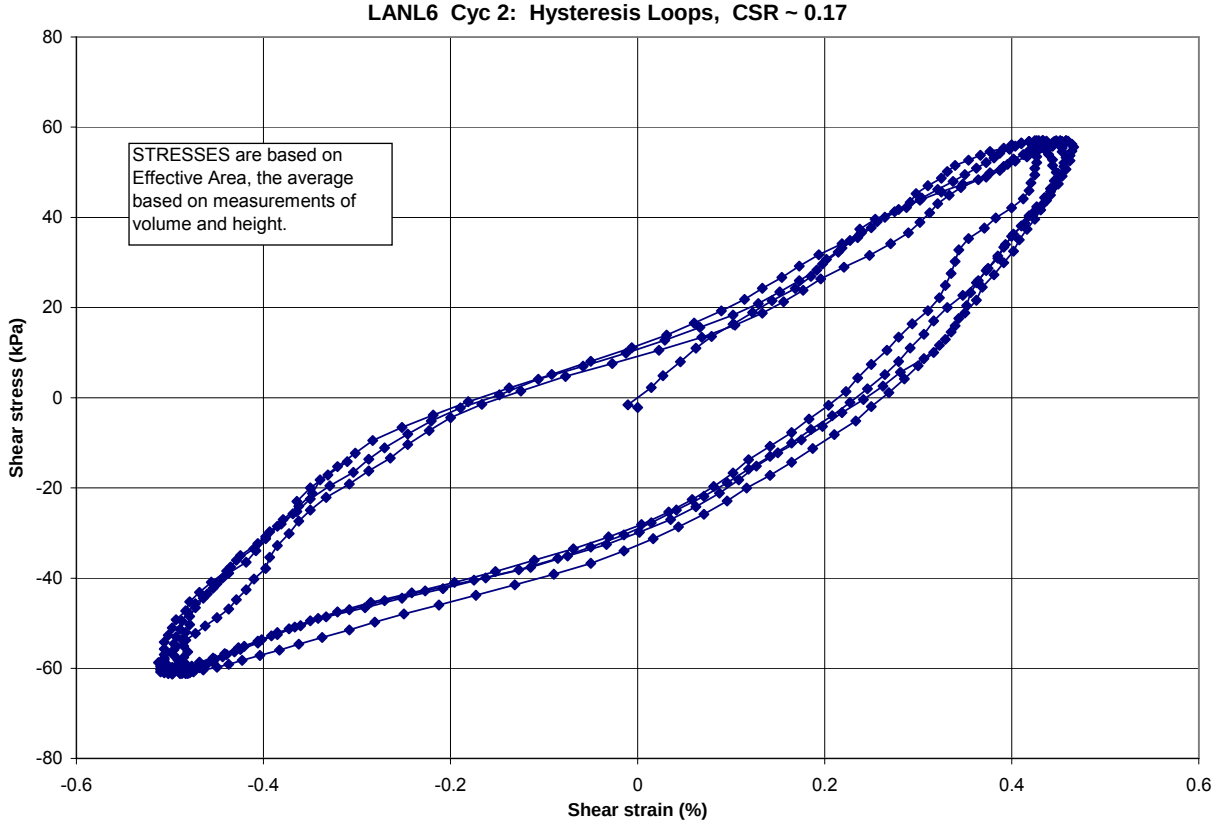

LANL6 Cyc 3: Vertical , radial and volumetric strains, CSR ~ 0.35

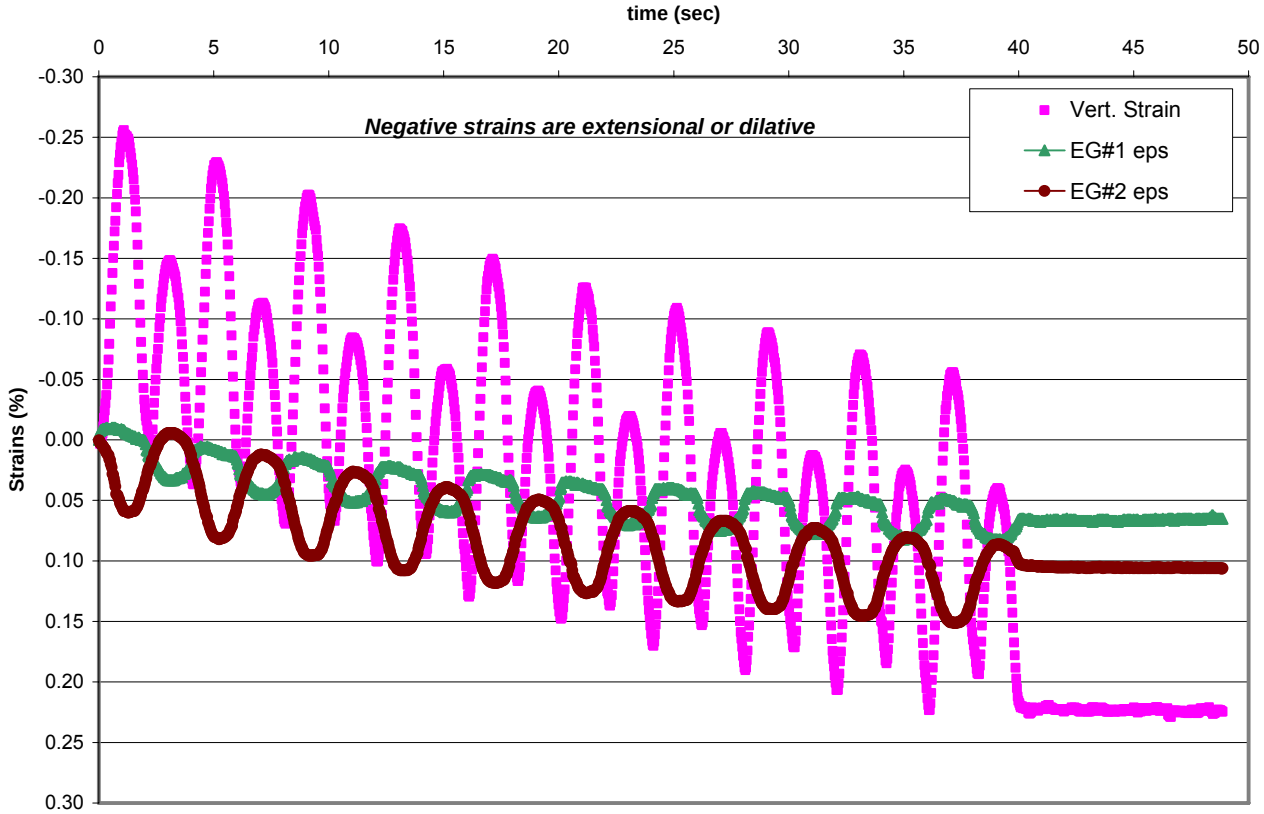

LANL6 Cyc 3: Hysteresis Loops, CSR ~ 0.35

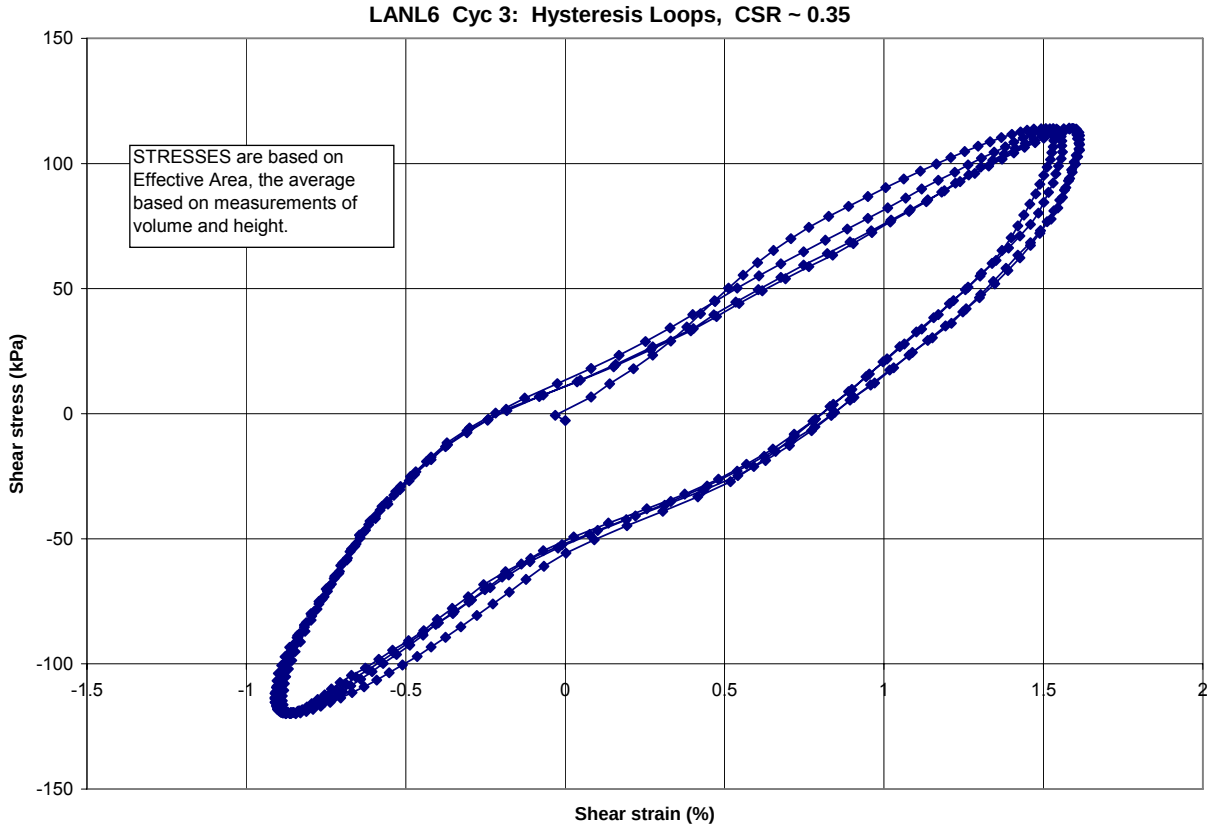

LANL # 7

Stage of testing					*Incremental Vert. Strain (%)*	*Average Radial Strain (%)*
Consol. #1	Raise vertical effective stress to 100 kPa				0.3	-0.035
Consol. #2	Raise lateral effective stress to 100 kPa, vertical to 150kPa				0.2	+0.08
Consol. #3	Raise vertical effective stress to 200 kPa				0.32	-0.04
Consol. #4	Raise lateral effective stress to 200 kPa, vertical to 300 kPa				0.33	+0.15
Consol. #5	Raise vertical effective stress to 400 kPa				0.65	-0.07
Consol. #6	Raise lateral effective to 225 kPa, vertical effective to 450 kPa				0.28	~0.0
	CSR	*# of cycles*	*s.a. shear strain (%)*	*Approx. G (kPa)*		
Cyclic loading 1	0.075	5	0.126	26,200	0.095	-0.01
Cyclic loading 2	0.15	10	0.317	21,450	0.3	-0.025
Cyclic loading 3	0.3	10	1.1	12,400	0.73	-0.06
Unloading	Reduce stresses, return to ~15 kPa vacuum confinement				-0.6	

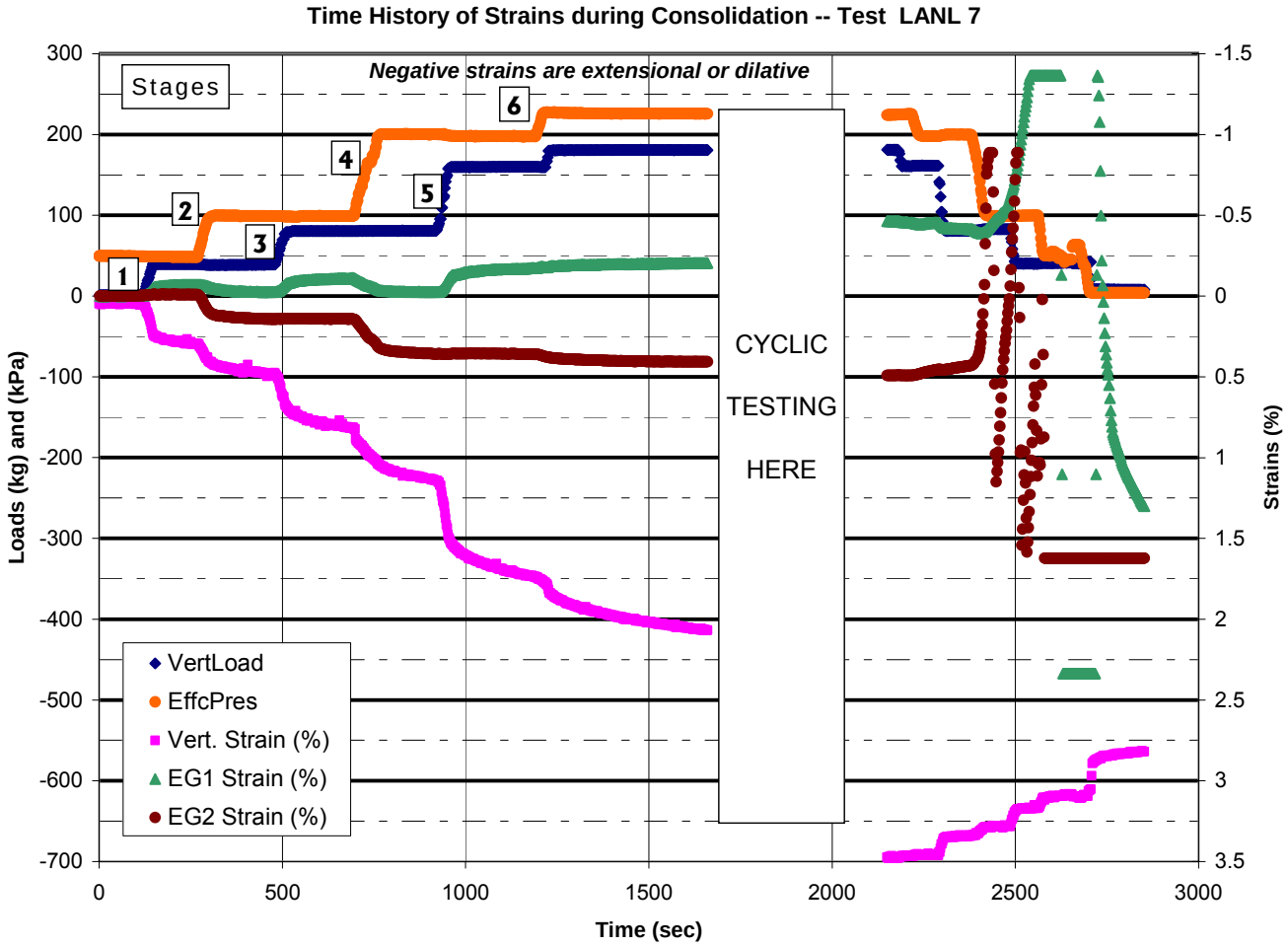

LANL7 Cyc 1: Vertical and radial strains, CSR ~ 0.075

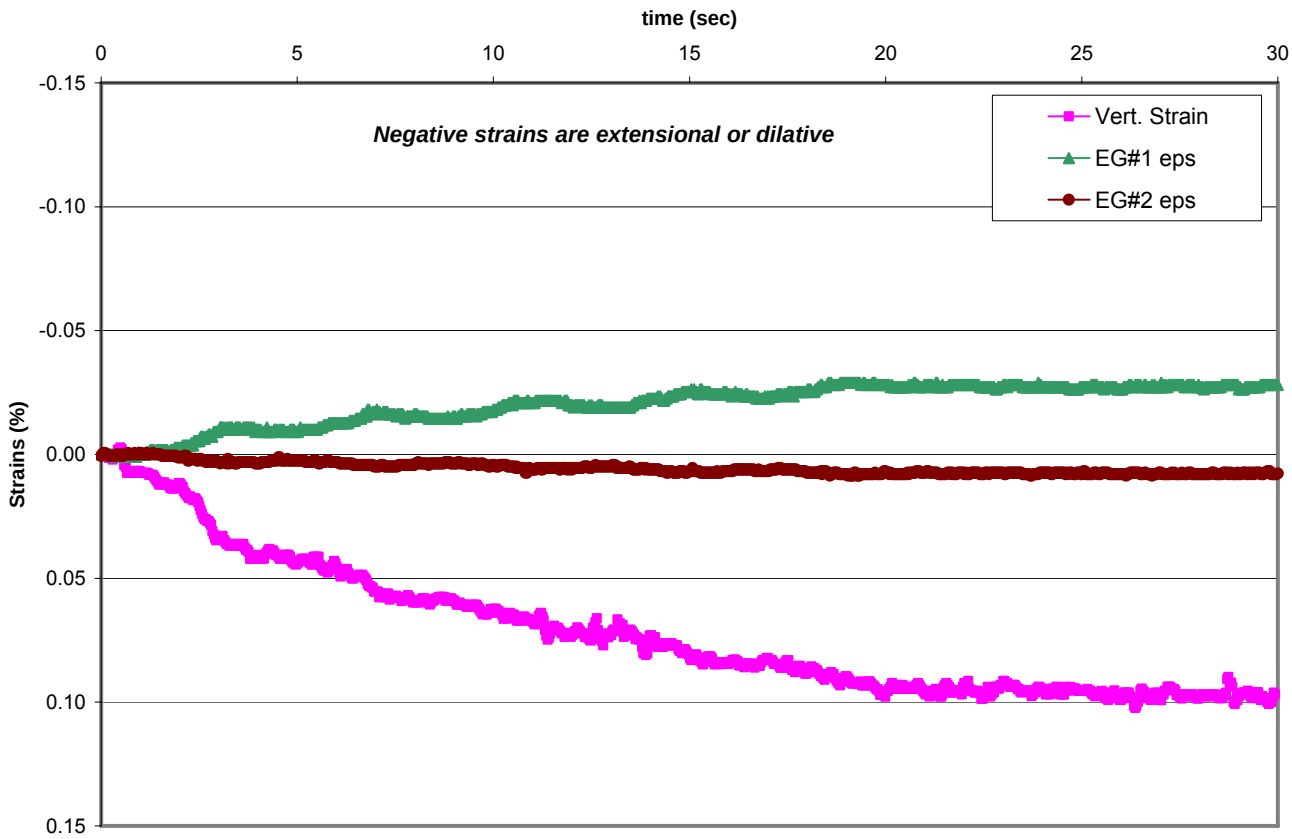

LANL7 Cyc 1: Hysteresis Loops, CSR ~ 0.075

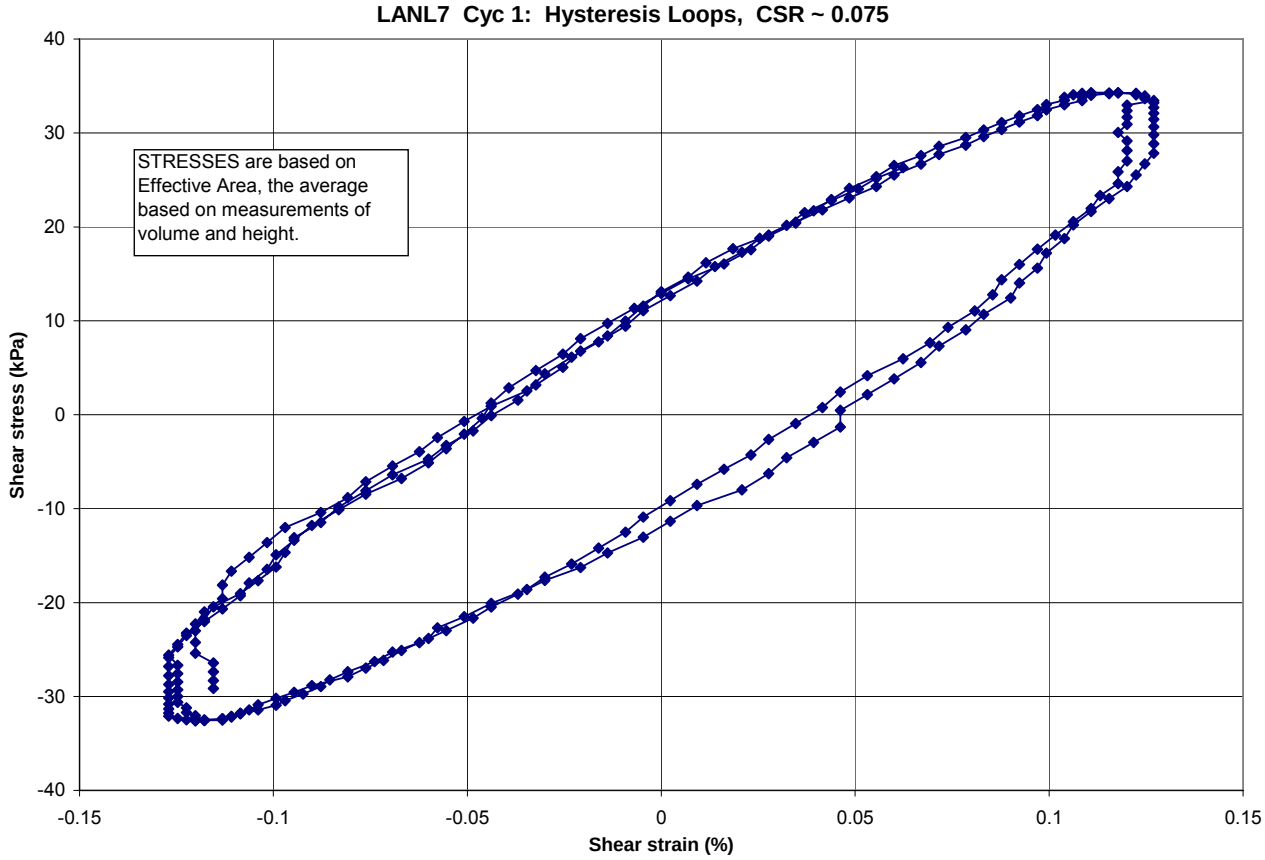

Copyright 2007, Kleinfelder

LANL7 Cyc 2: Vertical and radial strains, CSR ~ 0.15

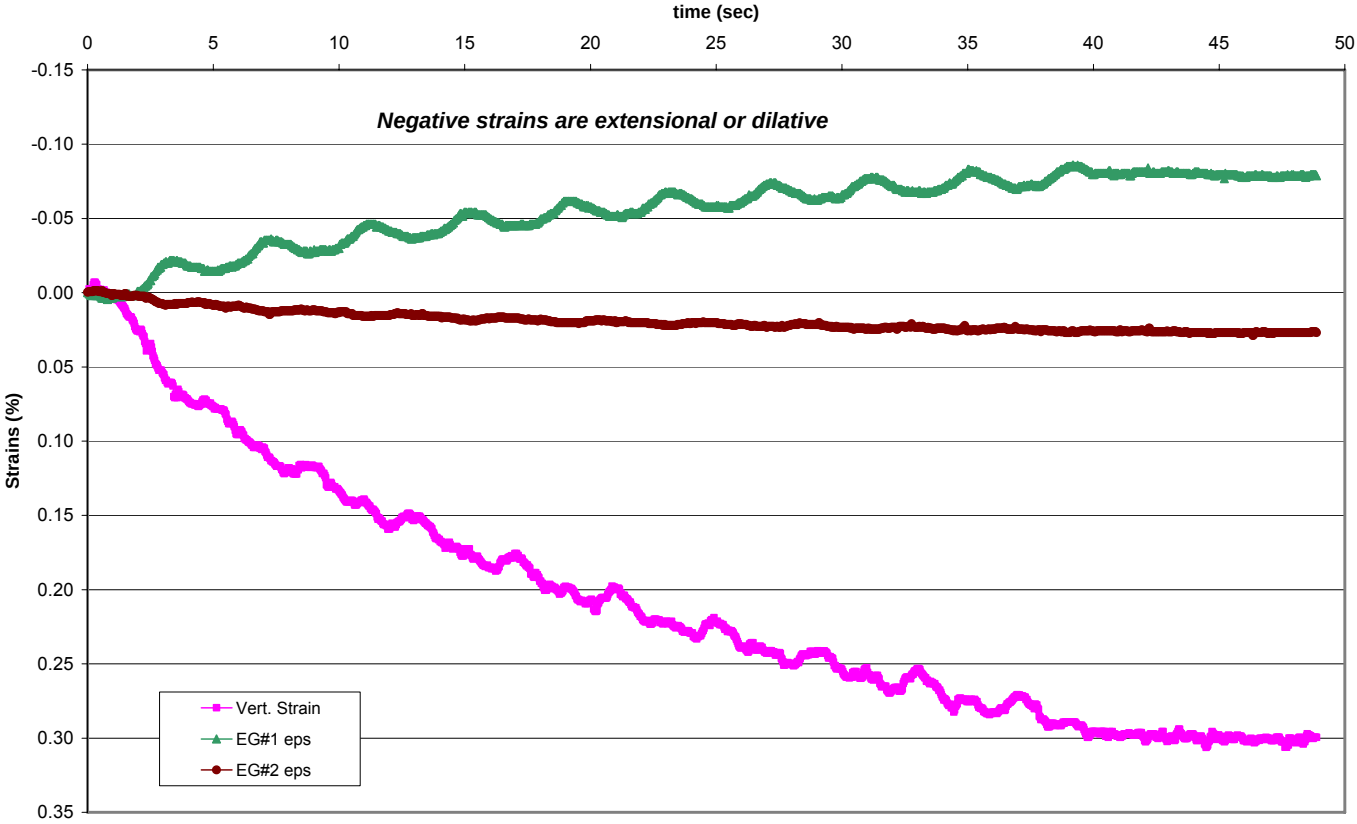

LANL7 Cyc 2: Hysteresis Loops, CSR ~ 0.15

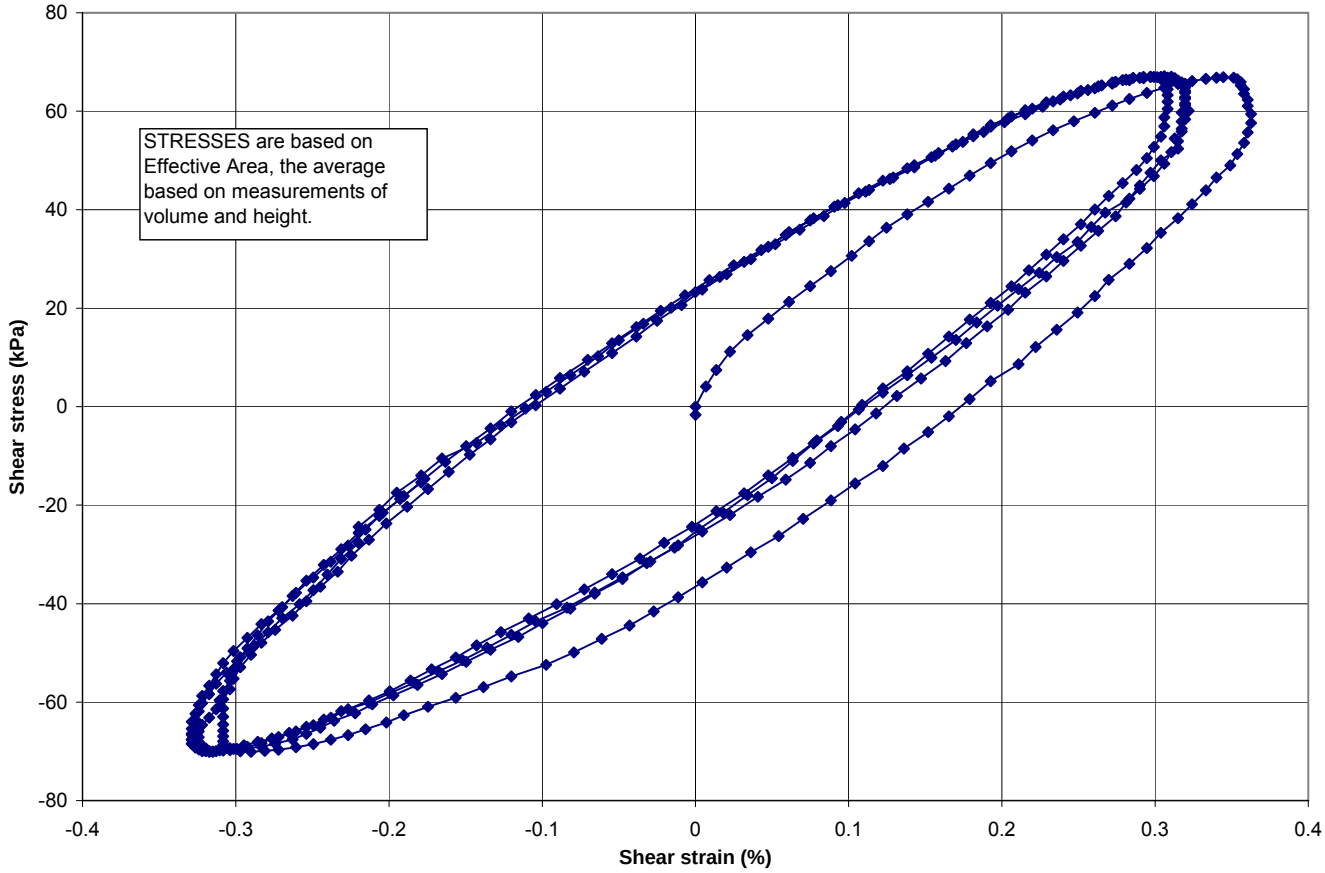

LANL7 Cyc 3: Vertical and radial strains, CSR ~ 0.30

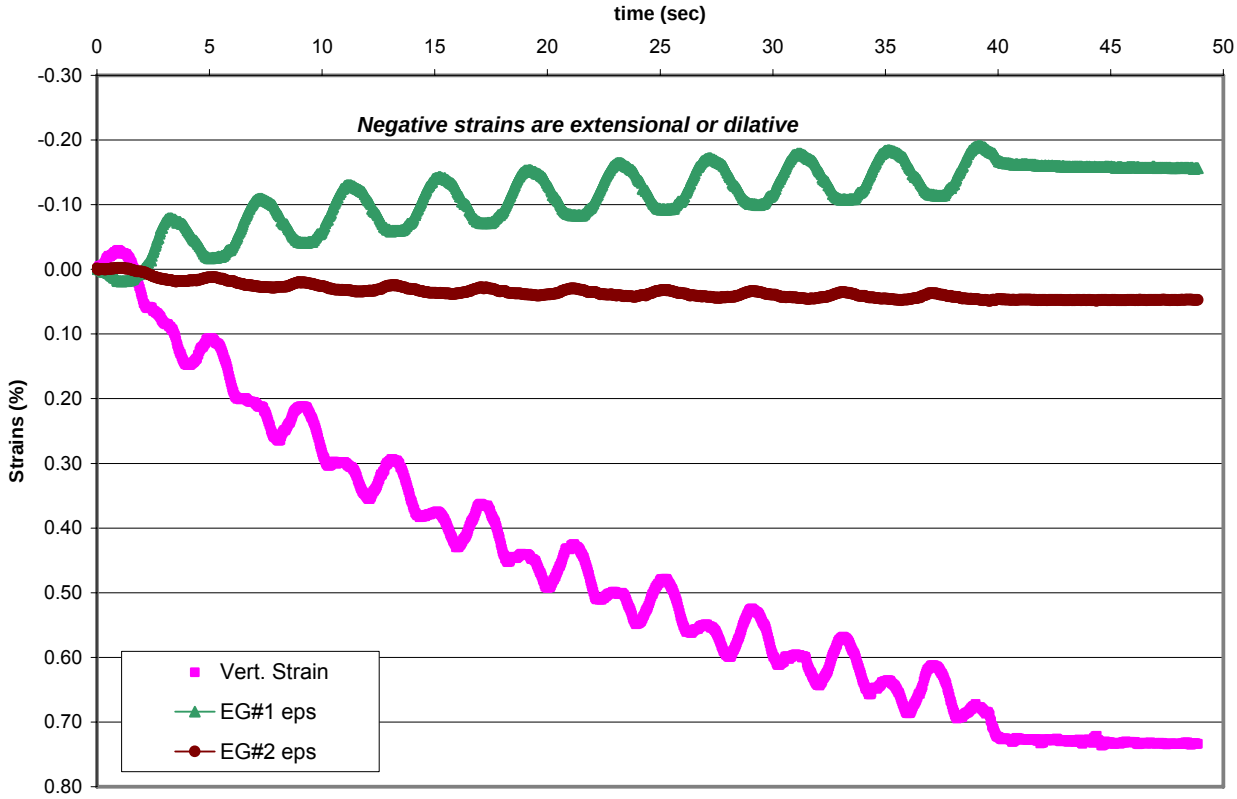

LANL7 Cyc 3: Hysteresis Loops, CSR ~ 0.30

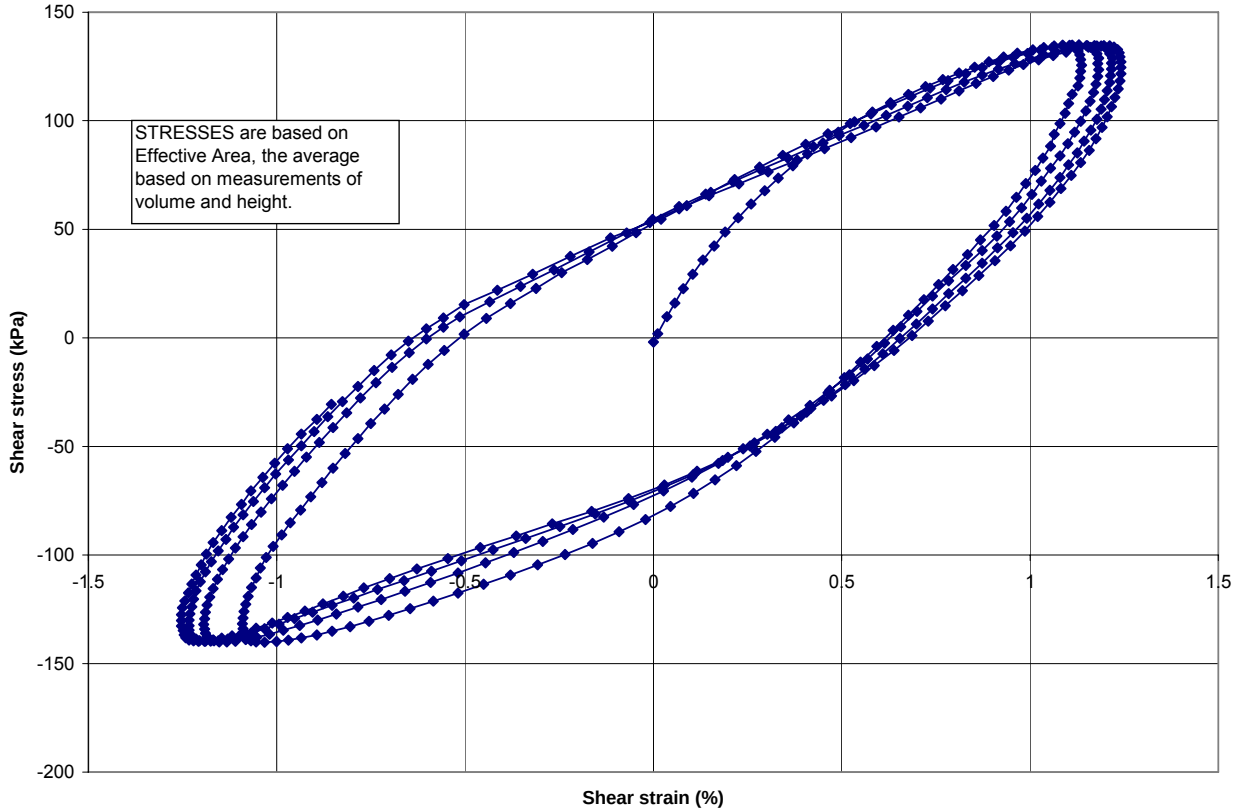

LANL # 8

Stage of testing					Incremental Vert. Strain (%)	Average Radial Strain (%)
Consol. #1	Raise lateral stress from 50 to 100, vertical from 77 to 154 kPa (K=0.65)				0.19	+0.075
#1A	Raise vertical stress to 182 kPa, establish K= 0.55				0.12	-0.010
Consol. #2	Raise lateral stress from 100 to 150, vertical from 182 to 272 kPa (K=0.55)				0.31	+0.040
#2A	Raise vertical stress to 300 kPa, establish K= 0.50				0.16	-0.008
Consol. #3	Raise lateral stress from 150 to 200, vertical from 300 to 400 kPa (K=0.50)				0.37	+0.029
#3A	Raise vertical stress to 444 kPa, establish K= 0.45				0.08	-0.008
Consol. #4	Raise lateral stress from 200 to 210, vertical from 444 to 467 kPa (K=0.45)				0.25	+0.003
	CSR	***# of cycles***	***s.a. shear strain***	***Approx. G***		
			(%)	***(kPa)***		
Cyclic loading 1	0.073	5	0.107	31,200	0.07	-0.01
Cyclic loading 2	0.15	10	0.26	26,100	0.26	-0.03
Cyclic loading 3	0.29	10	0.75	17,900	0.67	-0.07
Unloading	Reduce stresses thru same path, return to ~50 kPa vacuum confinement				-0.43	

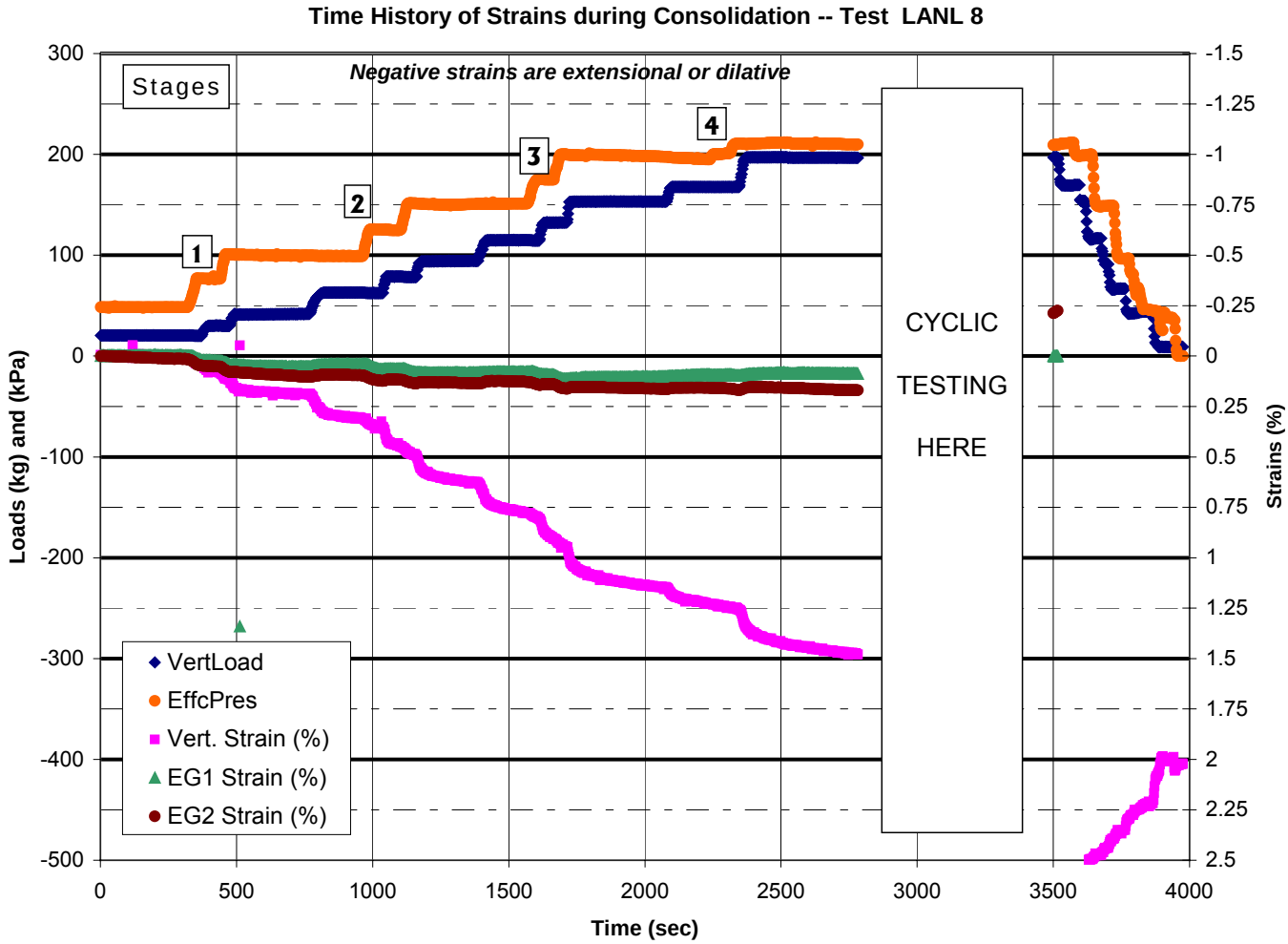

LANL8 Cyc 1: Vertical and radial strains, CSR ~ 0.073

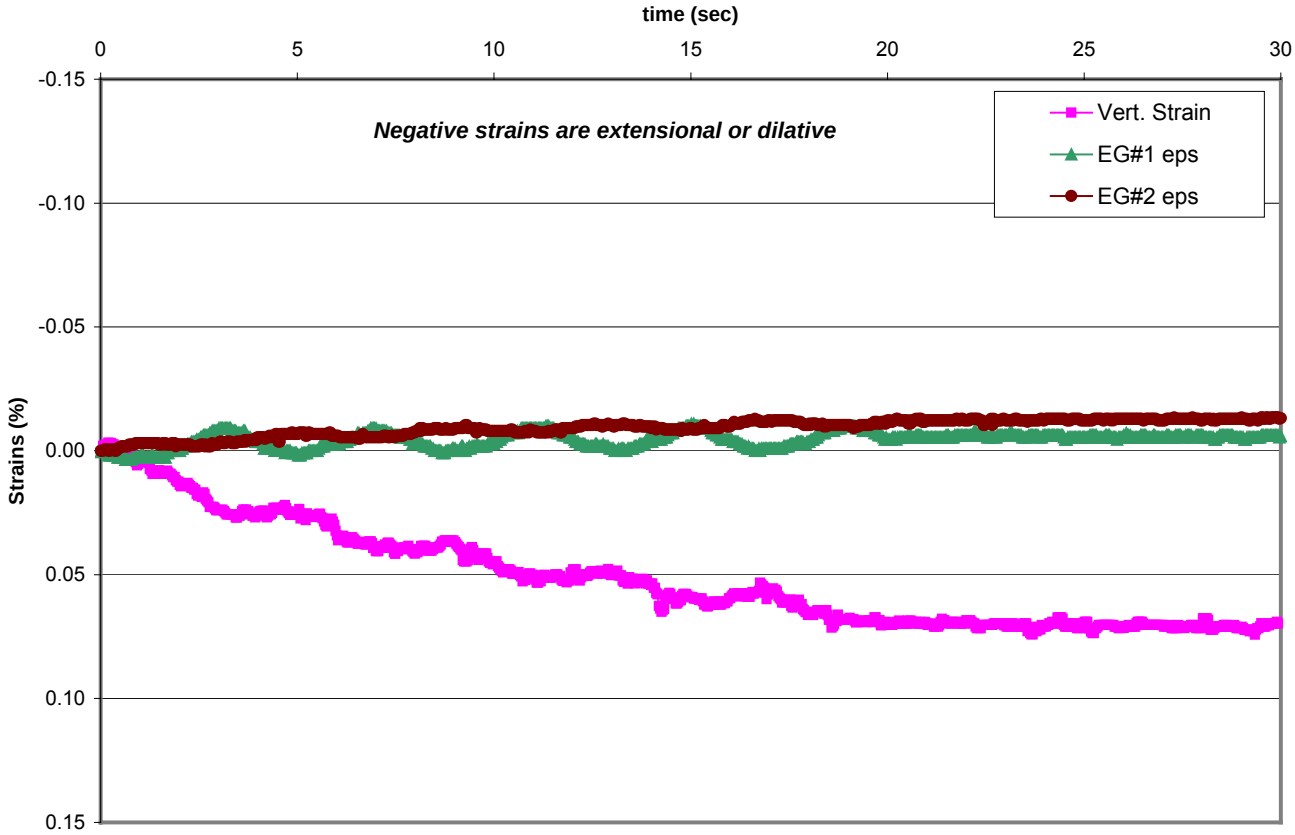

LANL8 Cyc 1: Hysteresis Loops, CSR ~ 0.073

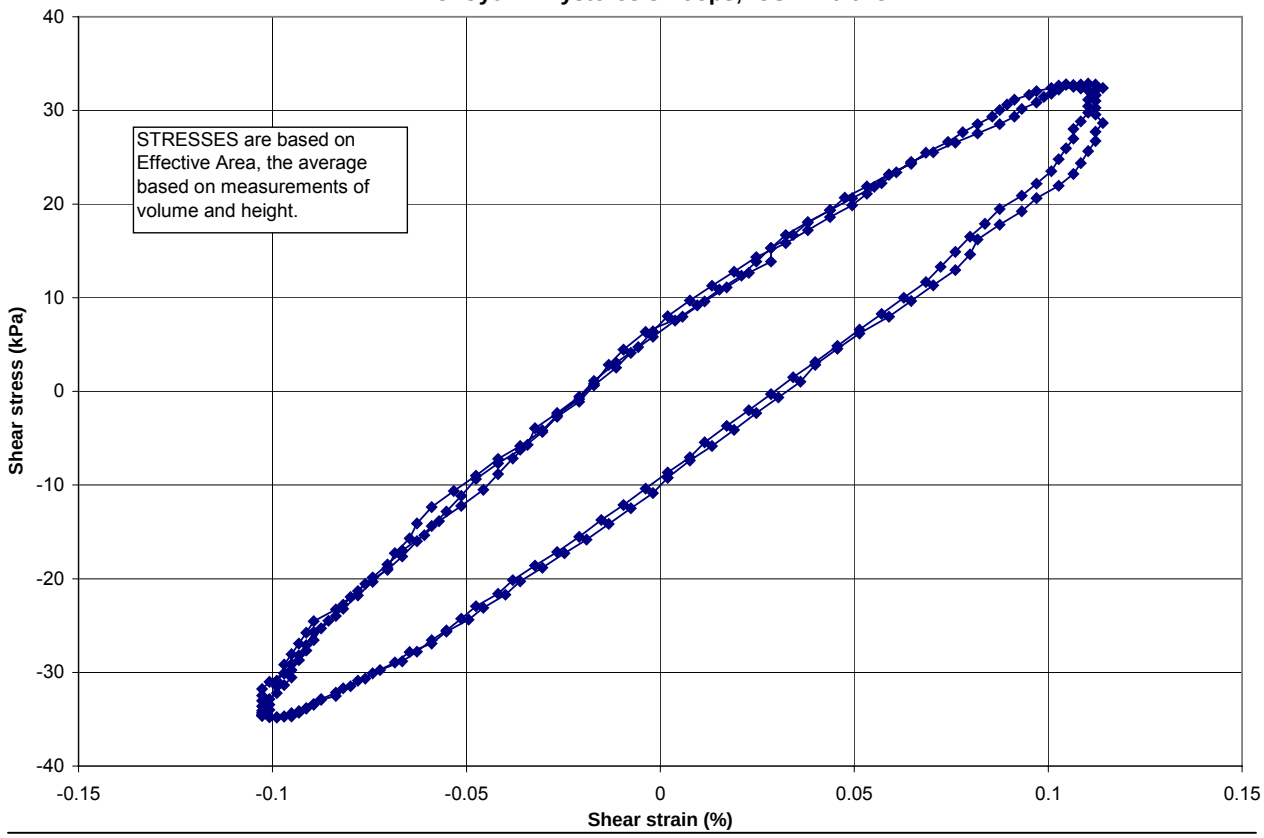

LANL8 Cyc 2: Vertical and radial strains, CSR ~ 0.15

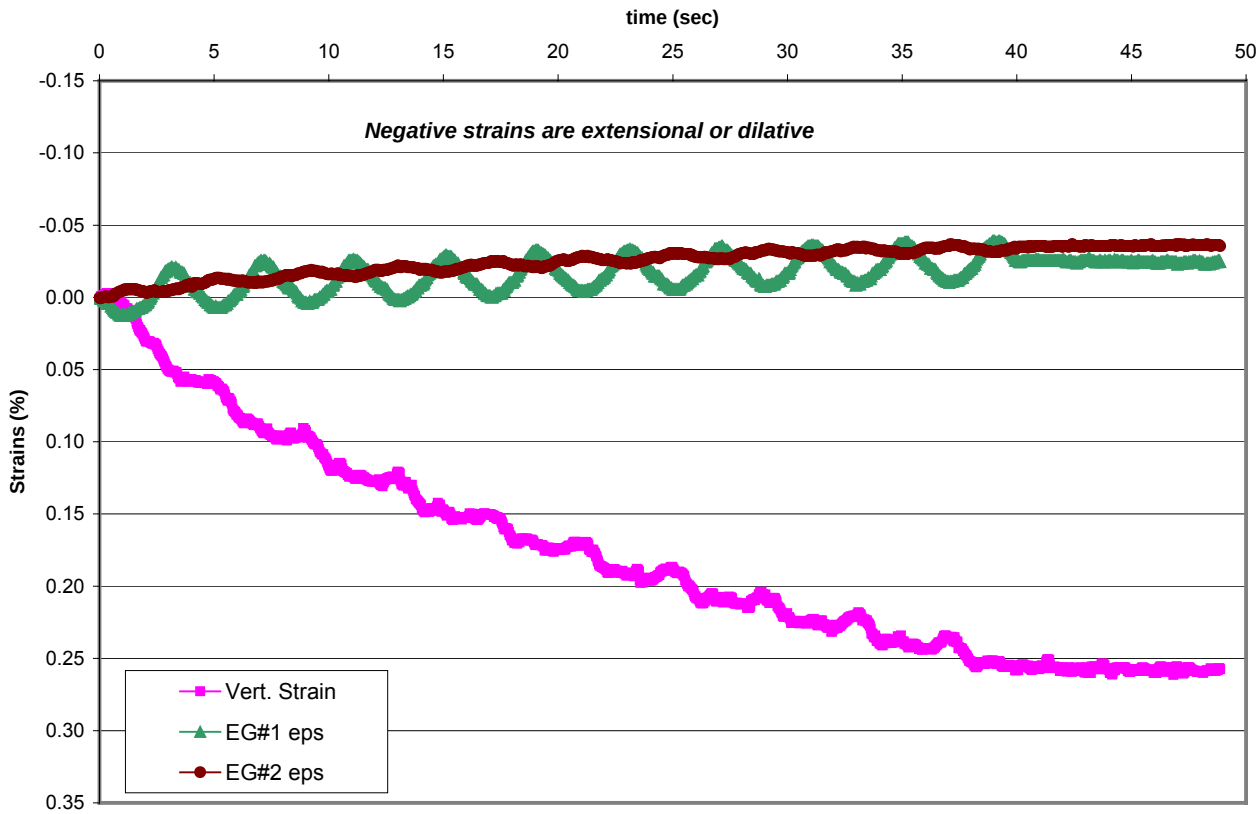

LANL8 Cyc 2: Hysteresis Loops, CSR ~ 0.15

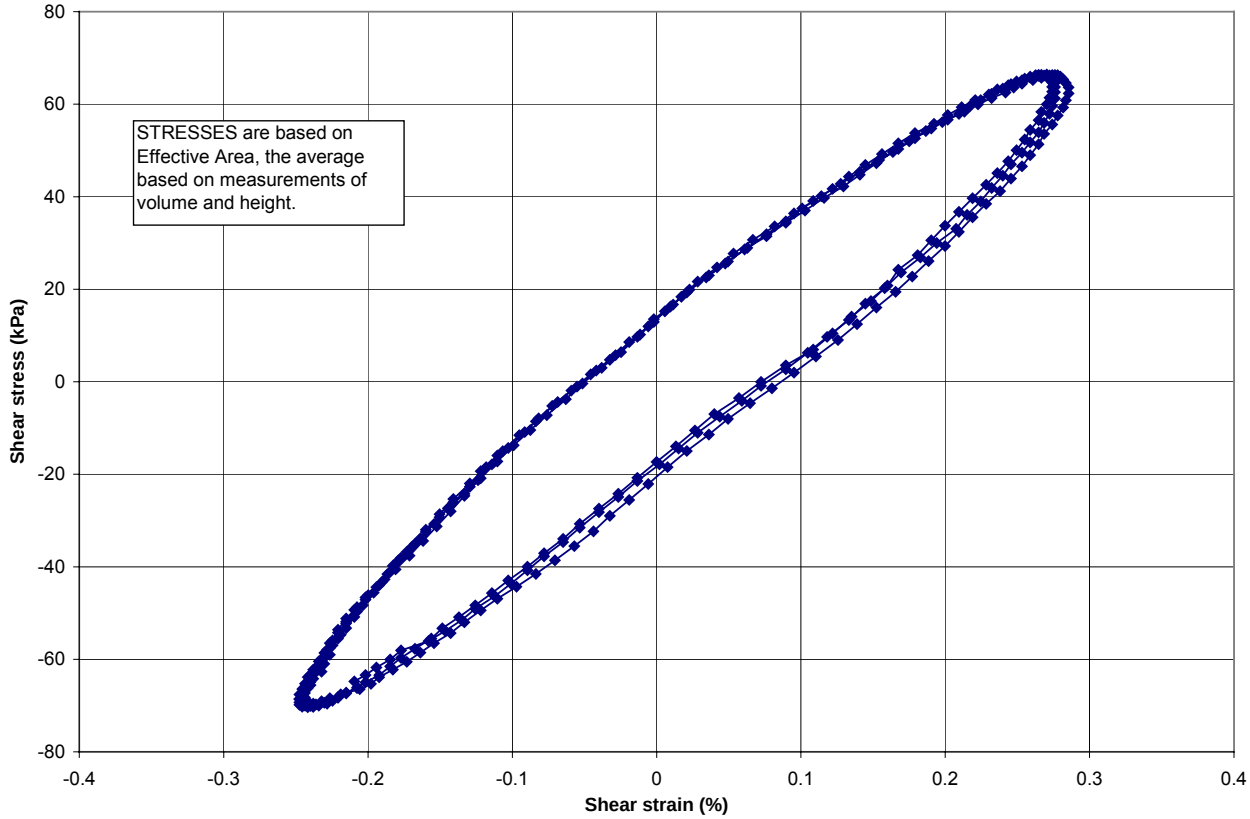

Copyright 2007, Kleinfelder

LANL8 Cyc 3: Vertical and radial strains, CSR ~ 0.29

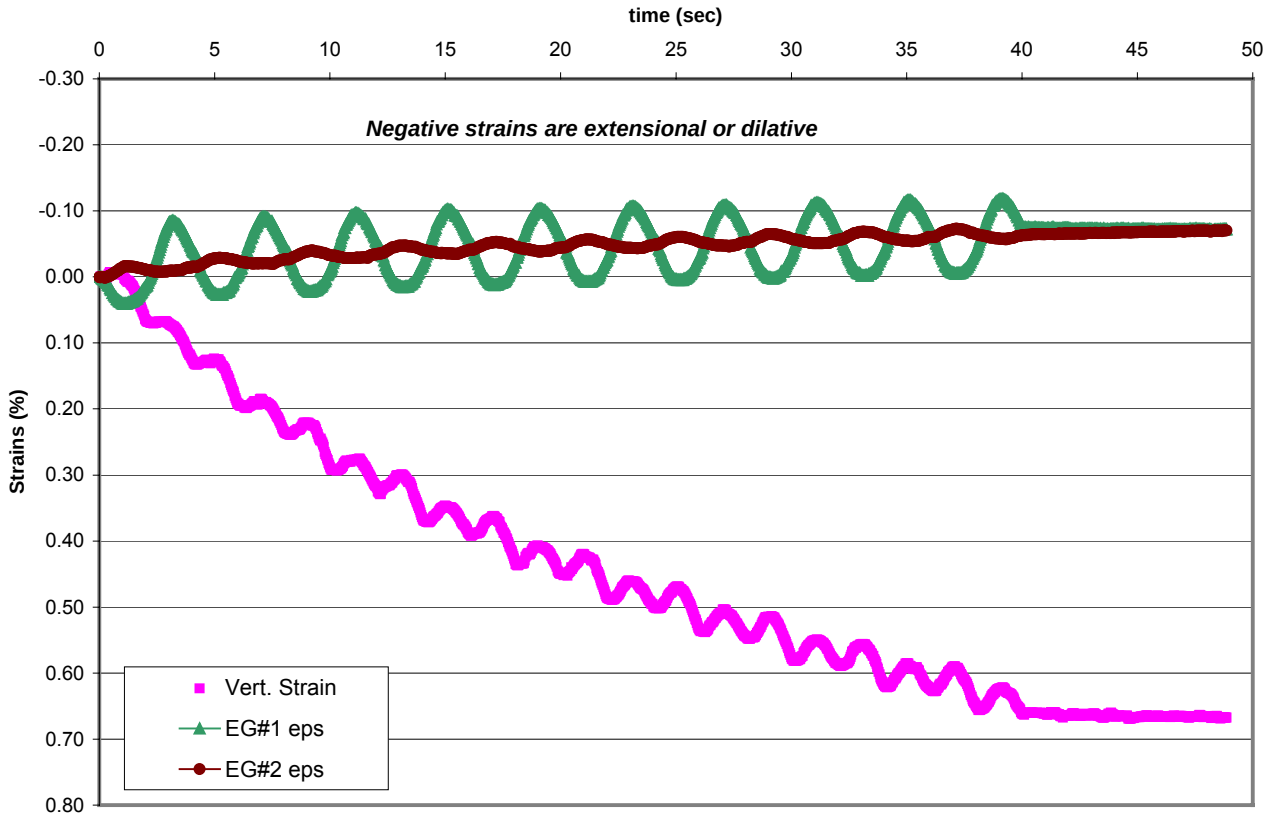

LANL8 Cyc 3: Hysteresis Loops, CSR ~ 0.29

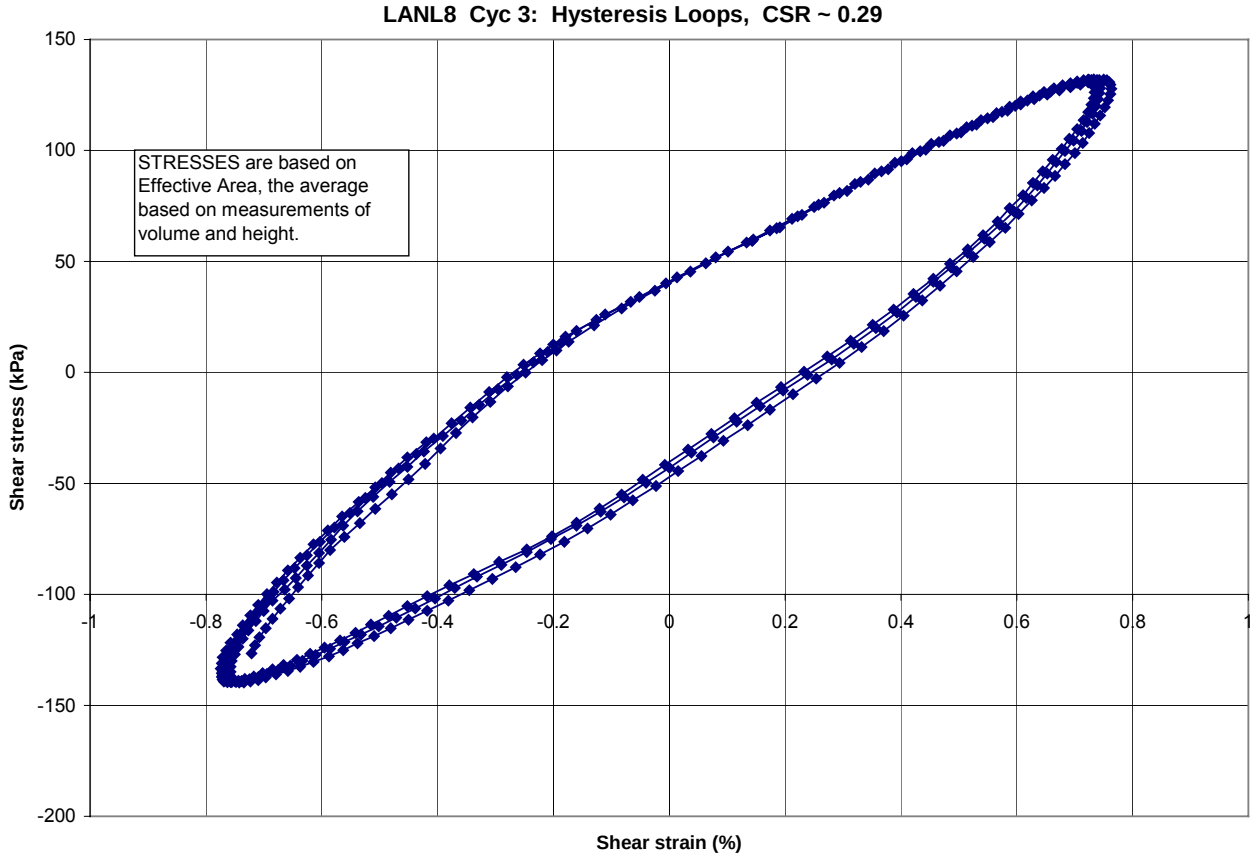

Copyright 2007, Kleinfelder

LANL # 9

Stage of testing					***Incremental Vert. Strain (%)***
Consol. #1	Raise vertical stress from 14 to 100 kPa				0.99
Consol. #2	Raise vertical stress from 100 to 200 kPa				0.59
Consol. #3	Raise vertical stress from 200 to 300 kPa				0.42
Consol. #4	Raise vertical stress from 300 to 402 kPa				0.41
					2.41
	CSR	***# of cycles***	***s.a. shear strain***	***Approx. G***	
			(%)	***(kPa)***	
Cyclic loading 1	0.077	5	0.119	26,200	0.09
Cyclic loading 2	0.15	10	0.3	20,400	0.23
Cyclic loading 3	0.3	10	0.86	14,200	0.8
Unloading	Reduce stresses thru same path, return to ~50 kPa vacuum confinement				-0.87

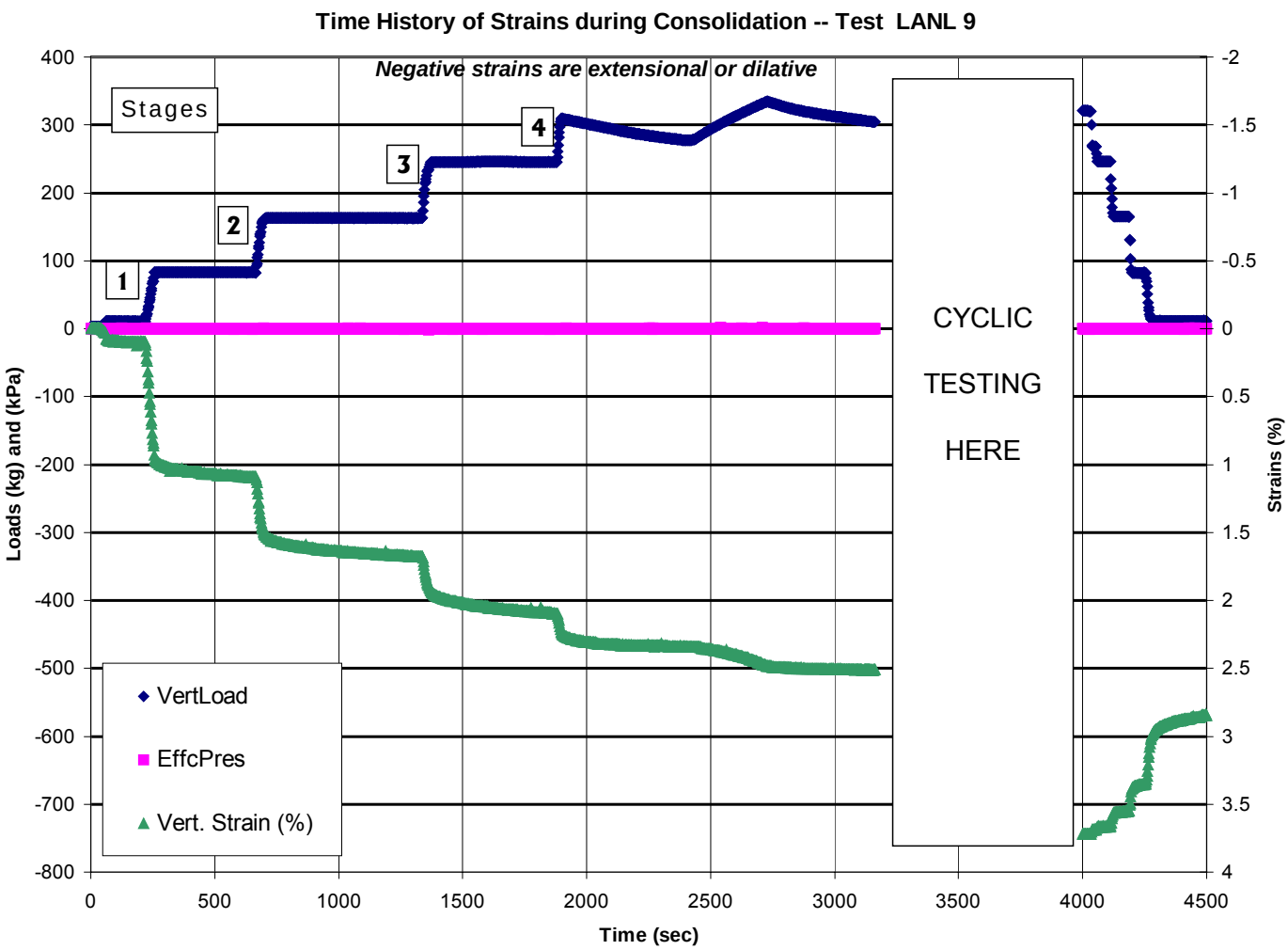

LANL9 Cyc 1: Vertical stress and strain, CSR ~ 0.077

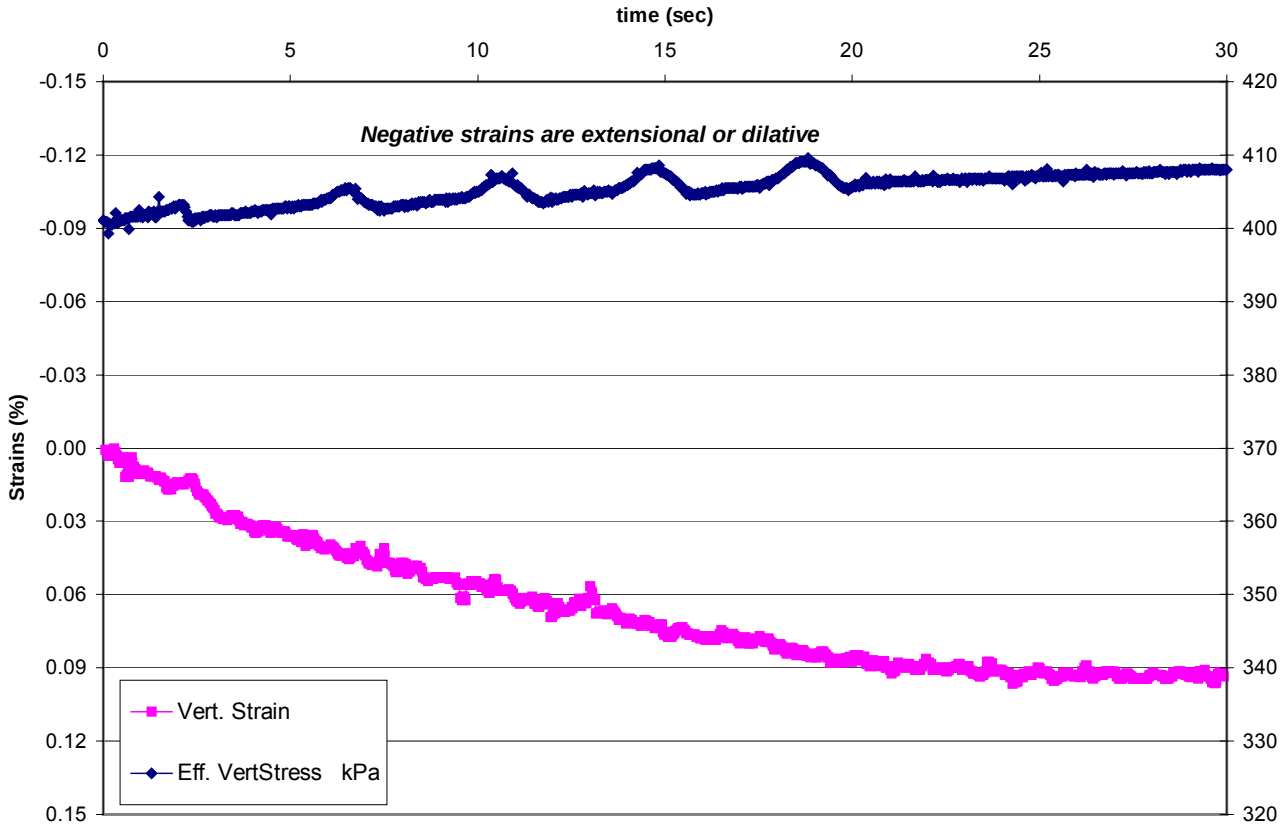

LANL9 Cyc 1: Hysteresis Loops, CSR ~ 0.077

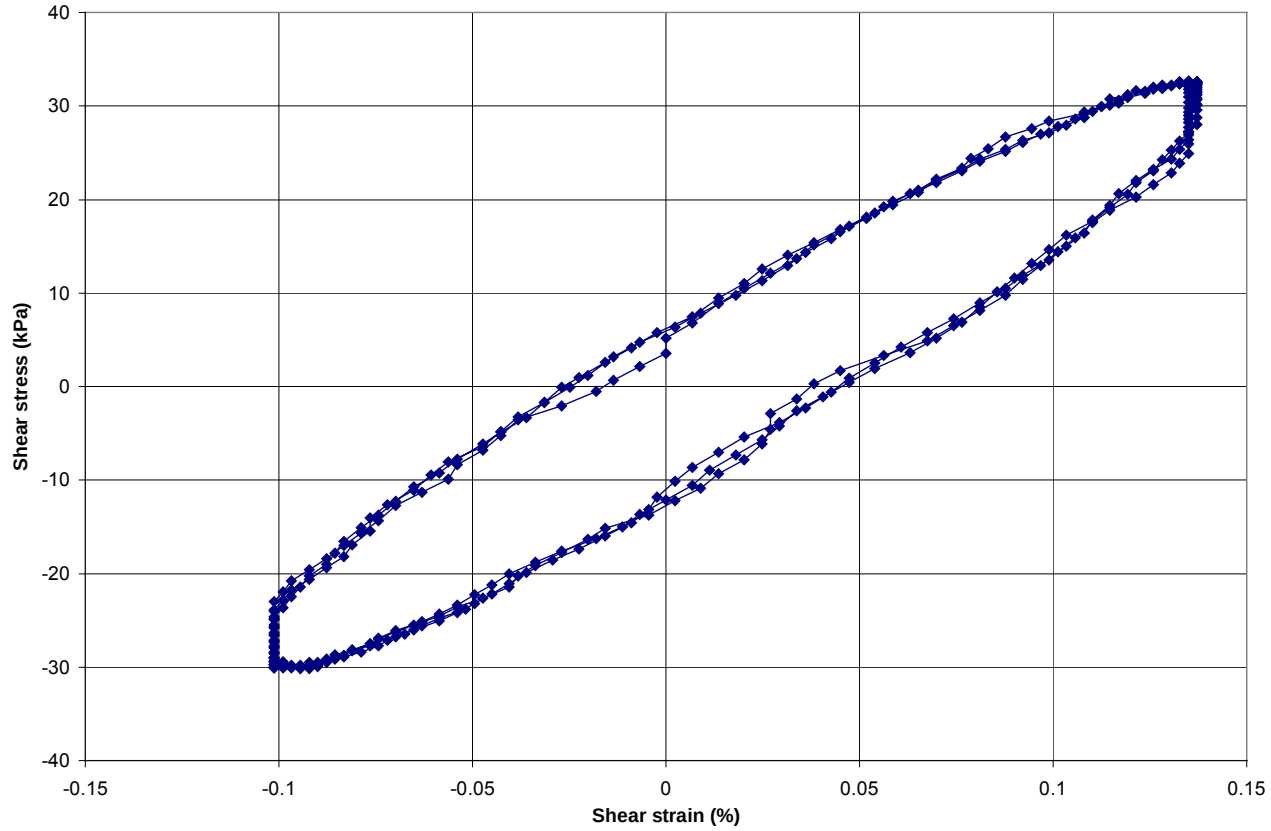

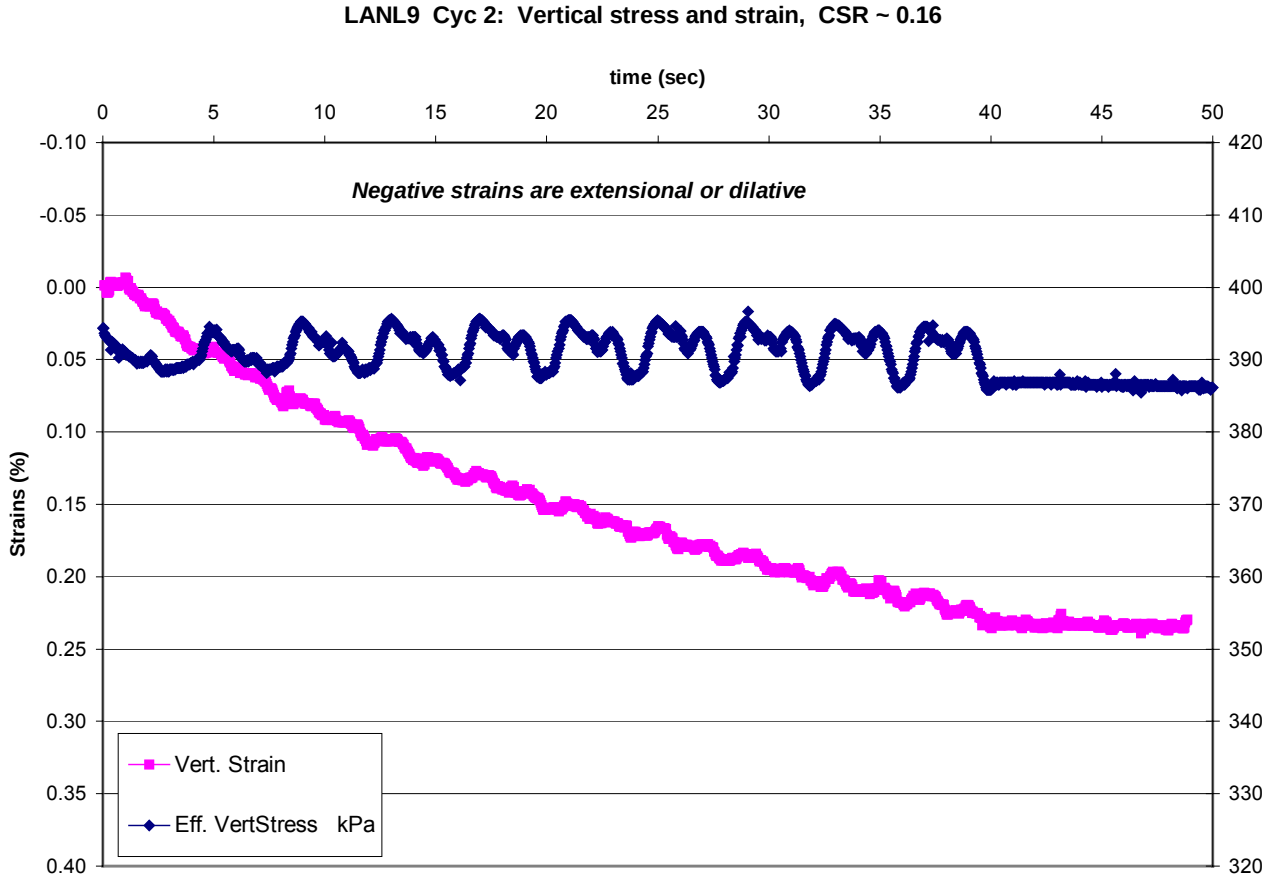
LANL9 Cyc 2: Vertical stress and strain, CSR ~ 0.16
time (sec)
0
5
10
15
20
25
30
35
40
45
50
Negative strains are extensional or dilative
Strains (%)
-0.10
-0.05
0.00
0.05
0.10
0.15
0.20
0.25
0.30
0.35
0.40
420
410
400
390
380
370
360
350
340
330
320
Vert. Strain
Eff. VertStress kPa

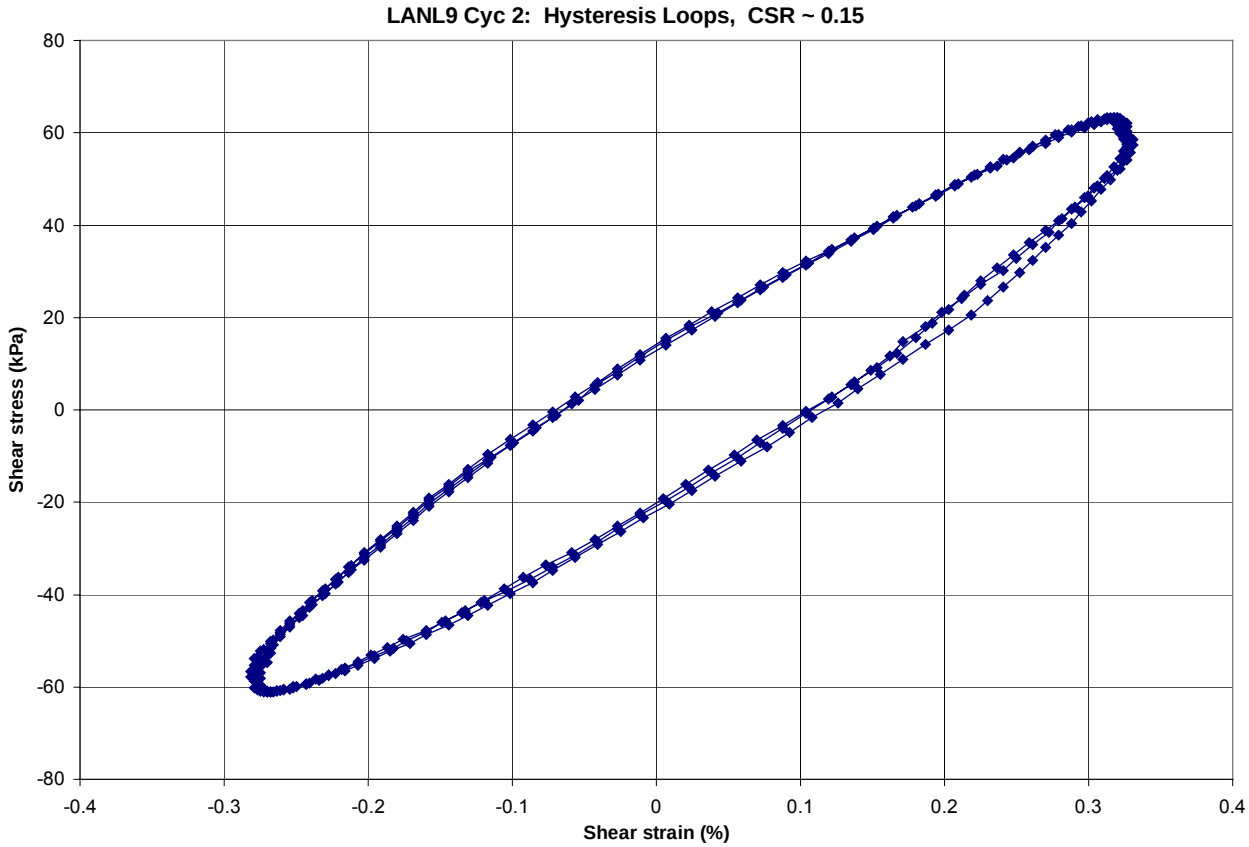
LANL9 Cyc 2: Hysteresis Loops, CSR ~ 0.15
Shear stress (kPa)
80
60
40
20
0
-20
-40
-60
-80
-0.4
-0.3
-0.2
-0.1
0
0.1
0.2
0.3
0.4
Shear strain (%)

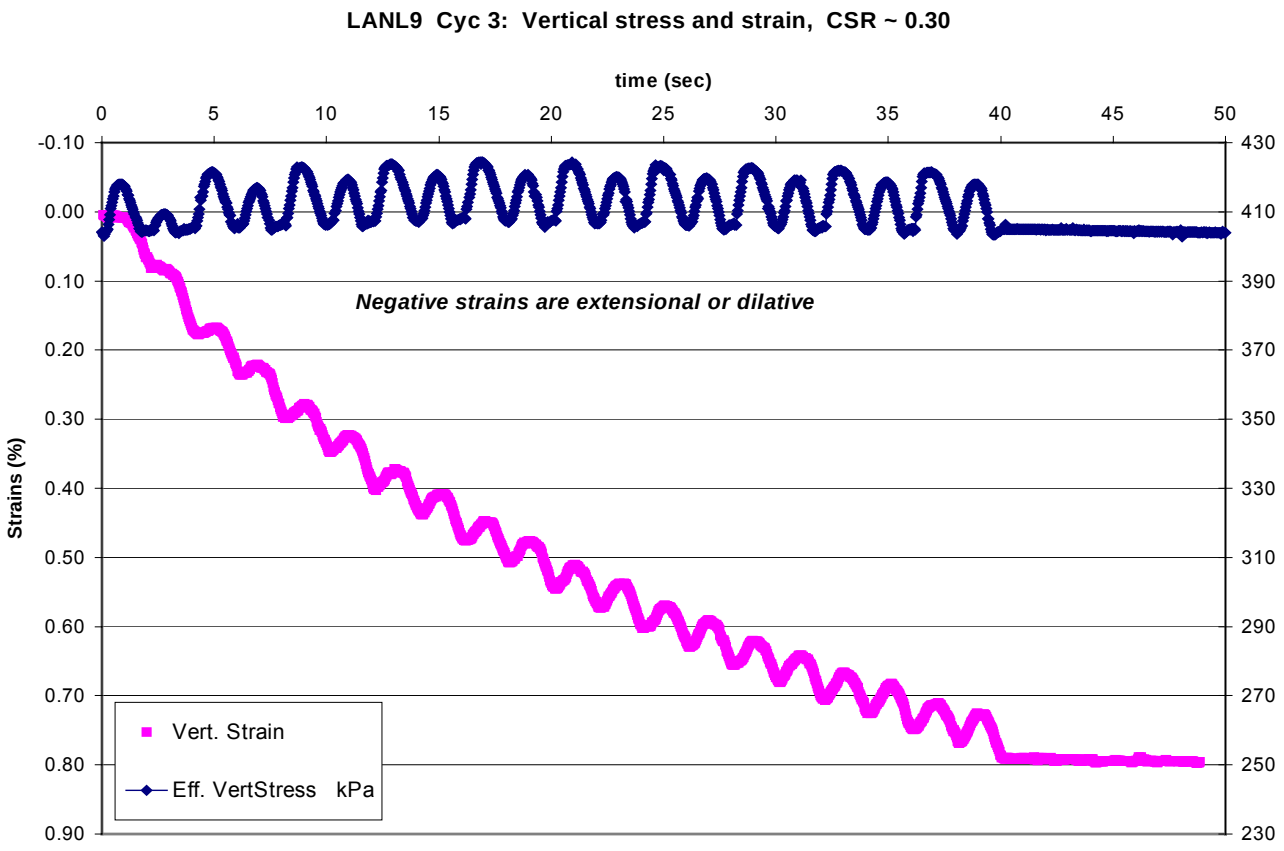
LANL9 Cyc 3: Vertical stress and strain, CSR ~ 0.30
time (sec)
0
5
10
15
20
25
30
35
40
45
50
-0.10
0.00
0.10
0.20
0.30
0.40
0.50
0.60
0.70
0.80
0.90
Strains (%)
430
410
390
370
350
330
310
290
270
250
230
Negative strains are extensional or dilative
Vert. Strain
Eff. VertStress kPa

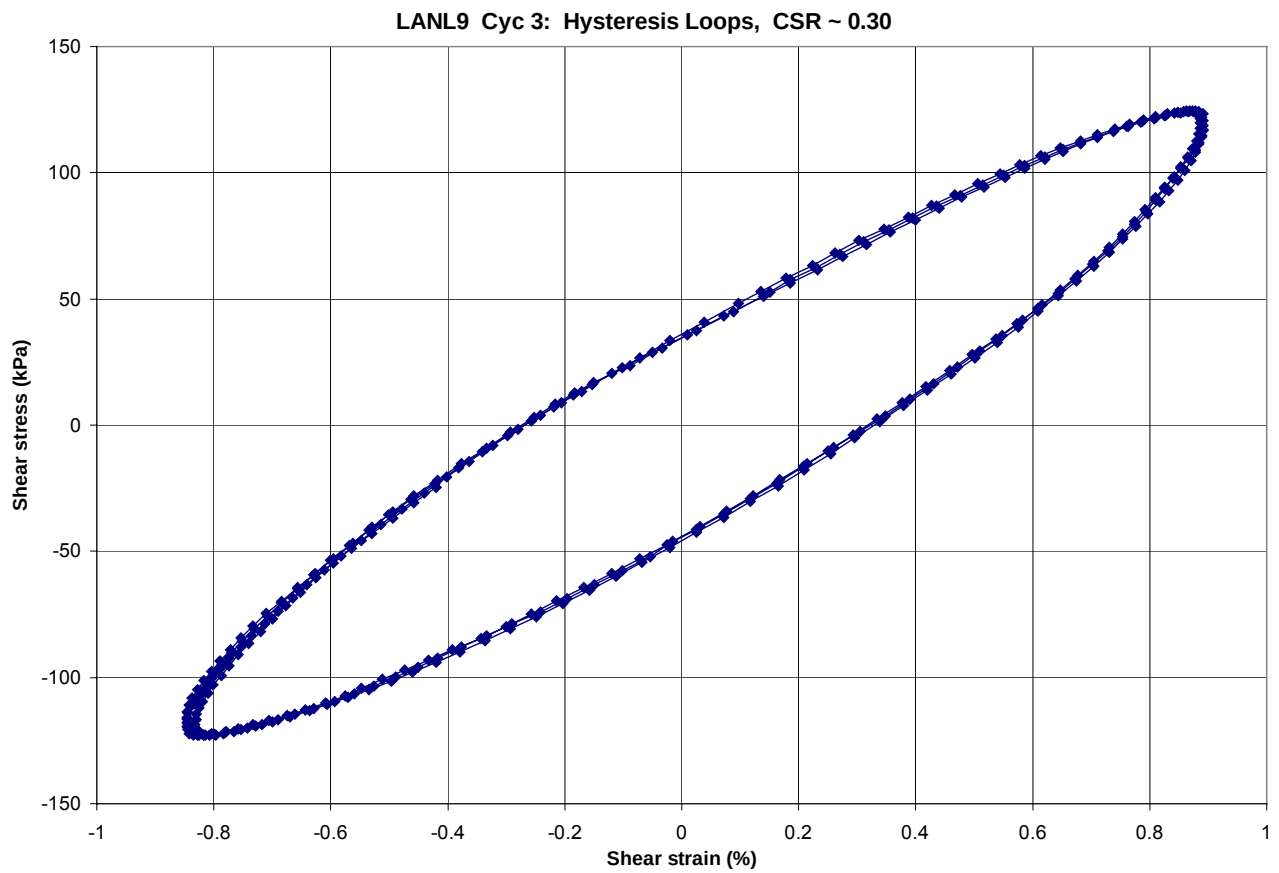
LANL9 Cyc 3: Hysteresis Loops, CSR ~ 0.30
150
100
50
0
-50
-100
-150
Shear stress (kPa)
-1
-0.8
-0.6
-0.4
-0.2
0
0.2
0.4
0.6
0.8
1
Shear strain (%)

Appendix F

Calculation – Estimate of Cyclic Stress Ratio for CMRR

CMRR Project Calculation Cover Sheet

LANL Subcontract No.:	13568	Calculation No.:	19435.SBT.16-ALB04CA001
LANL Task No.:	109	Calculation Title:	Estimation of Cyclic Shear Ratio for CMRR
LANL Project ID No.:	100320	Management Level:	1

Design Verification Required: ~~☒ Yes~~ 1/2/07 ☒ No

Calculation Type: ☐ Scoping ☐ Preliminary ☒ Final

☐ Superseded by Calculation No: _____ ☐ Voided

Original and Revised Calculation Approval

	Rev.0 Printed Name/ Signature/Initials/Date	Rev. Printed Name/ Signature/Initials/Date	Rev. Printed Name/ Signature/Initials/Date
Originator:	Joseph P. Laird Joseph P Laird JPL 12/21/04		
Checked By:	Chandra P Bhargin B Prakash CB 12/22/04		
Approved By:	1/4/05		
Other:			

Record of Revision

Rev.	Reason for Revision

Attachments

Attachment #	Title	Revision	Total Pages

Total Calculation Page Count – 9

CMRR Project Calculation Summary Sheet

Calculation No. 19435 SBT.16-ALB04CA001 ORIGINATOR JOSEPH P. LAIRA JPL DATE 12/21/04
Print & Initial Above

Rev No. 0 CHECKER: CHANDRA P. BHONGIR CB DATE 12/22/04
Print & Initial Above

Calculation Title ~~Engineering Properties and Design Parameters~~ JPL
ESTIMATION OF CYCLIC SHEAR RATIO FOR CHEE

Table of Contents

1.0 INTRODUCTION Page 3 of 9
1.1 Purpose Page 3 of 9
1.2 Scope Page 3 of 9

2.0 BASIS Page 3 of 9
2.1 Design Inputs Page 3 of 9
2.2 Criteria Page 3 of 9
2.3 Assumptions Page 3 of 9

3.0 REFERENCES Page 4 of 9

4.0 METHODS Page 4 of 9

5.0 RESULTS AND CONCLUSIONS Page 4 of 9

6.0 CALCULATIONS AND ANALYSIS Page 4 of 9

Copyright 2007, Kleinfelder

1.0 INTRODUCTION

1.1 Purpose

The purpose of this calculation brief is to estimate the Cyclic Stress Ratio (CSR) for the Bandelier Tuff, Unit 3 Lower (Qbt_{3L}) at the CMRR site. This parameter will be used as a correlation to targeted laboratory cyclic shear stresses to be applied during the planned Cyclic Simple Shear (CSS) tests.

1.2 Scope

The CSR will be estimated at the approximate mid-depth of Qbt_{3L} at the CMRR site using published correlations. A site specific CSR will be estimated at a later date by Walt Silva, Consultant, based on the modeled dynamic response of the site using subsequent field and laboratory data.

2.0 BASIS

2.1 Design Inputs

Design inputs include laboratory test results from the RLUOB report, as detailed in Calculation Brief 1197.109.X.001, Engineering Properties and Design Parameters. The laboratory test data includes total unit weight for the intact Bandelier Tuff, Units 3 and 4, which is used to calculate vertical effective stress and mean effective stress.

- An average unit weight of 93 pcf was utilized for Qbt_{3U}.
- An average unit weight of 88 pcf was utilized for Qbt_{3L}.

Probabilistic Seismic Hazard Analysis (PSHA) and Deterministic earthquake magnitude, maximum ground accelerations, and average shear wave velocity at 40 feet, $V_{s,40\,ft}$ were selected according to the 1995 Woodward Clyde Consultants Seismic Investigation.

- PSHA: Earthquake Magnitude, M = 6.0, Amax = 0.33 g
- Deterministic: Earthquake Magnitude, M = 7.0, Amax = 0.5 g
- Average shear wave velocity = 1,000 feet per second

2.2 Criteria

The design inputs for this calculation were used based on field and laboratory data of this and previous LANL investigations, as well as empirical design correlations taken from the references presented in Section 3, namely Seed and Idriss (1982) and Seed et al. (2003).

2.3 Assumptions

- The depth range of Qbt_{3L} is about 75 to 130 below ground surface at the CMRR site. Thus, the depth at the approximate middle of the layer is 102.5 feet

Copyright 2007, Kleinfelder

3.0 REFERENCES

The following references have been peered reviewed and are commonly used in standard practice. The exact page number, table, or figure will be called out in the calculations as they are used, since various parts of the references have been used.

1.) Conference Call Discussing Cyclic Simple Shear Test Plan, August 20, 2004, including John North, Alan Kuhn, Joe Laird, Ed Rinne, Michael Riemer and Bob Pyke.

2.) Keller and Oliver, "Engineering Report on the Properties and Characteristics of Volcanic Tuff at the Los Alamos National Laboratory", Merrick Engineers and Associates, 1995.

3.) Seed, H.B. and Idriss, I.M., 1982, Ground Motions and Soil Liquefaction During Earthquakes, Earthquake Engineering Research Institute

4.) Seed, R.B., et al., 2003, "Recent Advances in Soil Liquefaction Engineering – A Unified and Consistent Framework", 26th Annual ASCE Geotechnical Spring Seminar.

5.) Woodward Clyde Federal Services (WCFS), 1995, "Seismic Hazards Evaluation of the Los Alamos National Laboratory".

4.0 METHODS

Methods used included published correlations and laboratory test data to determine the engineering properties. Refer to Pages 5 through 7 of 9 for the Seed and Idriss Analysis and and Page 8 and 9 of 9 for the Seed et al equations.

5.0 RESULTS AND CONCLUSIONS

We recommend the use of an average CSR taken from the two correlations.

CSR (Seed and Idriss Method) = 0.12

CSR (Seed et al. Method) = 0.19

CSR Average = 0.155

6.0 CALCULATIONS AND ANALYSES

Refer to Pages 5 through 7 of 9 for the Seed and Idriss Analysis and and Page 8 and 9 of 9 for the Seed et al equations

Simplified Procedure for Evaluating Stresses Induced by Earthquakes

The shear stresses developed at any point in a soil deposit during an earthquake appear to be due primarily to the vertical propagation of shear waves in the deposit. This leads to a simplified procedure for evaluating the induced shear stresses (Seed and Idriss, 1971). If the soil column above a soil element at depth h behaved as a rigid body, the maximum shear stress on the soil element would be

$$(\tau_{max})_r = \frac{\gamma h}{g} \cdot a_{max} \qquad (1)$$

where a_{max} is the maximum ground surface acceleration and γ is the unit weight of the soil; see Fig. 39(a). Because the soil column behaves as a deformable body, the actual shear stress at depth h, $(\tau_{max})_d$, as determined by a ground response analysis will be less than $(\tau_{max})_r$ and might be expressed by

$$(\tau_{max})_d = r_d \cdot (\tau_{max})_r \qquad (2)$$

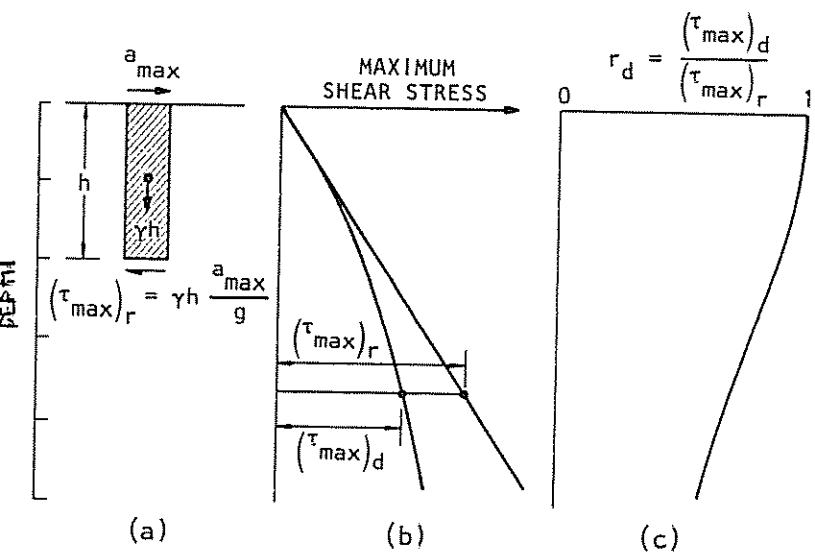

Figure 39. Procedure for determining maximum shear stress, $(\tau_{max})_r$.

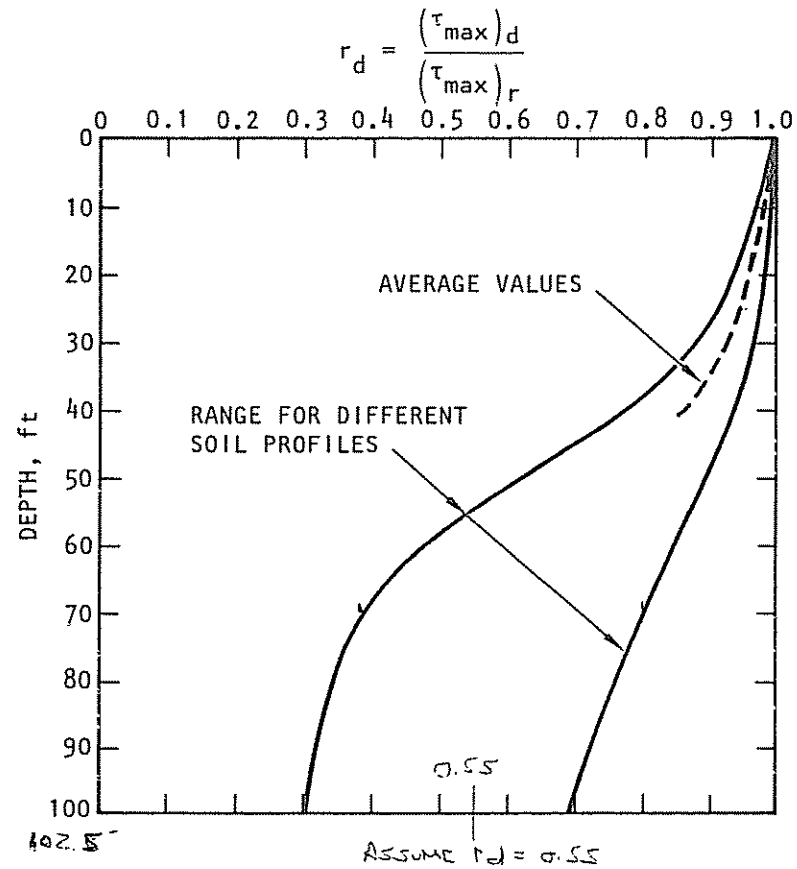

Figure 40. Range of values of r_d for different soil profiles.

where r_d is a stress reduction coefficient with a value less than 1. The variations of $(\tau_{max})_r$ and $(\tau_{max})_d$ will typically have the form shown in Fig. 39(b) and, in any given deposit, the value of r_d will decrease from a value of 1 at the ground surface to much lower values at large depths, as shown in Fig. 39(c).

Computations of the value of r_d for a wide variety of earthquake motions and soil conditions having sand in the upper 50 ft. have shown that r_d generally falls within the range of values shown in Fig. 40. It may be seen that in the upper 30 or 40 ft., the scatter of the results is not great and, for any of the deposits, the error involved in using the average values shown by the dashed line would generally be less than about 5%. Thus

(SEED, H.B, AND IDRISS, I.M., 1982)

LANL PROJECT NUMBER: 13568-109-100320
CALCULATION No. 19435.SBT.16-ALB04.CA001
PAGE 5 OF 9
12/21/2004

Ave Unit Weight, Qbt3 upper = 93 pcf a_{max}= 0.33 g

Ave Unit Weight, Qbt3 lower = 88 pcf r_d = 0.55

Cyclic Shear Stress, $\tau_{ave} = 0.65 * \sigma_o * (a_{max} / g) * r_d$

Cyclic Stress Ratio, CSR = τ_{ave} / σ_o'

Location	Depth, ft	Vertical Effective Stress, psf	Cyclic Shear Stress, psf	Cyclic Stress Ratio	Mean Effective Stress, psf (Ko = 1.0)	Mean Effective Stress, psf (Ko = 0.5)
Block Sample, Pre-Quarry	100	9275	1094	0.12	9275	6184
Block Sample, Post-Quarry	5	440	52	0.12	440	293
CMRR, Top Qbt3 lower	75	6975	823	0.12	6975	4650
CMRR, Middle Qbt3 lower	102.5	9395	1108	**0.12**	9395	6264
CMRR, Bottom Qbt3 lower	130	11815	1394	0.12	11815	7881

Cyclic Stress Ratio (CSR)

According to Seed et al. (2003),

$$CSR_{peak} = \left(\frac{a_{max}}{g}\right)\left(\frac{\sigma_v}{\sigma'_v}\right)(r_d) \qquad \text{(Eq. 1)}$$

where

a_{max} = the peak horizontal ground surface acceleration,
g = the acceleration of gravity,
σ_v = total vertical stress,
σ'_v = effective vertical stress, and
r_d = the nonlinear shear mass participation factor

d < 65 ft:

$$r_d(d, M_w, a_{max}, V^*_{s,40'}) = \frac{\left[1 + \dfrac{-23.013 - 2.949\ a_{max} + 0.999\ M_w + 0.016\ V^*_{s,40'}}{16.258 + 0.201\ e^{0.304(-d + 0.0785\ V^*_{s,40'} + 24.333)}}\right]}{\left[1 + \dfrac{-23.013 - 2.949\ a_{max} + 0.999\ M_w + 0.016\ V^*_{s,40'}}{16.258 + 0.201\ e^{0.304(0.0785\ V^*_{s,40'} + 24.333)}}\right]} \pm \sigma_{\epsilon_{r_d}} \qquad \text{(Eq 2)}$$

d ≥ 65 ft:

$$r_d(d, M_w, a_{max}, V^*_{s,40'}) = \frac{\left[1 + \dfrac{-23.013 - 2.949\ a_{max} + 0.999\ M_w + 0.016\ V^*_{s,40'}}{16.258 + 0.201\ e^{0.304(-65 + 0.0785\ V^*_{s,40'} + 24.333)}}\right]}{\left[1 + \dfrac{-23.013 - 2.949\ a_{max} + 0.999\ M_w + 0.016\ V^*_{s,40'}}{16.258 + 0.201\ e^{0.304(0.0785\ V^*_{s,40'} + 24.333)}}\right]} - 0.0014\ (d - 65) \pm \sigma_{\epsilon_{r_d}}$$

where

$\sigma_{\epsilon_{r_d}}(d) = d^{0.650}\ 0.0072$ [for d < 40 ft], and $\sigma_{\epsilon_{r_d}}(d) = 40^{0.650}\ 0.0072$ [for d ≥ 40 ft]

where d is the depth in feet, M_w is the moment magnitude, and $V^*_{s,40'}$ is average shear wave velocity over the top 40 feet of the site (in feet/sec), taken as 40 feet divided by shear wave travel time in traversing this 40 feet.

$$CSR_{eq} = (0.65)\ CSR_{peak} \qquad \text{(Eq. 3)}$$

LANL PROJECT NUMBER: 13568-109-100320
CALCULATION No. 19435-SBT, 16-ALB04CA001

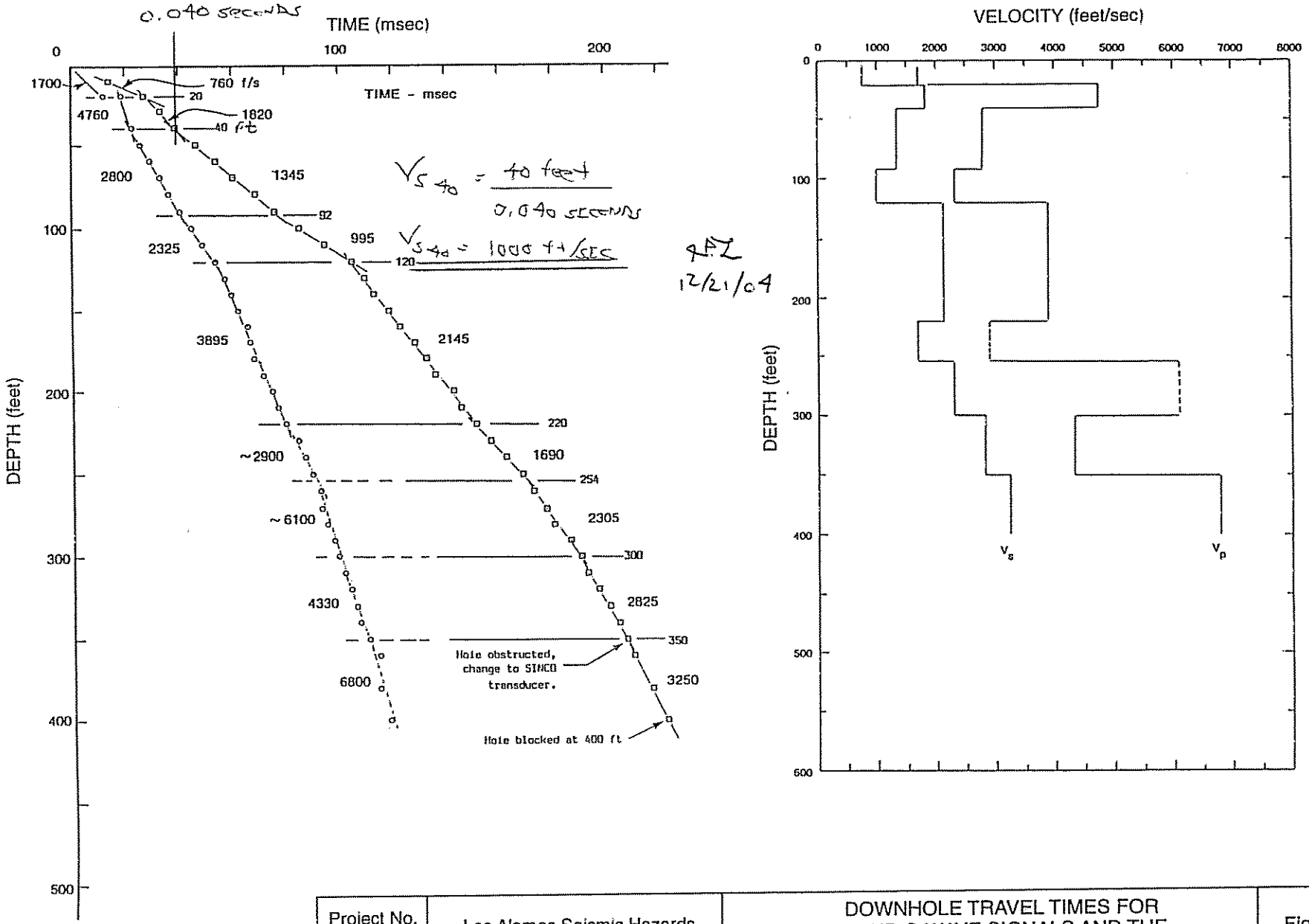

PAGE 8 OF 9
12/21/2004

Project No. 91C0509	Los Alamos Seismic Hazards	DOWNHOLE TRAVEL TIMES FOR P- AND S-WAVE SIGNALS AND THE RESULTING VELOCITY PROFILES FOR SHB-1 (NOTE TA-55)	Figure 6-6
	Woodward-Clyde Federal Services		

91C0509A-1300/101994

Ave Unit Weight, Qbt3 upper = 93 pcf
Ave Unit Weight, Qbt3 lower = 88 pcf

Cyclic Shear Stress, $\tau_{ave} = 0.65 * \sigma_o * (a_{max} / g) * r_d$

Cyclic Stress Ratio, CSR = τ_{ave} / σ_o'

$V_{s,40\,ft}$ in ft/sec = 1000
depth, d in ft = 102.5
$\sigma_{r,rd}$ for d > 40 ft = 0.166

	M_w	Amax/g	Mean Value r_d for d > 65 ft	$-\sigma_{r\,rd}$ r_d for d > 65 ft	$+\sigma_{r\,rd}$ r_d for d > 65 ft
PSHA	6.0	0.33	**0.87**	0.71	1.04
Deterministic	7.0	0.50	0.89	0.73	1.06

	Location	Depth below Current Ground at CMRR, feet	Vertical Effective Stress, psf	Cyclic Shear Stress, psf	Cyclic Stress Ratio	Ko = 1.0 Mean Effective Stress, psf	Ko = 0.5 Mean Effective Stress, psf
PSHA	CMRR, Top Qbt3 lower	75	6975	1762	**0.19**	6975	4650
	CMRR, Middle Qbt3 lower	102.5	9395			9395	6264
	CMRR, Bottom Qbt3 lower	130	11815			11815	7881
Deterministic	CMRR, Top Qbt3 lower	75	6975	2725	0.29	6975	4650
	CMRR, Middle Qbt3 lower	102.5	9395			9395	6264
	CMRR, Bottom Qbt3 lower	130	11815			11815	7881

Components of Rd equation (Seed, et al, 2003) for d > 65 feet, final answer in bold above

	Numerator 1	Denominator 1	Numerator 2	Denominator 2	end
PSHA	-1.9922	27.1486	-1.9922	9410.9641	0.0525
Deterministic	-1.4945	27.1486	-1.4945	9410.9641	0.0525

Copyright 2007, Kleinfelder

Appendix G

Summary Description of Quality Control Plan

APPENDIX G

SUMMARY DESCRIPTION OF QUALITY CONTROL PLAN

Kleinfelder, Inc. (Kleinfelder), as a subcontractor to DMJM H+N on the Chemistry and Metallurgical Research Replacement (CMRR) Project, uses the DMJM H+N Quality Assurance (QA) Program and applicable QA procedures in its CMRR work. The DMJM H+N QA Program satisfies Los Alamos National Laboratory QA requirements as defined in Contract #13568-109-02-CX, Request for Proposal 2002-109, "A/E Services for Chemistry and Metallurgy Research Building Replacement Project." DMJM H+N's QA Program meets 10 CFR 830.120 and DOE 414.1A by implementation of NQA-1.

A Subcontractor Quality Assurance Plan (SQAP) defining the QA requirements for Kleinfelder's support of the CMRR Project has been developed and is being followed. The DMJM H+N QA Program and the SQAP are supplemented by Kleinfelder's Quality System Manual, Quality Control Review Procedure Manual, and Technical Standard Operating Procedures Manual, which prescribe how Kleinfelder will document field and laboratory activities and observations, data acquisition and review, and reporting required by the Kleinfelder-DMJM H+N contract Scope of Work. All of these references are on file and available for review.

Copyright 2007, Kleinfelder